



UNIVERSITAT POLITÈCNICA
DE CATALUNYA
BARCELONATECH

Aggregation techniques for energy flexibility

Emmanouil Valsomatzis

ADVERTIMENT La consulta d'aquesta tesi queda condicionada a l'acceptació de les següents condicions d'ús: La difusió d'aquesta tesi per mitjà del repositori institucional UPCommons (<http://upcommons.upc.edu/tesis>) i el repositori cooperatiu TDX (<http://www.tdx.cat/>) ha estat autoritzada pels titulars dels drets de propietat intel·lectual **únicament per a usos privats** emmarcats en activitats d'investigació i docència. No s'autoritza la seva reproducció amb finalitats de lucre ni la seva difusió i posada a disposició des d'un lloc aliè al servei UPCommons o TDX. No s'autoritza la presentació del seu contingut en una finestra o marc aliè a UPCommons (*framing*). Aquesta reserva de drets afecta tant al resum de presentació de la tesi com als seus continguts. En la utilització o cita de parts de la tesi és obligat indicar el nom de la persona autora.

ADVERTENCIA La consulta de esta tesis queda condicionada a la aceptación de las siguientes condiciones de uso: La difusión de esta tesis por medio del repositorio institucional UPCommons (<http://upcommons.upc.edu/tesis>) y el repositorio cooperativo TDR (<http://www.tdx.cat/?locale-attribute=es>) ha sido autorizada por los titulares de los derechos de propiedad intelectual **únicamente para usos privados enmarcados** en actividades de investigación y docencia. No se autoriza su reproducción con finalidades de lucro ni su difusión y puesta a disposición desde un sitio ajeno al servicio UPCommons No se autoriza la presentación de su contenido en una ventana o marco ajeno a UPCommons (*framing*). Esta reserva de derechos afecta tanto al resumen de presentación de la tesis como a sus contenidos. En la utilización o cita de partes de la tesis es obligado indicar el nombre de la persona autora.

WARNING On having consulted this thesis you're accepting the following use conditions: Spreading this thesis by the institutional repository UPCommons (<http://upcommons.upc.edu/tesis>) and the cooperative repository TDX (<http://www.tdx.cat/?locale-attribute=en>) has been authorized by the titular of the intellectual property rights **only for private uses** placed in investigation and teaching activities. Reproduction with lucrative aims is not authorized neither its spreading nor availability from a site foreign to the UPCommons service. Introducing its content in a window or frame foreign to the UPCommons service is not authorized (*framing*). These rights affect to the presentation summary of the thesis as well as to its contents. In the using or citation of parts of the thesis it's obliged to indicate the name of the author.



Universitat Politècnica de Catalunya
Escola Tècnica Superior de Enginyeria Industrial de Barcelona

Ph.D. Thesis

Sustainable plastics derived from renewable resources

Elena Zakharova

Thesis advisors: Dr. Sebastián Muñoz-Guerra
Dr. Antxon Martínez Ilarduya

Barcelona, December 2017

*Границ научному познанию и предсказанию предвидеть
невозможно.*

Д.И. Менделеев

To all my family and friends...

Summary

In this century, the major use of synthetic polymers have been as replacements for more traditional materials, particularly in packaging. Today the packaging industry is by far the major user of plastics. Over 60% of post-consumer plastics waste is produced by households, most of it as single use packaging. Another interesting application of these materials is drug delivery systems. Polymers have played an integral role in the advancement of drug delivery technology by providing controlled release of therapeutic agents in constant doses over long periods, cyclic dosage and tunable release of both hydrophilic and hydrophobic drugs. Modern advances in drug delivery are now predicated upon the rational design of polymers tailored for specific cargo and engineered to exert distinct biological functions. Aliphatic polyesters such as poly(L-lactic acid), poly(butylene succinate), and polyhydroxyalkanoates among others, constitute primary examples of bio-based polymers that distinguish by being fully renewable and displaying partial or total biodegradability.

This Ph.D. Thesis is devoted to the synthesis of aliphatic random and block polyesters from renewable resources with application for packaging and drug delivery. The main goal of this project is to develop new bio-based polymers with similar or even improved properties compared to those of conventional plastics obtained from non-renewable sources.

The two cyclic acetals, 2,3-di-O-methylene-L-threitol and dimethyl 2,3-di-O-methylene-L-threarate, were used for the synthesis of two series of PBS copolyesters differing in which unit, butylene or succinate, was replaced, in addition of the corresponding parent homopolyesters. 2,4:3,5-di-O-methylene-D-glucitol was used for the synthesis of PBS copolyesters by melt polycondensation. Three series of polyalkanoates (adipates, suberates and sebacates) were synthesized using as monomers three sugar-based bicyclic diols derived from D-glucose and D-mannose. ABA triblock copolyesters were synthesized by ROP of L-lactide in solution initiated by telechelic D-glucose- and L-tartaric-based polyester macroinitiators.

The synthesized polyesters were characterized by nuclear magnetic resonance (NMR) spectroscopy, gel permeation chromatography (GPC) and viscosimetry. Thermal properties were analyzed by differential scanning calorimetry (DSC) and thermogravimetry (TGA). Crystalline structure of polyesters was studied by X-ray and its mechanical properties were evaluated as well. Hydrolytic degradation and biodegradation assays were followed by GPC and NMR. Nanoparticles made from triblock copolyesters were characterized by scanning electron microscopy (SEM) and dynamic light-scattering (DLS).

Table of content

Summary	6
Glossary	12
Aim and outline of the Thesis	15
1. Introduction	18
1.1. Bio-based and biodegradable polymers	19
1.2. Aliphatic polyesters	22
1.2.1. Biodegradable aliphatic polyesters	22
1.2.2. Poly(butylene succinate) and its copolyesters	27
1.2.3. Biodegradable block copolyesters	29
1.3. Carbohydrate-based polyesters	30
1.3.1. Acyclic carbohydrate-based monomers: resulting polyesters	30
1.3.2. Cyclic carbohydrate-based monomers: resulting polyesters	33
1.3.2.1. Cyclic acetalized aldaric acids and alditols	33
1.3.2.2. Bicyclic acetalized aldaric acids and alditols	34
1.3.2.3. Isohexides	40
1.3.2.4. Other cyclic carbohydrate-based monomers: resulting polyesters	43
1.4. Synthetic methods	45
1.4.1. Melt polycondensation	45
1.4.2. Ring-opening polymerization	46
1.5. Nanoparticles for drug carriers	48
1.5.1. Biodegradable polymeric nanoparticles	48
1.5.2. Techniques for nanoparticle formation	50
1.5.3. Drug encapsulation and release	52
1.6. References	54
2. Materials and methods	59
2.1. Materials	61
2.2. Synthesis of copolyesters	61
2.2.1. Melt polycondensation	61
2.2.2. Ring-opening polymerization in solution	61
2.3. Methods	62
3. Modification of properties of poly(butylene succinate) by copolymerization with tartaric acid-based monomers	64
3.1. Introduction	65
3.2. Experimental part	66

3.2.1. Monomer synthesis	66
3.2.2. Polymer synthesis	67
3.2.3. Hydrolytic degradation and biodegradation	68
3.3. Results and discussion	69
3.3.1. Synthesis and chemical structure	69
3.3.2. Thermal and mechanical properties	73
3.3.3. Crystalline structure and crystallizability	77
3.3.4. Biodegradation and hydrolytic degradation	79
3.4. Conclusions	82
3.5. References	84
4. Bio-based PBS copolyesters derived from a bicyclic D-glucitol	85
4.1. Introduction	86
4.2. Experimental part	87
4.2.1. Monomer synthesis	87
4.2.2. Polymer synthesis	88
4.2.3. Hydrolytic degradation and biodegradation	89
4.3. Results and discussion	90
4.3.1. Synthesis and chemical structure	90
4.3.2. Thermal properties and crystallization	95
4.3.3. Stress-strain behavior	99
4.3.4. Hydrolytic degradation and biodegradation	100
4.3.5. Sugar-based bicyclic diols compared	102
4.4. Conclusions	106
4.5. References	108
5. Sugar-based bicyclic monomers for aliphatic polyesters: A comparative appraisal of acetalized alditols and isosorbide	109
5.1. Introduction	110
5.2. Experimental part	111
5.2.1. Monomer synthesis	111
5.2.2. Polymer synthesis	112
5.3. Results and discussion	113
5.3.1. Synthesis and chemical structure	113
5.3.2. Thermal properties and crystallinity	116
5.3.3. Stress-strain behavior	124
5.4. Conclusions	126
5.5. References	127
6. Triblock copolyesters derived from lactic acid and glucose: Synthesis, nanoparticle formation and simulation	128
6.1. Introduction	129

6.2. Experimental part	130
6.2.1. Monomer synthesis	130
6.2.2. Synthesis of telechelic OH-(PGLuxS) _x -OH homopolyester	130
6.2.3. Synthesis of PLA _y -(PGLuxS) _x -PLA _y triblock copolyesters	130
6.2.4. Synthesis of PLA homopolyester	131
6.2.5. Hydrolytic degradation and biodegradation	131
6.2.6. Preparation of nanoparticles	132
6.2.7. Simulation studies	132
6.3. Results and discussion	132
6.3.1. Synthesis and chemical structure	132
6.3.2. Thermal properties	136
6.3.3. PLA _y -(PGLuxS) _x -PLA _y nanoparticles	139
6.3.4. Simulation studies	141
6.4. Conclusions	146
6.5. References	147
7. Bio-based triblock copolyesters synthesized from tartaric acid derivative and poly(lactic acid), nanoparticle formation	148
7.1. Introduction	149
7.2. Experimental part	149
7.2.1. Synthesis of telechelic OH-(PBiThx) ₁₉ -OH homopolyester	149
7.2.2. Synthesis of PLLA _y -(PBiThx) ₁₉ -PLLA _y triblock copolyesters	150
7.2.3. Removal of isopropylidene groups of triblock copolyesters	150
7.2.4. Hydrolytic degradation	150
7.2.5. Nanoparticle formation	151
7.2.6. Simulation studies	151
7.3. Results and discussion	152
7.3.1. Synthesis and chemical structure	152
7.3.2. Thermal properties	157
7.3.3. Hydrolytic degradation	161
7.3.4. Nanoparticle formation	163
7.3.5. Simulation studies	165
7.4. Conclusions	166
7.5. References	167
8. General conclusions	168
Annex A.	171
Annex B.	178
Annex C.	182
Annex D.	190

Annex E.	199
Acknowledgements	203
Curriculum Vitae	204
Publications	205

Glossary

BD	1,4-butanediol
COSY	2D ^1H - ^1H Homonuclear Correlation NMR spectrum
d	Doublet
DCM	Dichloromethane
DLS	Dynamic light scattering
D₂O	Deuterated water
DMS	Dimethyl succinate
Đ	Dispersity
DBTO	Dibutyltin (VI) oxide
d_{hkl}	Bragg spacings
DFT	Density functional theory
DMA_{di}	Dimethyl adipate
DMSeb	Dimethyl sebacate
DMSO	Dimethylsulfoxide
DMSub	Dimethyl suberate
DSC	Differential Scanning Calorimetry
DMT	Dimethyl terephthalate
Galx-diester	Dimethyl 2,3:4,5-di- <i>O</i> -methylene galactarate
Galx-diol	2,3:4,5-di- <i>O</i> -methylene galactitol
Glux-diol	2,4:3,5-di- <i>O</i> -methylene-D-glucitol
Glux-diester	Dimethyl 2,4:3,5-di- <i>O</i> -methylene-D-glucarate
GPC	Gel Permeation Chromatography
HFIP	1,1,1,3,3,3-hexafluoro-2-propanol
IIDC	Isoidide dicarboxylic acid
Is	Isosorbide
Manx-diol	2,4:3,5-di- <i>O</i> -methylene-D-mannitol
M_n	Number average molecular weight (g/mol)
m	Multiplet
M_w	Weight average molecular weight (g/mol)
NaTFA-HFIP	Trifluoroacetate-hexafluoroisopropanol
NOESY	2D ^1H - ^1H Nuclear Overhauser Effect Spectroscopy
OH-(PBiThx)_x-OH	Hydroxyl capped poly(butylene isopropylidene-L-threarate)
OH-(PGLuxS)_x-OH	Hydroxyl capped poly(2,4:3,5-di- <i>O</i> -methylene-D-glucitol succinate) homopolyester
MALDI-TOF-MS	Matrix-Assisted Laser Desorption/Ionization Time-of-Flight Mass Spectroscopy
PEF	Poly(ethylene furanoate)
PBS	Poly(butylene succinate)
PLA	Poly(lactic acid)
PLA_y-(PGLuxS)_x-PLA_y	Triblock poly(2,4:3,5-di- <i>O</i> -methylene-D-glucitol succinate)- <i>co</i> - poly(lactic acid) copolyester
PLLA_y-(PBiThx)_x-PLLA_y	Triblock poly(butylene 2,3-di- <i>O</i> -isopropylidene)- <i>co</i> -poly(lactic acid) copolyester
PLLA_y-(PBThxOH)_x-PLLA_y	Triblock poly(butylene 2,3-di- <i>O</i> -isopropylidene)- <i>co</i> -poly(lactic acid) copolyester

PMMA	Poly(methyl metacrylate)
PBS_xThx_y	Poly(butylene succinate-co-butylene-2,3-di-O-methylene-L-threarate) copolyesters
PBT	Poly(butylene terephthalate)
PBThx	Poly(butylene-2,3-di-O-methylene-L-threarate) homopolyester
PB_xGlux_yS	Poly(butylene succinate-co-2,4:3,5-di-O-methylene-D-glucitol succinate) copolyesters
PB_xIs_yS	Poly(butylene succinate-co-isosorbide succinate) copolyesters
PB_xManx_yS	Poly(butylene succinate-co-2,4:3,5-di-O-methylene-D-mannitol succinate) copolyesters
PB_xThx_yS	Poly(butylene succinate-co-2,3-di-O-methylene-L-threitylene succinate) copolyesters
PCL	Poly(ϵ -caprolactone)
PET	Poly(ethylene terephthalate)
PGA	Poly(glycolic acid)
PGLuxAdi	Poly(2,4:3,5-di-O-methylene-D-glucitol adipate)
PGLuxS	Poly(2,4:3,5-di-O-methylene-D-glucitol succinate)
PGLuxSeb	Poly(2,4:3,5-di-O-methylene-D-glucitol sebacate)
PGLuxSub	Poly(2,4:3,5-di-O-methylene-D-glucitol suberate)
PHB	Poly(hydroxybutyrate)
PHBV	Poly(3-hydroxybutyrate-co-3-hydroxyvalerate)
PIsAdi	Poly(isosorbide adipate)
PIsS	Poly(isosorbide succinate)
PIsSeb	Poly(isosorbide sebacate)
PIsSub	Poly(isosorbide suberate)
PIsT	Poly(isosorbide terephthalate)
PManxAdi	Poly(2,4:3,5-di-O-methylene-D-mannitol adipate)
PManxS	Poly(2,4:3,5-di-O-methylene-D-mannitol succinate)
PManxSeb	Poly(2,4:3,5-di-O-methylene-D-mannitol sebacate)
PManxSub	Poly(2,4:3,5-di-O-methylene-D-mannitol suberate)
PPDO	Poly(<i>p</i> -dioxanone)
PThxS	Poly(2,3-di-O-methylene-L-threitylene succinate)
R	Degree of Randomness of copolymers
ROP	Ring-opening polymerization
RW	Remainig weight
s	Singlet
SEM	Scanning electron microscopy
T_m	Melting temperature (°C)
T_g	Glass transition temperature (°C)
TBD	1,5,7-triazabicyclo[4,4,0]dec-5-ene
Thx-diester	Dimethyl 2,3-di-O-methylene-L-tartrate
Thx-diol	2,3-di-O-methylene-L-threitol
TGA	Thermogravimetry
TMS	Tetramethylsilane
TFA	Trifluoroacetic acid
WAXS	Wide-angle X-ray scattering
¹H NMR	Proton Nuclear Magnetic Resonance spectroscopy
¹³C NMR	Carbon-13 Nuclear Magnetic Resonance spectroscopy

T_d^{\max}	Temperature of maximum decomposition rate
$T_{5\%}$	Onset decomposition temperature corresponding to 5% of weight loss
E	Young's modulus
ϵ_{\max}	Elongation at break
η	Intrinsic viscosity
ζ	Zeta potential
t_0	Onset crystallization time
$t_{1/2}$	Half crystallization time
σ	Tensile strength
ΔH_m	Melting enthalpy

Aim and outline of the Thesis

In recent years considerable research efforts have been undertaken to develop new plastic materials with low environmental impact. Utilization of carbohydrate derivatives for polymer synthesis has been paid much attention not only because of the huge abundance of these resources but also because the promising biodegradability and biocompatibility of the polymers obtained from them. Among the different natural resources, carbohydrates stand out as highly convenient raw materials because of low cost, its readily availability, great functional diversity and low cost.

The goal of this project is to develop new polymeric materials based on the utilization of renewable resources with potential application in packaging, biomedicine and drug delivery. Depending on compositions and structure, the bio-based materials are capable to cover a wide range of thermal and mechanical behaviors. This Ph.D. work is addressed to the research and development of aliphatic polyesters and copolyesters, containing cyclic and bicyclic acetalized sugar-based units derived from L-tartaric acid, D-glucose, D-mannose. The challenge of this Ph.D. project is to develop new bio-based polymers with similar or even improved properties compared to those of conventional plastics obtained from non-renewable sources. The main objective of the project is achieved through several specific objectives:

- Preparation and characterization by NMR of monocyclic and bicyclic acetalized monomers, like dimethyl 2,3-di-O-methylene-L-tartrate, 2,3-di-O-methylene-L-threitol, 2,4:3,5-di-O-methylene-D-mannitol and 2,4:3,5-di-O-methylene-D-glucitol.
- Synthesis of different classes of homopolyesters, random and triblock copolyesters by melt polycondensation and ROP in solution.
- Characterization of all polyesters by NMR, viscosimetry, GPC and evaluation of the influence of the sugar-based comonomers on physical, mechanical and thermal properties (T_g , T_m , thermal stability), determined by DSC and TGA, including crystallinity and crystallizability.
- Self-assembly of triblock amphiphilic copolyesters of PLA. Evaluation of the capacity of these triblock copolyesters to build biphasic nanoparticles suitable as hydrophobic drug carriers in aqueous media, and its suitability to be used as drug delivery systems.

- Evaluation of the influence of the sugar-based comonomers of synthesized copolyesters on hydrolytic degradation and biodegradation rates and comparison with those displayed by parent homopolyesters.

The PhD thesis consists of 8 chapters describing synthesis of polyesters from renewable resources by polycondensation in bulk or ring-opening polymerization in solution.

Chapter 1. The present chapter deals with the introductory review to aliphatic polyester synthesized from renewable resources with potential application in packaging and biomedicine.

Chapter 2. In this chapter general materials and methods are summarized.

Chapter 3. The following chapter describes synthesis of PBS copolymers by melt polycondensation, using acetalized tartaric acid derivatives. Two series of copolyesters are compared, regarding thermal and mechanical properties, crystalline structure and crystallizability, hydrolytic degradability and biodegradability.

Chapter 4. In this section properties of PBS were modified by insertion of a glucose derivative in the main chain. The properties of novel copolyesters containing Manx-diol and Is units were compared to PBS homopolymer. The study of thermal and mechanical behavior, crystal structure and degradability is also presented.

In **Chapter 5**, three series of polyalkanoates made from two diacetalized alditols Glux-diol, Manx-diol and doubly anhydridized glucitol Is were systematically compared. The characterization of homopolyesters showed that the diacetalized alditols were clearly superior to Is in producing higher molecular weight polyesters. Thermal and mechanical behavior were compared as well.

Chapter 6 describes the synthesis of ABA triblock copolyesters by ring-opening polymerization (ROP) of L-lactide in solution initiated by a telechelic D-glucose-based polyester macroinitiator, differing in the length of the polylactide blocks. Polymers characterization, thermal properties, degradability and nanoparticle formation by dialysis are discussed. The effect of the block lengths on size, ζ -potential values and physical

stability of the nanoparticles was evaluated. The experimental results were supported by a molecular dynamics simulation study.

Chapter 7 describes the synthesis of ABA triblock copolyesters by ring-opening polymerization (ROP) of L-lactide in solution initiated by a telechelic L-tartaric-based polyester macroinitiator, differing in the length of the polylactide blocks. Polymers characterization, thermal properties, degradability and nanoparticle formation by dialysis are discussed. The experimental results were supported by a molecular dynamics simulation study.

Chapter 8. The final section summarizes the general conclusions of the present research.

Chapter 1

Introduction

1.1. Bio-based and biodegradable polymers

Advances in science and technology have resulted in the rapid development of modern society, which is clearly unsustainable because of the strain it places on current resources. The energy and materials needed to sustain the present society come primarily from non-renewable fossil resources, which will be depleted at some point. Plastics are one example of an important commodity in the modern lifestyle. While plastics are undoubtedly superior materials in terms of their costs, processing and functional properties, they are currently produced from fossil resources and they are not readily assimilated by the various ecosystems.¹ The search for biodegradable plastics that are derived from renewable resources has been ongoing since the 1970s. Human activities have been altering the natural ecosystem by producing large quantities of wastes that are endangering the survival of all forms of life on earth. In addition to the increasing demand for energy, the rate of usage of materials in the modern lifestyle also has been increasing rapidly. Among the many different materials that mankind is currently dependent on, plastics are arguably the most important considering their widespread usage in food packaging, clothes, shelter, communication, transportation, construction, health care and leisure industry. Biodegradable plastics and bio-based plastics are often confused with each other as eco-friendly plastics, although they are not identical in terms of the original concept. Biodegradable plastics have been developed from the view point of biodegradability, whereas for bio-based plastics, biomass is used as the raw material instead of oil.² A sound classification that allows to distinguish among different types of bioplastics is shown in Figure 1.1.

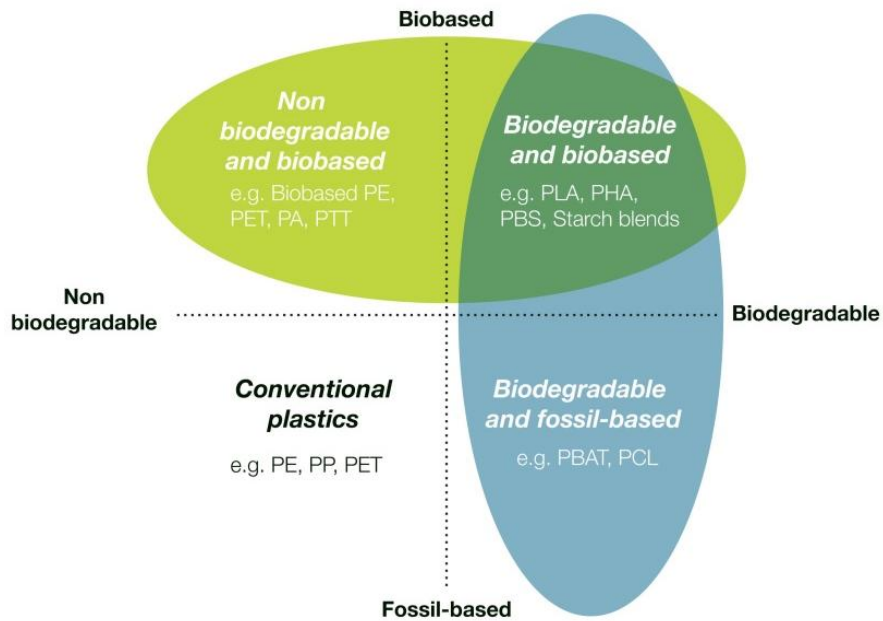


Figure 1.1. Classification of plastics regarding sustainability and biodegradability.

The term “bio-based polymers” applies not only to naturally occurring polymeric materials but also to those that have been polymerized from natural-occurring compound into high molecular weight materials by chemical and/or biological methods. Therefore, bio-based polymers include various synthetic polymers derived from renewable resources and CO₂, biopolymers, e.g., polynucleotides, polyamides, polysaccharides, polyoxoesters, polythioesters, polyanhydrides, polyisoprenoides and polyphenols, their derivatives, and their blends and composites. Accordingly, not all bio-based polymers are biodegradable. The recently discovered polythioesters^{3,4} are not biodegradable.⁵ Nevertheless, these types of bio-based polymers are important because one needs both biodegradable and non-biodegradable polymers that can be synthesized from renewable resources. The methods for the production of bio-based and biodegradable polymers can be classified into three main groups based on the processes involved and also the types of the polymers, *i.e.*, (i) chemical polymerization of monomers derived from biological processes, e.g., PLA, (ii) the direct biosynthesis of polymers by microorganisms, e.g., poly(hydroxyalkanoate) (PHA), and (iii) modification of natural polymers, e.g., cellulose acetate. Table 1.1. lists the commercially important bio-based and biodegradable polymers as well as information on past and current producers.

Table 1.1. Commercially important bio-based and biodegradable polymers for bulk applications and some of their sources.¹

Category	Bio-based polymer	Producer	Trade name
Bio-chemosynthetic polymers	Poly(lactic acid)	NatureWorks, U.S. Hycail, Netherlands Mitsui Chemicals, Japan Toyota, Japan	NatureWorks® Hycail HM; Hycail LM Lacea® U'z
	Poly(butylene succinate)	Mitsubishi Chemicals, Japan Showa High Polymer, Japan	GS Pla Bionolla
Biosynthetic polymers	Poly(hydroxyalkanoate)	Biomer, Germany Telles, USA Mitsubishi Gas, Japan PHB Industrial S/A, Brazil Metabolix, U.S. Kaneka, Japan	Biomer® Mirel™ Biogreen® Biocycle® Biopol®
Modified natural polymers	Starch polymers	Novamont, Italy Rodenburg, Netherlands BIOP, Germany Japan Corn Starch, Japan	Mater-Bi® Solanyl® BIOPar® Cornpol®
	Cellulose derivatives	Daicel Chemical Industries, Japan	Cellgreen

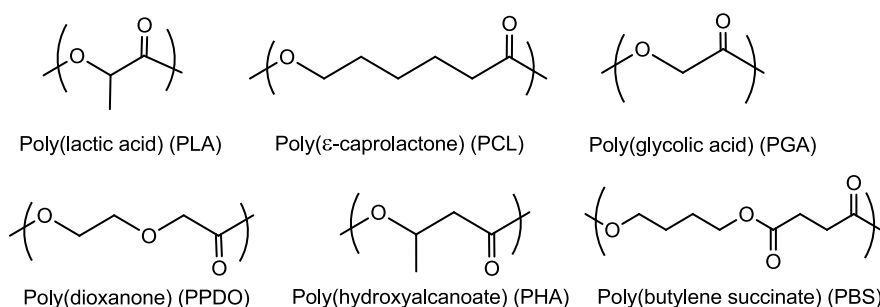
The main reason for the initial interest in biodegradable plastics is because non-biodegradable plastic packaging presents a major waste disposal problem. As a consequence, there has been much activity over the past 30 years in the development of biodegradable plastic packaging materials. Various biopolymers, biosynthetic polymers, chemosynthetic polymers, their blends and composites have been investigated for packaging applications. In order that biodegradable plastics are suitable for food packaging, several performance criteria need to be fulfilled such as suitable strength and flexibility, non-toxicity, impermeability to oxygen, good moisture resistance, stability during storage over a wide temperature range, and low cost for both the starting materials and the processing technology. As a result of these stringent criteria, many of the newly developed biodegradable plastics have not found widespread acceptance. Therefore, the focus has shifted towards the zero-emission concept largely because of global climate change due to increasing greenhouse gas emissions. This has given a very strong push for the development of biodegradable plastics that can be produced from renewable resources. Although many new approaches are being investigated for the production of bio-based and biodegradable plastics, it is important to keep in mind the stringent criteria that these materials must meet during their final applications.

2.2. Aliphatic polyesters

2.2.1. Biodegradable aliphatic polyesters

Aliphatic polyesters are a category of polymers that contains the ester functional group in their main chain repeating unit. It is an interesting class of materials that hold great promise in biomedical and pharmaceutical applications. Aliphatic polyesters are known to be the most promising category of biodegradable polymers and environmentally benign materials.⁶⁻⁸ Polyesters also have an advantage in their tunability; the crystallinity, thermal transitions, mechanical strength, and degradation can be altered based on molecular weight, composition (when used in copolymers), or addition of substituents to the polymer backbones.⁹⁻¹² The versatility provided by their tenability has enabled them to be used across a wide variety of biomedical applications such as drug delivery and tissue engineering.⁶

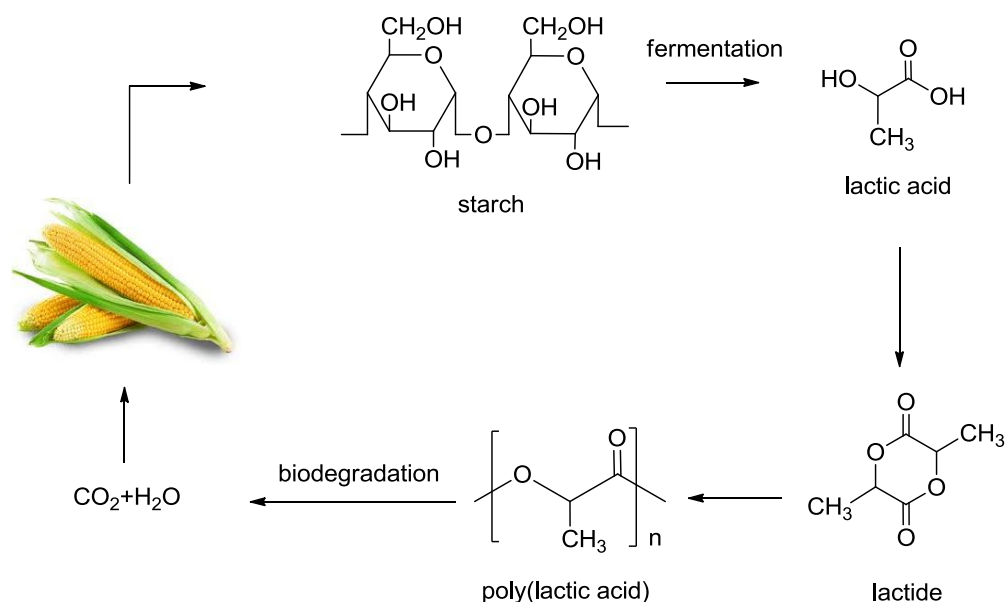
Depending on the structural composition, there are two types of polyester: poly(hydroxy acid)s, which are obtained by ROP of lactones or by polycondensation reactions of hydroxy acids, and poly(alkylene dicarboxylate)s, synthesized mostly by polycondensation reactions of diols with dicarboxylic acids or their esters. Monomers of this nature can be found within the carbohydrate framework; thus monosaccharides such as alditols, dianhydroalditols, lactones, aldonic acids, and aldaric acids with some hydroxyl groups protected, have been shown to be excellent candidates for the preparation of aliphatic polyesters.¹³ The most representative biodegradable aliphatic polyesters are depicted in Scheme 1.1.



Scheme 1.1. Biodegradable aliphatic polyesters.

Poly(lactic acid) (PLA) is renewable, biocompatible, biodegradable and it is one of the most widely used bioplastics (Scheme 1.2.). PLA is obtained either by ring-opening polymerization (ROP) of lactide or by direct polycondensation of lactic acid.¹⁴ The

molecular weight and yield of PLA depends on purity of the monomer used and the polymerization method used for its synthesis. Another important issue with PLA production via polycondensation reaction is the difficulty to remove water. Hence, the commercial production of PLA is mostly carried out by ROP of lactides.

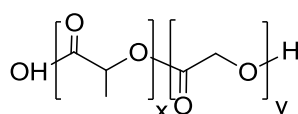


Scheme 1.2. The life cycle of PLA.

PLA's stereoregularity makes it a highly crystalline polymer.¹⁵ The chiral nature of lactic acid results in distinct forms of poly(lactide), namely poly(L-lactide), poly(D-lactide) and poly(DL-lactide) which are synthesized from the L-, D- and DL- lactic acid monomers, respectively, or from the corresponding L,L-lactide, D,D-lactide and D,L-lactide.¹⁶ Highly crystalline PLA can be obtained with low D content (<2%), while fully amorphous PLA can be obtained with high D content (>20%).^{15,17-19} Semicrystalline PLA are obtained with 2 to 20% of D content. Isotactic PLA, *i.e.* PLLA is a semicrystalline polymer and melts around 180 °C, the melting point can be increased to 230 °C by mixing equivalent proportions of L-PLA and D-PLA which will yield crystalline stereocomplex of PLA. The T_g of PLA can range from 50 to 65 °C depending on its molecular weight, polymer architecture and degree of crystallinity. The properties of PLA such as thermal stability and impact resistance are inferior to those of conventional polymers used for thermoplastic applications. To achieve this, copolymers of lactic acid and other monomers such as derivatives of styrene, acrylate, and poly(ethylene oxide) have been developed. Modification of PLA such as copolymerization with other monomers, and PLA composites are some approaches that are being used to improve the stiffness, permeability, crystallinity, and thermal stability of PLA.²⁰⁻²³

Poly(ϵ -caprolactone) (PCL) became commercially available following efforts to identify synthetic polymers that could be degraded by microorganisms.²⁴ PCL can be prepared by either ROP of ϵ -caprolactone using a variety of anionic, cationic and coordination catalysts or via free radical ROP of 2-methylene-1-3-dioxepane.²⁵ PCL is a hydrophobic, semicrystalline polymer; its crystallinity tends to decrease with increasing molecular weight. The good solubility of PCL, its low melting point and exceptional blend-compatibility has stimulated extensive research on its potential application in the biomedical field.^{8,26-28} Catalysts such as stannous octoate are used to catalyze the polymerization and low molecular weight alcohols can be used to control the molecular weight of the polymer.²⁹ PCL has a glass transition temperature (T_g) of -60 °C and melting point ranging between 59 and 64 °C, which enables easy processing at relatively low temperatures. In the 1970s it had already been recognized that PCL is particularly amenable to blending and polymer blends based on PCL were thus categorized with three types of compatibility; firstly exhibiting only a single T_g ; secondly as mechanically compatible, exhibiting the T_g values of each component but with superior mechanical properties and thirdly as incompatible, exhibiting the enhanced properties of phase-separated material.³⁰ Copolymers (block and random) of PCL can be formed using many monomers, e.g., ethyleneoxide, vinylchloride, ethylene glycol, diisocyanate, tetrahydrofuran, diglycolide, dilactide, methyl methacrylate, and vinyl acetate.⁸ PCLs can be biodegraded by outdoor living organisms (bacteria and fungi), but they are not biodegradable in animal and human bodies because of the lack of suitable enzymes.³¹

Poly(glycolic acid) (PGA) is a biocompatible aliphatic polyester with a T_g $35-40$ °C, T_m ranging from $224-227$ °C and excellent mechanical properties such as high tensile strength. PGA is widely used in surgical suture,³² artificial skin and vessel,³³ tissue engineering and drug delivery systems³⁴ due to its numerous unique characters including their biodegradable, biocompatible, and permeable properties.³⁵⁻³⁷ Because of its simple chemical structure and regularity, it occurs with different degree of crystallinity from completely amorphous to a maximum of 52% crystallinity.³² The crystallization temperature (T_c) of PGA is very high and its crystallization rate is also very fast even at high crystallization temperature. PGA is commonly used as a copolymer with PLA to form PLGA (Scheme 1.3.).



Scheme 1.3. Chemical structure of poly(lactic-co-glycolic acid).

PLGA is widely used in bone tissue engineering due to its suitable physico-chemical properties and biodegradability rate; however, compared to natural polymers such as collagen and chitosan which have numerous ionic molecular groups, the synthetic polymers have relatively few of these groups, making it very difficult to induce mineralization.^{39,40}

Poly(*p*-dioxanone) (PPDO), a typical aliphatic poly(ether-ester), is generally synthesized via ROP of 1,4-dioxan-2-one monomer. PPDO is a colorless bioresorbable synthetic polymer which undergoes hydrolytic degradation in vivo. PPDO is a semicrystalline polyester with a T_g at approximately -10 °C and T_m at around 110 °C. In early stages, PPDO was mainly used for sutures and it is the first clinically tested synthetic monofilament suture material.⁴¹ Compared with other aliphatic polyesters, such as poly(glycolide) (PGA) and poly(L-lactic acid) (PLLA), PPDO exhibits higher flexibility due to the presence of an ether bond and an additional $-CH_2-$ in its molecular structure. Furthermore, PPDO has proven to be tougher than poly(lactide) and high-density poly(ethylene). All the advantages mentioned above make PPDO a candidate not only for medical applications, but also for universal uses such as films, molded product laminates, non-woven materials, and coatings.^{42,43} The non-toxic and biodegradable nature of PPDO has led to the use of PPDO nanofiber scaffolds for antimicrobial drug delivery system for regenerative endodontics (Figure 1.2.).⁴⁴ PPDO plates and scaffolds are also being used for cosmetic procedures such as rhinoplasty and septal surgery where they guide cartilage regeneration.⁴⁵

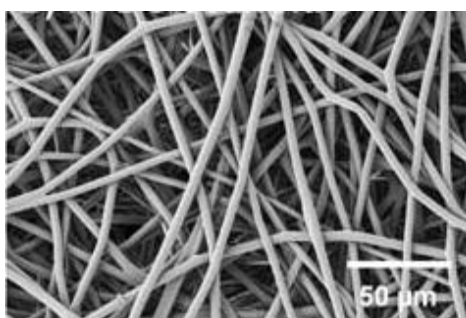
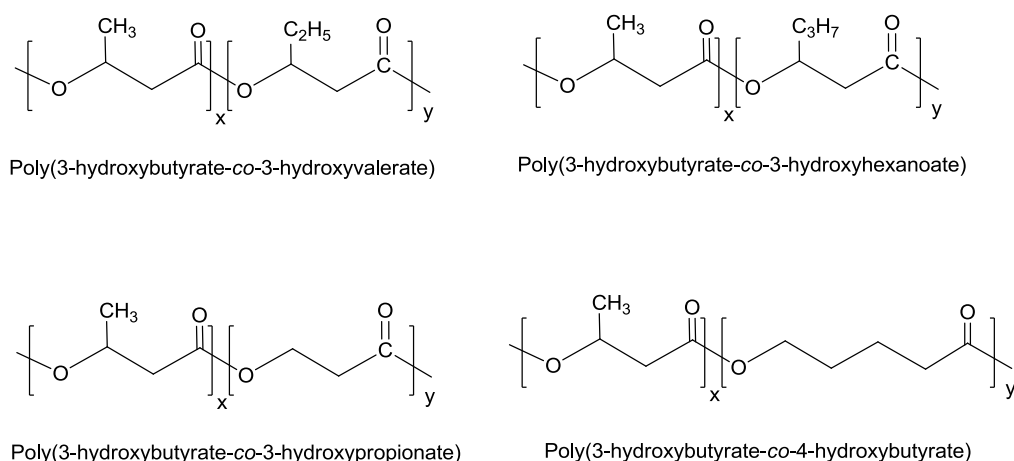


Figure 1.2. PPDO nanofibers.

As an aliphatic poly(ether-ester) (PPDO) exhibits excellent biodegradability and biocompatibility as well as good mechanical performance,⁴⁶⁻⁴⁸ moreover, it is worth to mention that PPDO can be called as ecofriendly polymer with excellent feedstock recyclability.^{49,50} Recently, the cost of its monomer, 1,4-dioxan-2-one decreased

significantly as the catalytic synthesis technology of PPDO from diethylene glycol had made breakthrough,⁵¹ which further reduced the cost of PPDO.

Poly(hydroxyalkanoate)s (PHA) are the family of biopolyesters which are totally synthesized by microorganisms from various substrates as carbon sources. Over 150 different types of PHAs, *i.e.* homopolymers and copolymers, can be synthesized by employing different bacterial species and growth conditions. Poly(hydroxybutyrate) (PHB) and poly(hydroxybutyrate-*co*-hydroxyvalerate) (PHBV) are the most well-known polymers of the poly(hydroxyalkanoate)s family. They are produced when bacteria are exposed to carbon source while all other necessary nutrients become limited.⁵² Poly(3-hydroxybutyrate-*co*-3-hydroxyvalerate), poly(3-hydroxybutyrate-*co*-3-hydroxyhexanoate), poly(3-hydroxybutyrate-*co*-3-hydroxypropionate), and poly(3-hydroxybutyrate-*co*-4-hydroxybutyrate) are four important copolymers produced by several bacterial strains (Scheme 1.4.).



Scheme 1.4. Chemical structure of poly(3-hydroxybutyrate) copolymers.

PHAs are very sensitive to processing conditions and exhibit a very narrow processing window. Under higher shears, they display rapid reduction in the molecular weight due to chain cleavage, and pose problems during most of the polymer processing operation. Impact strength increases with increasing hydroxyvalerate content, while T_m , T_g , crystallinity, water permeability and tensile strength decrease in the copolymers.^{6,53-63} The biodegradability of PHAs depends mainly on crystallinity and the polymer type; copolymers degrade faster than the homopolymers. The diversity of PHA's properties makes it suitable for wide range applications including packaging, fibers, and biomedical uses. Also, the PHA monomers can be used for biofuels, drugs or chiral intermediates.⁵⁵ Researchers are working on improve PHA's mechanical, biodegradation, and morphological properties to broaden its applicability in various industries. PCL⁵⁶, PLA⁵⁷ and starch⁵⁸ have been blended with PHBV for this purpose. Also, in another approach

various natural fibers such as wood fiber,⁵⁹ bamboo fiber,⁶⁰ jute,⁶¹ wheat straw,⁶² and coir fiber⁶³ have been used to fabricate lightweight and affordable composites.

1.2.2. Poly(butylene succinate) and its copolyesters

Poly(butylene succinate) (PBS) and its copolymers are a family of biodegradable polyesters synthesized from succinic acid and 1,4-butanediol, or other carboxylates and alkanediols. PBS is a white crystalline thermoplastic with T_m in the range of 90-120 °C and a low glass transition temperature (T_g) from -45 °C to -10 °C. It combines generally excellent mechanical properties and processing with excellent biodegradability.⁶⁴ The tensile yield strength of unoriented specimens reaches up to 30-35 MPa, which is comparable to that of polypropylene. PBS is flexible with Young's modulus in the range of 300–500 MPa, depending on the degree of crystallinity. PBS resins for extrusion, injection molding, thermoforming, fiber spinning and film blowing have been commercialized. They have been utilized to produce fast food packages, bottles, supermarket bags, flushable hygiene products, mulch film and compost bags, etc. PBS oligomers can also be used as building blocks for polyurethane elastomers as well. The synthesis of PBS can be separated into two steps: the first step is esterification of succinic acid with 1,4-butanediol (BD) or transesterification of dimethyl succinate with BD to obtain oligomers. The second step is polycondensation of the oligomers removing BD to form high-molecular weight PBS (see Scheme 1.5).⁶⁴

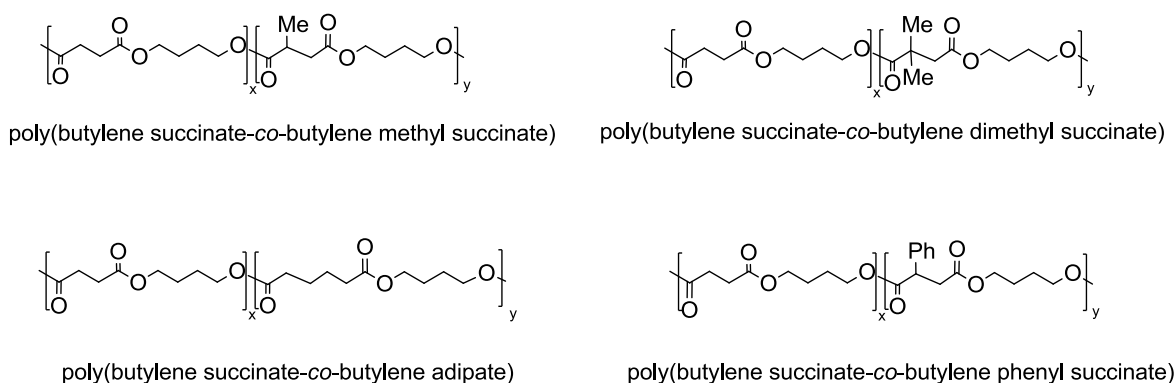


Scheme 1.5. Possible chemical synthesis of PBS by means of a two-stage process: esterification of succinic acid with 1,4-butanediol or transesterification of dimethyl succinate with 1,4-butanediol to obtain oligomers; oligomers are polycondensated to produce the final PBS. R: -H, -CH₃.

Different comonomeric units have been introduced along the PBS macromolecular chain such as dilinoleic acid,^{65,66} ω -pentadecalactone,⁶⁷ itaconic acid,⁶⁸ cyclic carbonates,^{69,70} and diethanolamine.⁷¹ Aliphatic/aromatic poly(butylene terephthalate/succinate) copolyesters have been also synthesized.⁷² On the other hand, by reactive blending, it has been possible to obtain multiblock copolymers with different block lengths by simply varying the mixing time. To this purpose, PBS has been

copolymerized with other aliphatic polyesters bearing ether and thioether-linkages, such as poly(triethylene succinate),⁷³ poly(diethylene glycol succinate),⁷⁴ and poly(butylene diglycolate).⁷⁵ PBS ionomers containing dimethyl 5-sodium sulfoisophthalate⁷⁶ or sulphonated succinate units⁷⁷ or ammonium side groups⁷⁸ have been synthesized and characterized, as well.

The biodegradation rate of PBS copolymers varies with their chemical structure, their physical properties in the solid state (such as crystallinity, orientation degree, specimen size) and the conditions of the biodegradation environment. The biodegradability may be tuned by copolymerization. For poly(butylene succinate) copolyesters containing 80% of butylene succinate as main comonomeric unit and the remaining 20% as different dicarboxylic acids, the biodegradation rate of the series changes as follows: poly(butylene succinate-co-butylene methyl succinate) \approx poly(butylene succinate-co-butylene dimethyl succinate) > poly(butylene succinate-co-butylene adipate) > poly(butylene succinate-co-butylene phenyl succinate) > poly(butylene succinate). The chemical formulae of these copolyesters are given in Scheme 1.6.



Scheme 1.6. Chemical structure of PBS copolyesters.

Compared to aliphatic copolyesters with the same comonomer content, PBS copolymerized with aromatic comonomers revealed slower biodegradation rates. However, PBS copolyesters with 20 %-mol of aromatic comonomers still showed high biodegradation rates in the activated sludge during the first three weeks. For aliphatic copolyesters, the biodegradation rate enhances with an increase of the comonomer content below 40 %-mol, resulting from the decreased degree of crystallinity.⁷⁹ For aliphatic-aromatic copolyesters, the biodegradation rate slows down with an increase in the aromatic content in the range of 10-70%-mol.⁸⁰ Consequently, the biodegradation

rate of PBS can be tailored via copolymerization with different types and contents of comonomer units to meet various requirements.

1.2.3. Biodegradable block copolyesters

Block copolymers are an example of amphiphiles that are capable of self-assembly into periodic geometry with long range order. These copolymers contain at least two distinct polymer chains, covalently bound at one point, which promote the miscibility of the two intrinsically dissimilar materials and phase separation is limited to the dimensions in the order of 100-400 Å. They are classified into several types according to what sequential arrangement of component segments is present (Figure 1.3.). The simplest block copolymer is an AB-type block copolymer, which is composed of one segment of A unit of homopolymer with B units of other homopolymer. In the second type of copolymer, both terminals of B units are connected at the terminal of A unit, and thus, it is referred to as an ABA type block copolymer. In the third type of block copolymers, A and B segments are connected many times and referred to as a multiblock copolymer. The fourth type of block copolymers is star block copolymers, where A unit has multi-arm functionality and copolymerizes with the blocks of B and shows a star-like shape.⁸¹

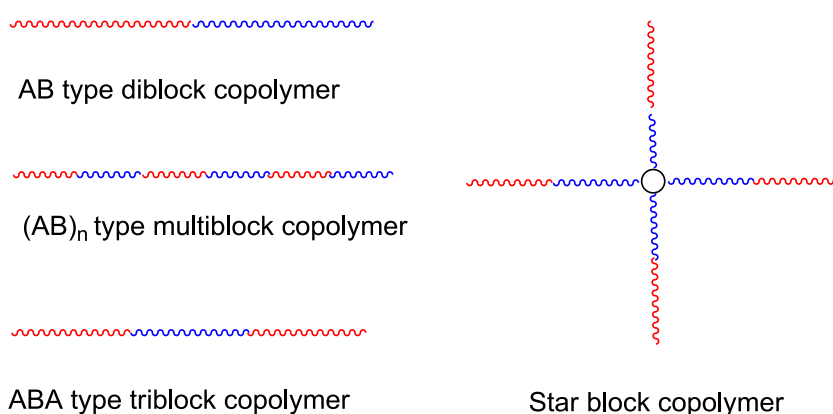


Figure 1.3. Types of block copolymers.

Many linear AB and ABA types of functional block copolymers have been synthesized via corresponding mono- and difunctional macroinitiators. For instance, amphiphilic poly(ethylene glycol-*b*-L-lactide) diblock copolymer, poly(L-lactide-*b*-ethylene glycol-*b*-L-lactide) triblock copolymer,^{82,83} and poly(L-lactide-*b*-trimethylene carbonate-*b*-

L-lactide),⁸⁴ have been successfully prepared, and they provided a broad spectrum of mechanical and biodegradation properties to meet the demands of different ultimate applications.

Recently, poly(ϵ -caprolactone)-*b*-poly(oxyethylene)-*b*-poly(ϵ -caprolactone) (PCL-*b*-POE-*b*-PCL) and poly(lactide)-*b*-poly(oxyethylene)-*b*-poly(lactide) (PLA-*b*-POE-*b*-PLA) were synthesized without any catalyst at 185 and 140 °C, respectively.⁸⁵ These triblock copolymers were used for the formation of Protein-C loaded nanospheres. It is suggested that hydrophilicity of copolymer increases with the increase of molar percentage of oxyethylene unit in the chain, and in general, PLA-*b*-POE-*b*-PLA is more hydrophilic than the PCL-*b*-POE-*b*-PCL one having the same molar composition.

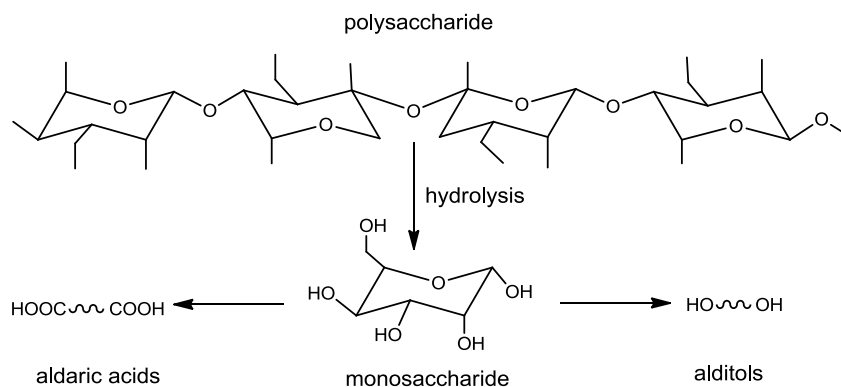
ABA triblock copolymer containing hydrophilic PEO blocks and hydrophobic PLA or PLGA were obtained by a bulk polymerization reaction using aluminium triisopropoxide as catalyst. After formation of the initiator complex between PEO and the catalyst, the PLA and PEO blocks were attached by ROP.⁸⁶ The degradation of ABA triblock copolymers was faster than degradation of its random copolymers.⁸⁷

The properties of PBS was modified by incorporation of poly(diethylene glycol succinate) segment by chain-extension reaction of dihydroxyl-terminated PBS and PDGS precursors using HDI as a chain extender to form PBS-*b*-PDGS multiblock copolymers.⁸⁸ The T_g and T_c increased, while T_m , crystallization rate and the crystallinity decreased with the increase in PDGS content of multiblock copolymers. In addition, the PBS-*b*-PDGS copolyesters showed excellent mechanical properties with higher strength and toughness than neat PBS, which can make the copolyesters suitable for a wide range of applications.

1.3. Carbohydrate-based polyesters

1.3.1. Acyclic carbohydrate-based monomers: resulting polyesters

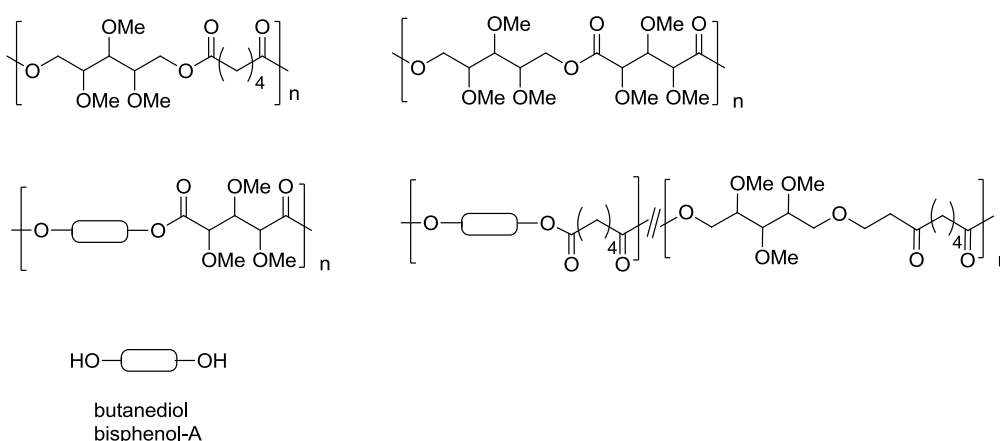
The carbohydrates are biological molecules consisting of carbon, hydrogen and oxygen atoms, usually with the empirical formula $C_x(H_2O)_y$. Carbohydrates are found in a wide variety of foods. The important sources are cereals (wheat, maize, rice), potatoes, sugarcane, fruits, table sugar (sucrose), bread, milk and etc. The term is most common in biochemistry, where it is a synonym of “saccharide”, a group that includes sugars, starch and cellulose. The saccharides are divided into monosaccharides, disaccharides, oligosaccharides and polysaccharides.



Scheme 1.7. Hydrolysis of carbohydrates leading to aldaric acids and alditols.

Readily available monosaccharides either produced by degrading polysaccharides or simply recovered from natural resources, are conveniently modified to afford aldaric acids, alditols and diaminoalditols suitable for polycondensation (Scheme 1.7.). A variety of polyamides,⁸⁹⁻⁹¹ polyesters,^{92,93} and polyesteramides^{94,95} derived from tetroses, pentoses and hexoses have been thus obtained and characterized, their structure examined, and some of their more relevant properties comparatively evaluated.

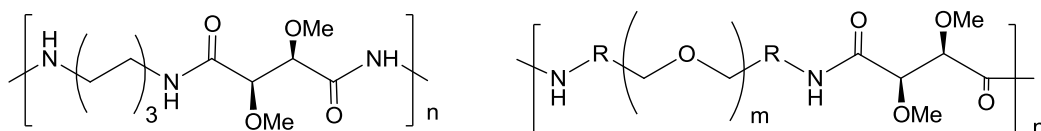
The carbohydrate-based linear polyesters of the poly(alkylene dicarboxylate) type were synthesized by polycondensation of 2,3,4-tri-*O*-methyl-L-arabinitol, 2,3,4-tri-*O*-methyl-xylitol, 2,3,4-tri-*O*-methyl-L-arabinaric acid and 2,3,4-tri-*O*-methyl-xylaric acid with 1,4-butanediol and adipic acid (Scheme 1.8.). These polymerizations were conducted in bulk or in solution, and copolyesters of the poly(alkylene-*co*-arylene dicarboxylate) type were also obtained using bisphenols as comonomers.⁹⁶



Scheme 1.8. Polyesters based on pentitols and pentaric acid.

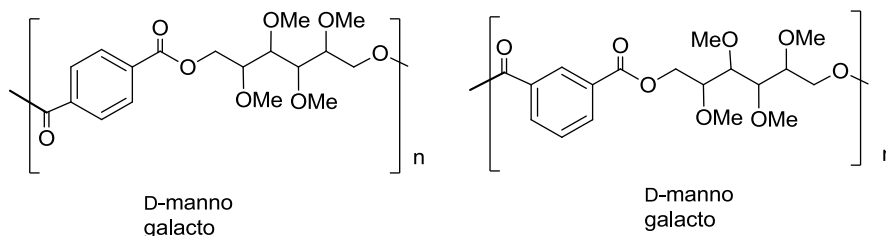
The effect of the stereochemical configuration of the tartaric unit on the crystal structure of poly(tartaramide)s deriving from 2,3-di-*O*-methyl-tartaric acid and hexamethylenediamine was studied. The purpose of the work was to elucidate how the replacement of the *L*-tartaric unit by its antipode may occur in the crystal without apparent distortion of the lattice.⁹⁷

The series of novel polyamides derived from *L* or *D*-tartaric acid and α,ω -diaminoethers were synthesized and characterized. Polycondensation in solution of the diaminoethers with di-*O*-methyl tartaric acid activated as pentachlorophenyl ester was used for the synthesis of these poly(ethertartaramide)s (Scheme 1.9.). These polyamides were highly hygroscopic and soluble in water. They were semicrystalline with T_m 's ranging from 50 to 190 °C, and thermally stable up to 250 °C. Chiro-optical properties were found to depend on the configuration of tartaric acid showing both high specific rotations and characteristic circular dichroism ellipticities.⁹⁸



Scheme 1.9. Poly(tartaramide) (left), poly(ether tartaramide) (right).

The synthesis and characterization of a new series of aromatic polyesters based on *D*-mannitol and galactitol were described (Scheme 1.10.). These polyesters were obtained by polycondensation reaction of the terephthaloyl chloride or isophthaloyl chloride and 2,3,4,5-tetra-*O*-methyl-*D*-mannitol or 2,3,4,5-tetra-*O*-methyl-galactitol in *o*-dichlorobenzene. They were soluble in chloroform, but insoluble in water and other polar oxygenated solvents. They showed a notable hygroscopicity, lower for those containing isophthalic units. DSC and X-ray diffraction studies showed that *D*-mannitol based polyesters were stiffer and less crystalline than those derived from galactitol, which presented a noticeably lower thermal stability.⁹⁹

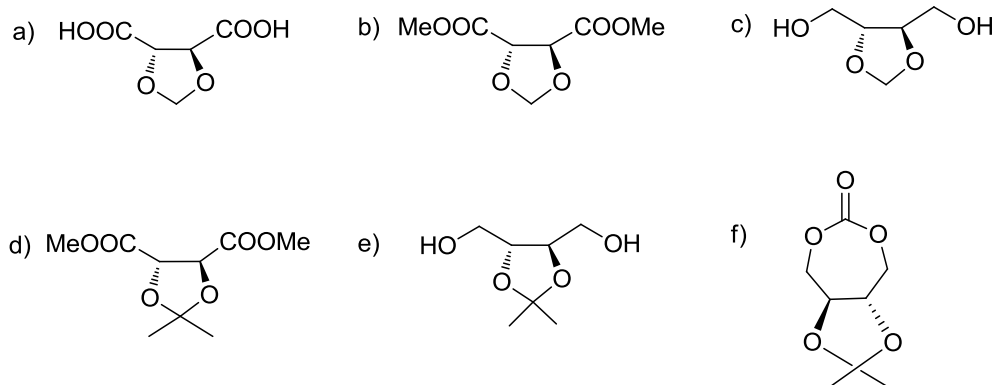


Scheme 1.10. Aromatic polyesters based on *D*-mannitol and galactitol.

1.3.2. Cyclic carbohydrate-based monomers: resulting polyesters

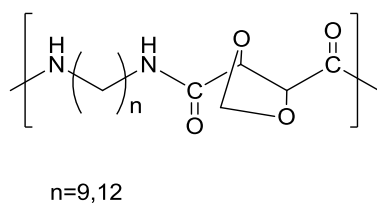
1.3.2.1. Cyclic acetalized aldaric acids and alditols

In most of cases, the two hydroxyl groups of tartaric acid are acetalized in order to avoid cross-linking reactions and the protected compound is used as either diacid or diol after reduction of the carboxylate groups (Scheme 1.11.).



Scheme 1.11. Chemical structure of cyclic acetalized monomers used in present thesis: 2,3-di-O-methylene-L-tartaric acid (a), dimethyl 2,3-di-O-methylene-L-tartrate (b), 2,3-di-O-methylene-L-threitol (c), dimethyl 2,3-di-O-isopropylidene-L-threarate (d), 2,3-di-O-isopropylidene-L-threitol (e), (5S,6S)-dimethyl 5,6-O-isopropylidene-1,3-dioxepin-2-one.

Stereoregular polyamides containing two chiral backbone carbons in the repeating unit were prepared by polycondensation of bis(pentachlorophenyl) 2,3-O-methylene-L-tartrate with 1,9 and 1,12-alcanediamines with the molecular weights which ranged between 6000 and 44000 (Scheme 1.12.). These poly(tartaramide)s were readily soluble in chloroform, displayed moderate optical activity in solution, and formed highly crystalline films.⁸⁹



Scheme 1.12. Chemical structure of poly(tartaramide)s.⁸⁹

Dimethyl of 2,3-di-O-methylene-L-tartaric acid and 2,3-di-O-methylene-L-threitol were also used as comonomer of dimethyl terephthalate and 1,6-hexanediol respectively in the melt polycondensation addressed to the preparation of PHT

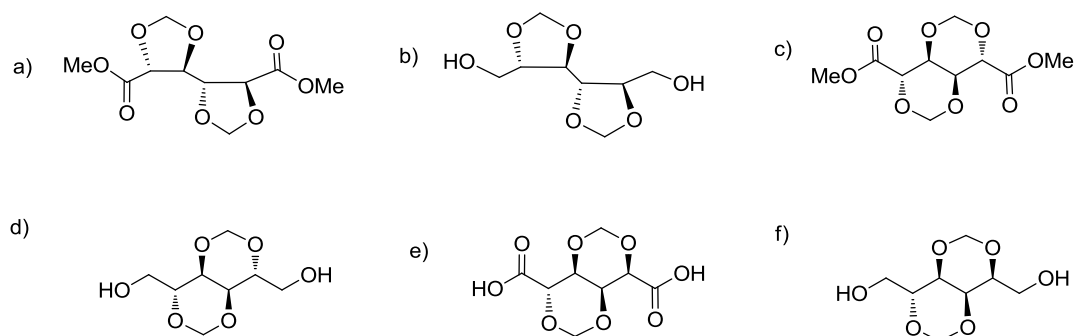
copolyesters with a higher sustainable content.¹⁰⁰ These copolyesters started to decompose above 300 °C. The T_g of the copolyesters oscillated between +9 and -9 °C with values steadily decreasing with increasing contents in Thx units. All the copolyesters as well as the homopolyester entirely made of tartrate units were semicrystalline with T_m falling from ~145 °C for PHT to ~70 °C for PHThx with intermediate values decreasing as the content in Thx increased. The PHT₇₀Thx₃₀ copolyester displayed significant hydrodegradability and also certain biodegradability when subjected to the action of porcine pancreas lipases.

Two different polyesters were prepared by polycondensation of dimethyl ester of 2,3-*O*-isopropylidene-L-tartaric acid¹⁰¹ with alkanediols, and the second one by reaction of 2,3-*O*-isopropylidene-L-threitol with diacid chlorides.¹⁰² Acid-catalyzed deprotection of the isopropylidene groups gave well-defined polyesters having pendant hydroxyl functional groups regularly distributed along the polymer chain.

Enantiomerically pure functional polycarbonate was synthesized from a cyclic carbonate monomer derived from naturally occurring L-tartaric acid.¹⁰³ The relationship between reaction time, monomer conversion, molecular weight, and weight distribution were investigated for Novozyme-435 catalyzing the polymerization. The deprotection of the ketal groups using trifluoroacetic acid offered polycarbonate with pendant hydroxy groups with minimal degradation in the polymer chain. The presence of hydroxy groups was expected to enhance the biodegradability and the hydrophilicity of the polymers.

1.3.2.2. Bicyclic acetalized aldaric acids and alditols

The carbohydrate-based diacetalized diols are bifunctional compounds suitable for the generation of linear polycondensates; the four secondary hydroxyl groups present in the genuine sugars are blocked as quite stable 5- or 6-membered cyclic acetals (Scheme 2.13.). Furthermore they all are highly stable to heat and capable to provide high stiffness to the polymer chain. *Galacto*, *manno* and *gluco* have been the stereochemical structures investigated so far.¹⁰⁴



Scheme 1.13. Chemical structure of dimethyl 2,3:4,5-di-*O*-methylene-galactarate (a); 2,3:4,5-di-*O*-methylene-galactitol (b); dimethyl 2,4:3,5-di-*O*-methylene-*D*-mannarate (c); 2,4:3,5-di-*O*-methylene-*D*-mannitol (d); dimethyl 2,4:3,5-di-*O*-methylene-*D*-glucarate (e); 2,4:3,5-di-*O*-methylene-*D*-glucitol (f).

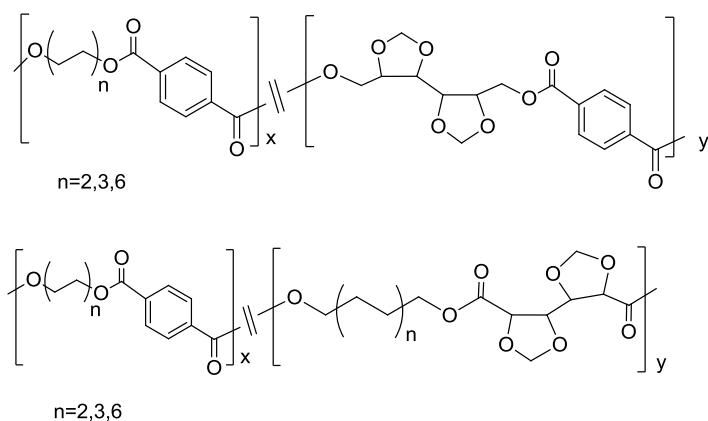
The two monomers with *galacto* configuration, 2,3:4,5-di-*O*-methylene-galactitol (Galx–diol) and dimethyl 2,3:4,5-di-*O*-methylene galactarate (Galx–diester), are prepared from commercially available galactaric acid.¹⁰⁵ The procedure consists essentially of the acetalization of the four secondary hydroxyl groups of methyl galactarate with paraformaldehyde followed by reduction of the carboxylate groups. A similar route is followed for the synthesis of the *gluco* monomers Glux–diol and Glux–diester, in this case using commercial *D*-gluconolactone as the starting material.¹⁰⁶ The synthesis of the *manno* diol Manx–diol is carried out from *D*-mannitol by acetalization of the previously prepared 1,6-di-*O*-benzoyl derivative and subsequent removal of the protecting group.¹⁰⁷ The synthesis of dimethyl mannarate (Manx–diester) in the amounts required for exploring its potential as a polycondensation monomer presented some difficulties that have prevented its inclusion in the studies carried out so far.

Whereas the Manx and Glux compounds share the same bicyclic structure made of two fused 1,3-dioxane rings that confers to the molecule a high stiffness, the diacetal arrangement adopted by the *galacto* configuration consists of two independent 1,3-dioxolane rings linked by a single C–C bond which allows a certain molecular flexibility. Whereas diols and diesters with *galacto* configuration are centrosymmetric and those with *manno* configuration have a C_2 axis, the *gluco* monomers lack any symmetry element. In the diacetalized compounds such differences are alleviated due to the high reactivity inherent to the primary character of the hydroxyl groups as well as to their farther distance from the cyclic structure.

Galx–diester was made to react in the melt with 1,*n*-alkanediols $\text{HO}(\text{CH}_2)_n\text{OH}$ containing even numbers of methylenes (*n* from 6 to 12) to produce linear polycyclic polyesters.¹⁰⁸ For comparative purposes a set of poly(alkylene adipate) polyesters (PE-*n*Ad) was also synthesized with molecular weights in the higher range using a similar procedure. The thermal stability of PE-*n*Galx was greater than that of PE-*n*Ad although it

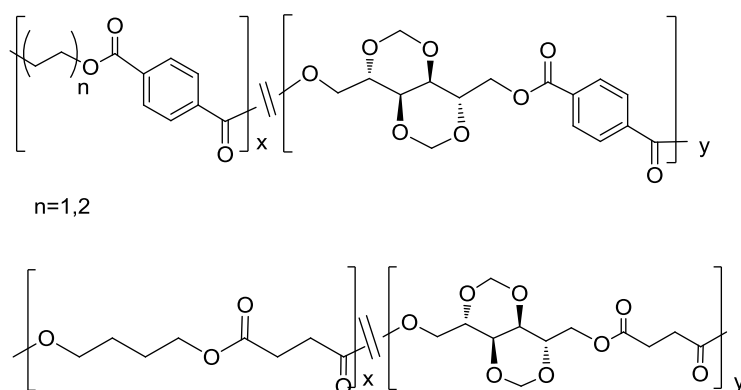
notably decayed as molecular weight decreased. The replacement of Ad by Galx in the polyesters caused increases in T_g of up to 70°C, and almost doubled the tensile mechanical parameters. All PE-nGalx were semicrystalline but only those made from 1,12-dodecanediol were able to crystallize from the melt with a crystallization rate that diminished as the molecular weight increased. In general, the galactarate containing polyesters displayed higher solubility and wettability than polyadipates, they hydrolyzed faster and exhibited comparable sensitivity to the action of lipases.

The copolyester series made from mixtures of Galx–diester and Galx–diol and DMT and 1,4-butanediol (BD), 1,6-hexanediol (HD) or 1,12-dodecanediol (DD) were described by Lavilla *et al.*¹⁰⁹ by melt polycondensation (Scheme 1.14.). Most of these copolyesters were able to crystallize from the melt with almost full recovery of the initial crystallinity and slightly diminished T_m 's. All PBT_xGalx_y displayed crystallinity upon precipitation from solution, and they retained the crystal structure of the PBT homopolymer. In all cases, the T_g steadily decreased as the terephthalate units were replaced by the galactarate ones. The thermal stability also decreased with the degree of replacement. Hydrolytic degradation and biodegradation essays performed on some of these polyesters demonstrated that hydrolysis was largely enhanced by copolymerization. Random copolyesters PB_xGalx_yT containing the Galx structure as a diol unit were semicrystalline only those containing up to 20% of Galx units were able to crystallize from the melt. It was found that, different from what happens with PBT_xGalx_y , the incorporation of the sugar as diol units in the PBT chain led to an increase in thermal stability. Furthermore, the presence of the Galx units in PB_xGalx_yT increased the T_g and the mechanical moduli, since in this case the substitution of the alkanediol by Galx–diol makes stiffer the polymer chain. Although PB_xGalx_yT copolyesters were not biodegradable in the presence of lipases, the presence of the Galx as diol units also enhanced the hydrodegradability of PBT.



Scheme 1.14. Chemical structure of Galx containing copolyesters.

Bio-based PET and PBT copolyesters were prepared when the bicyclic Manx-diol was made to react with mixtures of dimethyl terephthalate and ethylene glycol or 1,4-butanediol, respectively (Scheme 1.15).^{107,110} Lower temperatures and longer reaction times were used for copolyesters with higher contents in Manx units. PE_xManx_yT and PB_xManx_yT copolyesters containing up to 14% and 40%, respectively, of Manx units were semicrystalline, but only the latter were able to crystallize from the melt provided that their content in Manx did not go beyond 20%. Accordingly, thermal stability in the PB_xManx_yT series increased when BD was replaced by the Manx units, whereas the trend was opposite in the PE_xManx_yT series. It is worthy to mention however that in the latter the decrease in thermal stability is very slight with the decomposition temperature decreasing around 20 °C in the most detrimental case. In both series, the *T_g* and also the mechanical modulus steadily increased upon incorporation of Manx units. Neither PE_xManx_yT nor PB_xManx_yT was degraded by enzymes but both of them showed enhanced susceptibility to hydrolysis compared to their respective parent homopolyesters.

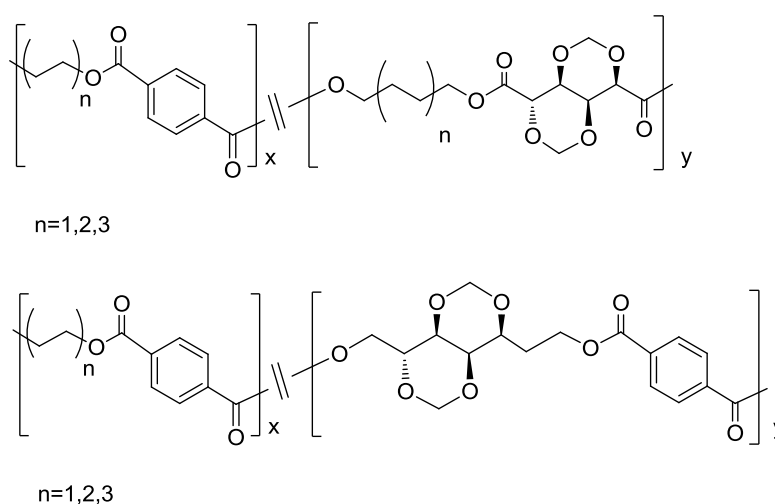


Scheme 1.15. Chemical structure of Manx containing copolyesters.

Recently, the properties of PBS were modified with Manx, as well.¹¹¹ These PB_xManx_yS copolyesters made from Manx, 1,4-butanediol and dimethyl succinate were semicrystalline with *T_m*'s lower than that of the parent homopolyester PBS. Since the thermal stability increases with the content in Manx, a wider range of temperatures between melting and decomposition exists in these copolyesters. Their *T_g* and, consequently, their elastic modulus and tensile strength increased with the content in Manx units. Hydrolytic degradation of Manx containing polyesters happened through hydrolysis of the main chain ester group without modification of the diacetal structure.

Degradation of both PManxS and the copolyester PB₇₀Manx₃₀S under physiological conditions was clearly favored by the action of enzymes.

Glux–diol was used as a comonomer of 1,6-hexanediol in the reaction with DMT in the melt to produce a set of random copolyesters (PH_xGlux_yT) with Glux contents ranging from 5 to 32%-mole (Scheme 1.16.).¹¹² Nevertheless PH_xGlux_yT copolyesters were thermally stable up to nearly 370 °C. All PH_xGlux_yT copolyesters were semicrystalline with *T_m*'s decreasing from 144 °C to 84 °C and only those containing 5 and 10% of Glux units were able to crystallize upon cooling from the melt. *T_g* notably increased with the incorporation of sugar diol going from 8 °C in PHT to nearly 60 °C in the copolyester containing 32%-mole of Glux. They showed not only an enhanced susceptibility to hydrolysis but also an appreciable biodegradability in the presence of lipases. Glux–diester was used in turn as a comonomer of DMT in the polycondensation with 1,6-hexanediol in the melt to produce random copolyesters PHT_xGlux_y with contents in glucarate units up to 50%.¹¹³ They start to decompose at a temperature well above 300 °C. Crystallinity of PHT is repressed by copolymerization so that copolyesters containing more than 20% of sugar-based units are essentially amorphous. PHT_xGlux_y displayed a *T_g* that increases monotonically with composition from 16 °C in PHT up to 73 °C in PHGlux. Compared with PHT, the copolyesters show an accentuated susceptibility to hydrolysis and are sensitive to the action of lipases upon incubation under physiological conditions. The degradability of PHT_xGlux_y increases with the content in Glux.



Scheme 1.16. Chemical structure of Glux containing copolyesters.

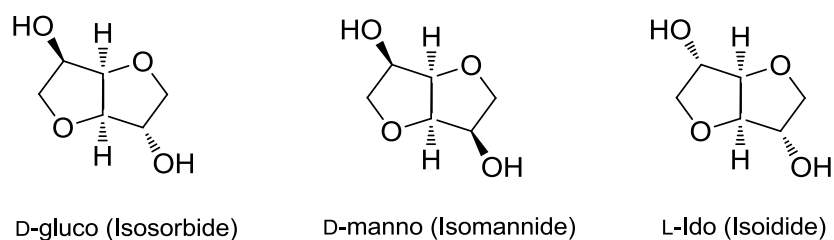
Glux–diol and Glux–diester have been later copolymerized with EG and DMT, respectively, by polycondensation in bulk to produce PET copolyesters PE_xGlux_yT and

PET_xGlux_y as well as their parent homopolyesters with 100% of substitution.¹⁰⁶ Thermal decomposition of the PE_xGlux_yT copolyesters started to be detectable above 350 °C following a single stage profile identical to PET. Conversely PET_xGlux_y copolyesters exhibited a more complex behavior involving a remarkable lower stability and a two-stage decomposition process at temperatures around 350 °C and 450 °C, respectively. Compared to PET, these copolyesters exhibited a higher hydrolysis rate and an appreciable susceptibility towards biodegradation. PE_xGlux_yT and PET_xGlux_y copolyesters containing up to ~10 to 15% of Glux units were semicrystalline, probably because at such low concentrations, the sugar units are selectively rejected from the crystalline phase. As expected, melting of these copolyesters occurred at temperatures notably lower than in PET and involved much smaller associated enthalpies and only those containing glucarate units were able to crystallize upon cooling from the melt but at much lower rates than PET. PE_xGlux_yT copolyesters T_g attained a value of 154 °C for the homopolyester, which is almost double the value of PET. In the PET_xGlux_y series, the increase in T_g was rather less noticeable because the stiff aromatic ring is replaced in this case. According to such enhancement in T_g and their poor crystallinity, the stress-strain curves of PE_xGlux_yT copolyesters showed an increase in Young's modulus and also in the elongation to break with the Glux content with the consequent increase in toughness.

Finally, the two series of PBT copolyesters, PB_xGlux_yT and PBT_xGlux_y, with contents in Glux units up to 50%.¹¹⁴ In the PB_xGlux_yT series, the thermal stability was found to increase steadily with the replacement of the butylene units whereas PBT_xGlux_y copolyesters showed a complex decomposition behavior at heating that takes place in two well differentiated stages with maximum decomposition rates at the proximities of 350 and 400 °C. The Glux-containing copolyesters displayed higher sensitivity to hydrolysis than PBT, in particular those containing glucarate units which are additionally distinguished by their sensitivity to the action of lipases. PBT copolyesters containing up to ~30% of Glux units were semicrystalline. It was found that the crystallization rate decreased with the insertion of the sugar units with a more pronounced depressing effect in the PB_xGlux_yT series. T_g 's of copolyesters was found to increase at a ratio of 3 and 1.5 °C per %-Glux point in the copolyesters made from Glux-diol and Glux-diester, respectively.

1.3.2.3. Isohexides

1,4:3,6-dianhydrohexitols, such as isosorbide, isomannide and isoidide (Scheme 1.17), have been used in the last thirty years for the synthesis of different condensation polymers.¹¹⁵⁻¹¹⁸



Scheme 1.17. Chemical structure of 1,4:3,6-dianhydrohexitols.

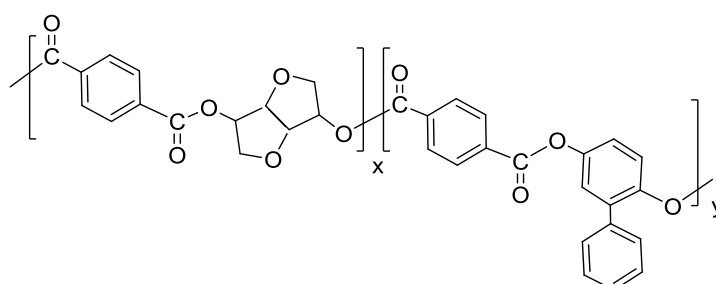
The isosorbide-based polymers are non-stereoregular, in contrast to those based on isomannide and isoidide, which are stereoregular. The most important features of these monomers are linked to their rigidity, chirality, and nontoxicity. Depending on the chirality, three isomers of the 1,4:3,6-dianhydrohexitols sugar diol exist, namely isosorbide, isomannide and isoidide (Scheme 1.17). The 1,4:3,6-dianhydrohexitols are composed of two *cis*-fused tetrahydrofuran rings, nearly planar and V-shaped with a 120° angle between rings. The hydroxyl groups are designated, respectively, as *endo* or *exo*. Isoidide has two *exo* hydroxyl groups, whereas for isomannide they are both *endo*, and for isosorbide there is one *exo* and one *endo* hydroxyl group. *Exo* and *endo* groups exhibit different reactivities since they are more or less accessible depending on the steric requirements of the studied reaction.^{119,120} Among the three isomers, isosorbide is the sole product produced at an industrial scale.

The synthesis of high molecular weight aromatic polyesters based on isosorbide, isomannide and isoidide by polycondensation in solution with terephthaloyl chloride and 2,5-diethoxyterephthaloyl chloride was reported.¹²¹ It was observed that the T_g of the 2,5-diethoxy substituted poly(terephthalate)s was around 70 °C lower than those of non-substituted ones, a reasonable result according to the free volume increase caused by the presence of the ethoxy side groups.

A diol-ether of isosorbide was made to react with terephthaloyl chloride to produce aromatic poly(ether-ester).¹²² It was observed that the reaction proceeds five times faster under microwave irradiation.

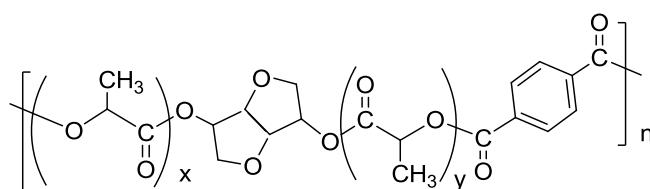
A serie of random PET terpolyesters containing variable amounts of 1,4-cyclohexanedimethanol and isosorbide were prepared.¹²³ The T_g of these copolyesters increased and the crystallization rate decreased with the total content on cyclic diol but these effects were more pronounced when isosorbide was the replacing comonomer. On the other hand, the use of the furanic monomer 5,5'-isopropylidene-bis(ethyl 2-furoate) together with isosorbide allowed the synthesis of new amorphous PET terpolyesters with T_g between 104 and 127 °C according to the terephthalate/furoate and ethylene glycol/isosorbide ratios with good thermal stability and enhanced solubility in common solvents.¹²⁴

The stiff nature of isosorbide allows its use as a monomer for the synthesis of a rigid polymer chain with liquid crystal properties and several examples are given in the literature. If isosorbide is partially replaced in PIsT by aromatic diols such as phenylhydroquinone, cholesteric thermotropic materials with good thermal stability can be obtained (Scheme 1.18).¹²⁵ Its replacement by monomers containing azobenzene mesogenic groups allowed the synthesis of liquid crystal copolyesters with high T_g 's and good thermal stability useful for the preparation of materials for nonlinear optical applications.



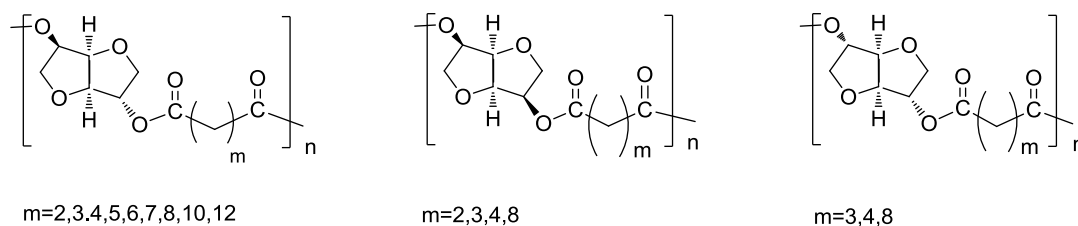
Scheme 1.18. Chemical structure of thermotropic liquid crystalline copolyesters.

Biodegradable isosorbide terephthalate copolyesters containing lactate units were prepared by polycondensation of the oligomer obtained from lactide and isosorbide with terephthaloyl chloride (Scheme 1.19.); the segmented lactate–terephthalate copolyesters had T_g 's within the 90-180 °C range decreasing linearly with the composition in lactate units.¹²⁶ Aliphatic–aromatic copolyesters obtained from mixtures of lactic and terephthalic acids with ethylene glycol and isosorbide are claimed to show excellent thermal and color properties; these copolyesters have been recently patented for use as films, sheets, and optical products.¹²⁷



Scheme 1.19. Chemical structure of copolyester made of isosorbide, L-lactide and terephthaloyl chloride.

Aliphatic polyesters were synthesized by polycondensation of the isosorbide, isomannide and isoidide with numerous aliphatic dicarboxylic acid chlorides according to Scheme 1.20.¹²⁸ The authors have tested the ability of these polymers to act as plasticizers for poly(vinyl chloride).¹²⁹ When the number of methylene groups, m , in the diacid chloride was >4 , only one T_g was observed that decreased with the proportion of polyester mixed with poly(vinyl chloride). Several studies were focused on the biodegradability of the same polyesters with methylene units ranging from 2 to 10.¹³⁰⁻¹³²



Scheme 1.20. Chemical structure of aliphatic polyesters prepared from 1,4:3,6-dianhydrohexitols with aliphatic dicarboxylic acid dichlorides.

The polymers with a methylene sequence >6 were semicrystalline. The effect of the diol configuration was considered and the polyester issued from isosorbide was found to degrade better while that based on isomannide was less degraded owing to the *endo* position of the hydroxyl limiting the approach of the enzymes. The polyesters based on isoidide were highly crystalline and thus were not degraded much despite the fact that the *exo* position of the hydroxyl should favor the approach of the enzymes.

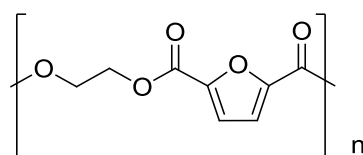
The renewable diacid monomers such as succinic and citric acid were associated with renewable diol monomers, such as isosorbide, 2,3-butanediol, 1,3-propanediol, and neopentylglycol. A classical melt polycondensation between diacids and diols was run at a maximum temperature of 250 °C during about 10 h. For such a long polymerization time, relatively low-molecular number average weights were obtained ~ 2000 , illustrating the difficulty to polymerize isosorbide-containing polycondensates. In order to obtain a $T_g > 45^\circ\text{C}$, a minimum isosorbide content of 65 mol% of the total diol amount was required. The advantage of aliphatic diacids compared to aromatic ones was a lower yellowing of

the coating, but the only possibility to obtain the required T_g was to introduce large amounts of isosorbide. Depending on the cross-linking agent, the polyester must be either fully hydroxyl or acid functionalized. For example, the linear OH-functional polyesters, based on isosorbide and succinic acid, were reacted with citric acid to obtain polyesters with carboxylic acid end groups.¹³⁴ Finally, hydroxyl and acid functionalized polyesters were crosslinked with different conventional cross-linking agents; the properties were found to compete with those of classical formulations in terms of resistance to solvent, impact, and hardness.

2.3.2.4. Other cyclic carbohydrate-based monomers: resulting polyesters

Furanic–aliphatic polyesters are one of the most actively investigated families of furan polymers, essentially due to the vast array of aliphatic monomers available to tailor these polyesters, and obviously also due to a wide variety of end properties that these monomers can impart to the ensuing polyesters.¹³⁵⁻¹³⁸ Entirely aromatic polyesters, the furanic–aromatic polyesters, were also pursued,¹³⁹⁻¹⁴¹ essentially aiming to prepare novel materials with enhanced thermal and mechanical properties and/or liquid crystalline character. In this field, the aromatic vanillic, syringic, salicylic and 4-hydroxybenzoic acids and 2,5-bis(hydroxymethyl) furan have attracted particular attention, owing to, among other features, their renewable origin.

The most spotlighted member of furandicarboxylic acid (FDCA) polyesters family is definitely the high performance poly(ethylene 2,5-furandicarboxylate) (PEF) (Scheme 1.21.). This homopolyester is semicrystalline with a T_g of around 75-80 °C and T_m at 210-215 °C. PEF was also shown to be thermally stable up to approximately 300 °C.



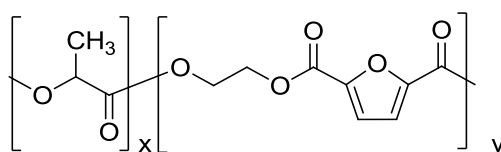
Scheme 1.21. Chemical structure of poly(ethylene 2,5-furandicarboxylate).

An extensive and systematic study of a series of homopolyesters, poly(1,3-propylene 2,5-furandicarboxylate), poly(1,4-butylene 2,5-furandicarboxylate), poly(1,6-hexylene 2,5-furandicarboxylate) and poly(1,8-octylene 2,5-furandicarboxylate)¹⁴² and poly(2,3-butylene 2,5-furandicarboxylate)¹⁴³ was published. Additionally, poly(1,9-nonylene 2,5-furandicarboxylate), poly(1,10-decylene 2,5-furandicarboxylate) and

poly(1,12-dodecylene 2,5-furandicarboxylate) were added to this list.¹⁴⁴ Results show a consistent decrease of T_g and T_m with increasing the number of methylene groups, except for the polyester prepared from 2,3-butanediol which has a higher T_g than parent poly(1,4-butylene 2,5-furandicarboxylate) or even poly(1,3-propylene 2,5-furandicarboxylate) and no melting transition due to its amorphous nature.

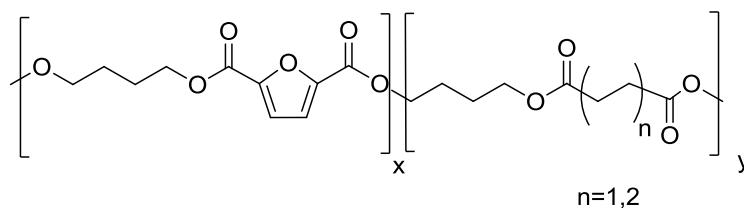
Various copolyesters of poly(ethylene 2,5-furandicarboxylate-*co*-1,4-butylene 2,5-furandicarboxylate) incorporating ethylene glycol and 1,4-butanediol in several amounts were prepared.¹⁴⁵ Results demonstrated that the composition of these copolyesters had little influence on the thermal stability of these materials. Indeed, T_g increased, with increasing the amount of ethylene units, according to an increased chain stiffness. T_m followed a more complex pattern, displaying higher melting events when either ethylene or butylene units were incorporated in lower amounts. This is in accordance with the disruption of polymer chain packaging interrupted by the random insertion of different alkylene units.

Promising poly(ethylene 2,5-furandicarboxylate)-*co*-poly(lactic acid) copolyesters were developed as well (Scheme 1.22).¹⁴⁶ These copolyesters were essentially stiff amorphous polymers possessing high T_g 's. Importantly, it was also shown that they have an improved degradability when compared with the PEF homopolymer counterpart. For example, the incorporation of only 8 mol% of lactyl units into the copolymer backbone was enough to improve substantially the degradability of this copolyester, which has still a very high T_d and high T_g values such as its PEF homologue.



Scheme 1.22. Chemical structure of poly(ethylene 2,5-furandicarboxylate)-*co*-poly(lactic acid) copolyesters.

Some studies in the field were performed aiming to produce completely renewable copolyesters, such as poly(butylene 2,5-furandicarboxylate-*co*-butylene succinate) and poly(butylene 2,5-furandicarboxylate-*co*-butylene adipate) copolyesters (Scheme 1.23).^{147,148} These copolymers were prepared from FDCA, succinic acid and/or adipic acid and 1,4-butanediol by a similar two-stage procedure, at high temperatures. Results showed that all copolymers had random microstructures but with a final well controlled composition, and high molecular weights.



Scheme 1.23. Chemical structure of poly(butylene 2,5-furandicarboxylate-co-butylene succinate) and poly(butylene 2,5-furandicarboxylate-co-butylene adipate) copolyesters.

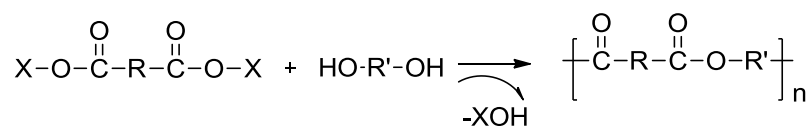
Poly(butylene 2,5-furandicarboxylate-co-succinate) copolyesters have been synthesized by ROP by high dilution condensation.¹⁴⁹ They all start to decompose above 300 °C and display melting enthalpy and temperatures that decrease with copolymerization, attaining minimum values when the comonomer contents are approximate to balance. On the contrary, the T_g increased almost linearly with the content of butylene furandicarboxylate units, covering the whole range of values between those of the two parent homopolyesters. Hydrolytic and enzymatic degradation studies revealed that the copolyesters became more degradable with increasing content of succinic units.

1.4. Synthetic methods

1.4.1. Melt polycondensation

Polycondensation is a process for the production of polymers from bifunctional and polyfunctional compounds, accompanied by the elimination of low-molecular weight by-products (water, alcohols and etc.) (Scheme 1.24.). Polyesters were historically the first family of synthetic condensation polymers.¹⁵⁰⁻¹⁵² Linear polyesters can typically be formed by a stepwise condensation reaction from difunctional monomers such as diols and diacids.¹⁵¹ Polycondensations under mild conditions are very important from an environmental technology viewpoint.¹⁵³ Recent concerns toward environmental problems prompted to explore an ideal polycondensation system taking low temperature, avoiding organic solvent, atomic economy and lack of catalyst toxicity. Polycondensation or step-growth polymerization processes are difficult to design. The polymerization is usually carried out under conditions such that the reactions are reversible and thus equilibrium-limited. One of the most pressing problems for polycondensation polymer processes is the removal of a condensate byproduct of the reaction in order to shift the reaction equilibrium to higher molecular weights. Without such condensate removal the production of high molecular weight polymer is practically unfeasible. The removal of the

condensate, however, is difficult due to limited rates of diffusion of the condensate through the polymer and limited rates of interphase mass transfer.¹⁵⁴



X=H, alkyl, halogen, vinyl, etc.

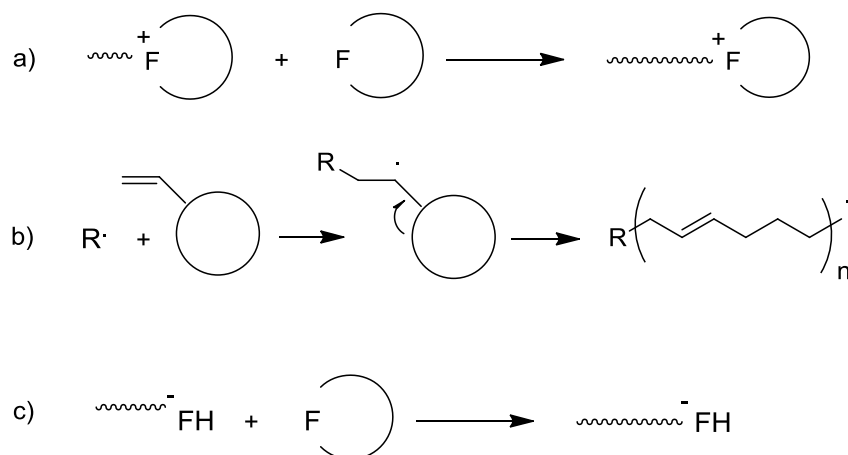
Scheme 1.24. Step-growth polycondensation of carboxylic acids or their ester derivatives and alcohols.

An understanding of the physical and kinetic processes occurring is important for developing and modifying polycondensation processes. By approaching these problems from the basics of fundamental modeling, it is possible to develop useful design tools for polycondensation processes. A general kinetic modeling technique¹⁵⁵ has been developed based on general kinetics mechanisms for polycondensation. This technique provides a unified approach to modeling polycondensation kinetics and can model a host of polycondensation polymers.

1.4.2. Ring-opening polymerization

ROP is a form of chain-growth polymerization, in which the terminal end of a polymer chain acts as a reactive center where further cyclic monomers can react by opening its ring system and form a longer polymer chain. The propagating center can be cationic, anionic or radical.

Most cationic ROP involves the formation and propagation of oxonium ion centers (Scheme 1.25a). Reaction involves the nucleophilic attack of monomer on the oxonium ion, where F represents a functional group such as O, NH, Si-O, C(=O)-O, and C(=O)-NH in ethers, amines, siloxanes, esters, and amides, respectively.¹⁵⁶



Scheme 1.25. Mechanism of cationic (a), radical (b) and anionic (c) ROP.

Via radical ROP it is possible to produce polymers with the same or lower density than the monomers. This is interesting for applications where it is desirable to maintain a constant volume during the polymerization such as tooth fillings, coatings and accurate molding of electrical and electronic components. Radical ROP offers novel routes to polyesters and polyketones particularly using vinyl substituted cyclic monomers (Scheme 1.25b). A less common group of monomers which undergo radical ROP are the bicyclobutanes, where by the bridge across the four-membered ring can be viewed as a concealed double bond.¹⁵⁷

The typical anionic ROP involves the formation and propagation of anionic centers (Scheme 1.26c). Reaction proceeds by nucleophilic attack of the propagating anion on monomer, where F represents an anionic propagating center, such as alkoxide or carboxylate, derived from the cyclic monomer. This is the mechanism usually used for the synthesis of polyesters by ROP.¹⁵⁶

ROP of lactone could be initiated by carboxylic acid. In the first step, a hydrogen proton of carboxylic acid transfer to the oxygen atom of the carbonyl group in lactone. Then, coordination of the alkyl–oxygen scission occurs by the nucleophilic attack of the carboxyl anion on the carbon atom of the alkyl-oxygen bond with part of a positive charge.¹⁵⁸

The presence of a heteroatom in the ring provides a site for nucleophilic or electrophilic attack by initiator species, resulting in initiation and subsequent propagation by ring opening. Thus, these type monomers are both kinetically and thermodynamically favored to be polymerized. In general, the polymerizability is higher for rings of 3, 4, and 7-11 members, lower for rings of 5 members, and much lower for rings of 6 members. However, there are exceptions. For instance, 6-membered rings with two or more

heteroatoms in the ring undergo polymerization. The 6-membered lactam undergoes polymerization as well.

Enthalpy-driven ROP of the cycles (5-8 atoms) show that the high levels of strain evident in their structures can be determined semiquantitatively in terms of the enthalpy released during ROP¹⁵⁹ and entropy-driven ROP stainless macrocyclic monomers and/or oligomers (>14 atoms) employs the ring-chain equilibria between macrocycles and their corresponding polymers and the associated increase of conformational freedom to achieve high molecular weight materials.^{160,161}

ROP is like a chain polymerization, consisting of a sequence of initiation, propagation, and termination. On the other hand, only monomer adds to the growing chains of propagation that is similar to step polymerization. However, unlike step polymerization, monomer and larger sized species do not generally react themselves or with each other in ROP. Many ROPs proceed as living polymerization. Block copolymer can be synthesized by this way. The ROP has the advantage over step polymerization for high molecular weight polymer. The molecular weight of ROP depends on conversion and the monomer/initiator ratio. On the other hand, the molecular weight of step polymerization depends on the conversion and stoichiometric balance which is more difficult to control as compared with ROP.

1.5. Nanoparticles for drug carriers

1.5.1. Biodegradable polymeric nanoparticles

Nanoparticles prepared from synthetic or natural polymers have applications in various technological and biomedical fields, because their chemical structures, surface functionalities, and particle size can be easily controlled. Nanoparticles can be defined as colloidal systems with a diameter smaller than 1000 nm.^{162,163} A colloidal delivery system is one of the most promising because it may reduce unwanted toxic side effects and improve the therapeutic effect. These delivery systems could be classified in monophasic dense nanoparticles, core-shell nanoparticles, hollow nanoparticle vesicles or nanocapsule polymersomes, and porous nanoparticles (Figure 1.4.).

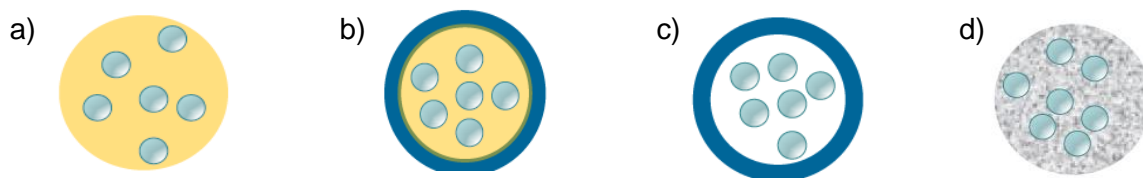


Figure 1.4. Schematic illustration of dense nanoparticle (a), core-shell nanoparticle (b), hollow nanoparticle vesicle (c), porous nanoparticle (d).

Considering the potential offered by polymer chemistry today, there are only a limited number of polymers which can be used as constituent of nanoparticles designed to deliver drugs *in vivo*.^{8,164,165} To explain this fact, one should consider that a suitable polymer needs to fulfil several requirements to be used in such an application. Firstly, it needs to be biodegradable or at least totally eliminated from the body in a short period of time allowing to repeat administration without any risk of uncontrolled accumulation. Secondly, it must be non toxic and non immunogenic. Thirdly, it should be formulated under the form of polymer nanoparticles with suitable properties regarding the drug delivery goal for which the nanoparticles are designed. At present, only a few of them are accepted by health authorities for parenteral administration. Others received agreements to be used in oral or topical formulations or they are used in the food industry. In general, self-assembled nanoparticles are composed of an inner hydrophobic core and an outer shell of hydrophilic groups. Hydrophobic blocks form the inner core of the structure, which act as a drug incorporation site, especially for hydrophobic drugs. Hydrophobic drugs can thus be easily entrapped within the inner core by hydrophobic interactions.

Several amphiphilic block and graft copolymers based on poly(amino acid) have been employed such as poly(L-glutamic acid),¹⁶⁶ poly(L-aspartic acid),¹⁶⁷ poly(L-lysine),¹⁶⁸ poly(L-arginine),¹⁶⁹ poly(L-asparagine),¹⁷⁰ and poly(γ -glutamic acid)^{171,172} as hydrophilic segments, and poly(β -benzyl-L-aspartate),¹⁷³ poly(γ -benzyl-L-glutamate),¹⁷⁴ and poly(L-histidine)¹⁷⁵ as hydrophobic segments. Amphiphilic copolymers based on poly(amino acid) form micelles through self-association in water. The formed micelles can act as hydrophobic drug carriers such as for the anticancer agent adriamycin. Amphiphilic block copolymers, such as poly(ethylene glycol)-*b*-poly(lactic acid) or poly(ethylene glycol)-*b*-poly(ϵ -caprolactone) are very attractive for use as drug delivery applications.^{176,177}

1.5.2. Techniques for nanoparticle formation

The selection of appropriate method for the preparation of nanoparticles depends on the physicochemical character of the polymer and the drug to be loaded. Emulsion-solvent evaporation method is one of the most frequently used methods for the preparation of nanoparticles (Figure 1.5). The first step requires emulsification of the polymer solution into an aqueous phase. During the second step polymer solvent is evaporated, inducing polymer precipitation as nanospheres. The nanoparticles are collected by ultracentrifugation and washed with distilled water to remove stabilizer residue or any free drug and lyophilized for storage.¹⁷⁸ For encapsulation of hydrophilic drug the double emulsion technique could be employed, which involves the addition of aqueous drug solutions to organic polymer solution under vigorous stirring to form w/o emulsions. This w/o emulsion is added into second aqueous phase with continuous stirring to form the w/o/w emulsion. The emulsion then subjected to solvent removal by evaporation and nanoparticles can be isolated by centrifugation at high speed.

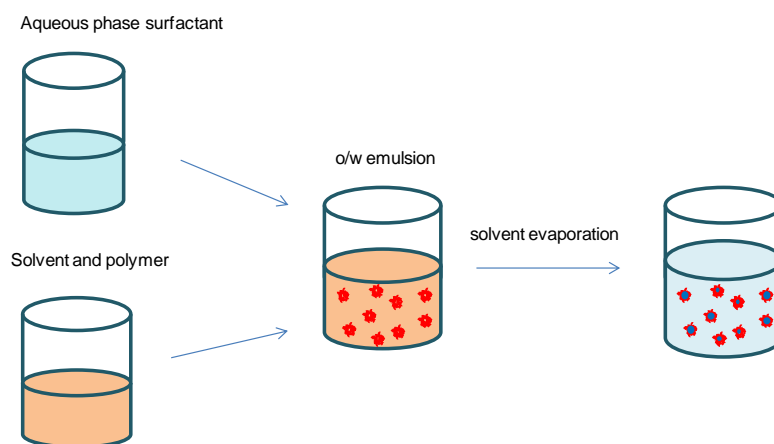


Figure 1.5. Nanoparticle formation by emulsion-solvent evaporation technique.

Salting out method is based on the separation of a water-miscible solvent from aqueous solution via a salting-out effect.¹⁷⁹ Polymer and drug are initially dissolved in a solvent which is subsequently emulsified into an aqueous gel containing the salting out agent (electrolytes, such as magnesium chloride and calcium chloride, or non-electrolytes such as sucrose) and a colloidal stabilizer. This oil/water emulsion is diluted with a sufficient volume of water or aqueous solution to enhance the diffusion of solvent into the aqueous phase, thus inducing the formation of nanospheres. The greatest

disadvantages are exclusive application to lipophilic drug and the extensive nanoparticles washing steps.

In emulsions-diffusion method, the encapsulating polymer is dissolved in a partially water-miscible solvent (such as propylene carbonate, benzyl alcohol), and saturated with water to ensure the initial thermodynamic equilibrium of both liquids. Subsequently, the polymer-water saturated solvent phase is emulsified in an aqueous solution containing stabilizer, leading to solvent diffusion to the external phase and the formation of nanospheres or nanocapsules, according to the oil-to-polymer ratio. Finally, the solvent is eliminated by evaporation or filtration, according to its boiling point. This technique presents several advantages, such as high encapsulation efficiencies (generally 70%), no need for homogenization, high batch-to-batch reproducibility, ease of scale up, simplicity, and narrow size distribution.

Solvent displacement/nanoprecipitation method involves the precipitation of a preformed polymer from an organic solution and the diffusion of the organic solvent in the aqueous medium in the presence or absence of surfactant. Polymers, drug, and lipophilic surfactant are dissolved in a semipolar water miscible solvent. The solution is then poured or injected into an aqueous solution containing stabilizer under magnetic stirring. Nanoparticles are formed instantaneously by the rapid solvent diffusion. The solvent is then removed from the suspensions under reduced pressure. The rates of addition of the organic phase into the aqueous phase affect the particles size. It was observed that a decrease in both particles size and drug entrapment occurs as the rate of mixing of the two phase increases.¹⁸⁰ Nanoprecipitation method is well suited for most of the poorly soluble drugs.

Dialysis method is a simple and effective preparation method for small and narrow size distributed nanoparticles using block, graft copolymers and amphiphilic materials (Figure 1.6.). Polymer should be dissolved in water-miscible solvent. The solution was introduced into dialysis tube with determined molecular cut-off and dialyzed against distilled water, replacing aqueous medium during several days. Then, the resultant solution was used for analysis. Although this approach is applicable to many solvent systems, the drug loading efficiency is usually low. While extensive dialysis can assist in the thorough purification of the product, it also can cause the release of the already encapsulated drug.

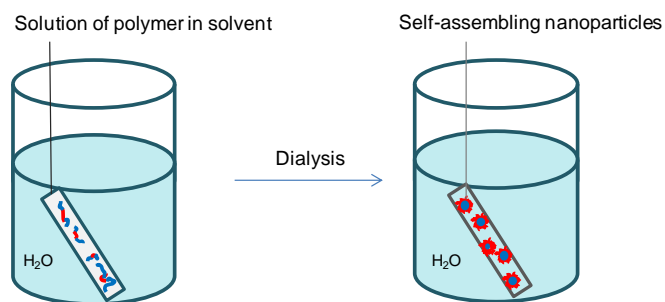


Figure 1.6. Nanoparticle formation by dialysis.

1.5.3. Drug encapsulation and release

The choice of drug delivery system determines the drug loading capacity, longevity of release, and the route best suited for administration. Furthermore, characteristics of the drug delivery system (size, surface charge and hydrophobicity, shape, flexibility, inclusion of targeting moieties) will affect performance and distribution in the body. Each drug delivery system has inherent advantages and limitations. It should be noted that drug release from any carrier is determined by a complex interaction between the drug properties, polymer characteristics, and environmental/in vivo conditions.

Careful polymer selection is essential to control the encapsulation efficiency, release rate, and duration of release. The diversity of polymer building blocks can further complicate formulation decisions. The most critical factor in polymer selection is considering the interaction of the drug and polymer. Polymer selection will determine the mechanism for drug release (bulk erosion, system degradation), and the choice of polymer properties (molecular weight, surface charge) will influence release rate and impact pharmacokinetics. Further fine-tuning of release from drug delivery systems can be achieved by using multiple types of polymers or including additives.

Independent of the drug-loading technique, the characterization of drug-loaded micelles is similar to other nanoparticles. Parameters of interest are the drug encapsulation efficiency (EE) and the drug-loading capacity (LC), where W_l is the weight of loaded drug, W_o the quantity of drug initially added, and W_n the weight of the nanoparticle.

$$EE\% = W_l/W_o \cdot 100\%$$

$$LC\% = W_l/W_n \cdot 100\%$$

For polymeric systems, “drug release” typically refers to how a drug molecule is transported from a starting position in a polymeric matrix to the polymer matrix’s outer surface and, finally, how it is released into the surrounding environment.^{181,182}

Drug molecules can be transported out of drug delivery systems via diffusion through water-filled pores. In addition to diffusion, drug molecules can be released from the polymer matrix by swelling, in which polymer hydration causes a volume increase of the polymeric structure and thus drug release. Another mechanism is by polymer hydrolytic degradation with release of its contents (erosion).

1.6. References

1. Sudesh, K.; Iwata, T. *Clean-Soil Air Water* **2008**, *36*, 433-442.
2. Iwata, T. *Angew. Chem. Int. Ed. Engl.* **2015**, *54*, 3210-3215.
3. Lutke-Eversloh, T.; Bergander, K.; Luftmann, H.; Steinbuchel, A. *Microbiology* **2001**, *147*, 11-19.
4. Lutke-Eversloh, T.; Fischer, A.; Remminghorst, U.; Kawada, J.; Marchessault, R.H.; Bogershausen, A.; Kalwei, M.; Eckert, H.; Reichelt, R.; Liu, S.J.; Steinbuchel, A.; Steinbuchel, A.T. *Nat. Mater.* **2002**, *1*, 236-240.
5. Steinbuchel, A. *Curr. Opin. Biotechnol.* **2005**, *16*, 607-613.
6. Amass, W.; Amass, A.; Tighe, B. *Polym. Int.* **1998**, *47*, 89-144.
7. Winzenburg, G.; Schmidt, C.; Fuchs, S.; Kissel, T. *Adv. Drug. Deliv. Rev.* **2004**, *56*, 1453-1466.
8. Okada, M. *Prog. Polym. Sci.* **2002**, *27*, 87-133.
9. Lutz, J.-F.; Meyer, T.Y.; Ouchi, M.; Sawamoto, M. *Sequence-Controlled Polymers: Synthesis, Self-Assembly, and Properties*, Washington, D.C. American Chemical Society, Washington D.C. **2014**.
10. Hakkarainen, M.; Höglund, A.; Odelius, K.; Albertsson, A.C. *J. Am. Chem. Soc.* **2007**, *129*, 6308-6312.
11. Xiong, X.B.; Falamarzian, A.; Garg, S.M.; Lavasanifar, A. *J. Control. Release* **2011**, *155*, 248-261.
12. Hao, J.; Rainbolt E.A.; Washington K.; Biewer M.C.; Stefan M.C. *Curr. Org. Chem.* **2013**, *17*, 930-942.
13. Galbis, J.A.; García-Martín M.G.; Violante de Paz M.; Galbis E. *Chem. Rev.* **2016**, *116*, 1600-1636.
14. Chen, G.Q. *Plastics from Bacteria: Natural Functions and Applications*. Heidelberg: Springer-Verlag, Berlin **2010**.
15. Madhavan Nampoothiri, K.; Nair, N.R.; John, R.P. *Bioresour. Technol.* **2010**, *101*, 8493-8501.
16. Huang, J.; Lisowski, M.S.; Runt, J.; Hall, E.S.; Kean, R.T.; Buehler, N.; Lin J.S. *Macromolecules* **1998**, *31*, 2593-2599.
17. Gupta, A.P.; Kumar, V. *Eur. Polym. J.* **2007**, *43*, 4053-4074.
18. Lunt, J.; Shafer, A.L. *J. Ind. Tex.* **2000**, *29*, 191-205.
19. Cicero, J.A.; Dorgan J.R. *J. Polym. Environ.* **2001**, *9*, 1-10.
20. Dorgan, J.R.; Lehermeier, H.; Mang, M. *J. Polym. Environ.* **2000**, *8*, 1-9.
21. Auras, R.; Harte, B.; Selke, S. *Macromol. Biosci.* **2004**, *4*, 835-864.
22. Urayama, H.; Moon, S.I.; Kimura, Y. *Macromol. Mater. Eng.* **2003**, *288*, 137-43.
23. Tsuji, H.; Ikada, Y. *Macromol. Chem. Phys.* **1996**, *197*, 3483-3499.
24. Dorgan, J.R.; Janzen, J.; Clayton, M.P.; Hait, S.B.; Knauss, D.M. *J. Rheol.* **2005**, *49*, 607-619.
25. Mark, F.; Bikales, N.; Overberger, C.; Menges, G.; Kroshwitz, J. *Encyclopedia of Polymer Science and Engineering*, John Wiley and Sons, New York **1985**.
26. Chasin, M.; Langer, R. *Biodegradable polymers as drug delivery systems*. Marcel Dekker, New York **1990**.
27. Chandra, R.; Rustgi, R. *Prog. Polym. Sci.* **1998**, *23*, 1273-335.
28. Nair, L.S.; Laurencin, C.T. *Prog. Polym. Sci.* **2007**, *32*, 762-798.
29. Storey, R.F.; Taylor, A.E. *Abstr. Pap. Am. Chem. Soc.* **1996**, *211*, 114-120.
30. Paul, D.; Newman, S. *Polymer Blends*, Academic Press, New York **1978**.
31. Vert, M. *J. Mater. Sci. Mater. Med.* **2009**, *20*, 437-446.
32. Singh, V.; Tiwari M. *Int. J. Polym. Sci.* **2010**, *278*, 1-23.
33. Fraunhofer, J.A.V.; Sichenab, W.J. *Biomaterials* **1992**, *13*, 715-720.

34. Athanasiou, K.A.; Niederauer, G.G.; Agrawal, C.M. *Biomaterials* **1996**, *17*, 93-102.
35. Wang, G.H.; Liu, S.J.; Ueng, S.W.; Chan, E.-C. *Int. J. Pharm.* **2004**, *273*, 203-212.
36. Ragauskas, A.J.; Williams, C.K.; Davison, B.H. et al. *Science* **2006**, *311*, 484-489.
37. Dechy-Cabaret, O.; Martin-Vaca, B.; Bourissou, D. *Chem. Rev.* **2004**, *104*, 6147-6176.
38. Mecking, S. *Angew. Chem.* **2004**, *43*, 1078-1085.
39. Kawasaki, K.; Aihara, M.; Honmo, J.; Sakurai, S.; Fujimaki, Y.; Sakamoto, K.; Fujimaki, E.; Wozney, J.M.; Yamaguchi, A. *Bone* **1998**, *23*, 223-231.
40. Meng, Z.X.; Li, H.F.; Sun, Z.Z.; Zheng, W.; Zheng, Y.F. *Mater. Sci. Eng. C Mater. Biol. Appl.* **2013**, *33*, 699-706.
41. Gesti, S.; Lotz, B.; Casas, M.T.; Aleman, C.; Puiggali, J. *Eur. Polym. J.* **2007**, *43*, 4662-4674.
42. Wang X.-L.; Yang, K.-K.; Wang, Y.-Z.; Wang D.-Y.; Yang, Z. *Acta Mater.* **2004**, *52*, 4899-4905.
43. Li, X.-Y.; Zhou, Q.; Wen, Z.-B.; Hui, Y.; Yang K.-K.; Wang, Y.-Z. *Polym. Degrad. Stab.* **2015**, *121*, 253-260.
44. Bottino, M.C.; Kamocki, K.; Yassen, G.H.; Platt, J.A.; Vail, M.M.; Ehrlich, Y.; Spolnik K.J.; Gregory, R.L. *J. Dent. Res.* **2013**, *92*, 963-969.
45. Rimmer, J.; Ferguson, L.M.; Saleh, H.A. *Arch. Facial Plast. Surg.* **2012**, *14*, 323-330.
46. Yang, K. K.; Wang, X. L.; Wang, Y. Z. *J. Macromol. Sci. Polym. Rev.* **2002**, *42*, 373-398.
47. Raquez, J. M.; Coulembier, O.; Duda, A.; Narayan, R.; Dubois, P. *Polimery* **2009**, *54*, 165-178.
48. Jin, C.; Liang, B.; Li, J.; Li, F. *J. Polym. Environ.* **2013**, *21*, 1088-1099.
49. Nishida, H.; Yamashita, M.; Hattori, N.; Endo, T.; Tokiwa, Y. *Polym. Degrad. Stab.* **2000**, *70*, 485-496.
50. Li, X. Y.; Zhou, Q.; Wen, Z. B.; Hui, Y.; Yang, K. K.; Wang, Y. Z. *Polym. Degrad. Stab.* **2015**, *121*, 253-260.
51. Wang, Y.Z.; Zhou, Q.; Zheng, C.Y.; Yang, K.K. *CN Patent* **2006**, *17*, 398, 52A.
52. Doi Y. *Microbial Polyesters*, Wiley-VCH, New York **1990**.
53. Shogren, R. *J. Environ. Polym. Degrad.* **1997**, *5*, 91-95.
54. Kotnis, M.A.; O'Brien, G.S.; Willett, J. *Environ. Polym. Degrad.* **1995**, *3*, 97-105.
55. Chen, G.Q. *Chem. Soc. Rev.* **2009**, *38*, 2434-2446.
56. Chun, Y.; Kim, W. *Polymer* **2000**, *41*, 2305-2308.
57. Nanda, M.R.; Misra, M.; Mohanty, A.K. *Macromol. Mater. Eng.* **2011**, *296*, 719-728.
58. Avella, M., Errico, M. *J. Appl. Polym. Sci.* **2000**, *77*, 232-236.
59. Singh, S.; Mohanty, A. *Compos. Sci. Technol.* **2007**, *67*, 1753-1763.
60. Jiang, L.; Huang, J.; Qian, J.; Chen, F.; Zhang, J.; Wolcott, M.P.; Zhu, Y. *J. Polym. Environ.* **2008**, *16*, 83-93.
61. Bledzki, A.; Jazzkiewicz, A. *Compos. Sci. Technol.* **2010**, *70*, 1687-1696.
62. Avella, M.; Rota, G.L.; Martuscelli, E.; Raimo, M.; Sadocco, P., Elegir, G.; Riva, R. *J. Mater. Sci.* **2000**, *35*, 829-836.
63. Javadi, A.; Srithep, Y.; Pilla, S.; Lee, J.; Gong, S.; Turng, L.S. *Mater. Sci. Eng. C* **2010**, *30*, 749-757.
64. Xu, J.; Guo B.-H. *Biotechnol. J.* **2010**, *5*, 1149-1163.
65. Tallawi, M.; Rai, R.; Gleixner, M.R.; Roerick, O.; Weyand, M.; Roether, J.A.; Schubert, D.W.; Kozłowska, A.; Fray, M.El.; Merle, B.; Goken, M.; Aifantis, K.; Boccacini, A.R.; *Macromol. Symp.* **2013**, *334*, 57-67.
66. Tallawi, M.; Zebrowski, D.C.; Rai, R.; Roether, J. A.; Schubert, D.W.; Fray, M.El.; Engel, F.B.; Aifantis, K.E.; Boccacini, A.R. *Tissue Eng. Part C Methods* **2015**, *21*, 585-596.
67. Liu, J.; Jiang, Z.; Zhang, S.; Saltzman, W.M. *Biomaterials* **2009**, *30*, 5707-5719.
68. Gowsika, J.; Nanthini, R. *J. Chem. Pharm. Res.* **2014**, *6*, 1452-1461.
69. Yang, J.; Tian, W.; Li, Q.; Li, Y.; Cao, A. *Biomacromolecules* **2004**, *5*, 2258-2268.
70. Yang, J.; Hao, Q.; Liu, X.; Ba, C.; Cao, A. *Biomacromolecules* **2004**, *5*, 209-218.
71. Wu, F.; Huang, C.L.; Zeng, J.B.; Li, S.L.; Wang, Y.Z. *Polymer* **2014**, *55*, 4358-4368.

72. Siracusa, V.; Lotti, N.; Munari, A.; Dalla Rosa, M. *Polym. Degrad. Stab.* **2015**, *119*, 35-45.
73. Gualandi, C.; Soccio, M.; Saino, E.; Focarete, M.L.; Lotti, N.; Munari, A.; Moroni, L.; Visai, L. *Soft Matter* **2012**, *8*, 5466-5476.
74. Gualandi, C.; Soccio, M.; Govoni, M.; Valente, S.; Lotti, N.; Munari, A.; Giordano, E.; Pasquinelli, G.; Focarete, M.L. *J. Bioact. Compat. Polym.* **2012**, *27*, 244-264.
75. Gigli, M.; Lotti, N.; Gazzano, M.; Finelli, L.; Munari, A. *Polym. Eng. Sci.* **2013**, *53*, 491-501.
76. Han, S.I.; Woong, S.W.; Kim, B.S.; Im, S.S. *Adv. Funct. Mater.* **2005**, *15*, 367-374.
77. Bautista, M.; Martínez de Ilarduya, A.; Alla, A.; Muñoz-Guerra, S. *Polymers* **2015**, *7*, 1232-1247.
78. Bautista, M.; Martínez de Ilarduya, A.; Alla, A.; Muñoz-Guerra, S. *Eur. Polym. J.* **2016**, *75*, 329-342.
79. Nikolic, M.S.; Djonlagic, J. *Polym. Degrad. Stab.* **2001**, *74*, 263-270.
80. Li, F.X.; Xu, X.J.; Yu, J.Y.; Cao, A. *Polym. Degrad. Stab.* **2007**, *92*, 1053-1060.
81. Kumar, N.; Ravikumar M.N.; Domb, A.J. *Adv. Drug Deliv. Rev.* **2001**, *53*, 23-44.
82. Kricheldorf, H. R.; Meier-Haack, J. *Makromol. Chem.* **1993**, *194*, 715-725.
83. Kim, K.-S.; Chung, S.; Chin, I.-J.; Kim, M. N.; Yoon, J. S. *J. Appl. Polym. Sci.* **1999**, *72*, 341-348.
84. Kim, J.-H.; Lee, J.-H. *Polym. J.* **2002**, *34*, 203-208.
85. Guerra, G.D.; Cerrai, P.; Tricoli, M.; Maltinti, S. *J. Mater. Sci. Mater. Med.* **2001**, *12*, 313-317.
86. Li, Y.X.; Kissel, T. *J. Control. Release* **1993**, *27*, 247-257.
87. Li, Y.X.; Volland, C.; Kissel, T. *J. Control. Release* **1994**, *32*, 121-128.
88. Lia, S.-L.; Wua, F.; Yanga, Y.; Wanga, Y.-Z.; Zengb, J.-B. *Polym. Adv. Technol.* **2015**, *26*, 1003-1013.
89. Rodríguez-Galán, A.; Bou, J.J.; Muñoz-Guerra, S. *J. Polym. Sci. Polym. Chem.* **1992**, *30*, 713-721.
90. Bou, J.J.; Rodríguez-Galán, A.; Muñoz-Guerra, S. *Macromolecules* **1993**, *26*, 5664-5670.
91. Regaño, C.; Martínez de Ilarduya, A.; Iribarren, I.; Rodríguez-Galán, A.; Galbis, J.A.; Muñoz-Guerra, S. *Macromolecules* **1996**, *29*, 8404-8412.
92. Zamora, F.; Hakkou, K.; Alla, A.; Espartero, J.L.; Muñoz-Guerra, S.; Galbis, J.A. *J. Polym. Sci. Polym. Chem.* **2005**, *43*, 6394-6410.
93. Zamora, F.; Hakkou, K.; Alla, A.; Marín-Bernabé, A.; de Paz, M.V.; Martínez de Ilarduya, A.; Muñoz-Guerra, S. *J. Polym. Sci. Polym. Chem.* **2008**, *46*, 5167-5179.
94. Alla, A.; Rodríguez-Galán, A.; Martínez de Ilarduya, A.; Muñoz-Guerra, S. *Polymer* **1997**, *38*, 4935-4944.
95. Villuendas, I.; Iribarren, I.; Muñoz-Guerra, S. *Macromolecules* **1999**, *32*, 8015-8023.
96. García-Martín, M.G.; Ruiz Perez, R.; Benito Hernández, E.; Galbis, J.A. *Carbohydr. Res.* **2001**, *333*, 95-103.
97. Iribarren, I.; Alemán, C.; Regaño, C.; Martínez de Ilarduya, A.; Bou, J.J.; Muñoz-Guerra, S. *Macromolecules* **1996**, *29*, 8413-8424.
98. Esquivel, D.; Bou, J.J.; Muñoz-Guerra, S. *Polymer* **2003**, *44*, 6169-6177.
99. Zamora, F.; Hakkou, K.; Alla, A.; Rivas, M.; Roffé, I.; Mancera, Muñoz-Guerra, S.; Galbis, J.A. *J. Polym. Sci. A: Polym. Chem.* **2005**, *43*, 4570-4574.
100. Japu, C.; Martínez de Ilarduya, A.; Alla, A.; Muñoz-Guerra, S. *Polymer* **2013**, *54*, 1573-1582.
101. Dhamaniya, S.; Jacob, J. *Polym. Bull.* **2012**, *68*, 1287-1304.
102. Dhamaniya, S.; Jacob, J. *Polymer* **2010**, *51*, 5392-5399.
103. Wu, R.; Al-Azemi, T.F.; Kirpal, S. *Biomacromolecules* **2008**, *9*, 2921-2928.
104. Muñoz-Guerra, S.; Lavilla, C.; Japu, C.; Martínez de Ilarduya, A. *Green Chem.* **2014**, *16*, 1716-1739.
105. Butler, K.; Lawrance, D. R.; Stacey, M. *J. Chem. Soc.* **1958**, 740-743.
106. Japu, C.; Martínez de Ilarduya, A.; Alla, A.; García-Martín, M.G.; Galbis, J.A.; Muñoz-Guerra, S. *Polym. Chem.* **2013**, *4*, 3524-3536.

107. Lavilla, C.; Martínez de Ilarduya, A.; Alla, A.; García-Martín, M.G.; Galbis, J.A.; Muñoz-Guerra, S. *Macromolecules* **2012**, *45*, 8257-8266.
108. Lavilla, C.; Alla, A.; Martínez de Ilarduya, A.; Benito, E.; García-Martín, M.G.; Galbis, J.A.; Muñoz-Guerra, S. *Biomacromolecules* **2011**, *12*, 2642-2652.
109. Lavilla, C.; Alla, A.; Martínez de Ilarduya, A.; Benito, E.; García-Martín, M.G.; Galbis, J.A.; Muñoz-Guerra, S. *J. Polym. Sci., Part A: Polym. Chem.* **2012**, *50*, 3393-3406. (b) C. Lavilla, C.; Alla, A.; Martínez de Ilarduya, A.; Benito, E.; García-Martín, M.G.; Galbis, J.A.; Muñoz-Guerra, S. *Polymer* **2012**, *53*, 3432-3445.
110. Lavilla, C.; Martínez de Ilarduya, A.; Alla, A.; Muñoz-Guerra, S. *Polym. Chem.* **2013**, *4*, 282-289.
111. Lavilla, C.; Martínez de Ilarduya, A.; Alla, A.; Muñoz-Guerra, S. *Biomacromolecules* **2013**, *14*, 781-793.
112. Japu, C.; Alla, A.; Martínez de Ilarduya, A.; García-Martín, M.G.; Benito, E.; Galbis, J.A.; Muñoz-Guerra, S. *Polym. Chem.* **2012**, *3*, 2092-2101.
113. Japu, C.; Martínez de Ilarduya, A.; Alla, A.; García-Martín, M.G.; Galbis, J.A.; Muñoz-Guerra, S. *Macromol. Chem. Phys.* **2014**, *215*, 2048-2059.
114. Japu, C.; Martínez de Ilarduya, A.; Alla, A.; García-Martín, M.G.; Galbis, J.A.; Muñoz-Guerra, S. *Polym. Chem.* **2014**, *5*, 3190-3202.
115. Kricheldorf, H.R. *J. Macromol. Sci., Rev. Macromol. Chem. Phys.* **1997**, *C37*, 599-631.
116. Fenouillot, F.; Rousseau, A.; Colomines, G.; Saint-Loup, R.; Pascault, J.P. *Prog. Polym. Sci.* **2010**, *35*, 578-622.
117. Van Es, D.S. *J. Renew. Mater.* **2013**, *1*, 61-72.
118. Wu, J.; Eduard, P.; Thiyagarajan, S.; van Haveren, J.; Koning, C.E.; Lutz, M.; Guerra, C.F. *ChemSusChem* **2011**, *4*, 599-603.
119. Matheson, N.K.; Angyal S.J. *J. Chem. Soc.* **1952**, 1133-1138.
120. Cope A.C.; Shen, T.Y. *J. Am. Chem. Soc.* **1956**, *78*, 3177-3182.
121. Storbeck, R.; Rehahn, M.; Ballauff, M. *Makromol. Chem.* **1993**, *194*, 53-64.
122. Chatti, S.; Bortoussi, M.; Bogdal, D.; Blais, J.C.; Loupy, A. *Eur. Polym. J.* **2006**, *42*, 410-424.
123. Quintana, R.; Martínez de Ilarduya, A.; Alla, A.; Muñoz-Guerra, S. *J. Polym. Sci. Part: A Polym. Chem.* **2011**, *49*, 2252-2260.
124. Abid, M.; Abid, S.; Gharbi, R.E. *J. Macromol. Sci., Pure Appl. Chem.* **2012**, *49*, 758-763.
125. Chavan, N.N. *Mater. Sci. Appl.* **2011**, *2*, 1520-1527.
126. Kricheldorf, H.R.; Weidner, S.M. *Macromol. Chem. Phys.* **2013**, *214*, 726-733.
127. Dong-Jin, K.; Jong-Ryang, K. *WO Pat* **2012**, 2012/134152.
128. Braun D, Bergmann M.. *J. Prakt. Chem.* **1992**, *334*, 298-310.
129. Okada, M.; Okada, Y.; Aoi, K. *J. Polym. Sci. Part A Polym. Chem.* **1995**, *33*, 2813-2820.
130. Okada, M.; Tsunoda, K.; Tachikawa, K.; Aoi, K. *J. Appl. Polym. Sci.* **2000**, *77*, 338-346.
131. Okada, M.; Aoi, K. *Curr. Trends Polym. Sci.* **2002**, *7*, 57-70.
132. Okada, M.; Okada, Y.; Tao, A.; Aoi, K. *J. Appl. Polym. Sci.* **1996**, *62*, 2257-2265.
133. Noordover, B.A.J.; van Staalduinen, V.G.; Duchateau, R.; Koning, C.E.; van Benthem, R.A.T.M.; Mak, M.; Heise, A.; Frissen, A.E.; van Haveren, J. *Biomacromolecules* **2006**, *7*, 3406-3416.
134. Noordover, B.A.J.; Duchateau, R.; van Benthem, R.A.T.M.; Ming, W.; Koning, C.E. *Biomacromolecules* **2007**, *8*, 3860-3870.
135. Jiang, M.; Liu, Q.; Zhang, Q.; Ye, C.; Zhou, G. *J. Polym. Sci., Part A: Polym. Chem.* **2012**, *50*, 1026-1036.
136. Knoop, R.J.I.; Vogelzang, W.; van Haveren, J.; van Es, D.S. *J. Polym. Sci., Part A: Polym. Chem.* **2013**, *51*, 4191-4199.
137. Burgess, S. K.; Leisen, J. E.; Kraftschik, B. E.; Mubarak, C. R.; Kriegel R. M.; Koros. W. J. *Macromolecules* **2014**, *47*, 1383-1391.
138. Cruz-Izquierdo, A.; van den Broek, L.A.M.; Serra, J.L.; Llama, M.J.; Boeriu, C.G. *Pure Appl. Chem.* **2015**, *87*, 59-69.

139. Gomes, M.; Gandini, A.; Silvestre, A.J.D.; Reis, B. *J. Polym. Sci., Part A: Polym. Chem.* **2011**, *49*, 3759-3768.
140. Gandini, A.; Coelho, D.; Gomes, M.; Reis, B.; Silvestre, A. *J. Mater. Chem.* **2009**, *19*, 8656-8664.
141. Moore, J.A.; Kelly, J.E. *Macromolecules* **1978**, *11*, 568-573.
142. Jiang, M.; Liu, Q.; Zhang, Q.; Ye, C.; Zhou, G. *J. Polym. Sci., Part A: Polym. Chem.* **2012**, *50*, 1026-1036.
143. Thiyagarajan, S.; Vogelzang, W.; Knoop, J.R.I.; Frissen, A.E.; van Haveren, J.; van Es, D.S. *Green Chem.* **2014**, *16*, 1957-1966.
144. Tsanaktis, V.; Papageorgiou, G.Z.; Bikiaris, D.N. *J. Polym. Sci., Part A: Polym. Chem.* **2015**, *53*, 2617-2632.
145. Ma, J.; Pang, Y.; Wang, M.; Xu, J.; Ma, H.; Nie, X. *J. Mater. Chem.* **2012**, *22*, 3457-3461.
146. Matos, M.; Sousa, A.F.; Fonseca, A.C.; Freire, C.S.R.; Coelho, J.F.J.; Silvestre, A.J.D. *Macromol. Chem. Phys.* **2014**, *215*, 2175-2184.
147. Wu, B.; Xu, Y.; Bu, Z.; Wu, L.; Li, B.-G.; Dubois, P. *Polymer* **2014**, *55*, 3648-3655.
148. Wu, L.; Mincheva, R.; Xu, Y.; Raquez, J.-M.; Dubois, P. *Biomacromolecules* **2012**, *13*, 2973-2981.
149. Morales-Huerta, J.C.; Ciulik, C.B.; Martínez de Ilarduya, A.; Muñoz-Guerra, S. *Polym. Chem.* **2017**, *8*, 748-760.
150. Edlund, U.; Albertsson A.-C. *Adv. Drug. Deliv. Rev.* **2003**, *55*, 585-609.
151. Carothers, W.H. *J. Am. Chem. Soc.* **1929**, *51*, 2548-2559.
152. Carothers, W.H.; Arvin, G.A. *J. Am. Chem. Soc.* **1929**, *51*, 2560-2570.
153. Shu, K.; Iwao, H.; Yoshinori, Y. *Bull. Chem. Soc. Jpn.* **1994**, *67*, 2342-2344.
154. Jacobsen, L.L.; Ray, W.H. *AIChE J.* **1992**, *38*, 911-925.
155. Jacobsen, L. L.; Ray, W.H. *J. Macromol. Sci., Rev. Macromol. Chem. Phys.* **1992**, *C32*, 407-519.
156. Su, W.-F. *Principles of Polymer Design and Synthesis, Lecture Notes in Chemistry* **82**, Springer-Verlag Berlin Heidelberg **2013**.
157. Nuyken, O.; Pask, S.D. *Polymers* **2013**, *5*, 361-403.
158. Jia, Z.; Huang, J. *J. Appl. Polym. Sci.* **2006**, *100*, 3713-3717.
159. Colquhoun, H.M.; Zhu Z.; Dudman, C.C. *Macromolecules* **2005**, *38*, 10421-10428.
160. Hodge, P. *Chem. Rev.* **2014**, *114*, 2278-2312.
161. Strandman, S.; Gautrot, J.E.; Zhu, X.X. *Polym.Chem.* **2011**, *2*, 791-799.
162. Soppimath, K.S.; Aminabhavi, T.M.; Kulkarni, A.R.; Rudzinski, W.E. *J. Control. Release* **2001**, *70*, 1-20.
163. Brigger, I.; Dubernet, C.; Couvreur, P. *Adv. Drug Deliv. Rev.* **2002**, *54*, 631-651.
164. Qiu, L.Y.; Bae, Y.H. *Pharm. Res.* **2006**, *23*, 1-30.
165. Slomkowski, S. *Acta Pol. Pharm.* **2006**, *63*, 351-358.
166. Holowka, E.P.; Pochan, D.J.; Deming, T.J. *J. Am. Chem. Soc.* **2005**, *127*, 12423-12428.
167. Arimura, H.; Ohya, Y.; Ouchi, T. *Biomacromolecules* **2005**, *6*, 720-725.
168. Wang, W.; Tetley, L.; Uchegbu, I.F. *Langmuir* **2000**, *16*, 7859-7866.
169. Holowka, E.P.; Sun, V.Z.; Kamei, D.T.; Deming, T.J. *Nat. Mater.* **2007**, *6*, 52-57.
170. Jeong, J.H.; Kang, H.S.; Yang, S.R.; Kim, J.D. *Polymer* **2003**, *44*, 583-591.
171. Liang, H.F.; Chen, S.C.; Chen, M.C.; Lee, P.W.; Chen, C.T.; Sung, H.W. *Bioconjugate Chem.* **2006**, *17*, 291-299.
172. Liang, H.F.; Yang, T.F.; Huang, C.T.; Chen, M.C.; Sung, H.W. *J. Control. Release* **2005**, *105*, 213-225.
173. Kataoka K, Matsumoto T, Yokoyama M, Okano T, Sakurai Y, Fukushima S, Okamoto, K.; Kwon, J.M. *J. Control. Release* **2000**, *64*, 143-153.
174. Lin, J.; Zhang, S.; Chen, T.; Lin, S.; Jin, H. *Int. J. Pharm.* **2007**, *336*, 49-57.
175. Lee, E.S.; Shin, H.J.; Na, K.; Bae, Y.H. *J. Control. Release* **2003**, *90*, 363-374.

176. Iijima, M.; Nagasaki, Y.; Okada, T.; Kato, M.; Kataoka, K. *Macromolecules* **1999**, *32*, 1140-1146.
177. Allen, C.; Han, J.; Yu, Y.; Maysinger, D.; Eisenberg, A. *J. Control. Release* **2000**, *63*, 275-286.
178. Song, C.X.; Labhasetwar, V.; Murphy, H.; Qu, X.; Humphrey, W.R.; Shebuski, R.J.; Levy, R.J. *J. Control. Release* **1997**, *43*, 197-212.
179. Catarina, P.R.; Ronald, J.N.; Antonio, J.R. *Nanomed.-Nanotechnol.* **2006**, *2*, 8-21.
180. Fessi, H.; Puisieux, F.; Devissaguet, J.-P.; Ammoury, N.; Benita, S. *Int. J. Pharm.* **1989**, *55*, R1-R4.
181. Langer, R. *Science* **1990**, *249*, 1527-1533.
182. Matalanis, A.; Jones, O.G.; McClements, D.J. *Food Hydrocolloid* **2011**, *25*, 1865-1880.

Chapter 2

Materials and methods

2.1. Materials

The reagents 1,4-butanediol (BD) (97%), 1,5-D-gluconolactone (99%), dimethyl succinate (DMS) (> 99%), dimethyl L-threarate (99 %), dimethyl 2,3-di-O-isopropylidene-L-tartrate (97%), dimethyl adipate (DMAdi) ($\geq 99\%$), dimethyl suberate (DMSub) (99%), diethyl sebacate (98%) (DESeb), 1,4:3,6-dianhydro-D-glucitol (Is) (98%), (3S,6S)-3,6-dimethyl-1,4-dioxane-2,5-dione (L-lactide, 98%), 1,5,7-triazabicyclo[4.4.0]dec-5-ene (TBD, 98%) lithium aluminium hydride (95%), paraformaldehyde (> 95%), sodium hydroxide (> 97%) were purchased from Sigma-Aldrich. Irganox 1010, Irgafos 126 antioxidants were a generous gift from BASF. Solvents used for purification, synthesis and characterization, such as chloroform, methanol, acetone, diethyl ether, ammonia (25%), sulphuric and dichloroacetic acids and sodium trifluoroacetate, all of either technical or high-purity grade, were purchased from Panreac and hexafluoroisopropanol was purchased from Apollo Scientific. All these products were used as received without further purification.

2.2. Synthesis of copolyesters

2.2.1. Melt polycondensation

Reactions were carried out in a three-necked, cylindrical bottom flask equipped with a mechanical stirrer, a nitrogen inlet and a vacuum distillation outlet. The reactants were stirred to a homogeneous mixture and DBTO (0.4-0.6 mol-% respect to the total of monomers) was added as catalyst. The transesterification step was performed under a nitrogen flow, and polycondensation under vacuum (0.03-0.06 mbar). The final reaction mixture was cooled to room temperature under a nitrogen flow to prevent degradation, the resulting solid mass was dissolved in chloroform, and the polymer precipitated with methanol, collected by filtration and dried under vacuum.

2.2.2. Ring-opening polymerization in solution

Telechelic homopolyesters were dissolved in 1M solution of L-lactide in dichloromethane. After dissolution of the prepolymer 5% mol TBD (relative to lactide) was added. The solution left stirred for 5 min under inert atmosphere and then precipitated in methanol, collected by filtration and dried under vacuum.

2.3. Methods

NMR-¹H and ¹³C NMR spectra were recorded on a Bruker AMX-300 spectrometer at 25.0 °C operating at 300.1 and 75.5 MHz, respectively. Polyesters were dissolved either in deuterated chloroform or in a mixture of deuterated chloroform/trifluoroacetic acid (TFA) (8/1), and spectra were internally referenced to tetramethylsilane (TMS). About 10 and 50 mg of sample dissolved in 1 mL of solvent were used for ¹H and ¹³C NMR, respectively. Sixty-four scans were acquired for ¹H and 1,000-10,000 for ¹³C with 32 and 64-K data points as well as relaxation delays of 1 and 2 s, respectively.

Intrinsic viscosities- Intrinsic viscosities of polyesters were measured in dichloroacetic acid at 25.00 ± 0.01 °C, using a capillary viscosimeter at concentrations ranging from 9 to 12 mg·mL⁻¹.

GPC- Gel permeation chromatograms were acquired at 35.0 °C with a Waters equipment provided with a refraction-index detector. The samples were chromatographed with 0.05 M sodium trifluoroacetate-hexafluoroisopropanol (NaTFA-HFIP) using a polystyrene-divinylbenzene packed linear column at a flow rate of 0.5 mL·min⁻¹. Chromatograms were calibrated against poly(methyl methacrylate) (PMMA) monodisperse standards.

MALDI-TOF- Matrix-assisted laser desorption ionization time-of-flight mass spectrometry (MALDI-TOF MS) was performed using a ABSciex 4800 plus MALDI TOF/TOF mass spectrometer. The spectrometer was equipped with a Nd:YAG laser. The detection was in the reflection mode and positive ionization was used.

TGA- Thermogravimetric analyses were performed under a nitrogen flow of 20 mL·min⁻¹ at a heating rate of 10 °C·min⁻¹, within a temperature range of 30 to 600 °C, using a Mettler Toledo TGA/DSC 1 thermobalance or a Perkin Elmer TGA 6 Thermogravimetric Analyzer under a nitrogen flow of 20 mL·min⁻¹ at a heating rate of 10 °C·min⁻¹ within a temperature range of 30 to 600 °C. Sample weights of about 10-15 mg were used in these experiments.

DSC- The thermal behavior of polyesters was examined by DSC using a Perkin Elmer DSC Pyris 1 and a Perkin Elmer DSC8000 apparatus. DSC data were obtained from 3 to 5 mg samples at heating/cooling rates of 10 °C·min⁻¹ under a nitrogen flow of 20 mL·min⁻¹. Indium and zinc were used as standards for temperature and enthalpy calibration. The glass-transition temperatures were determined by the tangent method

at a heating rate of $20\text{ }^{\circ}\text{C}\cdot\text{min}^{-1}$ from rapidly melt-quenched polymer samples. The treatment of samples for isothermal crystallization experiments was the following: the thermal history was removed by heating the sample up to $200\text{ }^{\circ}\text{C}$ and left at this temperature for 5 min, and then it was cooled at $20\text{ }^{\circ}\text{C}\cdot\text{min}^{-1}$ to the selected crystallization temperature, where it was left to crystallize until saturation.

XRD- X-ray diffraction patterns were recorded on the PANalytical X'Pert PRO MPD θ/θ diffractometer using the Cu $K\alpha$ radiation of wavelength 0.1542 nm from powdered samples coming from synthesis.

Mechanical tests- Films for mechanical properties with a thickness of $\sim 200\text{ }\mu\text{m}$ were prepared by hot-pressing. The tested samples were cut into strips with a width of 3 mm while the distance between testing marks was 10 mm. The tensile strength, elongation at break and Young's modulus were measured at a stretching rate of $30\text{ mm}\cdot\text{min}^{-1}$ on a Zwick 2.5/TN1S testing machine coupled with a compressor Dalbe DR 150. Each sample was measured five times.

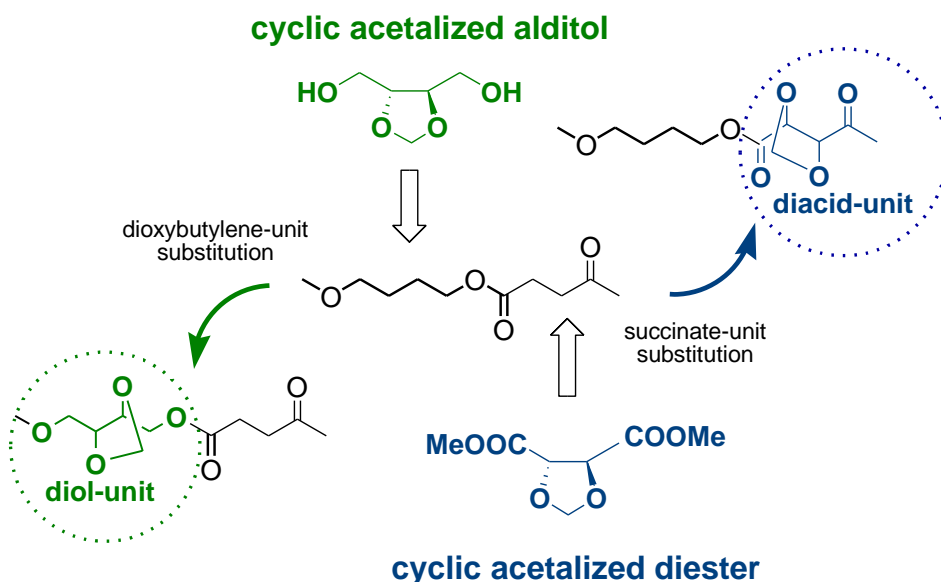
DLS- Dynamic light scattering for particle hydrodynamical size and ζ -potential measurements were performed with the Brookhaven NanoBrook, particle/protein size and zeta potential analyzer (Brookhaven Instruments Corporation, USA) with particles suspended in deionized water.

SEM- Scanning electron microscopy images were taken with a field-emission JEOL JSM-7001F instrument (JEOL, Japan) from platinum/palladium coated (PMLA/DOX conjugates) and uncoated samples.

Chapter 3

Modification of properties of poly(butylene succinate) by copolymerization with tartaric acid-based monomers

The two cyclic acetals, 2,3-di-O-methylene-L-threitol and dimethyl 2,3-di-O-methylene-L-threarate, were used for the synthesis of two series of PBS copolyesters differing in which unit, butylene or succinate, was replaced, in addition of the corresponding parent homopolyesters. Polycondensation reactions were carried out in the melt affording polymers with satisfactory molecular weights. Copolyesters were prepared with contents in tartaric acid-based units over the whole range of compositions and they all had a random chemical microstructure. The physical properties of the novel copolyesters varied widely depending not only on their composition but also on the type of unit that was replaced. They showed higher glass transition (T_g), lower melting temperatures (T_m), and lower crystallinity compared to the parent PBS homopolyester. Regarding mechanical properties, the presence of the stiff cyclic acetal units in the PBS chain caused an increase in the elongation at break and also a reduction in both elastic modulus and tensile strength of the polyester. Upon copolymerization the PBS notably increased its hydrolytic degradability and more slightly its susceptibility to be degraded by lipases.



This work was published as: E. Zakharova, C. Lavilla, A. Alla, A. Martínez de Ilarduya, S. Muñoz-Guerra, *Modification of properties of poly(butylene succinate) by copolymerization with tartaric acid-based monomers*, *Eur. Polym. J.* **2014**, 61, 263-273.

3.1. Introduction

Poly(butylene succinate) (PBS) is a partially bio-based polymer of current high interest because it exhibits a balanced performance in thermal and mechanical properties as well as a satisfactory thermoplastic processability.¹ The replacement of 1,4-butanediol by another diol of renewable origin that is able to increase the too low glass transition temperature of the polyester, would be highly desirable for increasing the sustainability of PBS and expanding its applications portfolio at the same time.

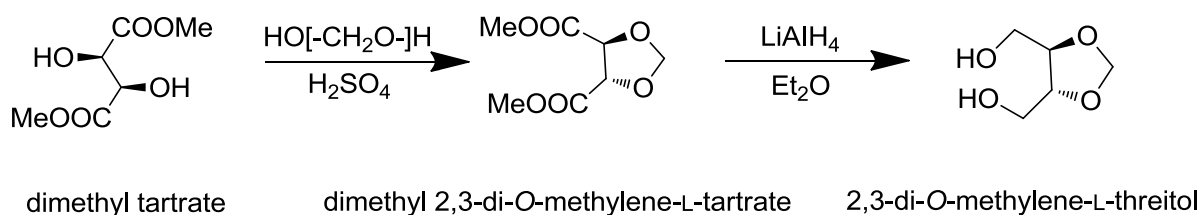
Utilization of carbohydrate derivatives as building blocks for polymer synthesis is currently receiving much attention not only due to their huge abundance and easy accessibility of resources but also because of the wide variety of structures that they can provide. L-Threonic acid ((2*R*,3*R*)-(+)-2,3-dihydroxybutanedioic acid), more commonly known as L-tartaric acid, is the aldaric acid derived from L-threose. It is a naturally-occurring compound frequently used as starting material for the production of an amazing array of products by well-developed synthetic procedures.² It has also attracted a great deal of interest as a substrate for the synthesis of fully or partially bio-based polycondensation polymers such as polyamides,^{3,4} polyesteramides,^{5,6} polyurethanes⁷ and polyesters.⁸ In most of cases, the two hydroxyl groups of tartaric acid are methylated in order to avoid cross-linking reactions and the protected compound is used as either diacid, or diol after reduction of the carboxylate groups. The outstanding interest in these monomers lies in their exceptional capability to rise the glass transition temperature of the polymers.⁹ L-Tartaric acid is able to provide after convenient acetalization both the cyclic diol and diacid counterparts required for linear polycondensation. The acetalized diester of L-tartaric acid is a readily accessible compound that can be obtained in high purity from the dimethyl ester of L-tartaric acid by acetalization with paraformaldehyde. The 2,3-di-*O*-methylene-L-threitol (Thx-diol) can be directly obtained from the dimethyl 2,3-di-*O*-methylene-L-tartrate (Thx-diester) by reduction with LiAlH₄.

The purpose of this work is to explore the use of Thx-diester and Thx-diol as comonomers of 1,4-butanediol, and dimethyl succinate respectively for the synthesis of PBS copolyesters with enhanced properties. The stiff nature of the cyclic acetalized compounds is expected to increase the glass transition temperature of PBS without too much detriment of other properties. Furthermore, given the bio-based nature of Thx compounds, the sustainability of PBS will be increased and its biodegradability very likely enhanced.

3.2. Experimental part

3.2.1. Monomer synthesis

The procedure applied to obtain 2,3-di-O-methylene-L-threitol (Thx-diol) was that recently described by Marín *et al.*¹⁰ To an ice bath cooled dispersion of LiAlH_4 (11 g) in dried diethyl ether (200 mL), a solution of dimethyl 2,3-di-O-methylene-L-tartrate (25 g) in the same solvent (130 mL) was added dropwise under energetic stirring under an inert atmosphere. The mixture was left under stirring overnight at room temperature and then the flask was reintroduced in the ice bath to add dropwise successively water (10 mL), 15% NaOH solution (10 mL) and water (60 mL). The mixture was left stirring for one hour further at room temperature, filtered and extensively washed with warm acetone. The filtrates were pooled, concentrated, and distilled under vacuum (100-110 °C, 0.01 mBar) to render the 2,3-di-O-methylene-L-threitol as a yellowish oil (9.5 g, 53% yield). Dimethyl 2,3-di-O-methylene-L-threarate (Thx-diester) was synthesized by reaction of dimethyl threarate (40 g) at 60 °C with paraformaldehyde (40 g) dissolved in 40 mL of 98%- H_2SO_4 . The reaction mixture was shaken for 6-8 hours at the same temperature and then extracted with chloroform. The extract was concentrated, washed extensively with water and ammonium hydroxide, distilled (84-86 °C, 0.05 mm) to give 16 g of dimethyl 2,3-di-O-methylene-L-threarate as a transparent liquid (40% yield). The NMR spectra of Thx compounds are provided in the Supporting Information (SI) of the Thesis.



Scheme 3.1. Synthesis of dimethyl 2,3-di-O-methylene-L-tartrate and 2,3-di-O-methylene-L-threitol.

3.2.2. Polymer synthesis

Copolyesters of PBS containing threitylene units (PB_xThx_yS) were synthesized by reaction of dimethyl succinate with mixtures of 1,4-butanediol and 2,3-di-O-methylene-L-threitol at different selected ratios. Analogously, the synthesis of copolyesters of PBS containing threarate units (PBS_xThx_y) was carried out by reacting 1,4-butanediol with mixtures of dimethyl succinate and dimethyl 2,3-di-O-methylene-L-threarate. PBS was obtained from 1,4-butanediol and dimethyl succinate and the homopolymers PThxS and PBThx from polycondensation of the bicomponent mixtures 2,3-di-O-methylene-L-threitol/dimethyl succinate and 1,4-butanediol/2,3-di-O-methylene-L-threarate, respectively. Since volatile diols were partially streamed off by the nitrogen flow and volatilized under vacuum, a 20%-mol excess of them respect to the diester monomer was used in all cases. The same synthesis protocol was applied in all cases. The specific experimental conditions used for the synthesis of homopolyesters and copolyesters are detailed in Table 3.1., and the NMR data ascertaining their constitution and purity are described below. A selection of illustrative NMR spectra is provided in the SI annex A.

Table 3.1. Reaction conditions selected for the preparation of PBS homopolyesters and copolyesters.

Polyester	First stage transesterification	Second stage polycondensation
PBS	160 °C, 3h	180 °C, 5h, 0.03-0.06 mm
PB ₉₅ Thx ₅ S	160 °C, 3h	180 °C, 5h, 0.03-0.06 mm
PB ₈₀ Thx ₂₀ S	160 °C, 3h	180 °C, 7h, 0.03-0.06 mm
PB ₆₀ Thx ₄₀ S	160 °C, 3h	180 °C, 7h, 0.03-0.06 mm
PB ₄₀ Thx ₆₀ S	140 °C, 6h	140 °C, 7h, 0.03-0.06 mm
PB ₂₀ Thx ₈₀ S	140 °C, 7h	140 °C, 7h, 0.03-0.06 mm
PThxS	140 °C, 7h	140 °C, 8h, 0.03-0.06 mm
PBS ₉₅ Thx ₅	160 °C, 3h	180 °C, 5h, 0.03-0.06 mm
PBS ₈₀ Thx ₂₀	160 °C, 3h	180 °C, 4h, 0.03-0.06 mm
PBS ₆₀ Thx ₄₀	160 °C, 5h; 180 °C, 1h	180 °C, 5h, 0.03-0.06 mm
PBS ₄₀ Thx ₆₀	160 °C, 4h; 170 °C, 3h	170 °C, 5h, 0.03-0.06 mm
PBS ₂₀ Thx ₈₀	160 °C, 7h	160 °C, 7h, 0.03-0.06 mm
PBThx	160 °C, 7h	160 °C, 8h, 0.03-0.06 mm

PBS homopolyester: ¹H NMR (300.1 MHz, CDCl₃/TFA), δ (ppm): 4.1 (t, 4H, OCH₂CH₂CH₂), 2.6 (s, 4H, COCH₂CH₂CO), 1.7 (t, 4H, OCH₂CH₂CH₂). ¹³C NMR (75.5 MHz, CDCl₃/TFA), δ (ppm): 172.2 (CO), 64.1, 29.0, 25.2.

PB_xTh_xyS copolyesters: ¹H NMR (300.1 MHz, CDCl₃/TFA), δ (ppm): 5.0 (m, y·2H, OCH₂O), 4.2 (m, y·4H, OCH₂CH), 4.1 (t, x·4H, OCH₂CH₂CH₂), 4.0 (m, y·2H, OCH₂CHCH), 2.7-2.6 (m, 4H, COCH₂CH₂CO), 1.9 (t, x·4H, OCH₂CH₂CH₂). ¹³C NMR (75.5 MHz, CDCl₃/TFA), δ (ppm): 171.8 (CO), 95.4, 76.6, 63.7, 62.1, 28.8, 25.2.

PBS_xTh_xy copolyesters: ¹H NMR (300.1 MHz, CDCl₃/TFA), δ (ppm): 5.2 (m, y·2H, OCH₂O), 4.7 (m, y·2H, COCHO), 4.2 (t, y·4H, OCH₂CH₂CH₂), 4.1 (m, x·4H, OCH₂CH₂CH₂), 2.6 (s, x·4H, COCH₂CH₂CO), 1.9-1.7 (m, 4H, OCH₂CH₂CH₂). ¹³C NMR (75.5 MHz, CDCl₃/TFA), δ (ppm): 172.2 (CO), 169.1 (CO), 97.5, 65.2, 64.1, 29.0, 25.2.

PTh_xS homopolymer: ¹H NMR (300.1 MHz, CDCl₃/TFA), δ (ppm): 5.0 (dd, 2H, OCH₂O), 4.2 (m, 4H, OCH₂CH), 4.0 (m, 2H, OCH₂CHCH), 2.7 (s, 4H, COCH₂CH₂CO). ¹³C NMR (75.5 MHz, CDCl₃/TFA), δ (ppm): 171.8 (CO), 95.4, 76.6, 62.1, 28.8.

PBTh_x homopolymer: ¹H NMR (300.1 MHz, CDCl₃/TFA), δ (ppm): 5.2 (dd, 2H, OCH₂O), 4.7 (m, 2H, COCHO), 4.2 (t, 4H, OCH₂CH₂CH₂), 1.8 (m, 4H, OCH₂CH₂CH₂). ¹³C NMR (75.5 MHz, CDCl₃/TFA), δ (ppm): 169.1 (CO), 97.5, 76.6, 64.1, 25.2.

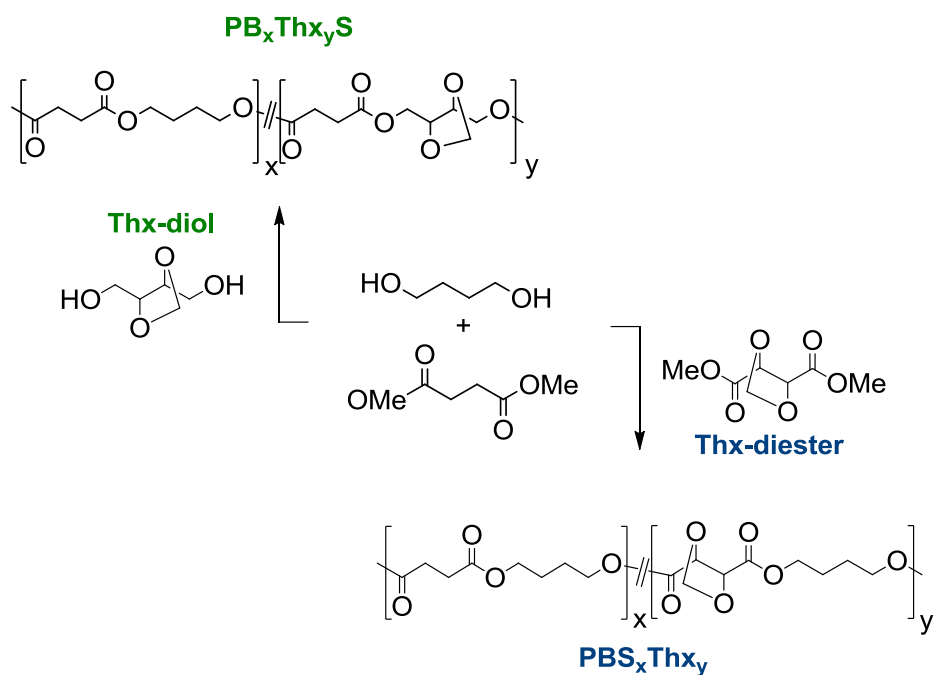
3.2.3. Hydrolytic degradation and biodegradation

Films for hydrolytic degradation and biodegradation studies were prepared with a thickness of ~200 μm by casting from chloroform solution at a polymer concentration of 100 g·L⁻¹. The films were cut into 10 mm diameter, 20–30 mg weight disks and dried under vacuum to constant weight. For hydrolytic degradation, samples were immersed in vials containing 10 mL of either citric acid buffer, pH 2.0 or sodium phosphate buffer, pH 7.4 at 37 °C. The enzymatic degradation was carried out at 37 °C in vials containing 10 mL of pH 7.4 buffered sodium phosphate solution with added lipase from porcine pancreas (10 mg). The buffered enzyme solution was replaced every 72 h to maintain the enzyme activity. In both cases, the disks were withdrawn from the incubation medium after scheduled periods of time, washed carefully with distilled water, dried to constant weight and analyzed by GPC chromatography and NMR spectroscopy. For the analysis of the products released to the incubation medium, samples were immersed in NMR tubes containing 1 mL of D₂O citric acid buffer pH 2.0 or sodium phosphate buffer, pH 7.4 and incubated at 37 °C for 42 days. The residual water after incubation was analyzed by NMR spectroscopy.

3.3. Results and discussion

3.3.1. Synthesis and chemical structure

The synthesis of the tartaric acid derived monomers, Thx-diol and Thx-diester, with the required purity and in satisfactory yield was accomplished without difficulty by following the methodology described in 3.2.1.section. The homopolyesters poly(2,3-di-O-methylene-L-threitylene succinate) (PThxS) and poly(butylene-2,3-di-O-methylene-L-threarate) (PBThx), as well as the copolyesters poly(butylene succinate-co-2,3-di-O-methylene-L-threitylene succinate) (PB_xThx_yS) and poly(butylene succinate-co-butylene-2,3-di-O-methylene-L-threarate) (PBS_xThx_y), were successfully synthesized using these monomers according to the reaction pathways outlined in Scheme 3.2. Reaction conditions regarding time and temperature had to be carefully selected in order to prevent decomposition of the relatively thermally unstable Thx compounds. The chemical constitution of the polyesters was definitely ascertained by both ¹H and ¹³C NMR, and their characterization data regarding composition, molecular weight and microstructure are collected in Table 3.2. Copolyester composition was determined by integration of the proton signals arising from the respective units. In the case of PB_xThx_yS, feed and copolyester compositions clearly diverged, indicating the occurrence of significant losses in Thx. Lower reactivity or/and higher volatility of the Thx-diol comonomer could be invoked to explain the observed differences. Conversely, compositions of PBS_xThx_y copolyesters, were fairly close to those used in their respective feeds with a slight increase in the Thx content. GPC analyses showed that polyesters were obtained with weight average molecular weights in the 50,000-20,000 g mol⁻¹ range with dispersity indexes oscillating between 1.6 and 3.0. In both series the general trend is that molecular weights decrease with the increasing content of the polyesters in Thx units. Intrinsic viscosities decreased from 0.8 to near 0.4 dL·g⁻¹ according to the trend displayed by molecular weights.



Scheme 3.2. Polycondensation reactions leading to PB_xTh_yS and PB_xTh_yS copolyesters, and also to their respective parent homopolyesters.

Table 3.2. Composition, molecular weights and microstructure of polyesters.

Polyester	Composition (mol/mol)		Molecular weight				Microstructure		
	Feed	Copolyester ^a	$[\eta]^b$ (dL·g ⁻¹)	M_n^c (g·mol ⁻¹)	M_w^c (g·mol ⁻¹)	\mathcal{D}^c	Average sequence length		R^d
	X_{BD} / X_{Thx}						n_B	n_T	
PBS	100/0	100/0	0.80	15400	34500	2.2	-	-	-
PB ₉₅ Th ₅ S	90/10	95.1/4.9	0.78	13800	30500	2.2	18.6	1	1.05
PB ₈₀ Th ₂₀ S	70/30	78.8/21.2	0.76	12600	27900	2.2	4.5	1.3	0.99
PB ₆₀ Th ₄₀ S	50/50	60.1/39.9	0.58	11900	29300	2.5	2.5	1.7	0.98
PB ₄₀ Th ₆₀ S	30/70	42.7/57.3	0.41	11400	26400	2.3	1.8	2.2	1.01
PB ₂₀ Th ₈₀ S	10/90	22.5/77.5	0.44	9900	27600	2.8	1.3	3.5	1.06
PThxS	0/100	0/100	0.41	8600	25500	3.0	-	-	-
	X_S / X_{Thx}						n_S	n_T	
PBS ₉₅ Th ₅	95/5	93.9/6.1	0.79	25300	48600	1.9	9.0	1.0	1.11
PBS ₈₀ Th ₂₀	80/20	77.9/22.1	0.73	20300	33100	1.6	4.5	1.4	0.95
PBS ₆₀ Th ₄₀	60/40	57.7/42.3	0.42	8500	20100	2.4	2.3	2.0	0.93
PBS ₄₀ Th ₆₀	40/60	36.5/63.5	0.37	8100	22200	2.7	1.6	2.2	1.05
PBS ₂₀ Th ₈₀	20/80	16.9/83.1	0.38	9600	26500	2.8	1.1	5.3	1.06
PBThx	0/100	0/100	0.43	13400	31700	2.4	-	-	-

^aMolar composition determined by integration of ¹H NMR spectra.

^bIntrinsic viscosity measured in dichloroacetic acid at 25 °C.

^cDetermined by GPC in HFIP against PMMA standards.

^dDegree of randomness of copolyesters calculated on the basis of the ¹³C NMR analysis.

The microstructure of the copolyesters was determined by ^{13}C NMR taking benefit from the sensitivity of the methylene signals to the sequence distribution at the dyad level (Figure 3.1). In the $\text{PB}_x\text{Th}_y\text{S}$ series, the signal corresponding to the methylene of the succinate unit appeared between 28.7 and 29.3 ppm split into four peaks corresponding to the four types of dyads (BB, BT, TB and TT) feasible for these copolyesters. In the case of the PBS_xTh_y series, it is the signal arising from the β -methylene of the butylene unit within the 24.9-25.3 ppm range that reflects the content in SS, ST, TS and TT dyads in the copolyesters. In both cases, integration of the four dyad-associated peaks and the application of the 1 and 2 equations led to estimate the number average sequence lengths and to the evaluation of the microstructure of $\text{PB}_x\text{Th}_y\text{S}$ and PBS_xTh_y copolyesters, respectively. The values resulting from these calculations for the two series are given in Table 3.2. which indicate that a very close to random microstructure is shared by all the copolyesters ($R \sim 1$).

$$n_T = \frac{\text{BB} + 0.5(\text{BT} + \text{TB})}{0.5(\text{BT} + \text{TB})} \quad n_T = \frac{\text{TT} + 0.5(\text{TB} + \text{BT})}{0.5(\text{TB} + \text{BT})} \quad R = 1/n_B + 1/n_T \quad (\text{Eq. 1})$$

$$n_T = \frac{TT + 0.5(TS + ST)}{0.5(TS + ST)} \quad n_S = \frac{SS + 0.5(ST + TS)}{0.5(ST + TS)} \quad R = 1/n_S + 1/n_T \quad (\text{Eq. 2})$$

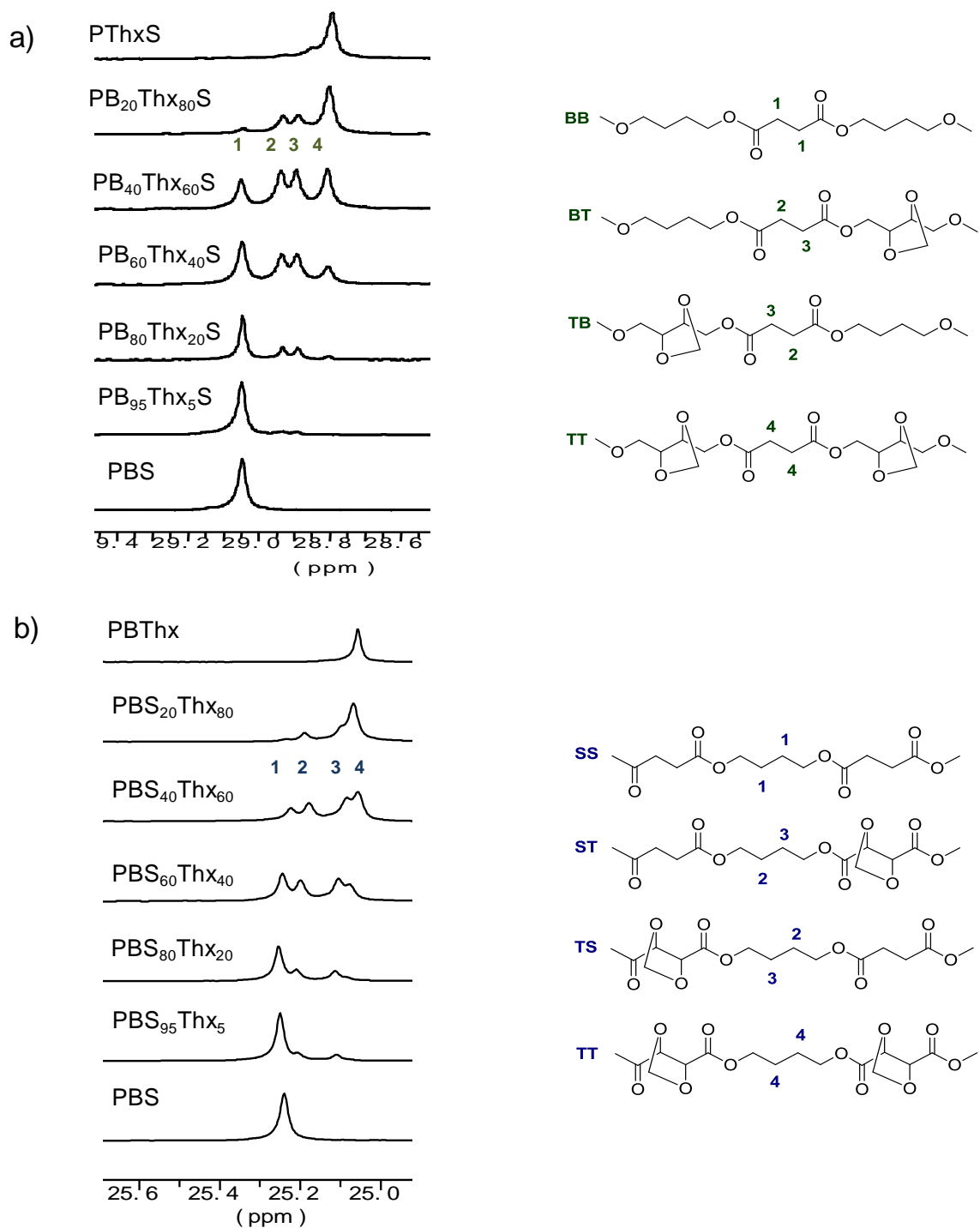


Figure 3.1. ^{13}C NMR spectra showing the changing of the CH_2 signal of the succinate unit of $\text{PB}_x\text{Thx}_y\text{S}$ (a) and the $\beta\text{-CH}_2$ signal of the butylene unit of PBS_xThx_y copolyesters (b).

3.3.2. Thermal and mechanical properties

To evaluate the thermal stability of polyesters, TGA analyses were performed in the 30-600 °C temperature range under a nitrogen atmosphere. The TGA traces obtained for the two series are compared in Figure 3.2, and decomposition thermal data are collected in Table 3.3. A slight decreasing in the decomposition temperatures with the content in Thx units is in general observed although such trend becomes less clear in the case of the PB_xThx_yS series. Remaining weights are always far below 10% of the initial sample and no clear tendency of values with composition can be appreciated. According to what has been previously reported for other related copolyesters containing Thx units,^{11,12} the thermal stability loss can be attributed to the relatively lower stability of the Thx unit although the simultaneous influence of the molecular weight, which is decreasing in the same sense, cannot be discarded.

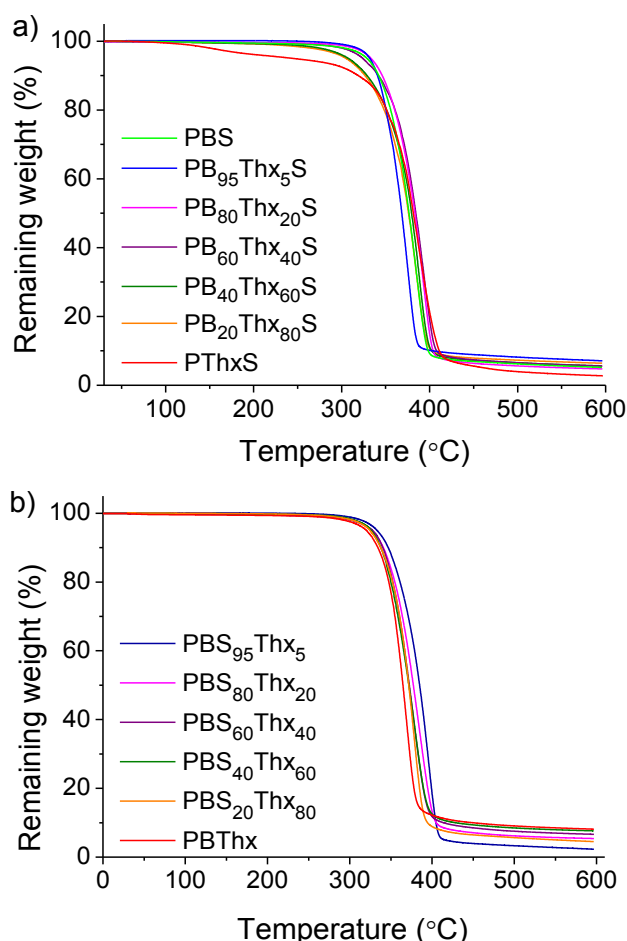


Figure 3.2. TGA traces of PB_xThx_yS (a) and PBS_xThx_y (b).

Table 3.3. Thermal properties of PB_xThx_yS and PBS_xThx_y polyesters.

Polyester	First heating ^b			Cooling ^b	Second heating ^b			TGA		
	T_g^a (°C)	T_m (°C)	ΔH_m (J·g ⁻¹)	T_c (°C)	T_c (°C)	T_m (°C)	ΔH_m (J·g ⁻¹)	$T_{d5\%}^c$ (°C)	T_{max}^d (°C)	RW^e (%)
PBS	-37	117	82	75	98	115	63	329	386	5
PB ₉₅ Thx ₅ S	-33	108	73	71	95	108	56	332	376	7
PB ₈₀ Thx ₂₀ S	-24	90	44	39	74	90	42	333	392	5
PB ₆₀ Thx ₄₀ S	-13	64	31	-	-	-	-	324	394	6
PB ₄₀ Thx ₆₀ S	-8	35	6	-	-	-	-	308	387	6
PB ₂₀ Thx ₈₀ S	7	-	-	-	-	-	-	304	384	6
PThxS	13	-	-	-	-	-	-	245	386	3
PBS ₉₅ Thx ₅	-36	109	79	69	91	109	65	333	396	2
PBS ₈₀ Thx ₂₀	-30	90	56	28	67	89	47	327	383	5
PBS ₆₀ Thx ₄₀	-25	61	35	-	-	-	-	328	378	7
PBS ₄₀ Thx ₆₀	-18	44	21	-	-	-	-	326	380	8
PBS ₂₀ Thx ₈₀	-6	53	34	-	-	-	-	324	379	5
PBThx	-3	104	27	-	64	104	22	320	370	8

^a Glass-transition temperature taken as the inflection point of the heating DSC traces of melt-quenched samples recorded at 20 °C·min⁻¹.

^b Melting (T_m) and crystallization (T_c) temperatures, melting enthalpy (ΔH_m) measured by DSC at heating/cooling rates of 10 °C·min⁻¹.

^c Temperature at which 5 % weight loss was observed.

^d Temperature for maximum degradation rate.

^e Remaining weight at 600 °C

The thermal properties of the synthesized polyesters and copolyesters were evaluated by differential scanning calorimetry giving special attention to the influence exerted by the Thx units on melting and glass transition temperatures. Transition temperatures and enthalpies measured by DSC are listed in Table 3.3. The DSC heating traces registered from the two polyester series are shown in Figure 3.3 bringing into evidence that both T_m and crystallinity decrease with the degree of replacement by Thx units. The effect is common to the two series but the influence is more perceivable for PB_xThx_yS copolyesters. In this series crystallinity is hardly observable when the content in Thx units exceeds 50%, and the homopolymer PThxS is definitely amorphous. The fact that the depressing effect is more pronounced in the PB_xThx_yS series is a reflect of the higher structural change that is introduced in the polyester chain when the flexible butylene segment is replaced by the 4,5-dimethylene-1,3-dioxolane cycle. Conversely, endothermal peaks indicative of crystallinity are observed for the whole PBS_xThx_y series and the homopolymer PBThx is clearly semicrystalline. The observed decreasing in T_m and ΔH_m enthalpy reflects a smaller crystallite size and lower crystalline fraction motivated by the lack of regularity of the copolymer chain and

restricted mobility caused by the relatively stiffer Thx structure. T_g was measured on heating traces recorded from samples that had been rapidly cooled from the melt. It was observed in both series that T_g increased with the incorporation of Thx units in the polyester chain although the enhancing effect was significantly stronger when the diol unit was the replacing one. In fact T_g values of 13 and -3 °C were obtained for the PThxS and PBThx homopolyesters, respectively, which are 50 and 34 °C higher than the T_g of PBS.

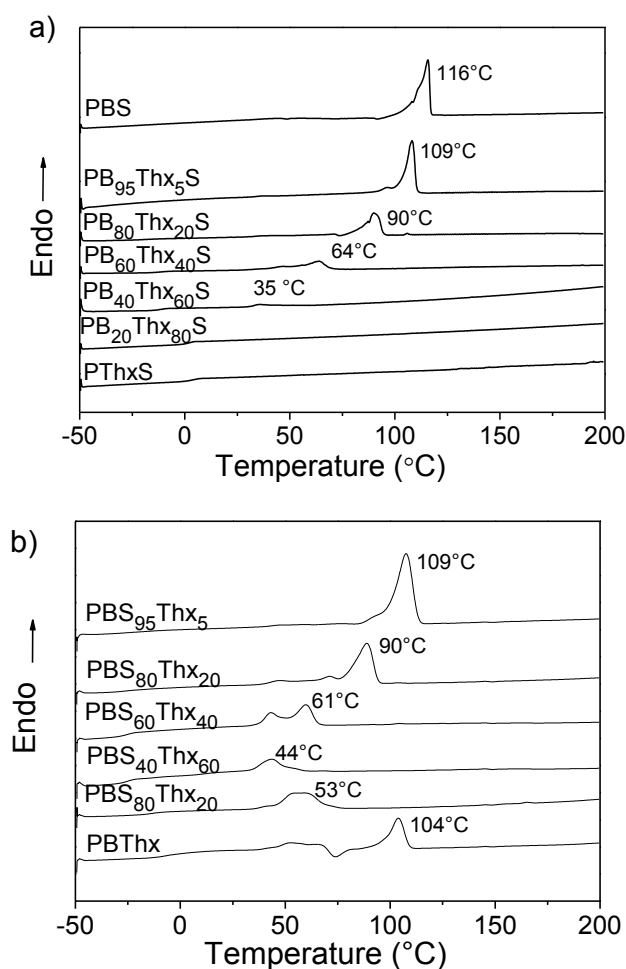


Figure 3.3. DSC heating traces of PB_xThx_yS (a) and PBS_xThx_y (b).

To have a preliminary appraisal of the influence of copolymerization on the mechanical behavior of PBS, films of several selected copolyesters and of PBS itself were prepared by hot-pressing and subjected to tensile testing. The films were previously examined by DSC in order to have an estimation of their crystallinity because the strong influence that it is known to have on mechanical properties. Thermal parameters of films samples were similar to those of the powder samples, with differences in the melting temperature of 2-3 °C and slightly lower melting enthalpies

according to what should be expected from the different treatment history followed in each case. The copolyesters tested were PB₉₅Thx₅S, PB₈₀Thx₂₀S and PB₆₀Thx₄₀S. Their stress-strain curves are compared to that of PBS in Figure 3.4 and mechanical parameters measured in these essays are gathered in Table 3.4. The copolyesters of the PB_xThx_y series were too fragile and could not be mechanically tested. Results demonstrate that the replacement of BD by Thx-diol gives rise to polymers with lower elastic modulus and tensile strength but with much higher elongation at break. In general it can be said that PB_xThx_yS copolyesters are softer and tougher than PBS. This tendency is contrary to what one would expect from the increased T_g displayed by the copolyesters and suggests that is crystallinity the factor playing the main role in the mechanical behavior of these copolyesters.

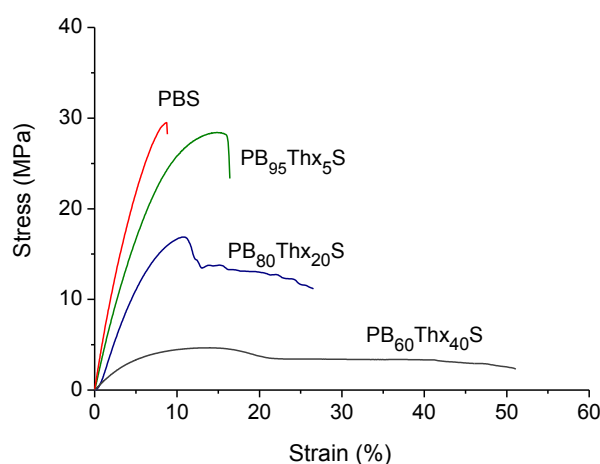


Figure 3.4. Stress-strain plots of the indicated polyesters.

Table 3.4. Mechanical parameters, powder X-ray diffraction and crystallization rate data of PB_xThx_yS and PBS_xThx_y polyesters.

Polyester	ΔH_m^a (J·g ⁻¹)	Mechanical parameters ^b			WAXS	Crystallization half-time (min)	
		E (MPa)	σ_{max} (MPa)	ϵ (%)	d^c (nm)	85 °C	90 °C
PBS	55	535	33	9	0.45, 0.40, 0.39	1.95	5.35
PB ₉₅ Thx ₅ S	59	396	30	17	n.d	6.20	19.50
PB ₈₀ Thx ₂₀ S	50	266	18	27	0.45, 0.40, 0.39		
PB ₆₀ Thx ₄₀ S	33	75	5	50	0.45, 0.40-0.39		
PThxS					-		
PBS ₉₅ Thx ₂₅					n.d	9.15	31.20
PBS ₈₀ Thx ₂₀					0.45, 0.40, 0.39		
PBS ₆₀ Thx ₄₀					0.45, 0.40-0.39		
PBS ₂₀ Thx ₈₀					0.85, 0.52, 0.45-0.39		
PBThx					0.85, 0.52, 0.44, 0.43 0.39		

^a Melting enthalpies obtained from film samples.

^b Elastic modulus (E), tensile strength (σ) and elongation at break (ϵ) measured in tensile tests.

^c Bragg spacings observed by WAXS with medium or high intensity. (n.d: not determined).

3.3.3. Crystalline structure and crystallizability

Powder X-ray diffraction analyses were performed for PBS, PThxS and PBThx homopolyesters as well as for a wide selection of copolyesters including Thx contents from 20 to 80%. Samples were previously subjected to annealing to improve the crystallinity. The recorded powder X-ray diffraction profiles are depicted in Figure 3.5., and the characteristic interplanar spacing values they provide are collected in Table 3.3. The diffraction pattern of PBS is characterized by three strong reflections at 0.45, 0.40, and 0.39 nm produced by the monoclinic crystal structure known for this polyester.¹³ The same reflections are observed for either of the two copolyester series with contents in Thx up to 40%. The occurrence of an ordered phase in these copolyesters with the crystal structure of PBS is explained by assuming the same semicrystalline model reported for other related aliphatic copolyester containing cyclic sugar-derived units.¹⁴ In this model, the crystal phase is assumed to be exclusively made of homogeneous segments made of butylene succinate units whereas segments containing cyclic units are rejected to the amorphous phase. For contents in Thx units higher than 40% the behavior is different for each series. Whereas the profiles of Thx enriched PB_xThx_yS copolyesters and PThxS do not show any sign indicative of crystallinity, both $PBS_{20}Thx_{80}$ and PBThx produce patterns clearly different to that observed for those members of the series containing minor amounts of Thx units. The X-ray diffraction profile arising from PBThx displays reflections at 0.88, 0.52, 0.50, 0.44, and 0.43 nm which are clearly different from those characteristic of PBS and therefore indicative that a new crystal form is adopted by this polyester. The crystallinity observed for $PBS_{20}Thx_{80}$ should be interpreted therefore as the result of the crystallization of homogeneous butylene threarate sequences whereas the segments that are segregated to the amorphous phase in this case would be those containing butylene succinate units. The occurrence of this crystal structure in PB_xThx_yS containing high amounts of Thx units is consistent with the trend observed for T_m by DSC along the series. While the two parent homopolyesters melt at nearly the same temperature (105-110 °C), the T_m of the copolyesters fall down to a minimum of about 50 °C lower when compositions are of similar contents in the two comonomers.

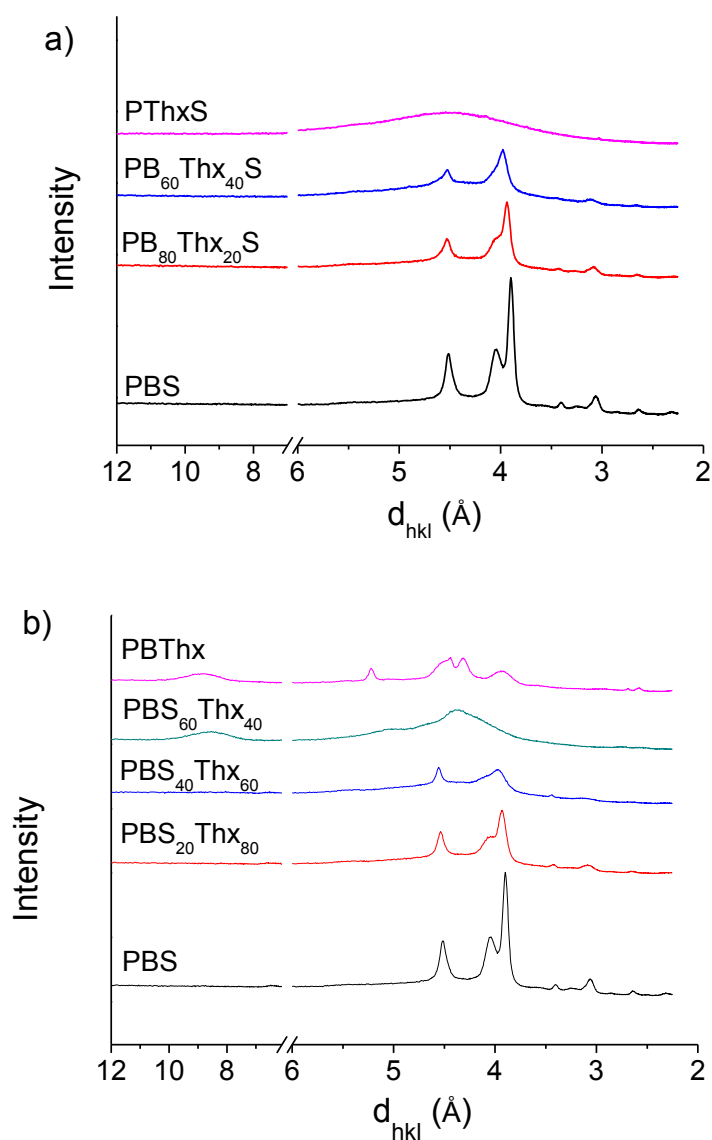


Figure 3.5. Powder WAXS profiles of homopolyesters and copolyesters from samples previously subjected to annealing.

As it is shown in Table 3.2., only those semicrystalline polyesters containing up to 20% of Thx units were able to crystallize at cooling from the melt and displayed cold crystallization on the second heating. These observations ascertain the depressing effect that Thx units have on crystallizability. Nevertheless, a comparative crystallization kinetics study was undertaken on PBS, PB₉₅Thx₅S and PBS₉₅Thx₅ in order to attain a precise evaluation of the effect that copolymerization exerts on crystallizability regarding the type of unit, diol or diacid, that is replaced. For that, polyester samples were melted at a common temperature, cooled rapidly to the selected crystallization temperature and the heat evolved while held isothermally at this temperature was measured. Two different crystallization temperatures were selected

for each sample to estimate also the influence of temperature on crystallization rate. Application of the widely known isothermal crystallization Avrami model^{15,16} allowed to determine the half-crystallization time for each polymer. The isothermal plots for PBS and the two copolyesters are depicted in Figure 3.6., and the resulting $t_{1/2}$ values are compared in Table 3.4. A detailed account of the procedure applied to these determinations including the representation of the Avrami plots as well as a table of kinetics parameters are given in the SI annex A.

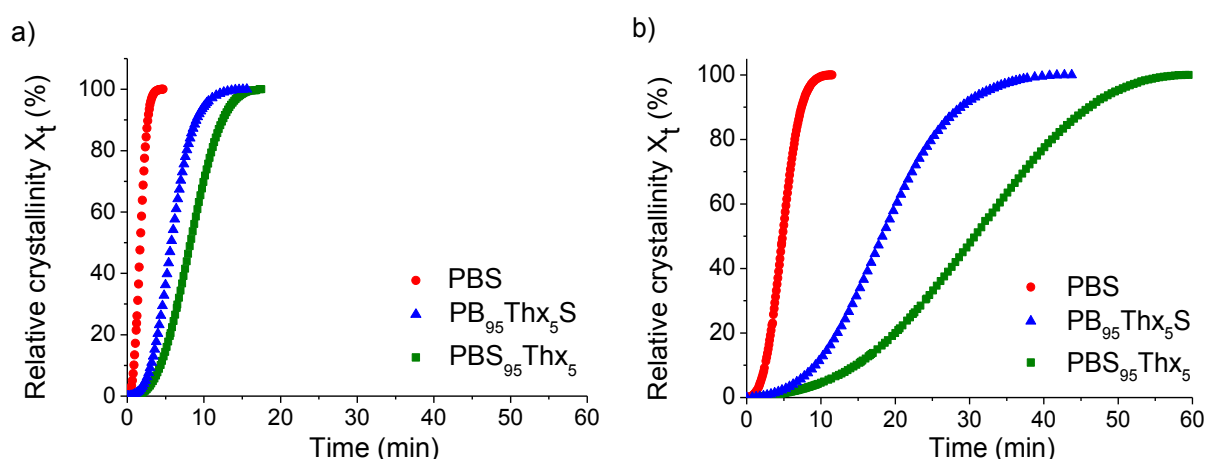


Figure 3.6. Isothermal crystallization of PBS, $PB_{95}Thx_5S$, $PBS_{95}Thx_5$ at 85 °C (a) and 90 °C (b).

The conclusions drawn from comparing the $t_{1/2}$ values are the following: a) The inverse dependence of crystallization rate on temperature indicates that in both PBS and copolyesters, the crystallization process is controlled by nucleating factors rather than by chain mobility. b) The incorporation of whatsoever kind of Thx units invariably entails a slowdown of the crystallization rate. c) The hindering effect due to copolymerization is markedly more pronounced when the succinate units are replaced ones.

3.3.4. Biodegradation and hydrolytic degradation

It is well known that PBS is readily hydrolysable and also biodegradable,¹ which is one merit favoring many applications of this polyester. It is desirable therefore retaining the degradability of PBS after modification or even enhancing it. In order to evaluate the effect of the Thx units on the behavior of PBS regarding its degradability several degradation essays were carried out in parallel using samples of PBS, PThxS and PBThx homopolyesters and $PB_{60}Thx_{40}S$, $PBS_{60}Thx_{40}$ copolyesters. First, samples

were incubated in pH 7.4 buffer at 37 °C, both in the presence and in the absence of porcine pancreas lipase. The changes taking place in sample weight and molecular weight of polyesters during incubation are depicted in Figure 3.7. After seven weeks, PBS had lost 15% of the initial weight, whereas the weight losses undergone by PB₆₀Thx₄₀S, PBS₆₀Thx₄₀, PThxS, PBThx were between 30 and 35%. In the presence of lipase, these weight losses increased up to 28% and ~45%, respectively. GPC analyses of the residue left after incubation revealed a progressive decay in molecular weight of the polyester that became more visible when polymers were incubated with enzymes added (Figure 3.7c.). The same polymers incubated at 37 °C in aqueous buffer at pH 2.0 displayed higher changes in both sample weight and molecular weight revealing their higher sensitivity to hydrolysis under acidic conditions (SI annex A figure). These results lead to conclude that the degradability of PBS is increased by the insertion of Thx units of whichever kind, and that the effect is particularly effective as far as biodegradability is concerned.

To get insight into the hydrolytic degradation mechanism, the same polyester samples were placed in NMR tubes at pH 2 aqueous buffer at 37 °C, and ¹H NMR spectra were recorded from the products released to the aqueous medium after every week. The ¹H NMR spectrum of the products released by PBThx after 7 weeks of incubation is shown in Figure 3.8. The spectrum contains signals corresponding to 1,4-butanediol, Thx-diacid, succinic acid and soluble oligomers. On the other hand, the analysis of the residue left by the copolyesters after incubation showed a decrease of more than 10% in the content of Thx units in the copolyester indicating that hydrolytic degradation happens mostly by breaking those ester groups in which the Thx units are directly implied. In all cases signals corresponding to -CH₂OH end groups were apparent whereas those arising from the 1,3-dioxolane ring remained unaltered, and no sign of hydrolysis of the acetal group was detected. The high resistance to hydrolysis of the Thx structure was confirmed by these results since no changes indicative of free secondary OH were detected in any ¹H NMR spectra of either polymer residue or released degraded products. Such extremely high resistance to hydrolysis displayed by the methylene acetal makes it an excellent permanent protecting group for polyesters made from hydroxylated monomers. This clearly differs from other C1-substituted acetals such as isopropylidene acetal, which are used for temporal protection of tartaric units that will be later deprotected for generating polyesters bearing free hydroxyl groups.^{17, 18}

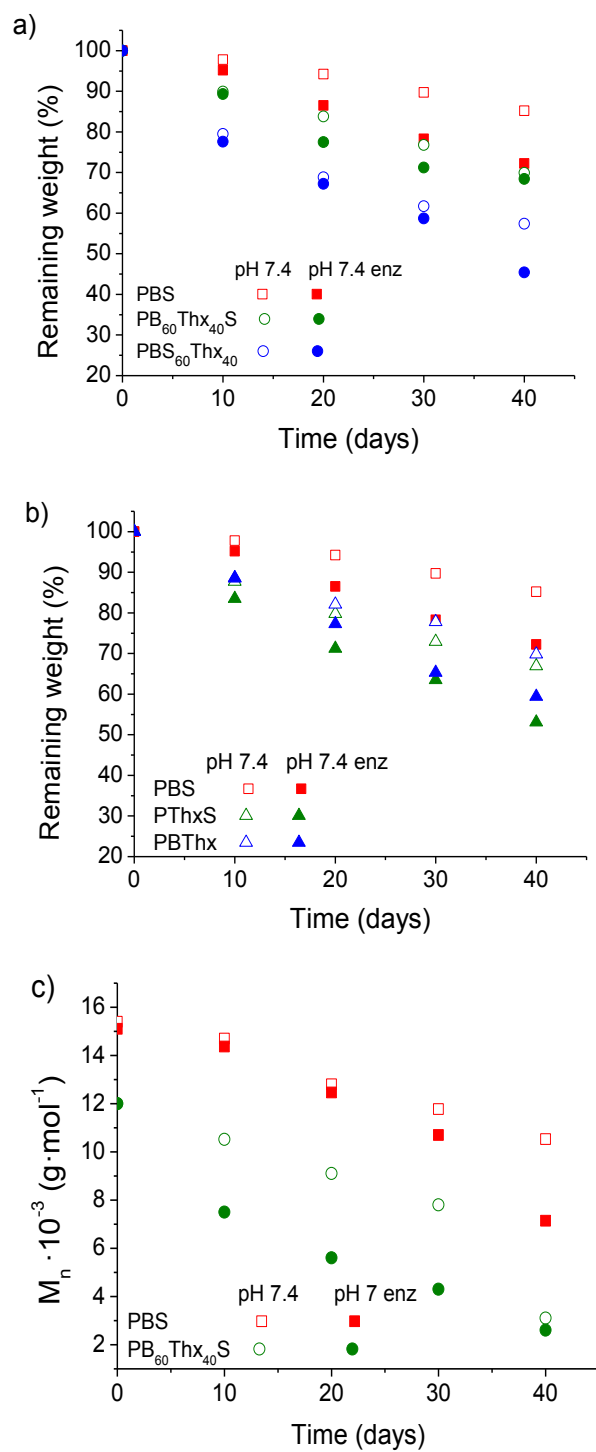


Figure 3.7. Remaining weight (a,b) and molecular weight (c) of polyesters vs. degradation time.

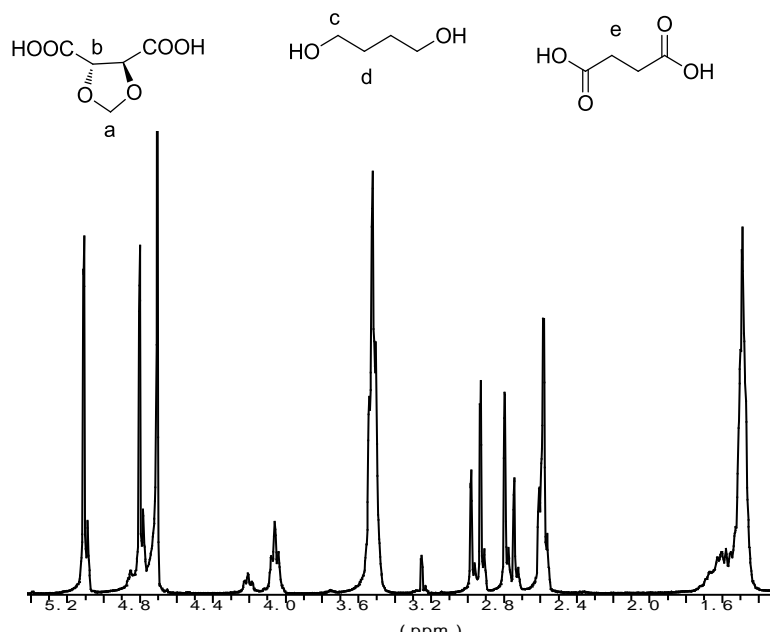


Figure 3.8. ^1H NMR spectrum (D_2O) of the products released to the aqueous medium after incubation of $\text{PBS}_{60}\text{Thx}_{40}$ at pH 2 for 7 weeks.

3.4. Conclusions

The cyclic acetals 2,3-di-O-methylene-L-threitol (Thx-diol) and dimethyl 2,3-di-O-methylene-L-threarate (Thx-diester) were used as comonomers for the synthesis of the PBS derived copolyesters poly(butylene-co-2,3-di-O-methylene-L-threitylene succinate) and poly(butylene succinate-co-2,3-di-O-methylene-L-thearate) as well as the two respective homopolyesters. All these polyesters could be successfully prepared by melt polycondensation with adjustable compositions and satisfactory molecular weights. The microstructure of the copolyesters was random in all cases, which appears to be a constant in copolyesters containing sugar-based acetalized cyclic units. The insertion of Thx units in the PBS chain gave rise to a decrease in the crystallinity and crystallizability of PBS whereas the glass transition temperature was greatly enhanced. These effects were more pronounced when the butylene unit of the polyester was the replaced unit as it could be expected from comparison of the stiffness of the molecular segments that are involved in each case. The influence of copolymerization on the mechanical behavior is very noticeable and also highly depending on the type of unit that is replaced. Copolyesters made from Thx-diol displayed lower elastic modulus and

tensile strengths but highly increased elongations at break whereas those made from Thx-diester became brittle. The presence of Thx units of whichever type increased the hydrolytic degradability of PBS and more specially with the concourse of enzymes. Hydrolysis of these polyesters was found to take place preferentially through hydrolysis of ester groups directly associated to Thx units.

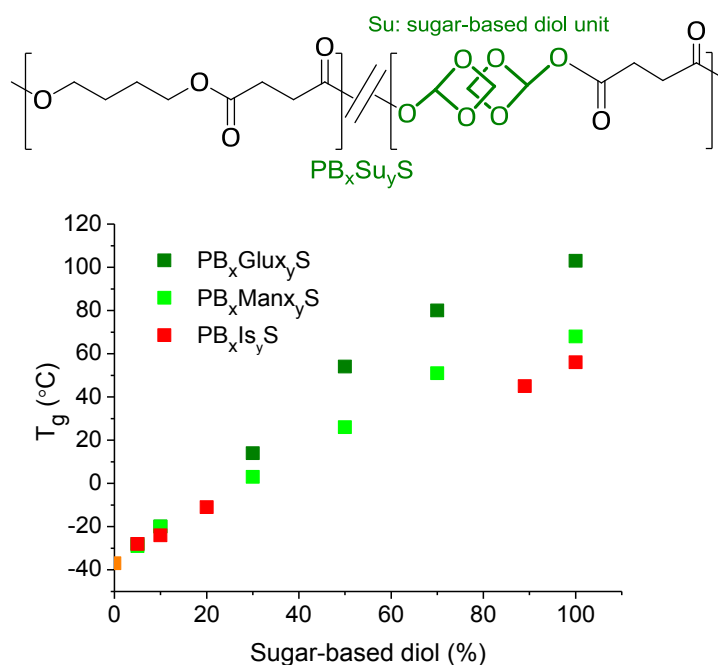
3.5. References

1. Jun, X.; Bao-Hua, G. *J. Biotechnol.* **2010**, *5*, 1149-1163.
2. Gawroński, J.; Gawrońska, K. *Tartaric and malic acids in synthesis*; Wiley-Interscience, Toronto, **1998**, xiii.
3. Bou, J.J.; Rodríguez-Galán, A.; Muñoz-Guerra, S. *Macromolecules* **1993**, *26*, 5664-5670.
4. a) Regaño, C.; Martínez de Ilarduya, A.; Iribarren, I.; Rodríguez-Galán, A.; Galbis, J.A.; Muñoz-Guerra, S. *Macromolecules* **1996**, *29*, 8404-8412. b) Bou, J.J.; Iribarren, I.; Martínez de Ilarduya, A.; Muñoz-Guerra, S. *J. Polym. Sci.: Polym. Chem.* **1999**, *37*, 983-993.
5. Villuendas, I.; Iribarren, I.; Muñoz-Guerra, S. *Macromolecules* **1999**, *32*, 8015-8023.
6. Villuendas, I.; Bou J.J.; Rodríguez-Galán, A.; Muñoz-Guerra, S. *Macromol. Chem. Phys.* **2001**, *202*, 236-244.
7. Marín, R.; Martínez de Ilarduya, A.; Muñoz-Guerra, S. *J. Polym. Sci.: Polym. Chem.* **2009**, *47*, 2391-2407.
8. Kint, D.; Wingstrom, E.; Martínez de Ilarduya, A.; Alla, A.; Muñoz-Guerra, S. *J. Polym. Sci.: Polym. Chem.* **2001**, *39*, 3250-3262.
9. Muñoz-Guerra, S.; Lavilla, C.; Japu, C.; Martínez de Ilarduya, A. *Green Chem.* **2014**, *16*, 1716-1739.
10. Marín, R.; Muñoz-Guerra, S. *J. Polym. Sci. Polym. Chem.* **2008**, *46*, 7996-8012.
11. Japu, C.; Martínez de Ilarduya, A.; Alla, A.; Muñoz-Guerra, S. *Polymer* **2013**, *54*, 1573-1582.
12. Lavilla, C.; Gubbels, E.; Alla, A.; Martínez de Ilarduya, A.; Noordover, B.A.J.; Koning, C.E.; Muñoz-Guerra, S. *Green Chem.* **2014**, *16*, 1789-1798.
13. Ihn, K.; Yoo, E.; Im, S. *Macromolecules* **1995**, *28*, 2460-2464.
14. Lavilla, C.; Alla, A.; Martínez de Ilarduya, A.; Muñoz-Guerra, S. *Biomacromolecules* **2013**, *14*, 781-793.
15. Bodor, G. *Structural investigation of polymers analysis*; Ellis Hordwood, Toronto, **1991**.
16. Martins, J.; Zhang, Wd.; Brito, A. *Rev. Sci. Instrum.* **2005**, *76*, 105105.
17. Dhamaniya, S.; Josemon, J. *Polymer* **2010**, *51*, 5392-5399.
18. Dhamaniya, S.; Jaggi, H.S.; Nimiya, M.; Sharma, S.; Satapathya, B.K.; Jacob, J. *Polym. Int.* **2014**, *63*, 680-688.

Chapter 4

Bio-based PBS copolyesters derived from a bicyclic D-glucitol

2,4:3,5-di-O-methylene-D-glucitol (Glux-diol) was used for the synthesis of poly(butylene succinate) (PBS) copolyesters by melt polycondensation. Glux-diol possess a rigid bicyclic asymmetric structure made of two fused 1,3-dioxane rings and two hydroxyl functions at the end positions. Copolyesters were prepared over the whole range of compositions with molecular weights varying from 26,000 to 46,000 g·mol⁻¹ and a random microstructure. The thermal stability of PBS did not significantly alter with the presence of Glux units. The glass transition temperatures (T_g) steadily increased from -28 to 80 °C along the whole copolyester series with the insertion of Glux. On the contrary, melting temperature (T_m) and crystallinity decreased because of lack of regularity of the polymer chain although copolyesters with contents of Glux units up to 30 mole-% were semicrystalline. The stress-strain behavior changed according to variations produced in thermal transitions. The replacement of 1,4-butanediol by Glux-diol slightly increased both the hydrolytic degradability and the biodegradability of PBS.



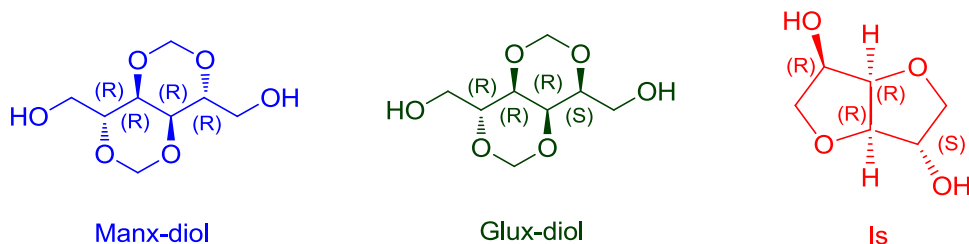
This work was published as: E. Zakharova, Alla, A. Martínez de Ilarduya, S. Muñoz-Guerra, Bio-based PBS copolyesters derived from a bicyclic D-glucitol, *RCS Adv.*, **2015**, 46395-46404.

4.1. Introduction

Aliphatic polyesters such as poly(L-lactic acid), poly(butylene succinate), and polyhydroxyalkanoates among others, constitute primary examples of bio-based polymers that distinguish by being fully renewable and displaying partial or total biodegradability. Poly(butylene succinate) (PBS) is one of the members of the aliphatic polyester family that is receiving greatest attention. This polyester not only may be built by using exclusively renewable feedstock but it also displays mechanical properties comparable to other extensively used conventional polymers.¹ Furthermore, PBS has been demonstrated to exhibit significant biodegradation in soil, activated sludge and sea water.² Due to its outstanding potential, PBS is today in the focus of an intensive research addressed to improve its thermal and mechanical properties without significant detriment to its sustainability and biodegradability. Copolymerization involving cyclic comonomers and blending with nanofillers are the main approaches followed in this regard.^{3,4}

Recently, carbohydrate-based bicyclic diols and diacids with a diacetal constitution have emerged as a new class of bio-based monomers with a potential at least comparable to that of isohexides.^{5,6} Most exciting results have been those attained with aromatic copolyesters containing fused diacetalized bicyclic units derived from D-mannose and D-glucose.^{7,8} These novel sugar-based copolyesters have been reported to exhibit enhanced thermal properties and biodegradability when compared to PET and PBT.^{9,10}

The purpose of this work is to explore the effects on properties of PBS caused by the presence of carbohydrate-based diacetalized bicyclic units in the polymer chain, more specifically of 2,4:3,5-di-O-methylene-D-glucitol, abbreviated as Glux-diol. Novel copolyesters will be compared with PBS copolyesters made from Manx-diol, the stereoisomer of Glux-diol that derives from D-mannose.¹¹ At difference with Manx-diol, Glux-diol is asymmetric so its two OH groups are spatially and hence chemically different (Scheme 4.1). Additionally, data obtained from this study can be related to those reported for PBS copolyesters containing isosorbide in order to assess diacetalized and dianhydride bicyclic diols as optional comonomers for their capacity to improve PBS properties. The study is also of practical relevance since Glux-diol is a compound coming from D-glucose, the most available monosaccharide in nature.

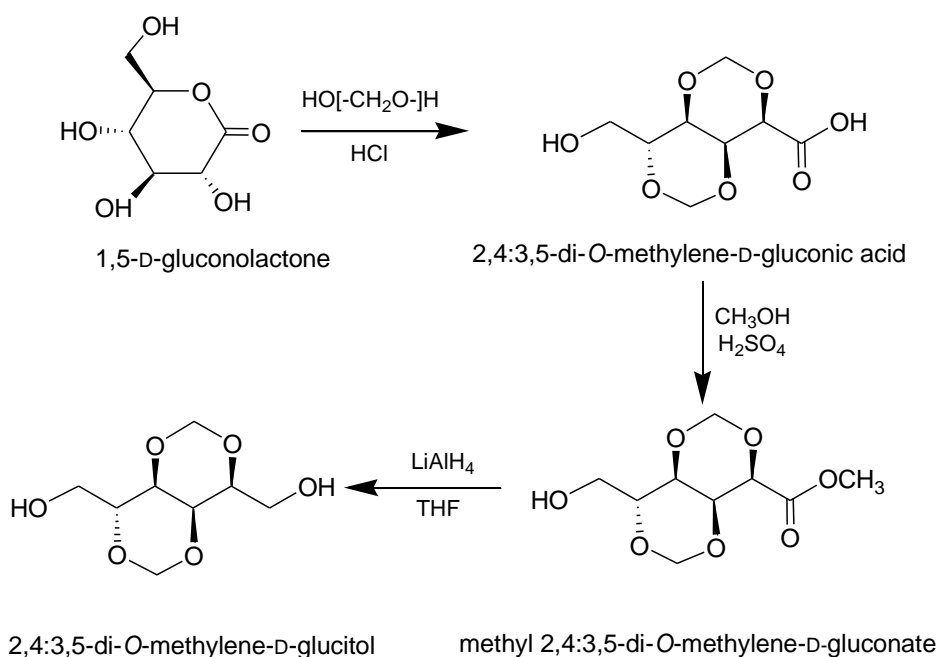


Scheme 4.1. Chemical structures of sugar-based bicyclic diols with specification of their respective stereocenters.

4.2. Experimental part

4.2.1. Monomer synthesis

The cyclic diol 2,4:3,5-di-O-methylene-D-glucitol (Glux-diol) has been prepared following a procedure well described in the recent literature.¹² A mixture of 1,5-D-gluconolactone, paraformaldehyde, and concentrated hydrochloric acid are refluxed at 110 °C for 1 h. The 2,4:3,5-di-O-methylene-D-gluconic acid precipitated from the solution on cooling. A mixture of di-O-methylidene-D-gluconic acid, methanol and concentrated sulfuric acid was refluxed until complete dissolution. The product precipitated from the solution on cooling, additional crops were obtained on concentrating the mother liquors. A suspension of LiAlH_4 in dry tetrahydrofuran is added to a suspension of methyl 2,4:3,5-di-O-methylene-D-gluconate in dry tetrahydrofuran at 0 °C under nitrogen atmosphere. The mixture is then refluxed for 24 h and cooled to 0 °C. Water, aqueous solution of NaOH, and water are sequentially and slowly added, and the mixture is then filtered and concentrated to an oily residue from which the title compound crystallized as a white solid.



Scheme 4.2. Synthesis of 2,4:3,5-di-O-methylidene-D-glucitol.

4.2.2. Polymer synthesis

Copolyesters of PBS containing Glux units (PB_xGlux_yS with subscripts x and y standing for mole-% of BD and Glux units in the feed respectively) were synthesized by reaction of dimethyl succinate with mixtures of 1,4-butanediol and 2,4:3,5-di-O-methylene-D-glucitol at different selected ratios. PBS and PGluxS homopolyesters were obtained by polycondensation of dimethyl succinate with 1,4-butanediol and 2,4:3,5-di-O-methylene-D-glucitol, respectively. Since volatile diols were partially streamed off by the nitrogen flow and volatilized under vacuum, a mole-10% excess of respect to the diester monomer was used in all cases. The antioxidants Irganox 1010 (0.2% w/w) and Irgafos 126 (0.6% w/w) were added to minimize degradation of thermally sensitive sugar-based monomers. The same reaction protocol was applied for all compositions. The transesterification step was performed for 3-5 h at 160 °C under nitrogen flow, and polycondensation for 7-8 h at 160-180 °C under vacuum (0.03-0.06 mbar). The NMR data ascertaining their constitution and purity are described below.

PBS homopolymer: ^1H NMR (300.1 MHz, CDCl_3), δ (ppm): 4.1 (t, 4H, $\text{OCH}_2\text{CH}_2\text{CH}_2$), 2.6 (s, 4H, $\text{COCH}_2\text{CH}_2\text{CO}$), 1.7 (t, 4H, $\text{OCH}_2\text{CH}_2\text{CH}_2$). ^{13}C NMR (75.5 MHz, CDCl_3/TFA), δ (ppm): 176.7 (CO), 65.1, 29.0, 25.2.

PB_xGlux_yS copolyesters: ^1H NMR (300.1 MHz, CDCl_3), δ (ppm): 5.2-4.8 (m, y·4H, OCH_2O), 4.6-4.4 (m, y·2H, OCH_2CH), 4.4-4.2 (m, y·4H, OCH_2CH), 4.2-4.1 (m, y·1H, OCH_2CHCH), 4.2-4.0 (t, x·4H, COCH_2CH_2), 3.9 (m, y·1H, OCH_2CHCH), 3.8-3.7 (t, y·1H, OCH_2CHCH), 3.7-3.6 (t, y·1H, $\text{OCH}_2\text{CHCHCHCH}$), 2.7-2.6 (t, x·4H, $\text{COCH}_2\text{CH}_2\text{CO}$), 2.7-2.6 (t, y·4H, $\text{COCH}_2\text{CH}_2\text{CO}$), 1.7 (t, x·4H $\text{OCH}_2\text{CH}_2\text{CH}_2$). ^{13}C NMR (75.5 MHz, CDCl_3/TFA), δ (ppm): 176.7 (CO), 93.2, 88.3, 76.2, 74.5, 71.5, 68.4, 67.0, 65.1, 61.8, 29.0, 25.2.

PGluxS homopolymer: ^1H NMR (300.1 MHz, CDCl_3), δ (ppm): 5.2-4.8 (m, 4H, OCH_2O), 4.6-4.4 (m, 2H, OCH_2CH), 4.4-4.2 (m, 4H, OCH_2CH), 4.2-4.1 (m, 1H, OCH_2CHCH), 3.9 (m, 1H, OCH_2CHCH), 3.8-3.7 (t, 1H, OCH_2CHCH), 3.7-3.6 (t, 1H, $\text{OCH}_2\text{CHCHCHCH}$), 2.7-2.6 (t, 4H, $\text{COCH}_2\text{CH}_2\text{CO}$). ^{13}C NMR (75.5 MHz, CDCl_3/TFA), δ (ppm): 176.7 (CO), 93.2, 88.3, 76.2, 74.5, 71.5, 68.4, 67.0, 61.8, 20.9.

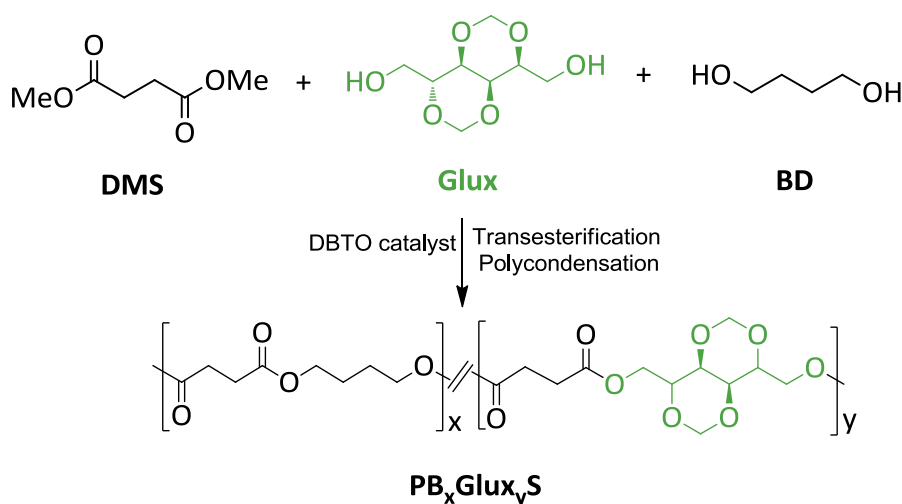
4.2.3. Hydrolytic degradation and biodegradation

Films for hydrolytic degradation and biodegradation studies were prepared with a thickness of $\sim 200\ \mu\text{m}$ by casting from chloroform solution at a polymer concentration of $100\ \text{g}\cdot\text{L}^{-1}$. The films were cut into 10 mm diameter, 20-30 mg weight disks and dried under vacuum to constant weight. For hydrolytic degradation, samples were immersed in vials containing 10 mL of either citric acid buffer pH 2.0 or sodium phosphate buffer pH 7.4 at 37 °C. The enzymatic degradation was carried out at 37 °C in vials containing 10 mL of a pH 7.4 buffered sodium phosphate solution with added lipase from porcine pancreas (10 mg) and replacing the supernatant every 72 h to maintain the enzyme activity. In both cases, the disks were withdrawn from the incubation medium after scheduled periods of time, washed carefully with distilled water, dried to constant weight, and analyzed by GPC chromatography and NMR spectroscopy.

4.3. Results and discussion

4.3.1. Synthesis and chemical structure

The monomer 2,4:3,5-di-O-methylene-D-glucitol (Glux-diol) with the required purity and in satisfactory yield was prepared from commercially available 1,5-D-gluconolactone.¹² Polycondensation in the melt was the method chosen to prepare both homopolyesters and copolyesters in agreement with that is usual in the industrial practice, and the applied procedure conditions were as close as possible to those reported for the synthesis of Manx-containing PBS copolyesters.¹¹ As it is depicted in Scheme 4.3., the polymerization procedure consisted in two steps, first generation of hydroxyl capped oligoesters by transesterification under a nitrogen flow to prevent decomposition of Glux, and second, polycondensation under vacuum to remove the excess of BD as much as possible. Reaction conditions regarding time and temperature were optimized for each individual case. Both the homopolyester PGluxS and the series of copolyesters PB_xGlux_yS containing Glux units from 5 up to 70 mole-% were thus synthesized.



Scheme 4.3. Polycondensation reactions leading to PB_xGlux_yS copolyesters. Only asymmetric carbons keeping a unique spatial orientation along the copolyester chain (3 and 4 carbons of the Glux unit) have been stereochemically represented.

The chemical constitution of the polyesters was assessed by NMR. As an example, both ¹H and ¹³C NMR spectra of PB₅₀Glux₅₀S with indication of all signals assignments are shown in Figure 4.1. NMR spectra of PB₉₀Glux₁₀S and PGluxS are

represented in ESI file. Data regarding composition, molecular weight and microstructure of PB_xGlux_yS copolyesters and homopolyesters are collected in Table 4.1. Copolyester compositions were determined by integration of the proton signals arising from BD and Glux units in the by ¹H NMR spectra. As it is seen in Table 4.1, copolyester compositions are very close to those used in their respective feeds with a slight excess in the Glux content. The GPC analysis revealed that polyesters were obtained with weight average molecular weights within the 46,000-26,000 range with dispersity degrees oscillating between 2.2 and 3.1. The general trend is that molecular weights slightly decrease with the increasing amount of Glux units in the polymer chain so that the minimum value is attained for the PGluxS homopolyester. Intrinsic viscosities decreased from 1.0 to near 0.4 dL·g⁻¹ in agreement with the trend observed for molecular weights. According to which has been repeatedly noticed for other polyesters containing sugar residues, such a trend is very likely determined by the high sensitivity to heat of 2,4:3,5-di-O-methylene-D-glucitol and the relatively high temperatures used in the polymerization reaction.

Table 4.1. Composition, molecular weights and microstructure of polyesters.

Polyester	Composition (mol/mol)		Molecular weight				Microstructure		
	Feed	Copolyester ^a	$[\eta]^b$ (dL·g ⁻¹)	M_n^c	M_w^c	D^c	Average sequence length		R^d
							n_B	n_G	
	X_{BD}/X_{Glux}						n_B	n_G	
PBS	100/0	100/0	1.00	17900	45600	2.5	-	-	-
PB ₉₅ Glux ₅ S	95/5	94.4/5.6	0.71	17000	43700	2.6	9.9	1	1.10
PB ₉₀ Glux ₁₀ S	90/10	88.9/11.1	0.65	14900	43400	2.9	6.3	1.2	0.96
PB ₇₀ Glux ₃₀ S	70/30	71.2/28.8	0.60	14000	39300	2.8	2.6	1.7	0.98
PB ₅₀ Glux ₅₀ S	50/50	46.2/53.8	0.59	12900	36700	2.8	1.6	2.6	1.00
PB ₃₀ Glux ₇₀ S	30/70	25.4/74.6	0.60	12600	38500	3.1	1.3	4.8	0.98
PGlucS	0/100	0/100	0.41	12300	26800	2.2	-	-	-

^a Molar composition determined by integration of ¹H NMR spectra.

^b Intrinsic viscosity measured in dichloroacetic acid at 25 °C.

^c Determined by GPC in HFIP against PMMA standards.

^d Degree of randomness of copolyesters calculated on the basis of the ¹³C NMR analysis.

The microstructure of the copolyesters was determined by ¹³C NMR taking benefit from the sensitiveness of the carbonyl groups to the sequence distribution at the dyads level (BB, BG, GB, GG). As a consequence of the occurrence of different dyads and also of the two orientations for the Glux unit, the CO signal splits into multiple peaks that appear spread within the 176.8–175.3 ppm interval (Figure 4.2).

Nevertheless, three groups of peaks may be discerned in such spectra which are arising from the four types of diol-dyads present in the copolyester chain. Although it is known that different carbons frequently have different relaxation times, it is not the case because the composition calculated using these carbon signals was the same as that obtained by ^1H NMR. Then, the integration of all the dyad-associated peaks and application of the equations given below, allowed estimating the number average sequence lengths to evaluate the microstructure of the copolyesters according to the degree of randomness R .

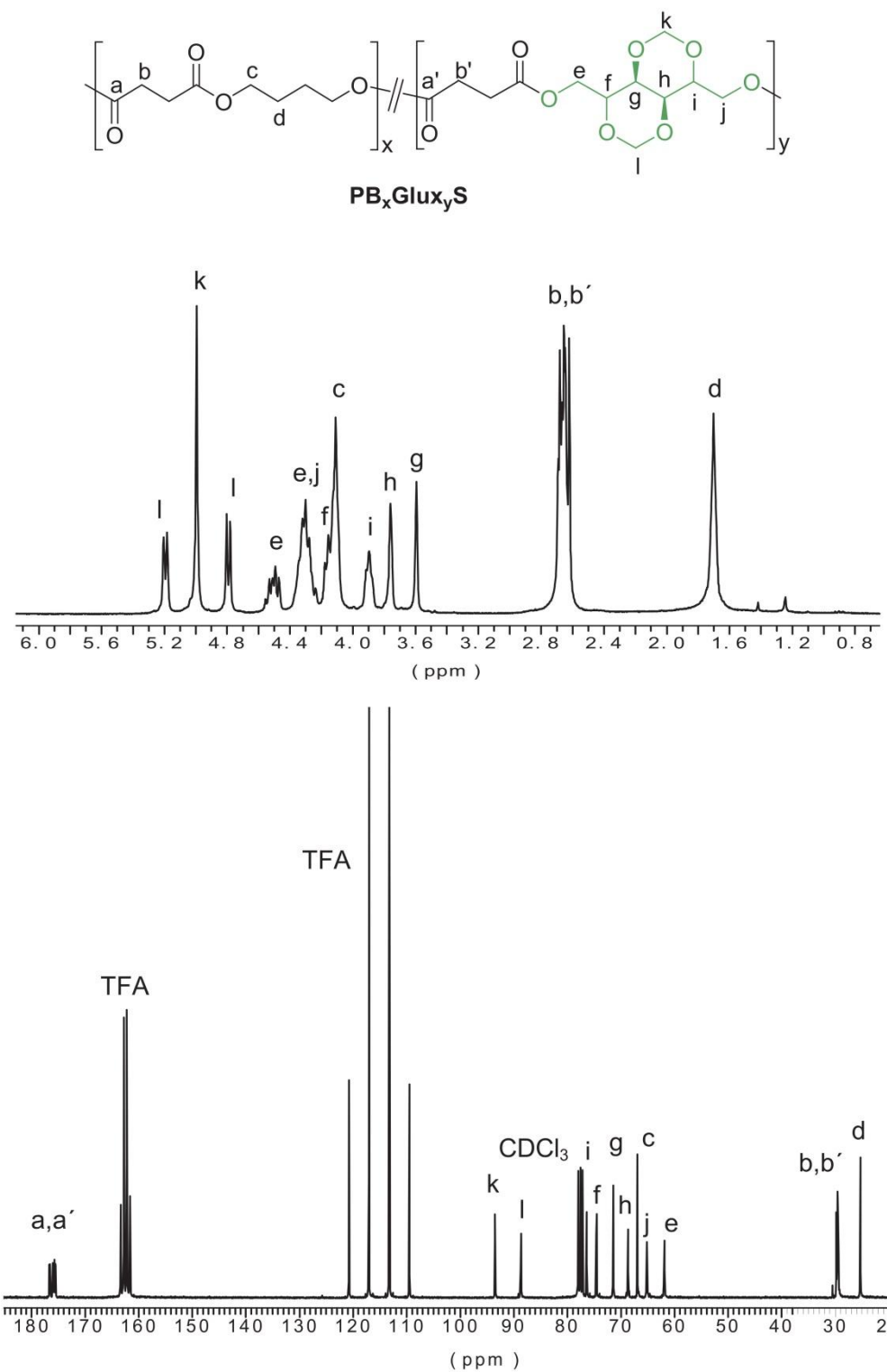


Figure 4.1. ¹H (top) and ¹³C (bottom) NMR spectra of PB₅₀Glux₅₀S copolyester.

The values resulting from these calculations are given in Table 4.1. and they indicate that an almost random microstructure is shared by all the copolyesters ($R \sim 1$).

$$n_B = (BB + 0.5(BG + GB)) / 0.5(BG + GB)$$

$$n_G = (GG + 0.5(GB + BG)) / 0.5(BG + GB)$$

$$R = 1/n_B + 1/n_G$$

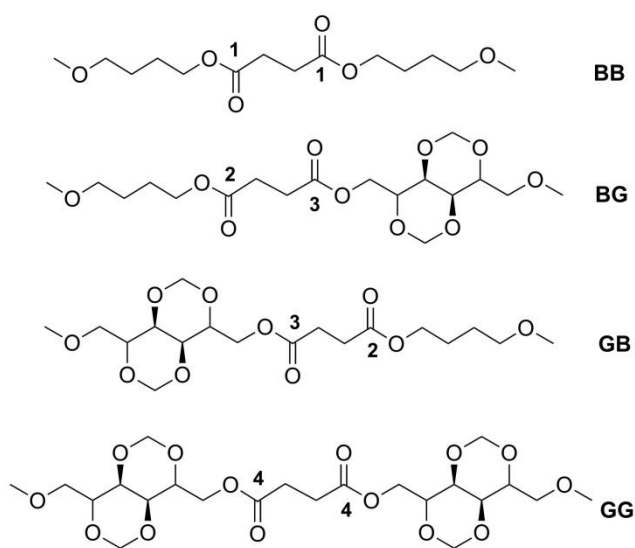
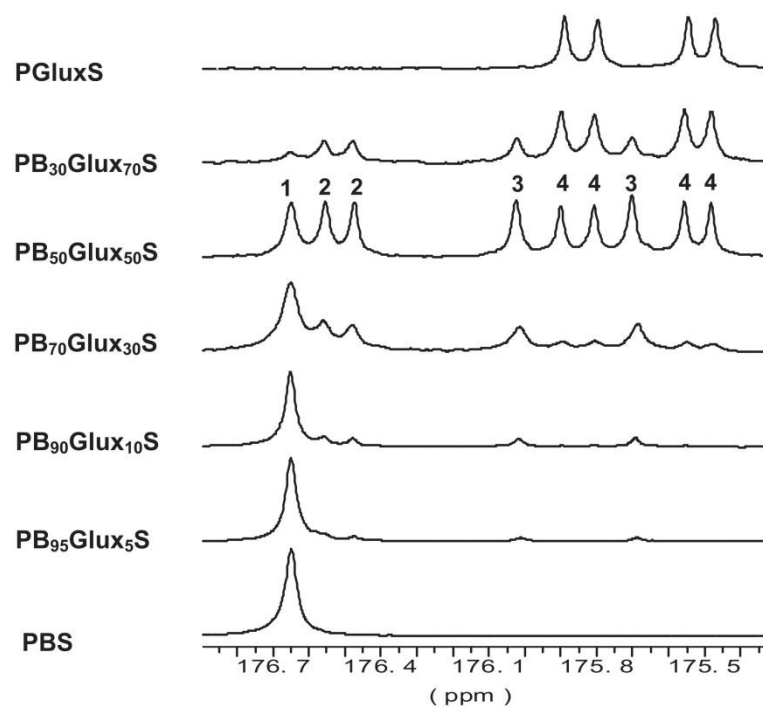


Figure 4.2. ^{13}C NMR spectra showing the changes undergone by the carbonyl signal of $\text{PB}_x\text{Glux}_y\text{S}$ copolyesters with variations in composition.

4.3.2. Thermal properties and crystallization

The basic thermal properties of the obtained copolyesters were evaluated by TGA and DSC with special attention to the influence of the presence of the Glux units on decomposition, melting and glass transition temperatures. Data afforded by these analyses are collected in Table 4.2.

TGA essays were carried out within the 30-600 °C temperature range under a nitrogen atmosphere, and the recorded TGA traces for the whole series are compared in Figure 4.3. All traces except that of PGluxS obey the same behavior pattern consisting of one only decomposition step that starts around 340 °C, falls down at the proximities of 400 °C (SI, annex B) and leaves less than 10% (w/w) of residual weight. A detailed comparison of the decomposition parameters reveals that the insertion of the Glux units in PBS does not alter significantly the thermal stability of the parent polyester if the case for homopolyester PGluxS is excluded. In fact, the maximum change observed for the onset temperature is a decrease in 10 °C whereas the maximum rate decomposition temperature slightly increases with copolymerization. The fact that an oppose tendency is observed for $^{\circ}T_d$ and $^{\max}T_d$ suggests the presence of small amounts of structural water associated to the Glux units in PB_xGlux_yS copolyesters. The exceptional behavior observed for PGluxS can be explained by assuming that it contains adsorbed water in much larger amounts than copolyesters, a conjecture that makes much sense given the 100 mole-% content of this homopolyester in Glux units. The high heat resistance displayed by PB_xGlux_yS is a really remarkable fact regarding the potential of these copolyesters to be used in applications involving thermal processing.

Table 4.2. Thermal and mechanical properties and X-ray spacings of PB_xGlux_yS polyesters.

Polyester	TGA ^a			DSC ^b							XRD ^c				Stress-strain essays ^d			
	^o T _d (°C)	^{max} T _d (°C)	RW (%)	First heating			Cooling	Second heating			<i>t</i> _{1/2} (min) (at °C)				<i>d</i> -(nm)	<i>E</i> (MPa)	<i>σ</i> _{max} (MPa)	<i>ε</i> (%)
				<i>T</i> _g (°C)	<i>T</i> _m (°C)	Δ <i>H</i> _m (J·g ⁻¹)	<i>T</i> _c (°C)	<i>T</i> _c (°C)	<i>T</i> _m (°C)	Δ <i>H</i> _m (J·g ⁻¹)	(75)	(80)	(85)	(90)				
PBS	340	396	3	-37	113	78	78	99	114	62	-	-	1.9	5.3	0.45, 0.40, 0.39	545 ± 11	32 ± 2	9 ± 1
PB ₉₅ Glux ₅ S	332	390	5	-28	106	70	62	90	106	63	1.2	2.3	-	-	0.45, 0.40, 0.39	482 ± 10	13 ± 2	4 ± 1
PB ₉₀ Glux ₁₀ S	330	392	3	-20	96	54	33	30	96	48	18.7	28.0	-	-	0.45, 0.40, 0.39	370 ± 13	16 ± 1	10 ± 2
PB ₇₀ Glux ₃₀ S	337	405	7	14	59	33	-	-	-	-	-	-	-	-	0.46, 0.40	348 ± 15	11 ± 1	4 ± 2
PB ₅₀ Glux ₅₀ S	343	407	9	54	-	-	-	-	-	-	-	-	-	-	-	1093 ± 16	15 ± 2	3 ± 2
PB ₃₀ Glux ₇₀ S	338	403	8	80	-	-	-	-	-	-	-	-	-	-	-	1356 ± 19	40 ± 3	6 ± 2
PGluxS	264	403	9	103	-	-	-	-	-	-	-	-	-	-	-	-	-	-

^a Onset decomposition temperature corresponding to 5% of weight loss (^oT_d), temperature for maximum degradation rate (^{max}T_d), and % of weight remaining after heating at 600 °C (RW).

^b Glass-transition temperature (*T*_g) taken as the inflection point of the heating DSC traces of melt-quenched samples recorded at 20 °C·min⁻¹. Melting (*T*_m) and crystallization (*T*_c) temperatures, and melting enthalpy (Δ*H*_m) measured at heating/cooling rates of 10 °C·min⁻¹. Isothermal crystallization half-time (*t*_{1/2}) determined at the indicated temperatures.

^c Bragg spacings measured by powder X-ray diffraction.

^d Elastic modulus (*E*), maximum stress (*σ*) and elongation to break (*ε*) measured by tensile testing from hot-pressing films.

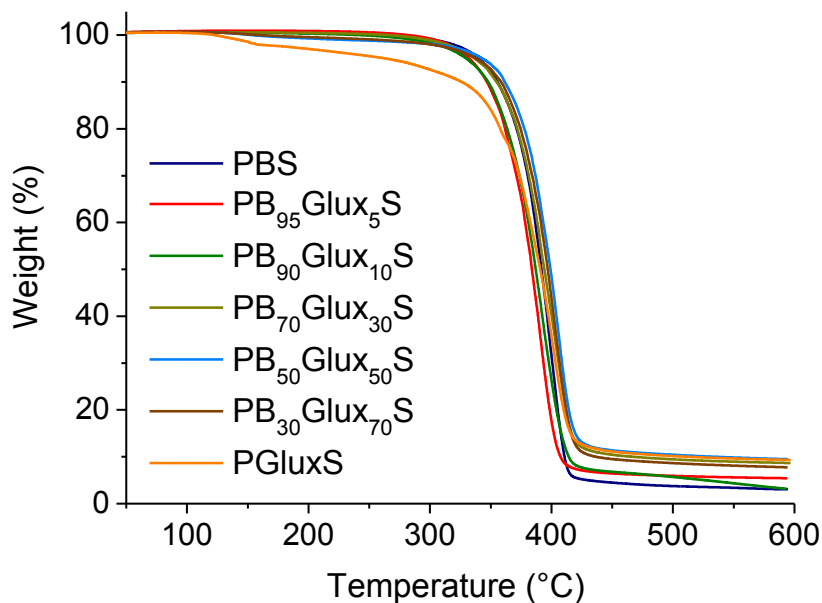


Figure 4.3. TGA traces of PB_xGlux_yS .

The glass transition and melting temperatures of PB_xGlux_yS copolyesters and homopolyesters were measured by DSC (SI, annex B). The T_g observed for copolyesters varied from -28 to 80 °C with values steadily increasing for increasing contents in Glux units (Table 4.2.). This range of values is fully consistent with the T_g values displayed by the parent homopolyesters (-37 °C and 103 °C for PBS and PGluxS, respectively). Such strong enhancing effect is just simply the consequence of the increasing in chain stiffness that is produced when the flexible butylene segment is replaced by the rigid bicyclic Glux structure.

The influence of copolymerization on the melting/crystallization behavior was brought into evidence by DSC. As it is shown in Figure 4.4.a, the DSC heating traces of copolyesters with contents in Glux units of 30 mole-% as maximum displayed an endothermic peak characteristic of melting and revealed therefore that they are semicrystalline. Both T_m and ΔH_m decreased as the presence of Glux units increased. Copolyesters with Glux contents above 30 mole-% as well as the PGluxS homopolyester produced plain traces without any vestige of crystallinity. This tendency is a consequence of the depressing in chain regularity that is caused by the partial replacement of butylene units by the Glux units.

The X-ray diffraction analysis corroborated the DSC results by showing discrete scattering diffraction for PBS and PB_xGlux_yS copolyesters containing up to 30% of Glux units with a peak sharpness and intensity decreasing with the increasing B/Glux ratio (Figure 4.4.b). Moreover the reflections observed for the semicrystalline copolyesters

were coincident in both spacing and intensity with those characteristic of PBS,¹³ which is indicative that the crystal structure of the homopolymer is retained after copolymerization.

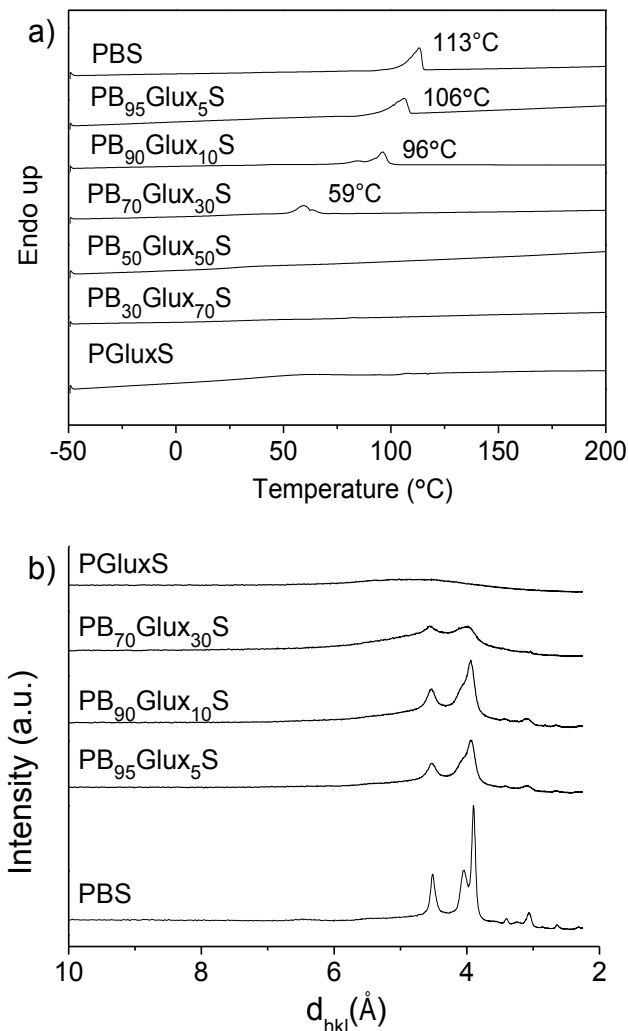


Figure 4.4. DSC heating traces of the whole series of PB_xGlux_yS recorded at heating at 10 °C·min⁻¹ from samples coming from synthesis (a), X-ray diffraction profiles of the indicated PB_xGlux_yS copolyesters (b).

The trend to crystallize is a relevant property of semicrystalline polyesters that has to be considered when they are intended to be used as thermoplastics. As it can be seen in Table 4.2. only PB_xGlux_yS copolyesters containing 10 mole-% of Glux as maximum are able to crystallize from the melt. Although these results clearly indicated that crystallizability of PBS is strongly depressed by the insertion of Glux units in the polyester chain, and that such effect has been reported to invariably occur for other related copolyesters containing sugar units, a comparative crystallization kinetics study has been undertaken in this work to quantify the influence of Glux in this regard.

PBS, PB₉₅Glux₅S and PB₉₀Glux₁₀S were compared regarding their isothermal crystallization although a common temperature could not be set for the three compounds due to their large differences in crystallizability. The study also included the crystallization of each polymer at two different crystallization temperatures in order to estimate the influence of temperature on crystallization rate. The graphical representations of crystallization data as a function of time are depicted in Figure 4.5. for the three compared polyesters. The kinetics was evaluated by the classical Avrami model,^{14,15} and the crystallization half-times afforded by this analysis are given in Table 4.2. It is clearly noticeable how $t_{1/2}$ is strongly influenced by composition so it increased more than ten times for an increase in the Glux content of only 5 mole-%. On the other hand, the observed inverse dependence of crystallization rate on temperature indicates that in both PBS and copolyesters, the crystallization process is controlled mainly by nucleating factors rather than by chain mobility.¹⁴

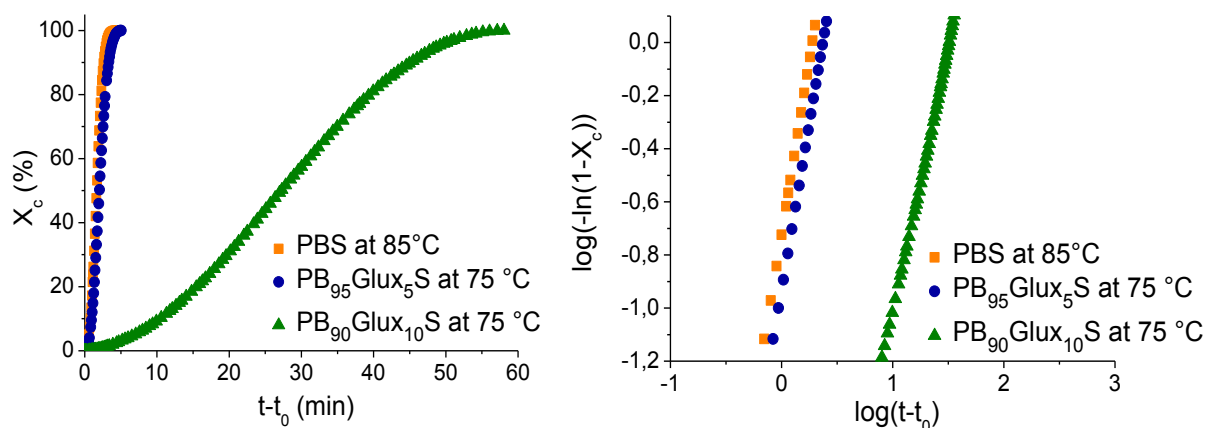


Figure 4.5. Isothermal crystallization of PBS, PB₉₅Glux₅S and PB₉₀Glux₁₀S at the indicated temperatures. Relative crystallinity vs. crystallization time (left), Avrami representation of crystallization data (right).

4.3.3. Stress-strain behavior

For a preliminary assessment of the mechanical behavior of PB_xGlux_yS, films of the copolyesters were prepared by hot-pressing and subjected to tensile testing in quintuplicates. Considering the strong influence that crystallinity has on mechanical properties, the samples prepared for testing were checked by DSC. These measurements proved that melting parameters (T_m and ΔH_m) of films were close to

those recorded for the powdered samples with the initial PBS crystallinity decreasing about 20, 30 and 50% for 5, 10 and 30 mole-% of Glux in the copolyester, respectively, to finally disappear for higher contents. The copolyesters were tested in parallel and compared with PBS. The mechanical parameters obtained in these essays are gathered in Table 4.2. Results showed that the copolyesters with amounts of Glux units till 30 mole-%, which are those displaying crystallinity, undergo a reduction in Young modulus and tensile strength whereas those with higher contents of Glux exhibit a sustained increasing in these parameters. Although rather wandering values were found for the elongation to break, probably due to sample heterogeneities and divergences in molecular weight, it can be reasonably concluded that ductility is not significantly modified by copolymerization. The ambiguous mechanical behavior exhibited by PB_xGlux_yS copolyesters reflects the ambivalent effect of the insertion of Glux unit in the PBS chain as far as crystallinity and chain mobility in the amorphous phase is concerning. For low contents in Glux, crystallinity is the main factor determining the stress-strain response, and E and σ_{max} decrease with copolymerization. Conversely, for high Glux contents crystallinity disappears and T_g becomes the only property affecting deformation. Consequently the mechanical performance is improved with copolymerization to the point that amorphous PB_xGlux_yS copolyesters arrive to be stiffer and stronger than PBS.

4.3.4. Hydrolytic degradation and biodegradation

In order to evaluate the effect of Glux on the behavior of PBS regarding its degradability and biodegradability, several essays were carried out in parallel using PBS, $PGluxS$ and $PB_{70}Glux_{30}S$ copolyester. Samples were incubated in the appropriate aqueous buffer solution, with or without lipases added, and degradation evolution was followed by monitoring the changes taking place in weight and molecular weight of the residue. Firstly, the degradation at pH 2.0 was performed to evaluate the influence of Glux on the chemical hydrolysis of PBS and results coming out from these essays have been plotted in Figure 4.6. (a and a'). According to what should be expected for aliphatic polyesters, a continuous decreasing in both sample weight and polymer molecular weight is observed for the three polyesters along incubation time with the noticeable remark that changes became more accentuated for Glux containing polyesters. In second place the degradation of the three polyesters incubated under approximately physiological conditions both with and without porcine pancreas lipases added, was examined, and results obtained therein are presented also in Figure 4.6. (b

and b'). As expected, degradation at pH 7.4 took place in much less extent than at pH 2.0 but the changes observed in both W and M_n continued being of the same sign as before for the three tested polyesters. Interestingly, degradation was notably enhanced when lipases were added to the incubation medium to the point that changes taking place in W and M_n were comparable to those observed at pH 2.0. To get insight into the hydrolytic mechanism, the residue left by the PB₇₀Glux₃₀S after incubation at pH 2.0 for 40 days was analyzed by ¹H NMR, which revealed that the content in Glux of this sample had decreased about 10%, *i.e.* about one third of the Glux units were released upon degradation. This result is demonstrative that hydrolysis of PBS containing Glux units mostly happens by breaking those ester groups in which the carbohydrate units are directly implied. All these results lead to conclude that not only the chemical degradation but also the biodegradability of PBS, becomes enhanced by the insertion of Glux units in the polyester chain.

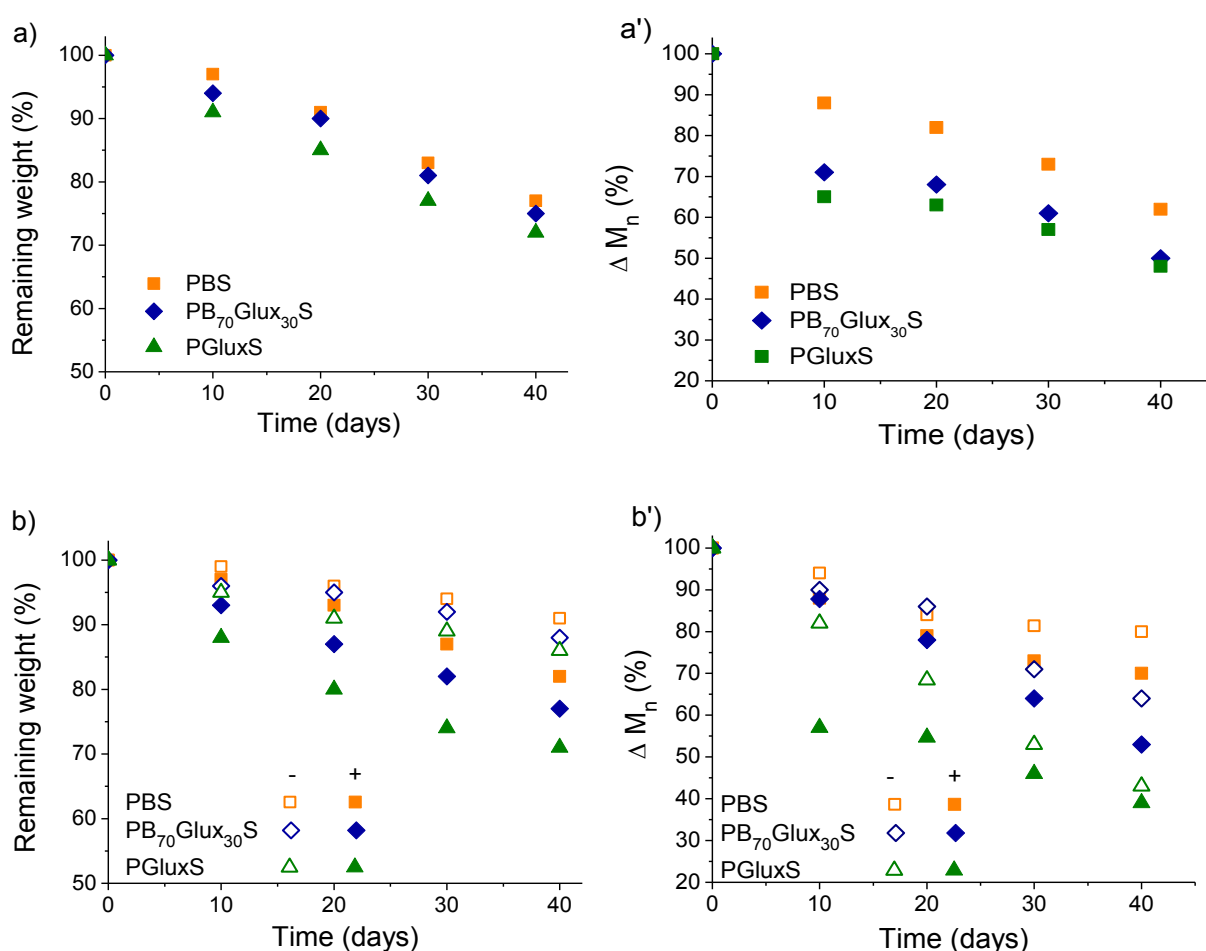


Figure 4.6. Degradation plots of PBS, PB₇₀Glux₃₀S, PGluxeS at pH 2.0 (a, a') and pH 7.4 with and without porcine pancreas enzyme added (b, b').

4.3.5. Sugar-based bicyclic diols compared

The results achieved in this work prove the ability of Glux-diol (2,4:3,5-di-O-methylene-D-glucitol) to be used as monomer for the preparation of PBS copolyesters with conveniently modified properties. Since Glux and Manx structures have the same chemical constitution but differ in configuration, and given the strong influence that the molecular symmetry usually has on polymerization and polymer properties, it is of interest comparing these two diols as comonomers of 1,4-butanediol in the preparation of PBS copolyesters.

In first place the results obtained in the synthesis of PB_xGlux_yS and PB_xManx_yS will be compared. Both types of copolyesters have a random microstructure and their compositions are in general close to those used in their respective polymerization feeds with divergences in the two cases due the higher volatility of the sugar-based diol. The Manx configuration has a C_2 symmetry and therefore the two hydroxymethyl groups of Manx-diol are indistinguishable and equatorially oriented. Conversely, in the asymmetrical Glux-diol, one CH_2OH group is equatorial and the other one is axial. A recent study on the use of Glux-diol as comonomer in the solid state modification of PBT has shown that the reactivity of the axially oriented hydroxyl function in transesterification reactions is significantly hindered.¹⁶ Therefore, smaller conversions, and consequently lower molecular weights would have to be expected for copolyesters made from Glux-diol compared to those from Manx-diol, provided that both are obtained under the same reaction conditions. The weight-average molecular weights of PB_xGlux_yS and PB_xManx_yS copolyesters obtained using the same procedure are compared in Figure 4.7a. for a broad range of compositions. As observed, M_w of the copolyesters are invariably lower than that of PBS and the reduction becomes more noticeable as the content in sugar-based units increases. Nevertheless divergences between Glux and Manx containing copolyesters are not large and they do not show any clear trend with their respective M_w differing between each other in less than 15% in any sense. It seems therefore that the limitations found in attaining high molecular weight PBS copolyesters containing large amounts of either Manx or Glux, must be caused by the sensitivity to heating of the sugar-based compounds, rather than by differences in the reactivity of the hydroxyl functions. Differences observed between the two series can be therefore attributed to small deviations in the preparation procedure that escape control at this stage of the study.

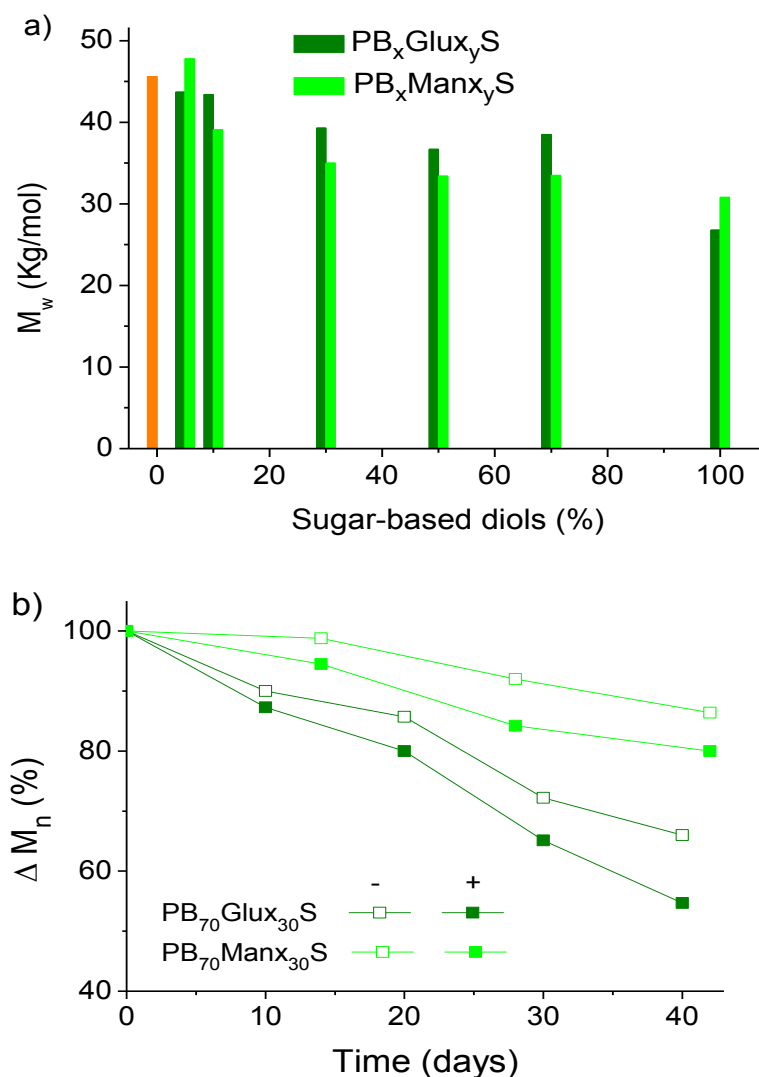


Figure 4.7. Compared weight-average molecular weight of PBS copolyesters made from Glux-diol and Manx-diol. PBS data in orange (a), degradation curves representing the decay in molecular weight against incubation time for isocompositional PBS copolyesters containing Glux and Manx at pH 7.4, (+) and (-) stand for presence and absence of lipases (b).

The symmetry properties of Glux and Manx will be directly reflected in the stereochemistry of their respective PBS homopolyesters and copolyesters. Although neither PB_xGlux_yS nor PB_xManx_yS copolyesters should be expected to be stereoregular due to the random distribution of the comonomers along their respective chains, the disorder will be less severe in the later due to the twofold symmetry of the Manx configuration. Since only one spatial arrangement is feasible for the Manx unit in the polyester chain, the PManxS homopolyester will be stereoregular. On the contrary, the insertion of Glux-diol in the PBS chain may happen with two different orientations. Therefore two spatially different Glux units will be found in both PB_xGlux_yS copolyesters and the PGluxS homopolyester and none of them will be stereoregular.

Accordingly PB_xMan_xS copolyesters show a greater ability to crystallize; they are crystalline over the whole range of compositions with crystallinity degrees oscillating between 50 and 65%. As it is shown in Figure 4.8a., T_m values in this series display a parabolic tendency with the minimum placed at comonomer compositions no far from 30 mole-% and with the maximum value at 100 mole-% (homopolyester $PManxS$). In contrast, only PB_xGlux_yS copolyesters with 30 mole-% of Glux units at maximum were found to be crystalline and no sign of crystallinity was detected for $PGluxeS$. Nevertheless practically identical T_m values are displayed by the two series over the interval in which PB_xGlux_yS are able to crystallize.

A highly pronounced increasing effect on T_g of PBS is exerted by the insertion of either Glux or Man_x units in the polyester chain due to their stiff structure compared to the rather flexible structure of the butylene group. This is perhaps the most interesting outcome of using bicyclic sugar-based compounds as comonomers in the synthesis of aliphatic polyesters because the importance that the glass transition has on their mechanical performance. A close comparison of the T_g values displayed by PB_xGlux_yS and PB_xMan_xS series is graphically afforded in Figure 4.8b. An almost linear trend is followed in both cases with slopes of ~ 1.5 and ~ 1.0 $^{\circ}C \cdot \text{mole-}\% \cdot \text{sugar unit}^{-1}$, respectively. The fact that higher T_g 's are displayed by copolyesters containing Glux units is really amazing since they are less crystalline than their isocompositional Man_x analogs. Apparently it is the more corrugated shape of the Glux structure which additionally contributes to hindering the mobility of the polyester chain and gives rise to an exceptionally increase in T_g .

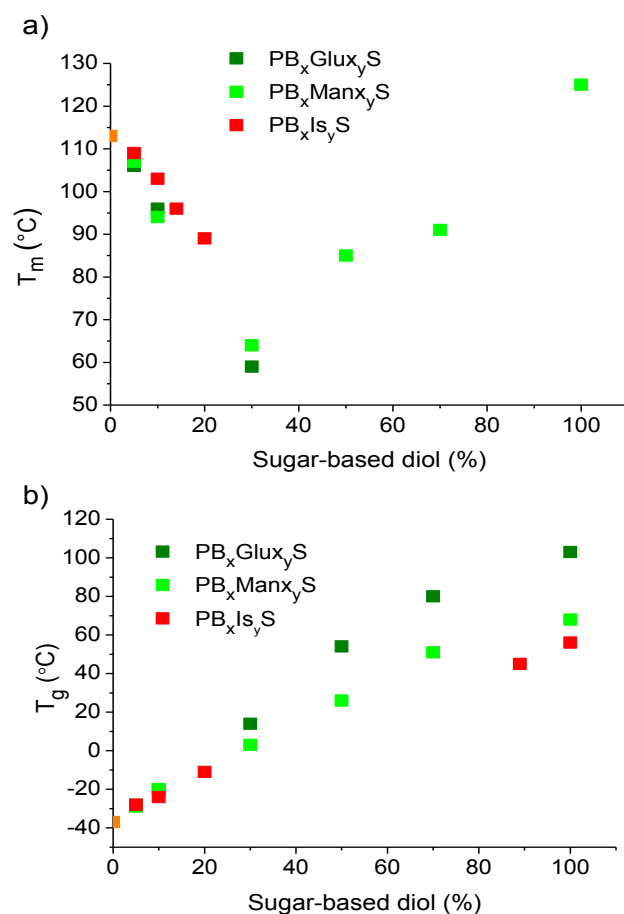


Figure 4.8. Compared melting (a) and glass transition (b) temperatures of PBS copolyesters made from Glux-diol, Manx-diol and isosorbide.^{17,18} PBS data in orange.

Biodegradability is a distinguishing feature of PBS of high relevance to its further development. PBS displays a partial biodegradability that enables it to be used as compostable material for packaging as well as a bioassimilable biomaterial for temporal applications. Attempts made in the past to improve the thermal and mechanical properties of PBS by inserting aromatic units in its chains invariably resulted in a notably reduction or even total suppression of the initial biodegradability of the polyester.² On the contrary, copolymerization of PBS with sugar-based monomers has proven to be not only non-detrimental in this regard but favoring both chemical hydrolysis and biodegradation.^{11,19} The presence of the sugar moiety in the polyester chain does not deactivate the enzyme function but favors its action due to increasing chain hydrophilicity. Furthermore, it has been shown that hydrolysis of the ester group in sugar-based copolyesters is hastened when a sugar residue is directly involved. In Fig. 4.7b, the reduction in molecular weight observed for two PBS copolyesters containing respectively similar amounts of Glux and Manx upon aqueous incubation,

either in absence or presence of lipases, is comparatively plotted against time. Both units show to have an enhancing effect of the degradability of PBS but apparently Glux is significantly more efficient than Manx. Such a difference is also observed when the homopolyesters PGluxS and PManxS are compared (SI). The higher enhancing effect displayed by Glux is most likely due to the strong depressing effect that this unit has on PBS crystallinity.

Since isosorbide (Is, 1,3:4,6-dianhydride-D-glucitol) is another glucose-derived bicyclic diol that has achieved in these last years wide recognition for the synthesis of bio-based copolyesters^{20,21} the present comparative analysis should be extended to this compound. Unfortunately only a few papers dealing with PBS copolyesters containing isosorbide are found in the accessible literature,^{17,18} and data afforded by them are incomplete or not fully suitable for a reliable comparison. Nevertheless some valuable inferences can be drawn by careful analysis of the available information. Several PlsS homopolyesters were reported with different molecular weights. These polyesters were intended for coating applications and were obtained with number-average molecular weights below $4,000 \text{ g}\cdot\text{mol}^{-1}$. The T_g reported for these copolyesters were between ~ 50 and ~ 70 °C with the maximum value corresponding to the homopolyester with M_n of $3,100 \text{ g}\cdot\text{mol}^{-1}$. The $\text{PB}_{11}\text{Is}_{89}\text{S}$ copolyester with M_n about 14,000 with T_g of ~ 45 °C and the PlsS homopolyester with M_n about 13,000 and T_g of ~ 56 °C. More recently, the $\text{PB}_x\text{Is}_y\text{S}$ copolyesters were prepared with astonishingly high molecular weights ($45,000 < M_n < 55,000$) although only polymers with low contents in Is (less than 15 mole-%) were described. These copolyesters were reported to be semicrystalline with T_m decreasing with composition down to 89 °C and T_g increasing from -28 up to -11 °C, and their mechanical properties were comparable to those displayed by PBS. The data available on $\text{PB}_x\text{Is}_y\text{S}$ copolyesters, although scarce, are enough to reveal that the effect of Is on PBS properties is in line with that exerted by Manx and Glux and rather closer to the former (Fig. 4.8). Unfortunately no data for $\text{PB}_x\text{Is}_y\text{S}$ copolyesters with higher contents in Is are available and no information about the influence of Is on the degradability of PBS have been published so far, at least to our knowledge.

4.4. Conclusions

A series of PBS copolyesters ($\text{PB}_x\text{Glux}_y\text{S}$) containing bicyclic acetalized units derived from D-glucose (Glux) in addition to the homopolyester PGluxS were synthesized by melt polycondensation from mixtures of 1,4-butanediol, Glux-diol and

dimethyl succinate. A complete incorporation of Glux-diol as well as satisfactory molecular weights were in general attained by careful selection of the reaction conditions. As it is usually observed for other sugar-based copolyesters, PB_xGlux_yS had a random microstructure. The presence of Glux in the polyester chain significantly modified the properties of PBS. Melting temperature and crystallinity were severely depressed so copolyesters containing more than 30 mole-% of Glux including the homopolyester were amorphous. Oppositely, the glass transition temperature of PBS dramatically increased with the content in Glux units with a slope not paragoned by any other sugar-based described up to date. Mechanical properties of the PB_xGlux_yS largely varying with composition with good results obtained for copolyesters with high contents in Glux. In line with the effect observed for other sugar-based copolyesters, PB_xGlux_yS display higher sensitivity to both hydrolytic degradation and biodegradation than PBS. All these results lead to finally conclude that Glux-diol is a highly appropriate bio-based comonomer to notably improve the properties of PBS as far as T_g and degradability are concerned. The exceptionally good accessibility of D-glucose as feedstock for Glux-diol is an additional merit of this compound if the modified PBS was intended to be used for industrial purposes.

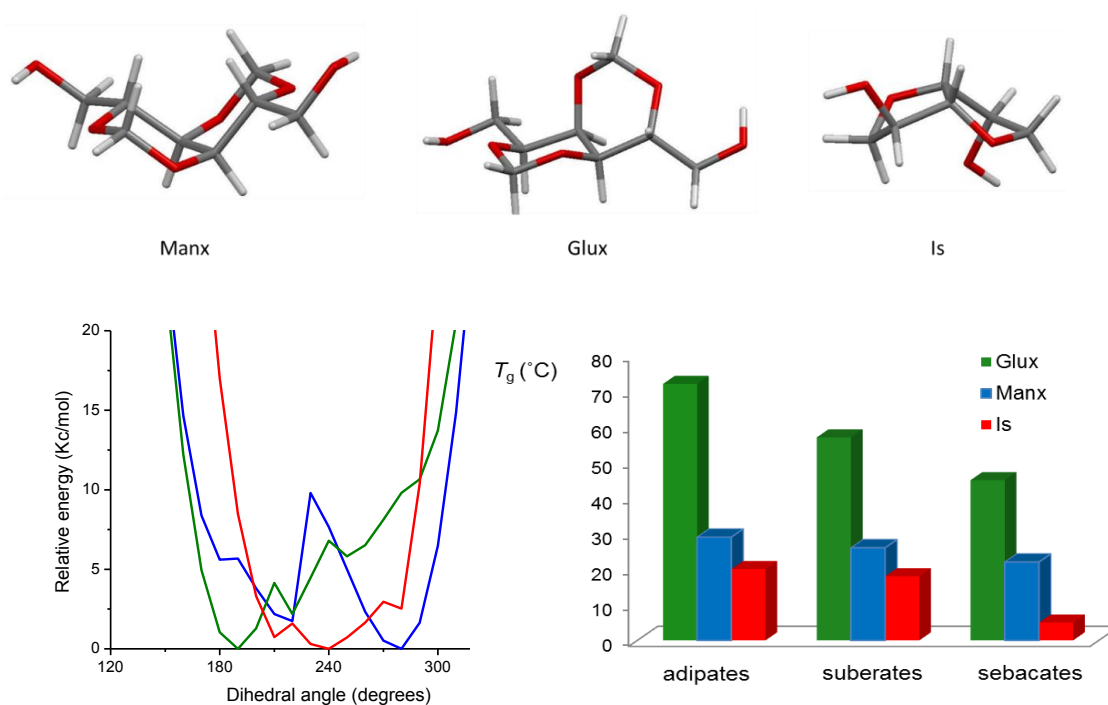
4.5. References

1. (a) Li, J.; Luo, X.; Lin, X. *Mater. Des.* **2013**, *46*, 902–909; (b) Li, J.; Luo, X.; Lin, X.; Zhou, Y. *Starch-Stärke* **2013**, *65*, 831-839.
2. Xu, J.; Guo, B.-H. *Biotechnol. J.* **2010**, *5*, 1149-1163.
3. Snowdon, M.; Mohanty, A.K.; Misra, M. *Macromol. Mater. Eng.* **2015**, *300*, 118-126.
4. Yang, J.; Hao, Q.; Liu, X.; Ba, C.; Cao, A. *Biomacromolecules* **2004**, *5*, 209-218.
5. (a) Lavilla, C.; Alla, A.; Martínez de Ilarduya, A.; Benito, E.; García-Martín, M.G.; Galbis, J.A.; Muñoz-Guerra, S. *Polymer* **2012**, *53*, 3432-3445; (b) Lavilla, C.; Muñoz-Guerra, S. *Green Chem.* **2013**, *15*, 144-151.
6. Muñoz-Guerra, S.; Lavilla, C.; Japu, C.; Martínez de Ilarduya, A.; *Green Chem.* **2014**, *16*, 1716-1739.
7. Japu, C.; Alla, A.; Martínez de Ilarduya, A.; García-Martín, M.G.; Benito, E.; Galbis, J.A.; Muñoz-Guerra, S. *Polym. Chem.* **2012**, *3*, 2092-2101.
8. Lavilla, C.; Martínez de Ilarduya, A.; Alla, A.; García-Martín, M.G.; Galbis, J.A.; Muñoz-Guerra, S. *Macromolecules* **2012**, *45*, 8257-8266.
9. Japu, C.; Martínez de Ilarduya, A.; Alla, A.; García-Martín, M.G.; Galbis, J.A.; Muñoz-Guerra, S. *Polym. Chem.* **2014**, *5*, 3190-3202.
10. Lavilla, C.; Martínez de Ilarduya, A.; Alla, A.; Muñoz-Guerra, S. *Polym. Chem.* **2013**, *4*, 282-289.
11. Lavilla, C.; Alla, A.; Martínez de Ilarduya, A.; Muñoz-Guerra, S. *Biomacromolecules* **2013**, *14*, 781-793.
12. Marín, R.; Muñoz-Guerra, S. *J. Appl. Polym. Sci.* **2009**, *114*, 3723-3736.
13. Ihn, K.J.; Yoo, E.S.; Im, S.S. *Macromolecules* **1995**, *28*, 2460-2464.
14. Bodor, G. *Structural investigation of polymers*; Ellis Hordwood, Toronto, 1991, ch. 6, 201-227.
15. Martins, J.A.; Zhang, Wd.; Brito, A.M. *Rev. Sci. Instrum.* **2005**, *76*, 105105.
16. Gubbels, E.; Lavilla, C.; Martínez de Ilarduya, A.; Noordover, B.A.J.; Koning, C.E.; Muñoz-Guerra, S. *J. Polym. Sci, Part A: Polym. Chem.* **2014**, *52*, 164-177.
17. Tan, L.; Chen, Y.; Zhou, W.; Wei, J.; Ye, S. *J. Appl. Polym. Sci.* **2011**, *121*, 2291-2300.
18. Jacquél, N.; Saint-Loup, R.; Pascault, J.-P.; Rousseau, A.; Fenouillot, F. *Polymer* **2015**, *59*, 234-242.
19. Zakharova, E.; Lavilla, C.; Alla, A.; Martínez de Ilarduya, A.; Muñoz-Guerra, S. *Eur. Polym. J.* **2014**, *61*, 263-273.
20. (a) Noordover, B.A.J.; Heise, A.; Malanowski, P.; Senatore, D.; Mak, M.; Molhoek, L.; Duchateau, R.; Koning, C.E.; Benthem, R.A.T.M. *Prog. Org. Coat.* **2009**, *65*, 187-196; (b) Noordover, B.A.J.; Staalduinen, V.G.; Duchateau, R.; Koning, C.E.; Benthem, R.A.T.M.; Mak, M.; Heise, A.; Frissen, A.E.; Haveren, J. *Biomacromolecules* **2006**, *7*, 3406-3416.
21. Sablong, R.; Duchateau, R.; Koning, C.E.; Wit, G.; Es, D.; Koelewijn, R.; Haveren, J. *Biomacromolecules* **2008**, *9*, 3090-3097.

Chapter 5

Sugar-based bicyclic monomers for aliphatic polyesters: A comparative appraisal of acetalized alditols and isosorbide

Three series of polyalkanoates (adipates, suberates and sebacates) were synthesized using as monomers three sugar-based bicyclic diols derived from D-glucose (Glux-diol and isosorbide) and D-mannose (Manx-diol). Polycondensations were conducted in the melt applying similar reaction conditions for all cases. The aim was to compare the three bicyclic diols regarding their suitability to render aliphatic polyesters with enhanced thermal and mechanical properties. The ensuing polyesters had molecular weights (M_w) in the 25,000-50,000 g/mol range with highest values being attained for Glux-diol. All the polyesters started to decompose above 300 °C and most of them did not display perceivable crystallinity. On the contrary, they had glass transition temperatures much higher than usually found in homologous polyesters made of alkanediols, and showed a stress-strain behavior consistent with their T_g values. Glux-diol was particularly effective in increasing the T_g and to render therefore polyesters with high elastic modulus and considerable mechanical strength.



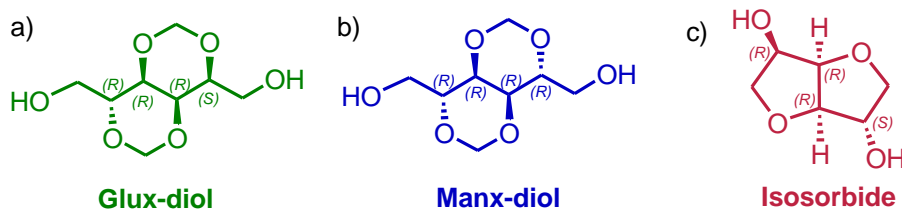
This work was published as: E. Zakharova, A. Martínez de Ilarduya, S. León, S. Muñoz-Guerra, Sugar-based bicyclic monomers for aliphatic polyesters: a comparative appraisal of acetalized alditols and isosorbide, *Des. Monomers Polym.* **2016**, *20*, 157-166.

5.1. Introduction

Polyesters are definitely among the most promising families of renewable polymers because the building-blocks needed for their synthesis, both diols and diacids, are relatively easy accessible.¹ Although aromatic polyesters (PET, PBT, etc...) are predominant at the industrial scale, aliphatic polyesters are rapidly increasing in importance due to their unique ability for combining a satisfactory performance with a good biocompatibility and significant biodegradability. Although ROP is the polymerization procedure usually preferred for producing some relevant aliphatic polyesters (poly(L-lactic acid), poly(ϵ -caprolactone), etc...), most of polyesters are usually obtained by melt polycondensation of alkanediols and either α,ω -alkanedioic acids or their methyl esters.²

Carbohydrate-based diols and diacids with a bicyclic structure are particularly interesting building-blocks for polyesters synthesis because they are unique in increasing chain stiffness and providing them therefore with high glass transition temperatures.^{3,4} The isohexide coming from D-glucose (dianhydro-1,4:3,6-D-glucitol) is commonly known as isosorbide, abbreviated as Is, and it is currently produced on industrial scale. Literature is plenty of references to polycondensation polymers and copolymers made from Is, and several Is containing copolyesters have achieved commercialization.⁵⁻⁷ In these last years, another family of based-carbohydrate bicyclic monomers has emerged. This comprises among others, alditols and aldaric acids methylene diacetals with a structure made of two fused 1,3-dioxane rings. The bicyclic diacetalized hexitols derived from D-mannose and D-glucose (2,4:3,5-di-O-methylene-D-mannitol and -D-glucitol), abbreviated as Manx-diol and Glux-diol, have been extensively explored as monomers for the synthesis of aromatic and aliphatic copolyesters.^{4,8} The results reported on these monomers have clearly shown that they may be efficiently used for melt polycondensation and that they are able to enhance the thermal and mechanical properties of polyesters while providing them with a significant biodegradability.^{9,10}

In the present chapter we wish to report a study comparing Glux-diol, Manx-diol and Is (Scheme 5.1.) for the synthesis of aliphatic homopolyesters by polycondensation in the melt. Three series of polyalkanoates made from dicarboxylic acids with 6, 8 and 10 carbon atoms have been chosen for this study. The value of this work relies on the high sustainable character of the sugar-based homopolyesters that are prepared as well as on the enhancing effect that the bicyclic structure exerts on their glass-transition temperature.

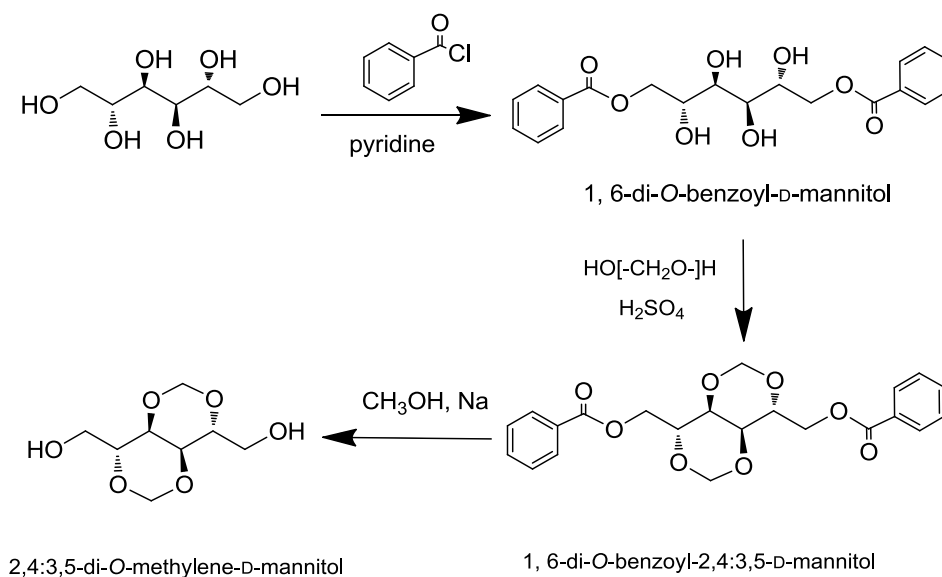


Scheme 5.1. Molecular structures of Glux-diol (a), Manx-diol (b) and Is (c).

5.2. Experimental part

5.2.1. Monomer synthesis

A solution of benzoyl chloride in dry pyridine is added drop-wise to a solution of D-mannitol in dry pyridine (Scheme 5.2.). The mixture is stirred at room temperature for 5 h and then poured into ice-water. The precipitated solid is filtered, washed with cold water and with chloroform, dried, and recrystallized from ethanol. To a mixture of 1,6-di-O-benzoyl-D-mannitol and paraformaldehyde, 96% sulfuric acid is added drop-wise, and the mixture is stirred for 3 h at room temperature. The reaction mixture is then repeatedly extracted with chloroform. The combined organic layers are washed with ammonia and water and dried over anhydrous sodium sulfate. The solution is evaporated to a solid residue, which is recrystallized from ethanol. A dispersion of 1,6-di-O-benzoyl-2,4:3,5-di-O-methylene-D-mannitol in dry methanol is stirred overnight with a small piece of sodium. The solution is treated with cation exchange resin, the resin is filtered, and the filtrate is concentrated to dryness. The resulting semisolid residue is washed with diethyl ether and recrystallized from ethanol.



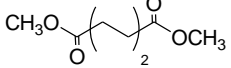
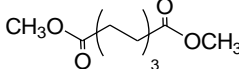
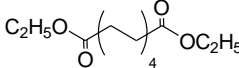
Scheme 5.2. Synthesis of 2,4:3,5-di-O-methylene-D-mannitol.

2,4:3,5-di-O-methylene-D-glucitol were synthesized by the protocol described in section 4.2.1.

5.2.2. Polymer synthesis

The three sets of sugar-based polyesters examined in this work, which amounts a total of nine different polymers, with indication of the monomers they come from, as well as the abbreviations used for naming them, are listed in Table 5.1. They all were synthesized by melt polycondensation of mixtures composed of the corresponding alkanedioic dialkyl ester and bicyclic diol using similar reaction conditions for all cases. It should be noted that 10%-mole excess of diol respect to diester was routinely used to compensate possible evaporation losses.

Table 5.1. Aliphatic polyesters studied in this work.

Alkylenediester	Sugar-based bicyclic diol		
	Glux-diol	Manx-diol	Is
Dimethyl adipate 	PGluxAdi	PManxAdi	PlsAdi
Dimethyl suberate 	PGluxSub	PManxSub	PlsSub
Diethyl sebacate 	PGluxSeb	PManxSeb	PlsSeb

The antioxidants Irganox 1010 (0.2% w/w) and Irgafos 126 (0.6% w/w) were then added to minimize possible degradation of the thermally sensitive sugar-based monomers. As usual, polymerization was made to proceed through two steps. Transesterification reactions taking place in the first step were conducted at temperatures increasing from 160 up to 200 °C for a period of time oscillating between 3 and 6 h depending on the case. A nitrogen flow was applied at this step to keep the pressure around one bar in order to minimize volatilization of diols and avoid oxidation of the sugar-based compounds. Polycondensation reactions occurring in the second step were performed at 180-220 °C for 3-8 h. High vacuum (0.03-0.06 mbar) was applied at this stage with the object of favoring the removal of by products and attaining high conversions. The chemical constitution and purity of the prepared polyesters were ascertained by NMR.

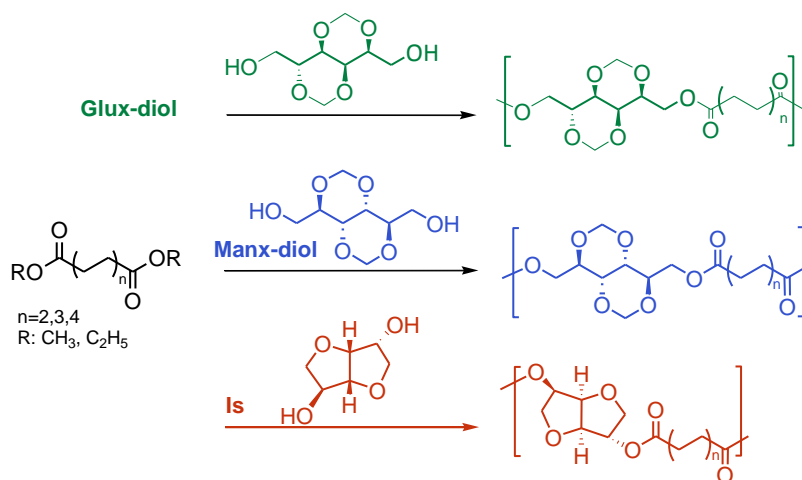
5.3. Results and discussion

5.3.1. Synthesis and chemical structure

The bicyclic acetalized alditols 2,4:3,5-di-O-methylene-D-glucitol (Glux-diol) and 2,4:3,5-di-O-methylene-D-mannitol (Manx-diol) were prepared from commercially

available 1,5-D-gluconolactone and D-mannitol respectively, in satisfactory yields and with the purity required for polycondensation.

Polycondensation reactions were performed according to Scheme 5.3. Reaction conditions were optimized for each individual system and for the two steps with the purpose of reaching high molecular weights without apparent decomposition of the sugar-based compounds. A detailed account of temperature and time values applied at each case is given in Table 5.2. Polycondensation proceeded invariably with a continuous increase in viscosity of the reaction mixture which usually became so high as to impede stirring.



Scheme 5.3. Polycondensation reactions leading to aliphatic polyesters.

Table 5.2. Molecular weights and reaction conditions selected for the preparation of aliphatic polyesters.

Polyester	Molecular weights				Reaction conditions	
	$[\eta]^a$ ($\text{dL}\cdot\text{g}^{-1}$)	M_n^b ($\text{g}\cdot\text{mol}^{-1}$)	M_w^b ($\text{g}\cdot\text{mol}^{-1}$)	\mathcal{D}^b	Transesterification (N_2)	Polycondensation (0.03-0.06 mm)
PGluxAdi	0.57	20100	41300	2.1	180 °C; 4 h	180 to 210 °C; 3 h
PGluxSub	0.71	20900	46500	2.2	180 °C; 4 h	180 to 220 °C; 4 h
PGluxSeb	0.69	16700	34400	2.1	170 °C; 6 h	180 °C, 4 h
PManxAdi	0.50	10400	29000	2.8	160 °C 3 h	180 to 210 °C; 8 h
PManxSub	0.69	16000	41600	2.6	160 °C 3 h	180 to 215 °C; 4 h
PManxSeb	0.70	13300	36200	2.7	160 °C 3 h	180 to 215 °C; 6 h
PIsAdi	0.48	10100	27400	2.7	180 to 200 °C; 5 h	220 °C; 8 h
PIsSub	0.68	16900	38400	2.3	180 °C; 3 h	200 to 215 °C; 6 h
PIsSeb	0.68	13000	34000	2.6	180 to 190 °C; 3 h	210 to 220 °C; 6 h

^aIntrinsic viscosity measured in dichloroacetic acid at 25 °C.

^bDetermined by GPC in HFIP against PMMA standards.

The chemical constitution and purity of all polyesters was ascertained by both ^1H and ^{13}C NMR spectroscopy. The recorded spectra together with their respective signal assignments are accessible in the SI (Annex C). The GPC analysis revealed that they were obtained with weight-average molecular weights within the 50,000-25,000 range and dispersity degrees oscillating between 2 and 3, meanwhile intrinsic viscosities varied from 0.5 and 0.7 $\text{dL}\cdot\text{g}^{-1}$ in good agreement with the tendency observed for molecular weights (Table 5.2). Molecular weights deserve particular attention due to their relevance to the properties of the polyesters, and also because their values are in some manner an indication of the reactivity of monomers. It is widely known that the difficulty in obtaining high enough molecular weights is a general drawback in the synthesis of polyesters which becomes critical when sugar-based monomers are concerned. For a more vivid comparative illustration, the weight-average molecular weight values obtained for the three series of the bicyclic sugar-based polyesters are represented in Figure 5.1. as a bar graphic. Although no clear correlation between constitution and molecular weights can be appreciated with a general validity, some valuable conclusions may be drawn when molecular weights are compared regarding the bicyclic diol used for building the polyesters. Whereas differences between Glux and Manx containing polyesters are not entirely systematic, maximum M_w values were attained for adipates and suberates when Glux-diol the chosen monomer. Furthermore, polyesters made from Is invariably show the lowest molecular weights in the all three groups. These results are in agreement with those obtained when polyterephthalate copolyesters prepared from similar bicyclic sugar-based monomers were compared.¹⁰

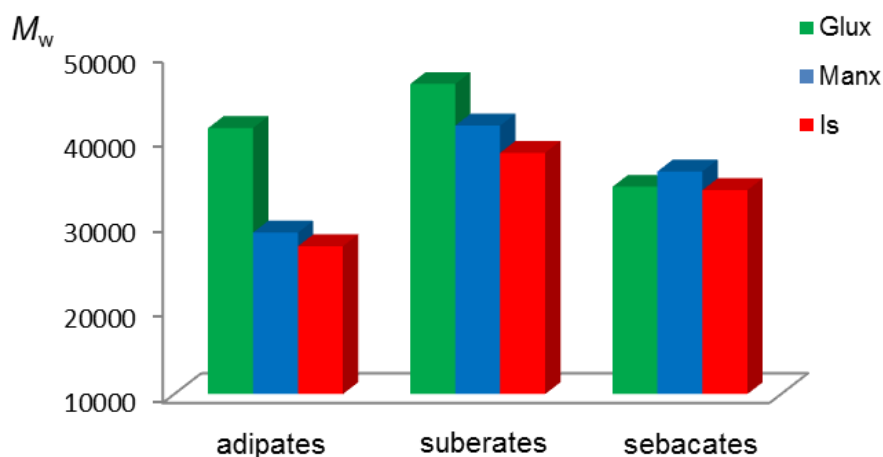


Figure 5.1. Compared weight-average molecular weight of aliphatic polyesters made from Glux-diol, Manx-diol and Is.

The fact that the two free hydroxyl functions of Is are secondary rationalizes the less reactivity displayed by this monomer compared to both Glux-diol and Manx-diol, each one bearing two hydroxymethyl groups. On the contrary, the differences in molecular weights observed between Glux and Manx containing polyesters are certainly striking. The two hydroxymethyl groups in the Manx-diol are spatially identical due to the C_2 symmetry of the Manx configuration whereas in the Glux structure such groups are allocated in different spatial positions (*exo* and *endo*). Accordingly, a greater reactivity for Manx-diol and in consequence a higher molecular weight for the Manx-containing polyester should be expected. However, the opposite result is found for both polyadipates and polysuberates whereas differences observed for polysebacates are not significant. These results reveal that, in contrast to what is reported for isosorbide,¹¹ the *exo-endo* influence on reactivity must be practically inoperating in Glux-diol. This is in agreement with the fact that a similar number of *exo* and *endo* hydroxyl end groups are detected in the NMR spectra of Glux containing polyesters whereas an excess of *endo* hydroxyl groups are found in the polymers made from Is (SI, Appendix C).

5.3.2. Thermal properties and crystallinity

The thermal behavior of the polyesters was evaluated by TGA and DSC, and the main thermal parameters recorded from these essays are collected in Table 5.3. The thermal stability was measured in a range of 30-600 °C under a nitrogen flow, and the registered TGA traces are compared in Figure 5.2. A rapid survey of these data leads

to conclude that the aliphatic polyesters containing bicyclic units derived from alditols are stable to temperatures well above ~350 °C and decompose in one step leaving less than ~10% of residue after being heated above ~450 °C. The relevant consequence of such pattern of behavior is that the resistance to heat of these polyesters is high enough as to allow their comfortable processing by conventional thermal methods. A closer comparison of data listed in Table 5.3 indicates that decomposition takes place at a maximum degradation rate temperature ($^{\text{max}}T_d$), located within the 420-430 °C range with differences among polyesters being less than ~2%. On the other hand, the differences observed for the onset temperature of decomposition, ($^{\circ}T_d$), measured for a loss of 5% of the initial weight, are also small although in this case polymers made from Is and Max-diol display respectively the highest and lowest values in every polyalkanoate group. It can be also stated that the thermal stability tends slightly to increase with the length of the alkanate moiety for whichever sugar-based diol is used in the synthesis of the polyester.

Table 5.3. Thermal properties of sugar-based aliphatic polyesters.

Polyester	TGA ^a			DSC ^b		
	$^{\circ}T_d$ (°C)	$^{\text{max}}T_d$ (°C)	RW (%)	T_g (°C)	T_m (°C)	ΔH_m (J·g ⁻¹)
PGluxAdi	380	422	8	72	-	-
PManxAdi	368	422	6	29	-	-
PlsAdi	386	423	10	20	-	-
PGluxSub	366	424	10	57	133	21.2
PManxSub	370	420	7	26	-	-
PlsSub	389	429	8	18	-	-
PGluxSeb	382	429	5	45	117	30.3
PManxSeb	375	420	5	22	-	-
PlsSeb	389	429	9	5	52	20.9

^aOnset decomposition temperature corresponding to 5% of weight loss ($^{\circ}T_d$), temperature of maximum degradation rate ($^{\text{max}}T_d$), and % of weight remaining after heating at 600 °C (RW).

^bGlass-transition temperature (T_g) taken as the inflection point of the heating DSC traces of melt-quenched samples recorded at 20 °C·min⁻¹. Melting temperatures (T_m) and melting enthalpy (ΔH_m) measured at a heating rate of 10 °C·min⁻¹ from pristine powdered samples.

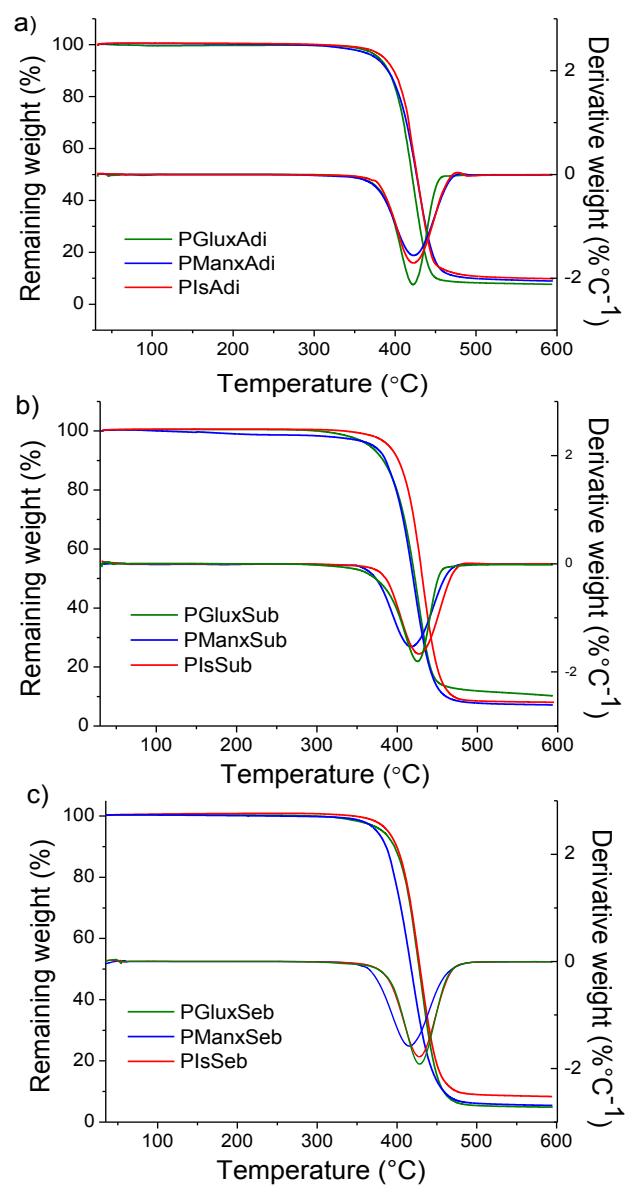


Figure 5.2. Compared TGA traces of aliphatic homopolyesters made from dimethyl adipate (a), dimethyl suberate (b), diethyl sebacate (c) and its derivative curves.

Comparison of melting and glass transition temperatures of the polyesters has been made on the basis of data collected by DSC. The DSC traces obtained at heating from samples coming directly from synthesis are depicted in Figure 5.3a, 5.3b, and 5.3c for the three respective sets of polyalkanoates. As a general rule, the presence of sugar-based bicyclic units in the polyester chain entailed a dramatic decreasing of crystallinity so that only PGluxSub, PGluxSeb, and PIsSeb displayed DSC containing endothermic peaks characteristic of melting. Conversely, plain traces typical of amorphous material were recorded from the three polyadipates as well as from the three Manx containing polyalkanoates. The greater ability of polyesters to crystallize as the length of the diacid moiety increases is highly expectable and may be explained by the higher spatial flexibility that is provided to the polymer chain. On the other side, the absence of crystallinity in polyesters containing Manx is not easily understandable since the Manx structure is the only one out that is able to render a polymer chain with stereoregular configuration. Nevertheless, what it is most noteworthy is that the Glux structure appears to be the more favorable one for developing crystallinity in aliphatic polyesters. Such effect has been previously observed in aromatic copolyesters containing the same sugar-based bicyclic units.^{12,13} Compared to PIsSeb, both PGluxSub and PGluxSeb have much higher melting temperatures and enthalpies. The greater ability of Glux containing polyesters to crystallize compared to those containing either Is or Manx should be related to the greater capacity of the Glux bicyclic structure to become accommodated in an ordered array of chains. However this effect is not easily explainable and its rationalization will require additional efforts.

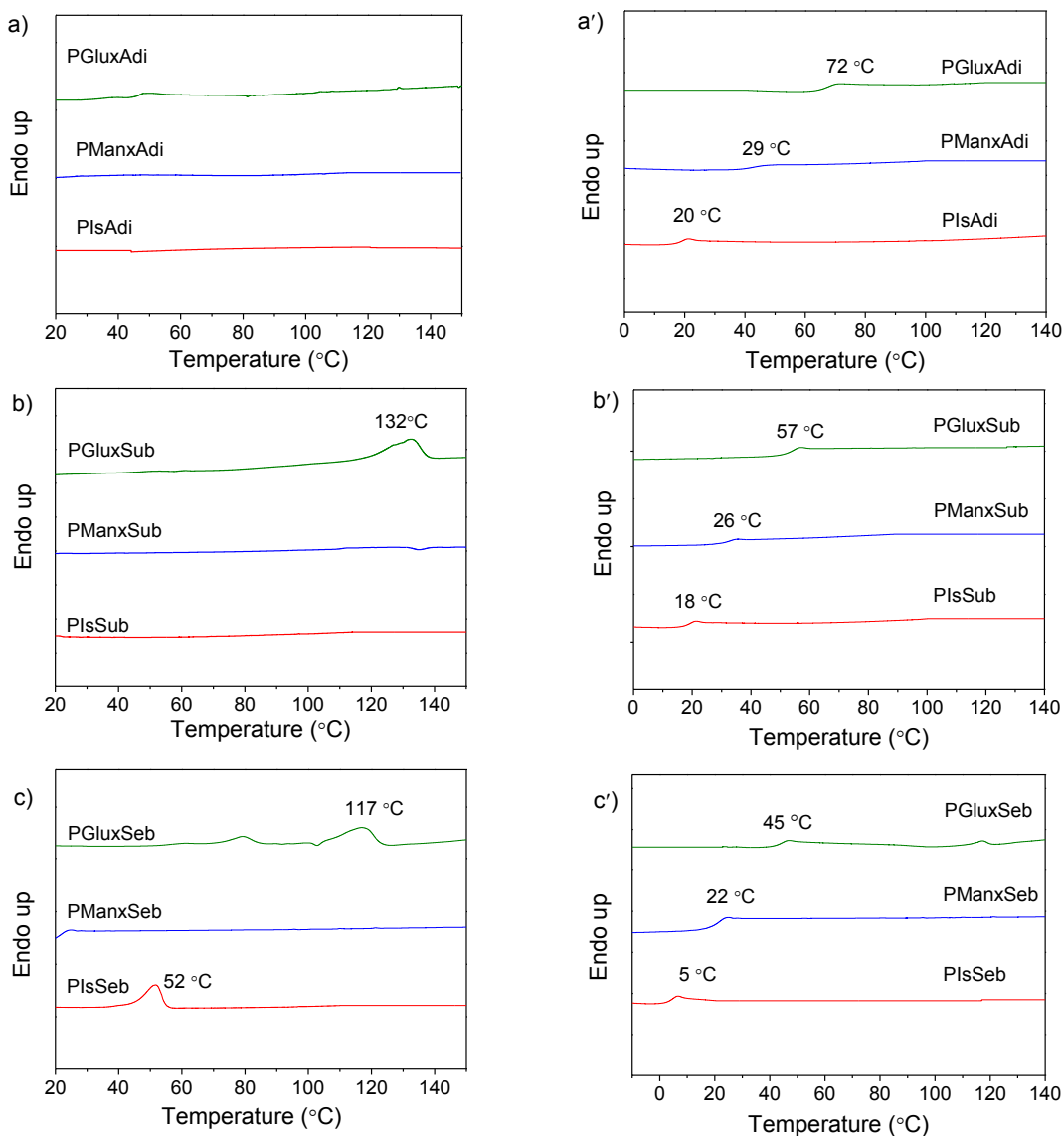


Figure 5.3. First heating DSC traces of aliphatic homopolyesters made from Glux-diol (a), Manx-diol (b) and Is (c). DSC traces of aliphatic homopolyesters made from Glux-diol (a'), Manx-diol (b') and Is (c') quenched from the melt for T_g observation.

The glass-transition temperature (T_g) is probably the property most greatly affected by the incorporation of cyclic units in an aliphatic polyester chain. Poly(alkylene alkanooate)s in general suffer from having very low T_g due to the very high flexibility inherent to the aliphatic polyester chain and in consequence displaying poor mechanical properties.¹⁴⁻¹⁶ Both the diacetalized Glux and Manx units as well as Is are highly rigid bicyclic structures that introduce a considerable stiffness in the polyester chain. The T_g values of the sugar-based bicyclic polyalkanoates examined in this work are listed in Table 5.3 and represented in the bar graphic of Figure 5.4 for a more straightforward comparison. As expected, all these polyalkanoates display T_g values much higher than those of their homologous made of alkanediols which are frequently below 0 °C.^{17,18} A more detailed comparison of the data presented in Figure 5.4 leads

to the following conclusions: a) The T_g of alkanooates made of a given diol, decreases almost linearly with the increase in length of the alkanooate unit. b) The polyesters containing bicyclic diacetalized units show T_g significantly higher than those containing Is. c) The Glux units are particularly effective in increasing the T_g of aliphatic polyesters with differences arriving to be larger than 50 °C between PGluxAdi and PIsAdi.

The exceptional effectiveness of the Glux structure to restrict chain mobility, and in consequence to rise the T_g of the polymer, was brought into evidence for the first time in several studies of aromatic polyesters^{10,12} in fact it was then reported that the polyterephthalate made of Glux-diol had a T_g of 154 °C, which is about 120 and 75 °C higher than those of PBT and PET, respectively. The reason for such strong effect could be attributed to the puckered molecular conformation adopted by the Glux bicyclic configuration compared to the more planar arrangement found in Manx. The bulkiness of Glux should be therefore a factor to be added to cyclic rigidity at explaining the reduction in free volume that apparently occurs in polyesters containing this structure.

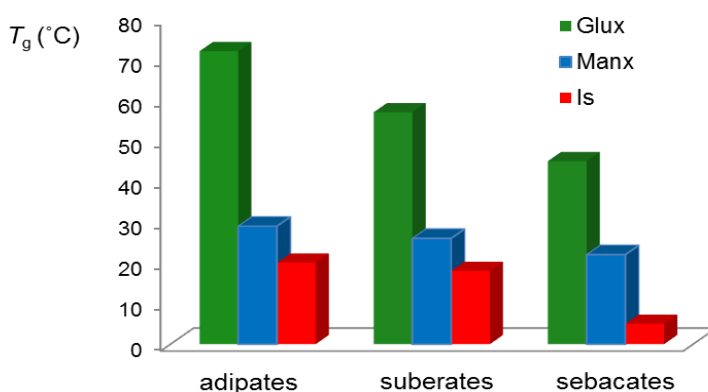


Figure 5.4. Compared glass transition temperatures of aliphatic homopolyesters made from Glux-diol, Manx-diol and Is.

The conformational preferences for Glux-diol, Manx-diol, and Is compounds have been evaluated by density functional theory (DFT) calculations. The molecular geometry of these molecules has been optimized, and the minimum character of such geometries has been verified by a frequency analysis. In addition, the torsional energy profile associated with the central bond of each molecule has been obtained, by fixing the corresponding torsion in intervals of 10° and allowing the rest of coordinates to relax. All the DFT calculations have been performed at the B3LYP/6-31G(d,p) level of theory with the GAMESS program.¹⁹ Figure 5.5. displays the torsional energy profiles for the rotation around the C-C central bond in the three units. It can be seen that for

the three monomers, complete rotation is precluded by the presence of the two fused rings. More specifically, the profiles for the Glux and Manx monomers are narrower than for Is (about 170-250° for Glux and 240-300° for Manx, as compared to about 190-290° for Is), suggesting that the associated rotation will be more restricted for the former two monomers. A larger flexibility could be therefore expected for the polymers based on the Is monomer.

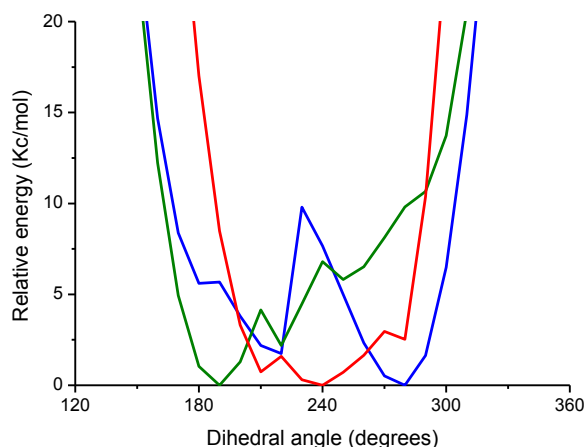


Figure 5.5. Energy profile obtained for the torsion respect to the central C-C bond for the three diol monomers under study: Glux-diol (green), Manx-diol (blue) and Is (red.).

Regarding Glux and Manx, their profiles display a similar width. However, the presence of two energy minima in the Manx profile could account for the comparatively greater flexibility observed for the polyesters containing this structure. Moreover, comparison of the minimum energy conformations reveals geometrical differences for the Glux and Manx units. The most favorable geometry for Manx (Figure 5.6.) is relatively planar with the two 1,3-dioxane ring units in a chair conformation and the two hydroxymethyl groups in equatorial positions. On the other hand, the optimal conformation for Glux corresponds to a puckered geometry with only one of the rings in a chair conformation while the other adopts a twisted boat conformation in order to accommodate its hydroxymethyl group in a non-axial position. Such differences could also contribute to the greater effect of Glux on the reduction of flexibility on its corresponding polymers.

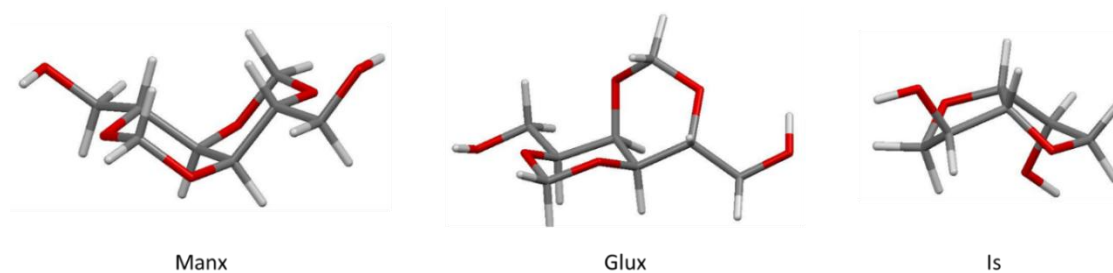


Figure 5.6. DFT-calculated minimum energy geometries for the three diol monomers under study.

To support DSC data, the polyesters showing crystallinity were examined by powder X-ray diffraction. The scattering profiles recorded for PGluxSub, PGluxSeb and PIsSeb are depicted in Figure 5.7 with indication of the Bragg spacings associated to the most prominent observed peaks. Only PIsSeb was able to render a crystalline diffraction pattern from the pristine sample. Sharp strong reflections at 5.0, 4.6, and 4.3 Å were present at the profile of this polyester together with another broad one centered on ~15 Å, which very probably arises from the axial repeat of the structure. In the other two cases, samples had to be subjected to annealing in order to obtain well-defined discrete scattering (SI. Annex C). The profiles recorded from PGluxSub and PGluxSeb annealed samples displayed a similar profile in the wider angle region with peaks at 6.5, 4.9, 4.5, 4.0, and 3.7 Å. The fact that the same diffraction pattern is observed over the 5-3 Å interval may be easily understandable because the reflections appearing therein are usually interpreted as arising from the side-by-side chain packing of the structure, which is expected to be essentially determined by the Glux bicyclic units. On the contrary, the spacing differences observed in the smaller angle region (14.5 and 12.5 for PGluxSeb and PGluxSub, respectively) are in agreement with the different repeat that would result for the packing of suberic and sebacic segments along the axial repeat of the structure. According to results, it seems that it is the packing of the sugar moiety that exclusively determines the geometry of the crystal structure in aliphatic polyesters containing Glux units.

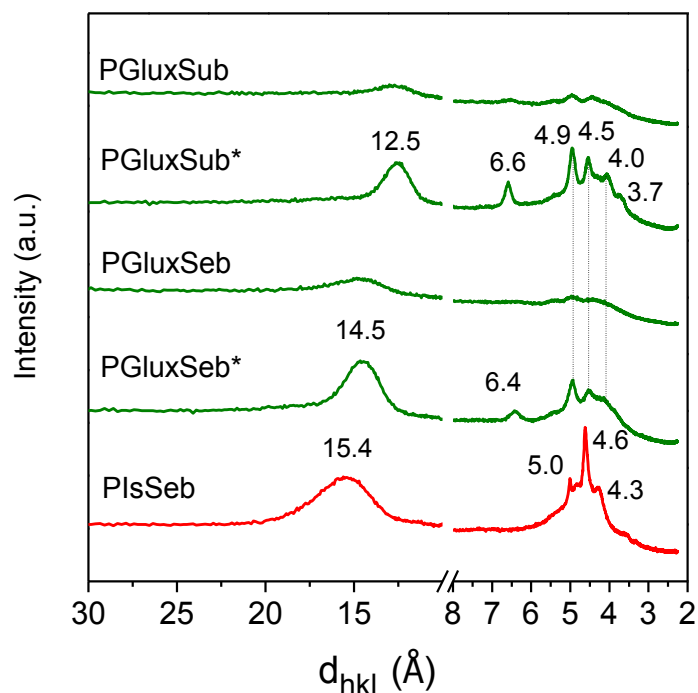


Figure 5.7. Powder WAXS profiles of PGLuxSub, PGLuxSeb and PIsSeb homopolyesters coming directly from synthesis.*Profile obtained of PGLuxSub annealed at 120 °C for 1 h and PGLuxSeb annealed at 105°C for 1 h.

5.3.3. Stress-strain behavior

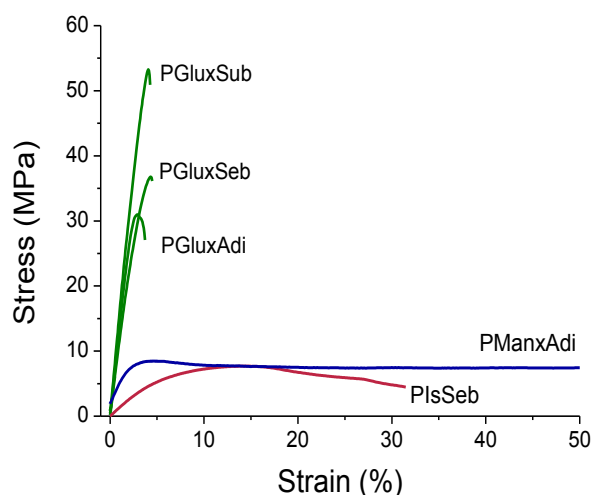
The evaluation of the mechanical properties of the sugar-based bicyclic polyesters was performed by tensile essays of films that were prepared by either hot pressing or casting (Figure 5.8). Unfortunately, not all the polyesters were evaluated because films suitable for testing could not be always obtained. All the Glux containing polyesters in addition to PManxAdi and PIsSeb could be tested whereas too brittle films unable for measuring under stretching were produced by all others. Given the strong influence that crystallinity is known to exert on mechanical behavior, the films were examined by DSC before being subjected to mechanical testing. DSC data and mechanical parameters obtained in these essays are gathered in Table 5.4.

Table 5.4. Mechanical properties of aliphatic polyesters.

Polyester	DSC ^a		Stress-strain essays		
	T_m (°C)	ΔH_m (J·g ⁻¹)	E (MPa)	σ_{max} (MPa)	ϵ (%)
PGluxAdi	-	-	1522 ± 70	30 ± 3	3 ± 1
PGluxSub	133	19.5	945 ± 10	49 ± 5	5 ± 1
PGluxSeb	115	3.6	1160 ± 20	32 ± 8	4 ± 2
PManxAdi	-	-	243 ± 20	9 ± 3	230 ± 20
PIsSeb	53	19.1	110 ± 10	8 ± 2	34 ± 7

^aMelting temperatures (T_m) and enthalpies (ΔH_m) of films measured by DSC at heating of 10 °C·min⁻¹

In general it can be stated that polyesters made from Glux-diol display much higher modulus and tensile strength than the others made from either Manx-diol or Is which are at their turn much less extensible. This behavior is a clear consequence of their comparatively higher T_g . In fact Young's moduli of Glux containing polyalkanoates are within 1.1-1.5 GPa range, which are amazingly high values for aliphatic polyesters. Tensile strengths ranged between 30 and 50 MPa and elongations to break were below 5%, which are usual values found for this type of polymers. On the other hand, the amorphous PManxAdi displayed a much lower modulus and tensile strength than its homologous PGluxAdi but it can be stretched up to more than 200% without breaking. Such great different behavior is doubtlessly due to the lower T_g displayed by the Manx containing polyadipate. Although only a polyester containing Is could be measured, PIsSeb, comparison of data with its Glux containing homologous, PGluxSeb, revealed mechanical behavior differences consistent with their T_g values. The polysebacate containing Is results to be a much softer and weaker polymer than that containing Glux although it was able to be stretched in a much longer extent.

**Figure 5.8.** Stress-strain curves of aliphatic polyesters containing sugar-based bicyclic units.

5.4. Conclusions

Polymerization results as well as thermal and mechanical properties of the ensuing polyesters were systematically compared for three series of polyalkanoates made from two diacetalized alditols (Glux-diol and Manx-diol) and from a doubly anhydridized glucitol (Is). The diacetalized alditols (Glux-diol and Manx-diol) were clearly superior to Is in producing higher molecular weight polyesters whichever alkanoate was concerned but no consistent differences between the two diacetals were apparent along the three polyester series. All polyesters displayed good thermal stability regardless the type of sugar-based unit involved with no significant differences among them. The repressing effect of the bicyclic alditol on crystallinity became obvious for the three diol monomers but it was less noticeable for Glux-diol. On the contrary, they all showed an enhancing effect on T_g whose intensity follows the order Glux>>Manx>Is in the three polyalkanoate series. As a consequence the mechanical behavior of the polyesters changed from strong and hard in those made of Glux-diol to soft and weak in those made of either Manx-diol or Is. The results provided by this study bring into evidence the intrinsic superiority of Glux-diol and Manx-diol on Is for polycondensation with dialkyl dialkanoates as well as for enhancing the thermal and mechanical behavior of the ensuing aliphatic polyesters. The commercial inaccessibility of the diacetalized diols is however a severe handicap in short term for both scientific and technical development of these monomers.

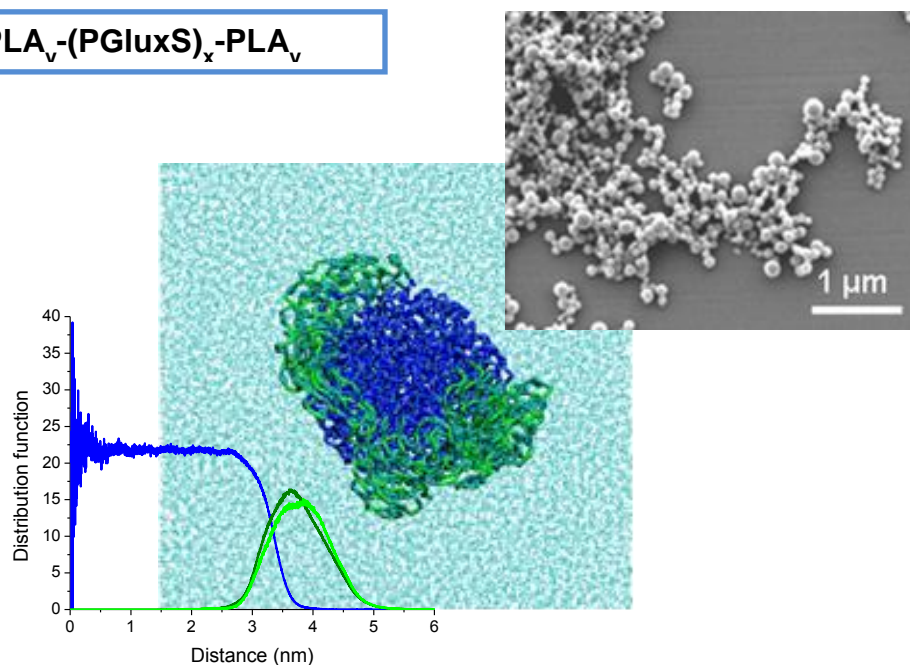
5.5. References

1. Edlund, U.; Albertsson, A.-C. *Adv. Drug. Delivery Rev.* **2003**, *55*, 585-609.
2. Vilela, C.; Sousa, A.F.; Fonseca, A.C.; Serra, A.C.; Coelho, J.F.J.; Freire, C.S.R.; Silvestre, A.J-D. *Polym. Chem.* **2014**, *5*, 3119-3141.
3. Galbis, J.A.; García-Martín, M.G.; Violante de Paz, M.; Galbis, E. *Chem. Rev.* **2016**, *116*, 1600-1636.
4. Muñoz-Guerra, S.; Lavilla, C.; Japu, C.; Martínez de Ilarduya, A. *Green Chem.* **2014**, *16*, 1716-1739.
5. Kricheldorf, H.R.; Behnken, G.; Sell, M. *J. Macromol. Sci. Part A Pure Appl. Chem.* **2007**, *44*, 679-684.
6. Fenouillot, F.; Rousseau, A.; Colomines, G.; Saint-Loup, R.; Pascault, J.-P. *Prog. Polym. Sci.* **2010**, *35*, 578-622.
7. Noordover, B.A.J.; Staalduinen, V.G.; Duchateau, R.; Koning, C.E.; Benthem, R.A.T.M.; Mak, M.; Heise, A.; Frissen, A.E.; Haveren, J. *Biomacromolecules* **2006**, *7*, 3406-3416.
8. Zakharova, E.; Alla, A.; Martínez de Ilarduya, A.; Muñoz-Guerra, S. *RSC Adv.* **2015**, *5*, 46395-46404.
9. Lavilla, C.; Alla, A.; Martínez de Ilarduya, A.; Muñoz-Guerra, S. *Biomacromolecules*, **2013**, *14*, 781-793.
10. Japu, C.; Martínez de Ilarduya, A.; Alla, A.; García-Martín, M.G.; Galbis, J.A.; Muñoz-Guerra, S. *Polym. Chem.* **2014**, *5*, 3190-3202.
11. Noordover, B.A.J.; van Staalduinen, V.G.; Duchateau, R.; Koning, C.E.; van Benthem, R.A.; Mak, M.; Heise, A.; Frissen, A.E.; van Haveren, J. *Biomacromolecules* **2006**, *7*, 3406-3416.
12. Japu, C.; Martínez de Ilarduya, A.; Alla, A.; García-Martín, M.G.; Galbis, J.A.; Muñoz-Guerra, S. *Polym. Chem.* **2013**, *4*, 3524-3536.
13. Lavilla, C.; Martínez de Ilarduya, A.; Alla, A.; Muñoz-Guerra, S. *Polym. Chem.* **2013**, *4*, 282-289.
14. Chen, Y.; Tan, L.; Chen, L.; Yang, Y.; Wang, X. *Braz. J. Chem. Eng.* **2008**, *25*, 321-335.
15. Diaz, A.; Katsarava, R.; Puiggali, J. *Int. J. Mol. Sci.* **2014**, *15*, 7064-7123.
16. Kang, E.Y.; Lih, E.; Kim, I.H.; Joung, Y.K.; Han, D.K. *Biomater. Res.* **2016**, *20*, 7.
17. Wu, B.; Xu, Y.; Bu, Z.; Wu, L.; Li, B.-G.; Dubois, P. *Polymer* **2014**, *55*, 3648-3655.
18. Shi, X.; Qiu, Z. *RSC Adv.* **2015**, *5*, 79691-79698.
19. Schmidt, M.W.; Baldrige, K.K.; Boatz, J.A.; Elbert, S.T.; Gordon, M.S.; Hensen, J.H.; Koseki, S.; Matsunaga, N.; Nguyen, K.A.; Su, S.; Windus, T.L.; Dupuis, M.; Montgomery, J.A. *J. Comput. Chem.* **1993**, *14*, 1347-1363.

Chapter 6

Triblock copolyesters derived from lactic acid and glucose: Synthesis, nanoparticle formation and simulation

ABA triblock copolyesters were synthesized by ring-opening polymerization (ROP) of L-lactide in solution initiated by a telechelic D-glucose-based polyester macroinitiator. The macroinitiator with a number-average molecular weight about 2500 g mol^{-1} was synthesized by non-stoichiometric polycondensation in the melt of 2,4:3,5-di-O-methylene-D-glucitol and dimethyl succinate. Two triblock copolyesters of M_n ranging between ~ 6000 and $\sim 9000 \text{ g mol}^{-1}$, and differing in the length of the polylactide blocks were prepared. These copolyesters started to decompose when heated at $\sim 220 \text{ }^\circ\text{C}$ and degraded slowly upon aqueous incubation under physiological conditions. They did not display any perceivable crystallinity and showed a single glass transition temperature (T_g) around $60 \text{ }^\circ\text{C}$ with the higher value corresponding to the larger content in glucitol units. The copolyesters were able to form nanoparticles with average diameters of $\sim 100\text{-}130 \text{ nm}$ and satisfactory dispersity. The effect of the block lengths on size, ζ -potential values and physical stability of the nanoparticles was evaluated. A molecular dynamics simulation study allowed modelling the two-phase structure of the nanoparticles and evidenced the preference of the glucose-based block to be peripherally located.



This work was published in: E. Zakharova, S. Leon, A. Martínez de Ilarduya, S. Muñoz-Guerra, Triblock copolyesters derived from lactic acid and glucose: Synthesis, nanoparticle formation and simulation, *Eur. Polym. J.* **2017**, *92*, 1-12.

6.1. Introduction

Biodegradable and biocompatible polymers are today the products of choice to build biomaterials that are intended to be used for temporal applications.¹⁻³ Among aliphatic polyesters, lactic acid derivatives, are outstanding due to their bio-based origin and exceptionally low immunogenicity.^{4,5} In fact, the literature is plenty of reports dealing with the potential application of PLA and its copolymers in the biomedical field as a variety of prostheses and scaffolds, and as drug delivery systems.⁶⁻⁸

The present paper is concerned with triblock copolyesters of poly(lactide) and their potential application in the preparation of particles, more specifically structured nanoparticles with interest as drug carriers. Amphiphilic block or graft copolymers are particularly suitable because they may be arranged in nanostructures with separated phases capable to embed specifically either hydrophobic or hydrophilic compounds. Block copolyesters based on polylactides stand out in this field due to their favorable physicochemical characteristics in terms of safety, stability, large-scale production, and lack of intrinsic immunogenicity.^{9,10} Nanostructured PLA-based particles are usually achieved when the lactide is copolymerized with a comonomer able to generate a highly hydrophilic polymer block,¹¹ such as polyether¹² or polypeptide.¹³ Incompatibility of this block with the relatively hydrophobic polylactide block promotes phase segregation and concomitant generation of shell-core particles.

In this paper we want to report on triblock copolyesters made of a hydrophilic block of poly(glucitylene succinate) (PGLuxS) attached to two dangling hydrophobic PLA blocks. PGLuxS is synthesized by melt polycondensation of 2,4;3,5-di-O-methylene-D-glucitol (Glux-diol) and dimethyl succinate. Glux-diol is a bicyclic diacetal derived from D-glucose that has been extensively explored by us as a bio-based comonomer appropriate for the synthesis of aromatic and aliphatic copolyesters.^{14,15} The novelty of the approach followed in this work relies on the fact that whereas racemic PLA and (PGLuxS) are compatible in the bulk or in films prepared by casting, the two blocks become segregated when they are confined in particles that are generated by emulsion in an aqueous environment. This paper describes the synthesis and characterization of the triblock $PLA_y-(PGLuxS)_x-PLA_y$ copolyesters and explores the formation of nanospheres paying particular attention to the effect of the length of the blocks on their thermal properties, particle size, ζ -potential and physical stability. The experimental work is supported by a modelling study carried out by

molecular dynamics that is addressed to substantiate the existence of differentiated phase domains in the copolyester nanoparticles

6.2. Experimental part

6.2.1. Monomer synthesis

The synthesis of 2,4:3,5-di-O-methylene-D-glucitol (Glux-diol) was described in Section 4.2.1.

6.2.2. Synthesis of telechelic OH-P(GluxS)_x-OH homopolyester

The hydroxyl capped telechelic homopolyester was synthesized by melt polycondensation of dimethyl succinate with Glux-diol using a 10 %-mole excess of diol respect to the diester. The two-steps reaction proceeded through transesterification at 175 °C for 4 h under a nitrogen flow followed by polycondensation at the same temperature for 2 h under vacuum (0.03-0.06 mbar). The NMR data ascertaining their constitution and purity are described below.

OH-(PGluxS)_x-OH homopolyester: ¹H NMR (300.1 MHz, CDCl₃), δ (ppm): 5.2-4.8 (m, 4H, OCH₂O), 4.6-4.2 (m, 2H, OCH₂CH), 4.4-4.2 (m, 4H, OCH₂CH), 4.2 (m, 1H, OCH₂CHCH), 3.9 (m, 1H, OCH₂CHCH), 3.8 (m, 1H, OCH₂CHCH), 3.6 (m, 1H, OCH₂CHCHCHCH), 2.7 (m, 4H, COCH₂CH₂CO). ¹³C NMR (75.5 MHz, CDCl₃), δ (ppm): 176.7 (CO), 93.2, 88.3, 76.2, 74.5, 71.5, 68.4, 67.0, 61.8, 20.9.

6.2.3. Synthesis of PLA_y-(PGluxS)_x-PLA_y triblock copolyesters

Briefly, the calculated amount of OH-(PGluxS)_x-OH was added to a 1M solution of L-lactide in dichloromethane at 25 °C in a round bottom three-necked flask and the mixture stirred until complete solution. Then TBD (5 %-mole relative to the lactide) was added and the solution was further stirred for 5 min under a nitrogen atmosphere at the same temperature. The triblock copolyester was precipitated with methanol, collected by filtration and dried under vacuum. Two copolyesters PLA_y-(PGluxS)_x-PLA_y with y/x ratios of approximately 2 and 3.5 were obtained by this procedure.

PLA_y-(PGLuxS)_x-PLA_y block copolyesters: ¹H NMR (300.1 MHz, CDCl₃), δ (ppm): 5.2-4.8 (m, 4H, x·OCH₂O), 5.2 (m, y·1H, OCHCH₃), 4.6-4.2 (m, x·2H, OCH₂CH), 4.4-4.2 (m, x·4H, OCH₂CH), 4.2 (m, x·1H, OCH₂CHCH), 3.9 (m, x·1H, OCH₂CHCH), 3.8 (m, x·1H, OCH₂CHCH), 3.7 (m, x·1H, OCH₂CHCHCHCH), 2.7 (t, x·4H, COCH₂CH₂CO), 1.5 (d, y·3H, OCHCH₃). ¹³C NMR (75.5 MHz, CDCl₃), δ (ppm): 172.0 (CO), 169.6 (CO), 92.9, 88.4, 75.3, 73.7, 70.8, 69.0, 67.2, 63.4, 61.0, 29.0, 16.66.

6.2.3. Synthesis of PLA homopolymer

Benzyl alcohol (1.6 %-mole relative to the lactide) was added to a 1M solution of L-lactide in dichloromethane at 25 °C in a round bottom three-necked flask and the mixture stirred until complete solution. Then TBD (5 %-mole relative to the lactide) was added and the solution was further stirred for 5 min under a nitrogen atmosphere at the same temperature. The homopolymer was precipitated with hexane, collected by filtration and dried under vacuum.

PLA homopolymer: ¹H NMR (300.1 MHz, CDCl₃), δ (ppm): 5.2 (m, 1H, OCHCH₃), 1.5 (m, 3H, OCHCH₃). ¹³C NMR (75.5 MHz, CDCl₃), δ (ppm): 172.0 (CO), 69.0, 16.7.

6.2.4. Hydrolytic degradation and biodegradation

Films for hydrolytic degradation and biodegradation studies were prepared with a thickness of ~200 μm by casting from a chloroform solution with a polymer concentration of 100 g·L⁻¹. The films were cut into 10 mm-diameter and ~20 mg-weight disks which were then dried under vacuum to constant weight. For hydrolytic degradation, the disks were incubated in vials containing 10 mL of sodium phosphate buffer pH 7.4 at 37 °C. The enzymatic degradation was carried out under the same conditions but in the presence of 10 mg of lipase from porcine pancreas and replacing the supernatant every 72 h in order to maintain the enzyme activity. In both cases, disks were withdrawn from the incubation medium at scheduled periods of time, washed carefully with distilled water, dried to constant weight, and analyzed by GPC chromatography and NMR spectroscopy.

6.2.5. Preparation of nanoparticles

Nanoparticles of $\text{PLA}_y\text{-(PGLuxS)}_x\text{-PLA}_y$ were prepared by the precipitation-dialysis method. 5 mg of the block copolymer were dissolved in 1 mL of DMSO and the same volume of water added to yield a translucent solution. This solution was dialyzed against distilled water for 72 h at room temperature using cellulose membrane tubes (2000 molecular weight cut-off) with frequent replacement of the external medium. The particles generated upon dialysis were subjected to SEM examination and light-scattering measurements.

6.2.6. Simulation studies

Molecular dynamics simulations in water solution have been carried out for model nanoparticles made up of copolymer chains with different sequences. Due to the large size of the systems under consideration, as well as the large time scales involved, the MARTINI¹⁶ coarse-grained force-field with explicit polarizable water solvent¹⁷ has been used in the simulations. Each mesoscopic simulation consisted on 15 ns of equilibration, and 15 ns of production run, with a time step of 0.03 ps, in the NVT ensemble at 300 K.

Energy parameters within the MARTINI CG model for the copolymers under study have been taken by fitting the results to short atomistic molecular dynamics simulations performed on model systems of limited size, i.e. $\text{PLA}_6\text{-P(GluxS)}_{12}\text{-PLA}_6$ chains, in a box of solvent. The GROMOS¹⁸ force-field has been used in the atomistic simulation, where the energy parameters for the three types of residue have been obtained through the ATB¹⁹⁻²¹ online tool. All the atomistic and mesoscopic simulations have been carried out with the GROMACS²² package.

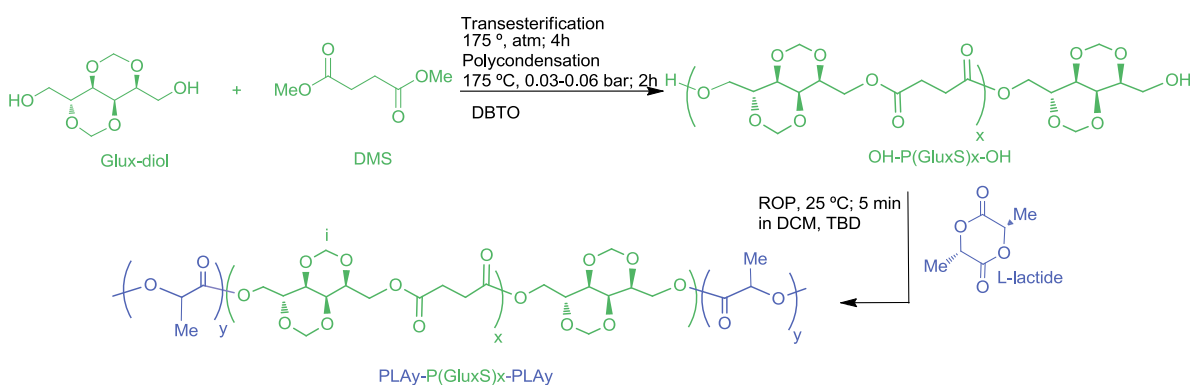
6.3. Results and discussion

6.3.1. Synthesis and chemical structure

The synthetic route followed in this work to obtain the triblock copolyesters is depicted in Scheme 6.1. 2,4:3,5-di-O-methylene-D-glucitol (Glux-diol) was prepared from commercially available 1,5-D-gluconolactone with satisfactory yield and high purity. The $\text{OH-(PGLuxS)}_x\text{-OH}$ telechelic homopolyester was synthesized by a two-

steps polymerization reaction in the melt from Glux-diol and dimethyl succinate assisted by DBTO catalyst. An excess of 10 %-mole of Glux-diol was used in order to generate hydroxyl capped oligoesters containing around ten repeating units. ^1H and ^{13}C spectra of $\text{OH}-(\text{PGLuxS})_x\text{-OH}$ homopolyester with indication of all signals assignments are provided in the SI (Annex D). These spectra ascertained the chemical constitution expected for this telechelic homopolyester and a comparative quantification of the proton resonance signals arising from inner and end glucitylene units was used to estimate its number average polymerization degree which resulted to be about 12. These data were well supported by MALDI-TOF spectra which showed peaks regularly separated by 288 m/z corresponding to the GluxS repeating unit and at values that included the additional ending Glux-OH (see SI, Annex D).

Triblock copolyesters $\text{PLA}_y\text{-(PGLuxS)}_x\text{-PLA}_y$ were synthesized by ring-opening polymerization of L-lactide in the presence of $\text{OH}-(\text{PGLuxS})_x\text{-OH}$ which operated as a double macroinitiator. In order to prevent undesirable transesterifications leading to randomization, the reaction was carried out at 25 °C in solution. The amounts of lactide and $\text{OH}-(\text{PGLuxS})_{12}\text{-OH}$ made to react were accurately adjusted to target copolyesters with two selected y/x ratios, *i.e.* 2 and 3.5.



Scheme 6.1. Synthetic route leading to $\text{PLA}_y\text{-(PGLuxS)}_x\text{-PLA}_y$ triblock copolyesters.

The strategy followed in this work to synthesize the block structure was especially suitable for a triblock design since the poly(glucitol succinate) telechelic with two ending hydroxyl groups could be readily prepared. In the triblock structure, the mobility of the glucitol succinate segment is more restricted than it would be in a diblock structure and therefore a higher particle stability can be expected.

Additionally, the presence of hydrophilic segments dangling from the particle surface is minimized.

The chemical constitution and composition of the triblock copolyesters synthesized in this work were definitely ascertained by NMR. The ^1H and ^{13}C NMR spectra of $\text{PLA}_{24}\text{-(PGLuxS)}_{12}\text{-PLA}_{24}$ copolyester are depicted in Figure 6.1. for illustrating purposes, and those recorded for its $\text{PLA}_{40}\text{-(PGLuxS)}_{12}\text{-PLA}_{40}$ homologue are included in the SI file. All signals could be straightforwardly assigned and no significant peaks revealing the presence of impurities were present in these spectra. It is well-known that NMR spectra of polymers are sensitive to neighboring and configurational effects. Stereoregular poly(L-lactic acid) is characterized by a quadruplet corresponding to methine group at 5.2 ppm and a doublet arising from the methyl group at 1.5 ppm. The simultaneous presence of D and L-lactate units will give rise to complex NMR spectra with lactate signals more or less split according to the different types of stereosequence present in the blocks. In fact, it could be observed that the ^1H spectra of $\text{PLA}_y\text{-(PGLuxS)}_{12}\text{-PLA}_y$ copolyesters as well as those of the PLA homopolymer contain multiplet peaks in the regions assigned to PLA blocks, proving the occurrence of a certain racemization of the L-lactide during polymerization. Conversely no additional succinate signals revealing the occurrence of transesterification reaction were detected in the copolyesters spectra.

Copolyester compositions were determined by integration of the proton signals arising from the respective block units. The obtained values were fairly close to those used in the respective feeds, which leads to conclude that L-lactide must have reacted almost completely by ROP. The characteristic peaks at 4.0 and 3.7 ppm corresponding to $-\text{CH}_2\text{OH}$ terminal groups disappeared as the conversion of $\text{OH-(PGLuxS)}_{12}\text{-OH}$ increased confirming the formation of ester functions (see details in the SI, Annex D). GPC measurements showed that polyesters were obtained with weight average molecular weights in the 4,000–10,000 g mol^{-1} range with dispersity indexes oscillating between 1.4 and 1.7. Number average molecular weights of copolyesters measured by GPC resulted to be slightly lower than those determined by ^1H NMR end group analysis; an inconsistency that can be accounted by the inaccuracy inherent to the chromatographic method when standards are used for calibration. Composition and molecular weight data obtained for the telechelic homopolymer and the triblock copolyesters are collected in Table 6.1.

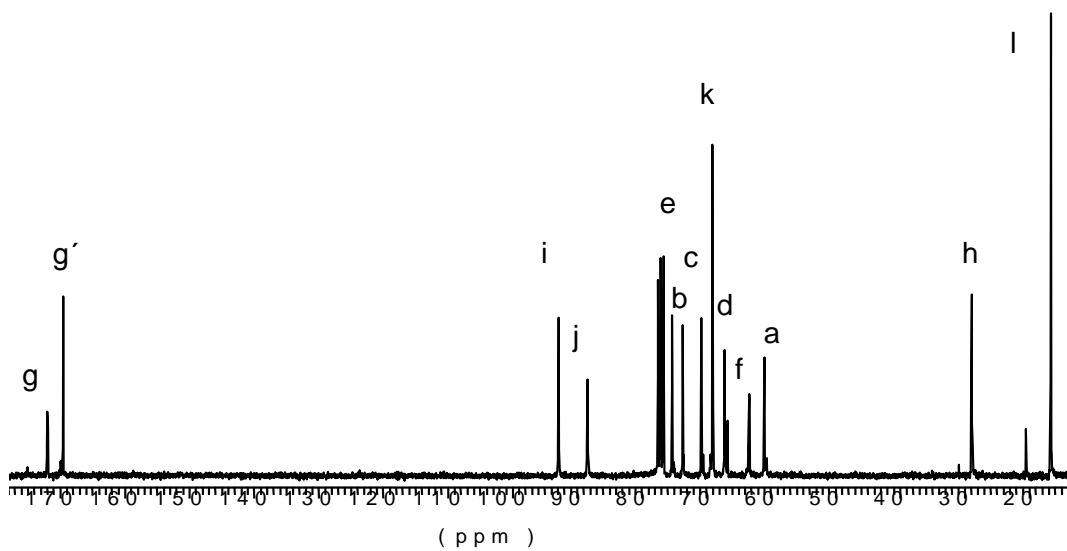
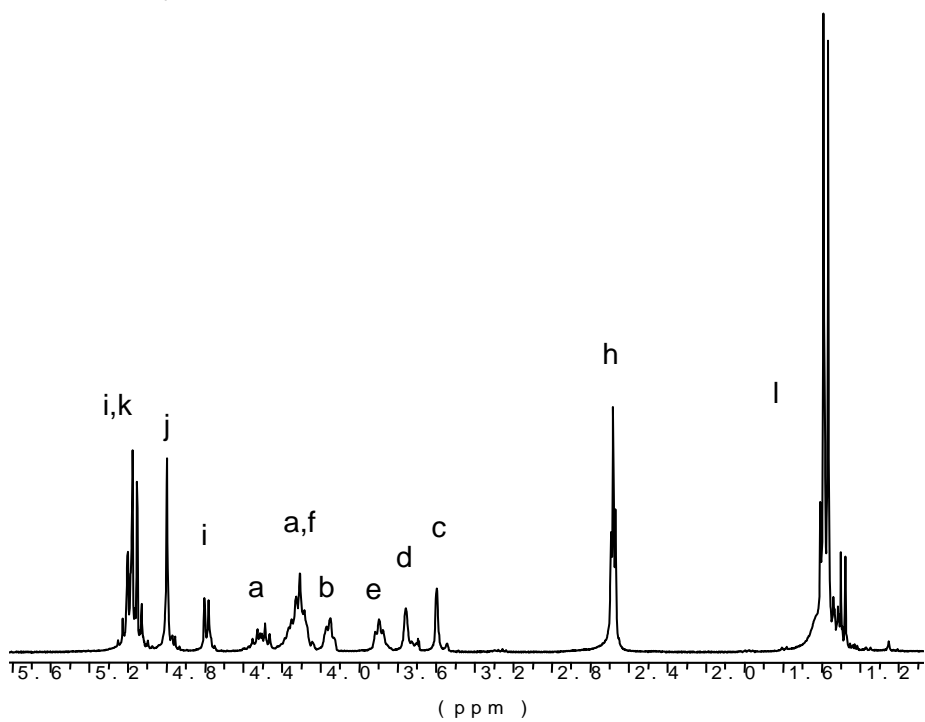
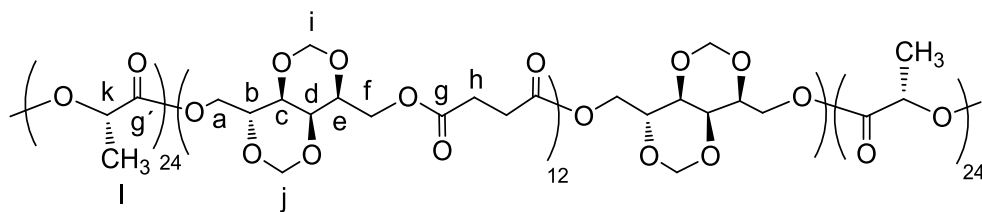


Figure 6.1. ^1H (top) and ^{13}C (bottom) NMR spectra of $\text{PLA}_{24}\text{-(PGLuxS)}_{12}\text{-PLA}_{24}$ triblock copolyester.

Table 6.1. Composition and molecular weights of homopolyesters and triblock copolyesters.

Polyester	Composition ^a ([LA] / [GluxS])		Molecular weight (g·mol ⁻¹)			
	Feed	Copolyester ^a	M_n^b	M_n^c	M_w^c	\mathcal{D}^c
OH-(PGLuxS) ₁₂ -OH	0/100	0/100	3500	2600	4500	1.7
PLA ₂₄ -(PGLuxS) ₁₂ -PLA ₂₄	80.0/20.0	81.0/19.0	6900	5500	7700	1.4
PLA ₄₀ -(PGLuxS) ₁₂ -PLA ₄₀	87.0/13.0	88.0/12.0	9200	6800	9400	1.4
PLA	100/0	100/0	8100	4400	10900	2.5

^aMolar composition in the feed and in the copolyester determined by integration of ¹H NMR spectra.

^bMolecular weights calculated by ¹H NMR.

^cMolecular weights and dispersities determined by GPC against PMMA standards.

6.3.2. Thermal properties

The thermal behaviour of the telechelic homopolyester and the two triblock copolyesters has been comparatively studied by thermal gravimetric analysis (TGA) and differential scanning calorimetry (DSC). The main thermal parameters recorded from these assays are collected in Table 6.2.

Table 6.2. Thermal properties of the polyesters.

Polyester	TGA ^a			DSC ^b		
	$^{\circ}T_d$ (°C)	$^{\max}T_d$ (°C)	<i>RW</i> (%)	T_g (°C)	T_m (°C)	ΔH (J·g ⁻¹)
OH-(PGLuxS) ₁₂ -OH	316*	398	11	94	-	-
PLA ₂₄ -(PGLuxS) ₁₂ -PLA ₂₄	223	287/395	6	61	-	-
PLA ₄₀ -(PGLuxS) ₁₂ -PLA ₄₀	216	278/347/384	8	58	-	-
PLA	218	283	5	40	-	-

^aOnset decomposition temperature corresponding to 5% of weight loss ($^{\circ}T_d$), temperature of maximum degradation rate ($^{\max}T_d$) and weight (%) remaining after heating at 600 °C (*RW*). *Before experiment telechelic homopolyester was heated at 130 °C during 5 min to eliminate moisture of the sample.

^bGlass-transition temperature (T_g) taken as the inflection point of the heating DSC traces recorded at 20 °C·min⁻¹ from melt-quenched samples. Melting temperature (T_m) and melting enthalpy (ΔH_m) measured at a heating rate of 10 °C·min⁻¹.

The thermal stability was measured in the range of 30-600 °C range under a nitrogen flow, and the registered TGA traces are compared in Figure 6.2. As can be seen, the telechelic homopolyester starts to decompose above 300 °C and displays a unique decomposition step that proceeds at maximum rate at a temperature close to

400 °C. The resistance to heating shown by this polyester is in agreement with data recently reported for their homologous polyesters made from other dicarboxylic acids and Glux-diol, which evidenced the ability of the bicyclic diol to enhance the thermal stability of aliphatic polyesters.²³ PLA homopolymer also decomposed in one step but at a considerable lower temperature.

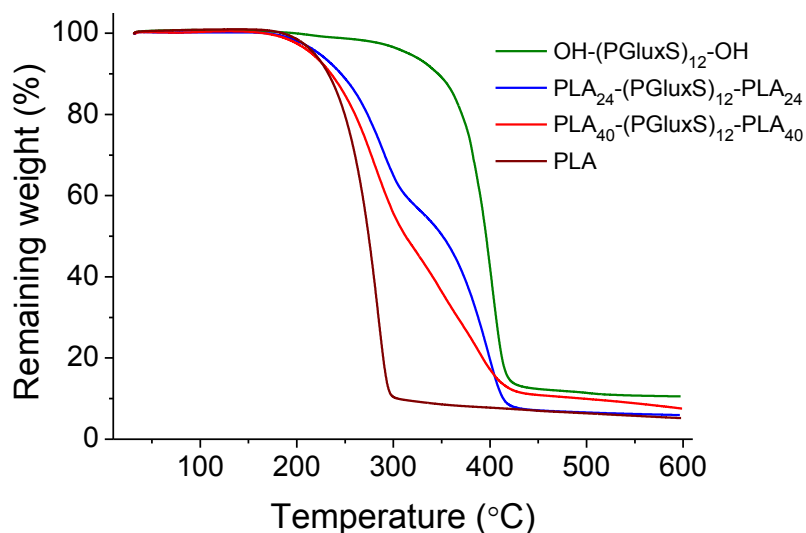


Figure 6.2. TGA traces of polyesters.

The triblock copolyesters started to decompose at ~220 °C due to the relative lower stability of PLA blocks. In contrast to the homopolyesters, $\text{PLA}_y\text{-(PGLuxS)}_x\text{-PLA}_y$ copolyesters decomposed through several degradation steps along a wide range of temperatures. Main peaks corresponding to temperatures of maximum degradation rates were observed for the derivatives curves of the TGA traces in the ~270-400 °C range (SI, Annex D). The weight loss taking place at the lower temperature step is in agreement with that should be expected for the complete degradation of the PLA blocks whereas that happening at higher temperature corresponds approximately to the decomposition of the $(\text{GluxS})_x$ block. According to the degradation process followed at each case, the residue left after heating at 600 °C was maximum for the telechelic homopolymer (11%) whereas remaining weights for the PLA homopolymer and triblock copolyesters oscillated within the 5-8% range. These TGA results lead to conclude that although the thermal stability of the copolyesters is significantly lower than that of the $\text{OH-P(GluxeS)}_{12}\text{-OH}$, these compounds continue being heat resistant enough as to be comfortably handled by thermal processing.

A DSC analysis of the OH-(PGLuxS)₁₂-OH and PLA homopolyesters and triblock copolyesters was carried out in order to appraise their behavior regarding reversible thermal transitions. The DSC traces recorded at first heating of powdered samples are accessible in the SI (Annex D). Plain traces characteristic of amorphous material were recorded from all samples including PLA. Although according to the optical purity of the L-lactic acid used for feeding, the PLA blocks could be expected to be crystalline, racemization of L-lactide occurring under the applied polymerization conditions led to generation of non-stereoregular blocks unable to crystallize.

The traces recorded from samples quenched from the melt showed inflections characteristic of glass-transitions (SI, Annex D) at temperatures between 40 and 60 °C (Table 6.2.). The telechelic OH-(PGLuxS)₁₂-OH homopolyester displayed a pretty high glass-transition temperature (94 °C) as logically corresponds to the chain stiffness induced by the presence of the of the Glux-diol units.^{23,24} As it is known, the T_g of PLA varies in the range of 50-80 °C depending on different parameters such as molecular weight and stereoisomeric content.²⁵ The PLA synthesized in this work showed a rather low T_g (40 °C) due to both absence of crystallinity and low molecular weight. The triblock copolyesters showed only one T_g at a value intermediate between those of OH-(PGLuxS)₁₂-OH and PLA, which increased with the GluxS/LA ratio as it should be expected. This result demonstrates the miscibility of the GluxS and LA blocks, a result that is striking given the constitutional differences between the two blocks. In fact, the GluxSucc structure is expected to be hydrophilic due to the presence of the two fused dioxane rings whereas PLA is unanimously considered a hydrophobic polyester. As we will see below, the two blocks will be however separated out when the copolyester is left to be self-assembled in an aqueous environment.

A preliminary evaluation of the hydrodegradability of the triblock copolyesters was carried out by monitoring the changes taking place in molecular weight as a function of time in samples incubated in aqueous buffer pH 7.4 at 37 °C, both in absence and presence of lipases. After three weeks of incubation, the PLA₂₄-(PGLuxS)₁₂-PLA₂₄ copolyester had lost less than 10% of its initial M_w indicating a moderate sensitivity to hydrolysis under physiological conditions. The ¹H NMR spectrum of the products released by the copolyester to the incubating medium revealed the presence of succinic and lactic acid as well as soluble oligomers of different lengths. The figures illustrating these results have been included in the SI (Annex D).

6.3.3. PLA_y-(PGLuxS)_x-PLA_y nanoparticles

Nanoparticles are known to be excellent systems for the adequate transport and distribution of drugs at both cell and organ levels. The nanometer-size ranges of these systems offer distinct advantages as effective permeation through cell membranes and good stability in the blood flow. Nanoparticles of PLA_y-(PGLuxS)₁₂-PLA_y were obtained by dialysis-precipitation method using DMSO as organic phase. The most characteristic parameters of the nanoparticles are collected in Table 6.3. As it is shown in Figure 6.3., well-shaped spherical particles with average diameters in the 100-130 nm range and satisfactory dispersities were obtained. The size distribution profiles of the nanoparticles obtained from the two copolyesters are compared in Figure 6.4. to show that an unimodal distribution is present in the two cases and that size slightly reduced as the length of the PLA block increased.

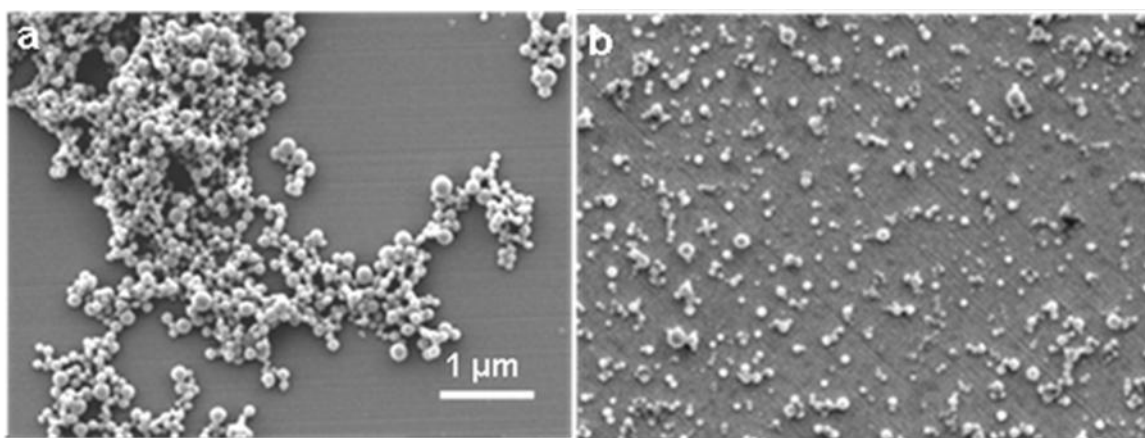


Figure 6.3. SEM images of nanoparticles made of PLA₂₄-(PGLuxS)₁₂-PLA₂₄ (a) and PLA₄₀-(PGLuxS)₁₂-PLA₄₀ (b) triblock copolyesters.

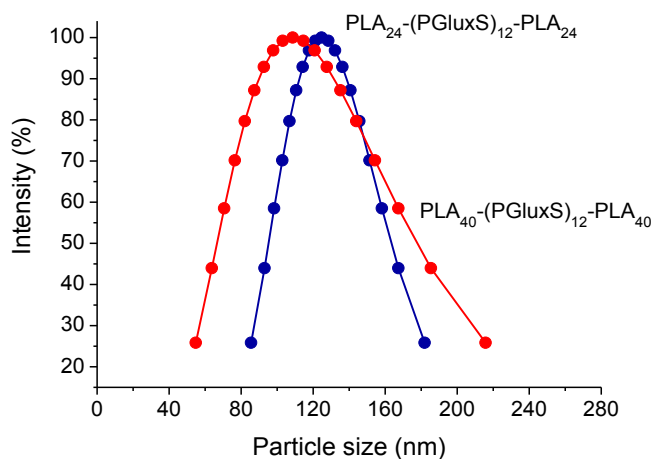


Figure 6.4. Size distribution profiles of nanoparticles.

Table 6.3. Nanoparticles properties.

Triblock copolyester	Particle size (nm)	<i>D</i>	ζ -potential (mV)	Radius of gyration (nm) ^a	
				I	II
PLA ₂₄ -(PGLuxS) ₁₂ -PLA ₂₄	123.4±7.5	0.04	-31.1±1.8	3.30±0.02	3.17±0.02
PLA ₄₀ -(PGLuxS) ₁₂ -PLA ₄₀	109.9±10.2	0.17	-13.9±1.4	3.08±0.01	3.11±0.01
PLA ₆₀ -(PGLuxS) ₁₂ -PLA ₆₀ ^b	-	-	-	3.05±0.01	3.04±0.01

^aSimulations starting with the chains separated (I), and the chains close to each other (II).

^bNo experimental data available for this composition.

The Zeta potential is a relevant parameter that is closely related to nanoparticle stability, cell adhesion and self-aggregation, and it has therefore significant implications on product performance. The Zeta-potential of the two triblock copolyesters was negative with values ranging between -30 and -10 mV. Such negative values are consistent with the presence of a high concentration of acetal groups on the particle surface. Accordingly the structure of these nanoparticles can be interpreted as the (GluxS)₁₂ segments are segregated to the outer part of the nanospheres whereas the PLA blocks remain preferably located in the inner part. The PLA₂₄-(PGLuxS)₁₂-PLA₂₄ nanoparticles distinguish in showing a significantly higher negative zeta potential value (~-30 mV), which is a favorable feature for nanoparticle stability since aggregation will be hindered by electrostatic repulsion. PLA₄₀-(PGLuxS)₁₂-PLA₄₀ nanoparticles exhibit much lower zeta potential values and therefore they should be expected to be more prone to degenerate in unspecific aggregates.

To evaluate the stability of these nanoparticles while standing at temperatures within the physiological range, a sample made of PLA₂₄-(PGLuxS)₁₂-PLA₂₄ was stored for 5 days in distilled water at temperatures comprised between 25 °C and 45 °C, and changes taking place in size, ζ -potential and shape with time were monitored. Results are shown in Fig.6.5. where it can be seen that both size and surface charge of the nanoparticles were essentially maintained after incubation at 25 °C whereas they significantly changed at higher temperatures. In fact, the particle distribution profiles move steadily to higher values and the ζ -potential rapidly increased with incubation temperature, as it should be expected from a disarrangement of the particle structure. These observations were confirmed by SEM which brought out the morphological changes concomitant to the variations observed in size and charge. A set of illustrative pictures is depicted in Figure 6.6. which shows how the particles tend to coalesce to form shapeless continuous aggregates that become more prominent as

temperature increased. It is worthy to mind that, in full agreement with light scattering measurements (Figure 6.5.), the appearance of the nanoparticles remained essentially unchanged when incubated at 25 °C. The influence of chain flexibility on particle stability should be considered for explaining these results. As incubation temperature increases the mobility of the copolyester chains is drastically enhanced since it is approaching to the T_g of the whole system.

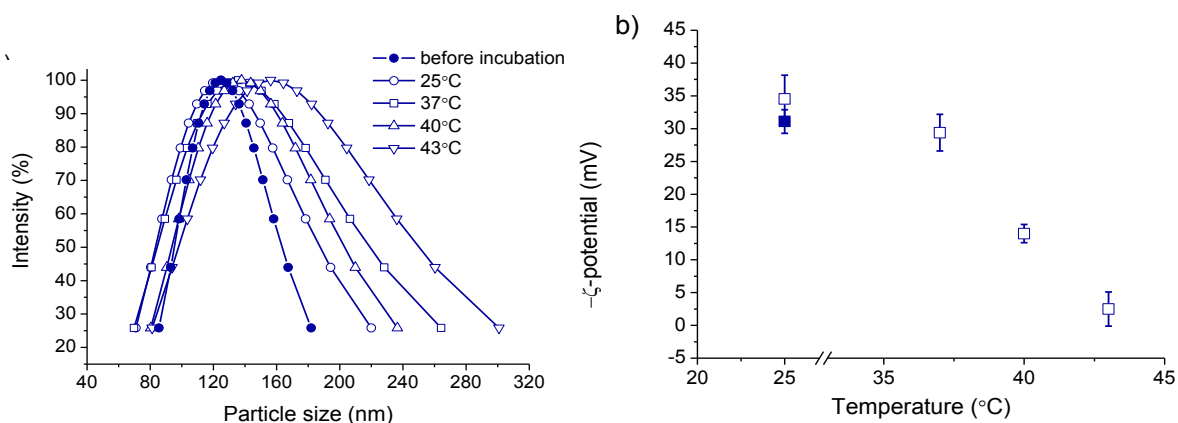


Figure 6.5. Particle size distribution (a) and ζ -potential (b) of PLA₂₄-(PGLuxS)₁₂-PLA₂₄ nanospheres versus temperature after 5 days of incubation in water.

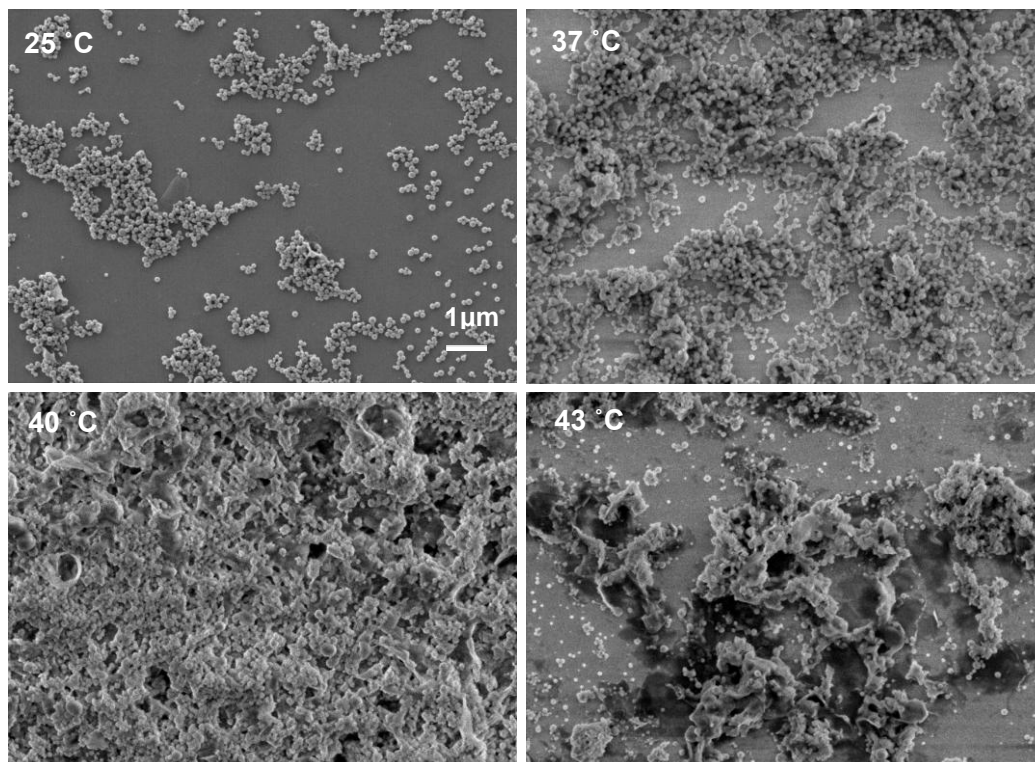


Figure 6.6. SEM nanoparticles of PLA₂₄-(PGLuxS)₁₂-PLA₂₄ at 25, 37, 40 and 43 °C after 5 days of incubation in water.

6.3.4. Simulation studies

Mesoscopic molecular dynamics simulations on model nanospheres in aqueous solution have been carried out using the MARTINI force-field.¹⁶ As it is shown in Figure 6.7., each repeat unit of the PLA blocks is described by a single non-polar bead, each succinate unit is represented by two polar beads and the Glux unit is represented by four small hydrogen-bonded acceptor beads. A detailed account of the representation used for the copolyester according to the MARTINI framework is given in the SI document.

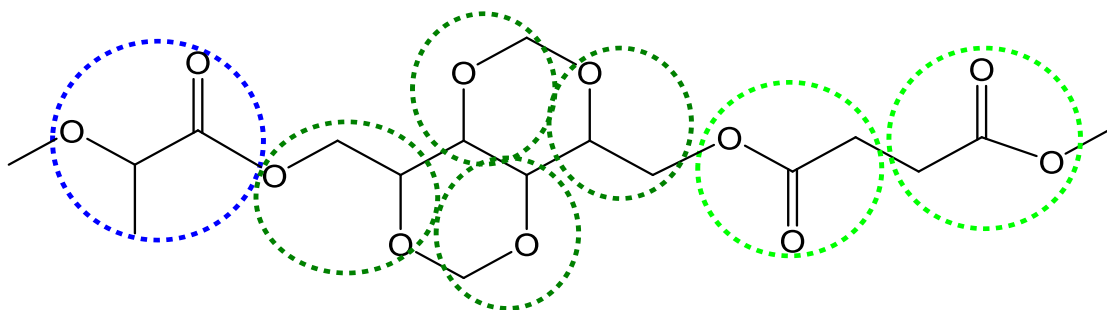


Figure 6.7. Scheme illustrating the definition adopted for the CG particles used for the mesoscopic model of the $\text{PLA}_y\text{-(PGLuxS)}_x\text{-PLA}_y$ copolymers. A more detailed sketch indicating the connectivity between the beads is shown in the SI (Annex D).

Triblock copolymer chains $\text{PLA}_y\text{-(PGLuxS)}_{12}\text{-PLA}_y$ with PLA blocks of 24, 42, 60 units have been considered in these simulations. In order to more readily compare the results of the different simulations, model nanoparticles with similar weights were built, thus corresponding to 26, 19 and 15 chains respectively, for the three lengths of the PLA blocks. All the nanoparticles were placed in a $15 \times 15 \times 15 \text{ nm}^3$ solvent box constituted by 27,092 polarizable water particles (equivalent to 108,368 water molecules). In order to avoid artifacts due to the selection of the starting geometry, two molecular dynamics differing in the initial relative chain positions (one with the chains separated from each other, and the other with the chains close to each other) have been performed for each system.

Figure 6.8. displays snapshots obtained from the mesoscopic molecular dynamics trajectories for the three selected model nanoparticles. It can be seen that in all cases, the chains tend to aggregate forming a nanoparticle with a roughly spherical shape. In all cases, the hydrophilic GluxS groups are distributed on the

outer region of the particles, while the more hydrophobic PLA blocks tend to occupy an inner region. The interior of the particles is compact and preferably occupied by units of the PLA blocks, as it could be further demonstrated by serial sectioning of the particle (see images in the SI, Annex D). The results obtained for a given copolymer appear to be in general quite irrespective of the starting geometry selected for the simulation. The only exception is the model particle for $\text{PLA}_{24}\text{-(PGLuxS)}_{12}\text{-PLA}_{24}$; in this case the simulation starting with the chains initially separated led to nanoparticle displaying a more irregular shape, and even two of the chains remained unjoined to the nanoparticle aggregate.

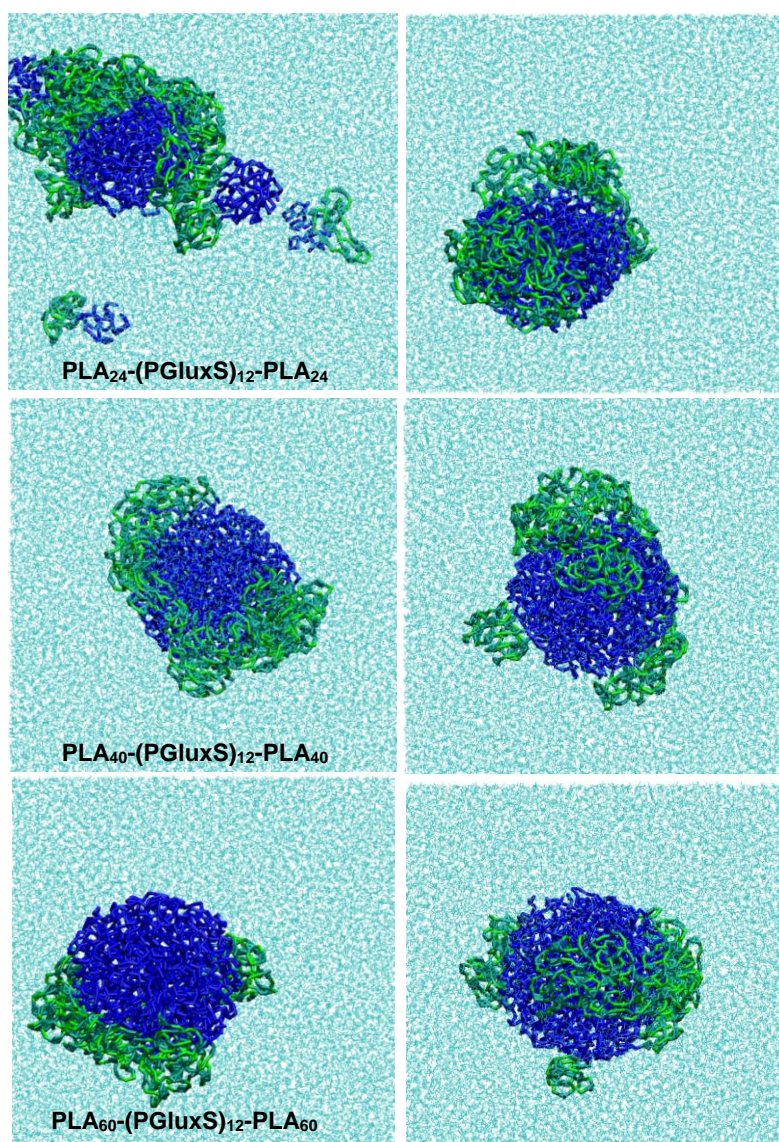


Figure 6.8. Snapshots for the solvated model nanospheres of the $\text{PLA}_y\text{-(PGLuxS)}_{12}\text{-PLA}_y$ copolyesters, from trajectories with two different starting geometries. Left: separated chains; Right: closed chains. LA groups are depicted in blue color, Glux groups in dark green and S groups in bright green. Water molecules are represented in cyan.

The size of the model nanoparticles has been evaluated in terms of the global radius of gyration, which is displayed in Table 6.3. Even though the model nanoparticle sizes used for simulations are much smaller than those experimentally produced, the values of the radius of gyration tend to decrease when the length of the PLA block increases, in agreement with experimental observations. The distribution of polymer mass and solvent molecules inside the nanoparticles has been analyzed and results are shown in Fig. 6.9. The dimensions and shape of the model nanospheres were analyzed in terms of the radial distribution of groups. Fig. 6.9a displays the radial distribution function of the copolymer units with respect to the center of mass of the nanoparticle. In all cases, the inner region presents a rather homogeneous distribution of groups, and extends up until about 3.5 nm from the center, while the outer groups extend up to 5 nm. Interestingly, although the differences between the three distributions are small, the groups for PLA₂₄-(PGLuxS)₁₂-PLA₂₄ are able to reach longer distances from the center.

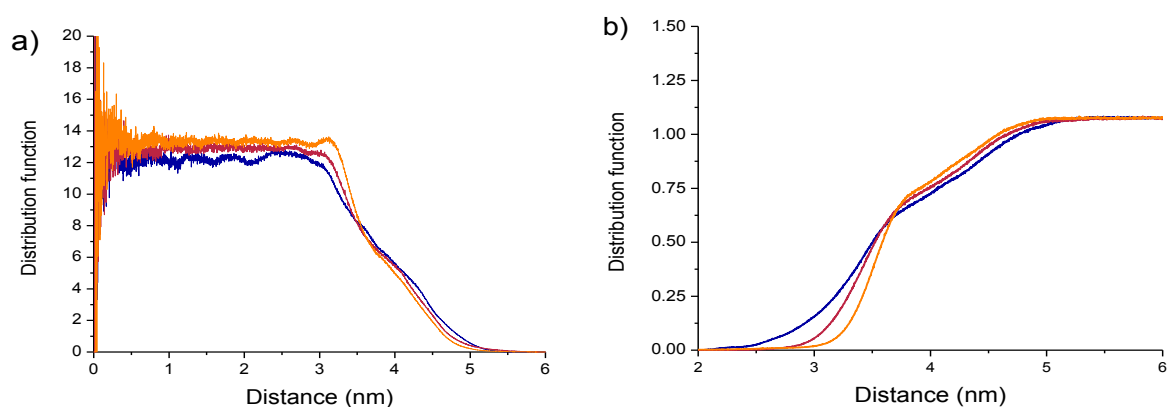


Figure 6.9. Radial distribution analysis of the model PLA_y-(PGLuxS)₁₂-PLA_y nanoparticles. Blue, red and orange colors refer to PLA block size $y = 24, 42, 60$, respectively. Only results for the simulations starting with a close arrangement of chains are shown a) Mass distribution b) Solvent distribution.

Regarding the distribution of solvent around the model nanoparticles, Figure 6.9b shows the radial density of solvent with respect to the center of mass of the nanoparticle, which evidences the inexistence of solvent in the interior of the particles. The presence of solvent starts to be detectable at a distance of 2.5-3 nm from the center and increases with the radius. It should be remarked that the presence of water at distances of 4-5 nm is due to the fact that the polymer groups are insufficient to fill the spherical space defined at such distances (this can be seen in Figure 6.8.).

Finally, the distribution of the different polymer building blocks within the model nanoparticles is illustrated in Figure 6.10. As it was reflected in the snapshots depicted in Figure 6.8., the inner region of the particles is preferably occupied by the hydrophobic PLA blocks, while the hydrophilic GluxSucc units are predominantly placed in the outer region. The differences among the radial density profiles mainly concern the distribution of the outer groups. Such distribution is broader for the systems with shorter PLA segments. This can be observed in more detail when the radial distribution function of the hydrophilic groups is compared for the three model nanoparticles (Figure 6.10d). For $\text{PLA}_{24}\text{-(PGLuxS)}_{12}\text{-PLA}_{24}$, the smaller proportion of PLA blocks with respect to the (PGLuxS) segment could allow a more readily covering of the outer region by the hydrophilic blocks, while for $\text{PLA}_{42}\text{-(PGLuxS)}_{12}\text{-PLA}_{42}$ and $\text{PLA}_{60}\text{-(PGLuxS)}_{12}\text{-PLA}_{60}$ the large proportion of PLA segments forces the outer region to have a smaller thickness to cover as much as possible the outer core. It is worth mentioning that the mass placed at the outer region does not cover the whole space around the hydrophobic core. In other words, the number of molecules used for modelling is not large enough as to build an arrangement in which the contact between water and the hydrophobic segments can be fully avoided. Unfortunately, the computational cost to simulate a nanoparticle with the experimental dimensions would exceed largely the scope of the present work.

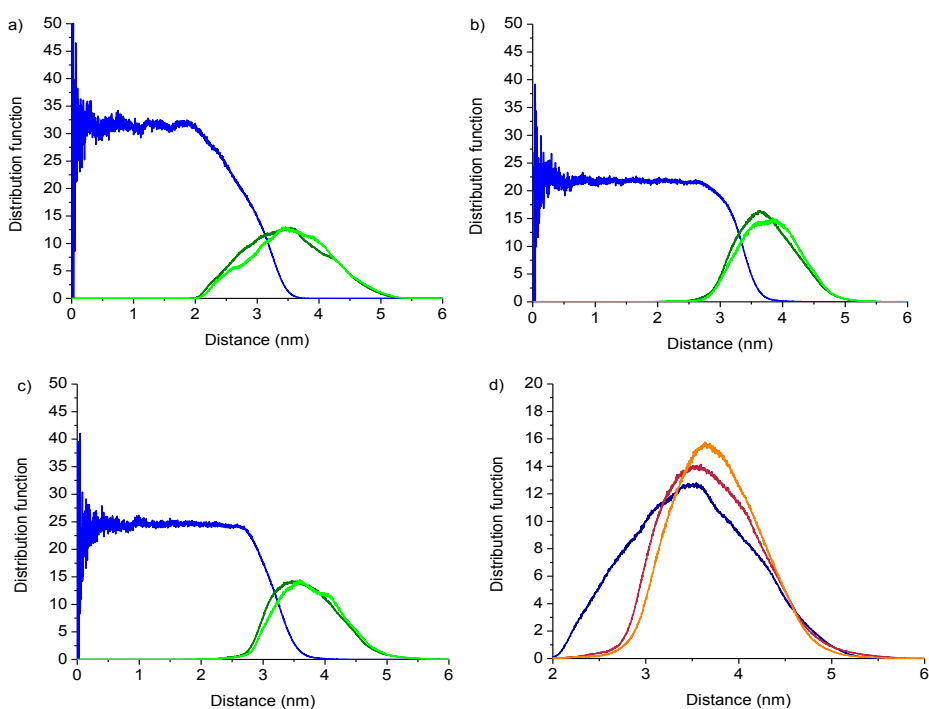


Figure 6.10. Radial density of individual LA, S and Glux groups with respect to the center of mass of the model $\text{PLA}_y\text{-(PGLuxS)}_{12}\text{-PLA}_y$ nanoparticles. Blue, dark green and bright green colors refer to LA, Glux and Succ groups, respectively. Only results for the simulation starting with a close arrangement of chains

are shown. a) PLA₂₄-(PGLuxS)₁₂-PLA₂₄ b) PLA₄₂-(PGLuxS)₁₂-PLA₄₂ c) PLA₆₀-(PGLuxS)₁₂-PLA₆₀ d) Radial density of the hydrophilic (GluxS) groups with respect to the center of mass of the model PLA_y-(PGLuxS)₁₂-PLA_y nanoparticles. Blue, red and orange colors refer to PLA block size y = 24, 42, 60, respectively.

6.4. Conclusions

Two bio-based triblock copolyesters PLA_y-(PGLuxS)₁₂-PLA_y for y = 24 and 40 were successfully synthesized via ROP of L-lactide using as initiator a telechelic hydroxyl-capped polysuccinate derived from D-glucose, i.e. OH-(PGLuxS)₁₂-OH. Racemization of the L-lactide happened in the polymerization led to the non-crystalline copolyesters. The copolyesters were slightly biodegradable and their thermal stability was found to increase with the content in Glux units. They showed an only T_g of value intermediate between those of PLA and (PGLuxS) indicative of the miscibility of the blocks. The copolyesters were found to be able to form nanoparticles with diameters in the 100 to 130 nm range which maintained their physical integrity during storage at room temperature but coalesced when temperature increased above 37 °C. The modelling of the nanoparticles by molecular dynamics using a system of moderate dimensions supported the existence of a biphasic structured arrangement with the GluxS units preferably located on the periphery and the polylactide blocks filling the inner space. The present research has shown the capacity of these triblock copolyesters to build biphasic nanoparticles suitable as hydrophobic drug carriers in aqueous media, and has brought into evidence their potential to be used as drug delivery systems with the release being controlled by mild temperature changes.

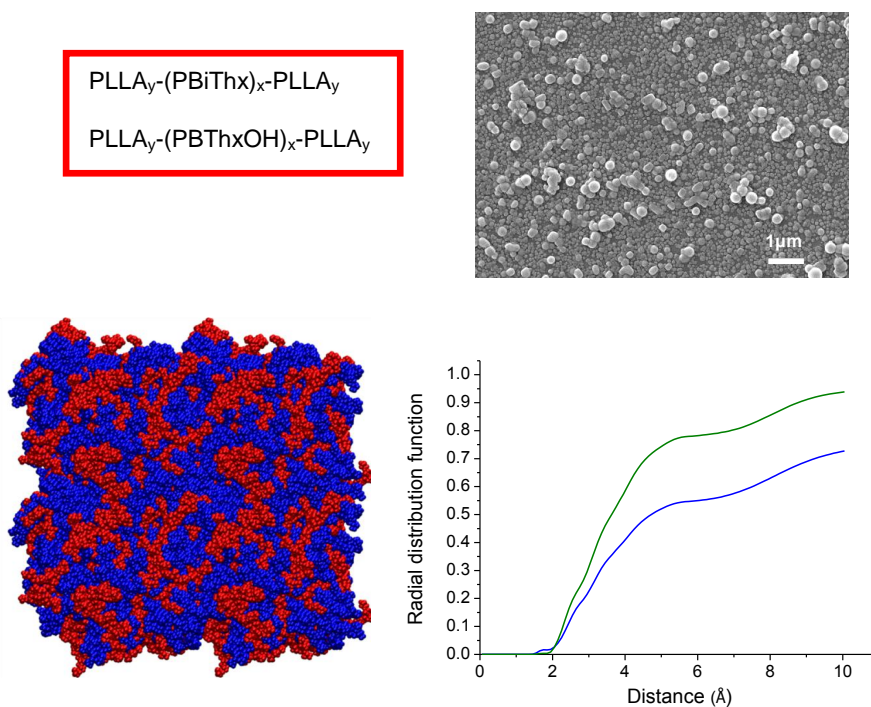
6.5. References

1. Nair, L.S.; Laurencin, C.T. *Prog. Polym. Sci.* **2007**, *32*, 762-798.
2. Tian, H.; Tang, Z.; Zhuang, X.; Chen, X.; Jing, X. *Prog. Polym. Sci.* **2012**, *37*, 237-280.
3. Doppalapudi, S.; Jain, A.; Khan, W.; Domb, A.J. *Polym. Adv. Tech.* **2014**, *25*, 427-435.
4. Gupta, A.P.; Kumar, V. *Eur. Polym. J.* **2007**, *43*, 4053-4074.
5. Hamad, K.; Kaseem, M.; Yang, H.W.; Deri, F.; Ko, Y.G. *Express Polym. Lett.* **2015**, *9*, 435-455.
6. Athanasiou, K.A.; Agrawal, C.M.; Barber, F.A.; Burkhart, S.S. *Arthroscopy* **1998**, *14*, 726-737.
7. Garvin, K.; Feschuk, C. *Clin Orthop Rel Res* **2005**, *437*, 105-110.
8. Dinarvand, R.; Sepehri, N.; Manoochehri, S.; Rouhani, H.; Atyabi, F. *Int. J. Nanomedicine* **2011**, *6*, 877-895.
9. Xiao, R.Z.; Zeng, Z.W.; Zhou, G.L.; Wang, J.J.; Li, F.Z.; Wang, A.M. *Int. J. Nanomedicine* **2010**, *5*, 1057-1065.
10. Wang, B.; Jiang, W.; Yan, H.; Zhang, X.; Li, Y.; Deng, L.; Singh, G.; Pan, J. *Int. J. Nanomedicine* **2011**, *6*, 1443-1451.
11. Oh, J.K. *Soft Matter* **2011**, *7*, 5096-5108.
12. Li, T.; Han, R.; Wang, M.; Liu, C.; Jing, X.; Huang, Y. *Macromol. Biosci.* **2011**, *11*, 1570-1578.
13. Arimura, H.; Ohya, Y.; Ouchi, T. *Biomacromolecules* **2005**, *6*, 720-725.
14. Japu, C.; Martínez de Ilarduya, A.; Alla, A.; García-Martín, M.G.; Galbis, J.A.; Muñoz-Guerra, S. *Polym. Chem.* **2014**, *5*, 3190-3202.
15. Zakharova, E.; Alla, A.; Martínez de Ilarduya, A.; Muñoz-Guerra, S. *RSC Adv.* **2015**, *5*, 46395-46404.
16. Marrink, S.J.; Risselada, H.J.; Yefimov, S.; Tieleman, D.P.; de Vries, A.H. *J. Phys. Chem. B* **2007**, *111*, 7812-7824.
17. Yesylevskyy, S.O.; Schafer, L.V.; Sengupta, D.; Marrink, S.J. *PLOS Comput. Biol.* **2010**, *6*, e1000810.
18. Oostenbrink, C.; Villa, A.; Mark, A.E.; van Gunsteren, W.F. *J. Comput. Chem.* **2004**, *25*, 1656-1676.
19. Malde, A.K.; Zuo, L.; Breeze, M.; Stroet, M.; Poger, D.; Nair, P.C.; Oostenbrink, C.; Mark, A.E. *J. Chem. Theory Comput.* **2011**, *7*, 4026-4037.
20. Canzar, S.; El-Kebir, M.; Pool, R.; Elbassioni, K.; Malde, A.K.; Mark, A.E.; Geerke, D.P.; Stougie, L.; Klau, G.W. *J. Comp. Biol.* **2013**, *20*, 188-198.
21. Koziara, K.B.; Stroet, M.; Malde, A.K.; Mark, A.E. *J. Comput. Aided Mol. Des.* **2014**, *28*, 221-233.
22. Eichenberger, A.P.; Allison, J.R.; Dolenc, J.; Geerke, D.P.; Horta, B.A.C.; Meier, K.; Oostenbrink, C.; Schmid, N.; Steiner, D.; Wang, D.Q.; van Gunsteren, W.F. *J. Chem. Theory Comput.* **2011**, *7*, 3379-3390.
23. Zakharova, E.; Martínez de Ilarduya, A.; León, S.; Muñoz-Guerra, S. *Des. Monomers Polym.* **2016**, *20*, 157-166.
24. Japu, C.; Martínez de Ilarduya, A.; Alla, A.; García-Martín, M.G.; Galbis, J.A.; Muñoz-Guerra, S. *Polym. Chem.* **2013**, *4*, 3524-3536.
25. Ahmed, J.; Zhang, J.X.; Song, Z.; Varshney, S.K. *J. Therm. Anal. Calorim.* **2009**, *95*, 957-964.

Chapter 7

Bio-based triblock copolyesters synthesized from tartaric acid derivative and poly(lactic acid), nanoparticle formation

Bio-based triblock copolyesters were synthesized by ring-opening polymerization (ROP) of L-lactide in solution using a telechelic L-tartaric-based polyester as double macroinitiator. The macroinitiator with a M_n about $3100 \text{ g}\cdot\text{mol}^{-1}$ was synthesized by non-stoichiometric melt polycondensation of dimethyl 2,3-di-O-isopropylidene-L-tartrate and 1,4-butanediol. Two triblock copolyesters of M_n ranging between $\sim 5,000$ and $\sim 7,000 \text{ g}\cdot\text{mol}^{-1}$, differing in the length of the polylactide blocks were prepared. Isopropylidene groups were hydrolyzed leading to unprotected copolyesters. All copolyesters started to decompose approximately at $260\text{--}280 \text{ }^\circ\text{C}$ and were found to be semicrystalline. Protected copolyesters had a single T_g , while deprotected ones showed two T_g . The copolyesters were able to form nanoparticles with average diameters of $\sim 190\text{--}440 \text{ nm}$ and satisfactory dispersity. The effect of the block lengths on size and ζ -potential values of the nanoparticles was evaluated. The copolyesters were highly hydrolysable especially under basic condition.



This work will be published as: E. Zakharova, S. Leon, A. Martínez de Ilarduya, S. Muñoz-Guerra. Bio-based triblock copolyesters synthesized from tartaric acid derivative and poly(lactic acid), nanoparticle formation. *React. Funct. Polym.*, to be submitted.

7.1. Introduction

Polymers from renewable resources, which are biodegradable and biocompatible, have been an attractive area of research. Of the different natural resources, carbohydrates because of their natural abundance and functional diversity stand out as highly convenient raw material and carbohydrate-based polymers have been extensively reported in literature. L-Tartaric acid, a widely available and relatively inexpensive natural resource from a large variety of fruits, has been extensively utilized in organic synthesis as a source of chirality but its use in polymers has been somewhat limited. L-Tartaric acid has been used in the synthesis of polyamides,¹⁻³ polyesters,⁴ polyesteramides,^{5,6} and polycarbonates.^{7,8}

In the present work dimethyl 2,3-di-*O*-isopropylidene-L-tartrate (iThxCOOMe) was polycondensed with 1,4-butanediol to obtain OH-(PBiThx)_x-OH telechelic homopolyester. This acetalized tartrate derivative has been previously explored for the synthesis of aliphatic copolyesters.⁹ This monomer also caused a great deal of interest, because acid-catalyzed deprotection of the isopropylidene groups gave well-defined polyesters having pendant hydroxyl functional groups regularly distributed along the polymer chain. Telechelic homopolyester was copolymerized with L-lactide to reach triblock copolyesters with evident structural difference between blocks. This chapter describes the thermal properties and the formation of nanospheres of triblock copolyesters with isopropylidene and free hydroxyl groups paying particular attention to the effect of the length of the blocks on particle size, ζ-potential.

7.2. Experimental part

7.2.1. Synthesis of telechelic OH-(PBiThx)₁₉-OH homopolyester

The aliphatic telechelic homopolyester was synthesized by melt polycondensation of 1,4-butanediol with 2,3-di-*O*-isopropylidene-L-tartrate. A 30% mole excess of diol respect to diester monomer was used. The reactants were stirred to get a homogeneous mixture and DBTO (0.5 mole-% respect to the total of monomers) was added as catalyst. The transesterification step was performed at 100 °C under nitrogen flow for 16 h, and polycondensation for 6 h at 110 °C under vacuum (0.03-0.06 mbar). The NMR data ascertaining their constitution and purity are described below.

OH-(PBiThx)₁₉-OH homopolymer: ¹H NMR (300.1 MHz, CDCl₃), δ (ppm): 4.69 (s, 2H, OCHCH), 4.25 (s, 4H, OCH₂CH₂), 1.76 (s, 4H, OCH₂CH₂), 1.54 (s, 6H, CH₃) ¹³C NMR (75.5 MHz, CDCl₃), δ (ppm): 169.5 (CO), 113.8, 77.0, 65.0, 26.2, 24.9.

7.2.2. Synthesis of PLLA_y-(PBiThx)₁₉-PLLA_y triblock copolyesters

Telechelic homopolymer OH-(PBiThx)₁₉-OH (0.30 g, 0.06 mmol) was dissolved in a 1M solution of L-lactide (0.34 g, 2.36 mmol) in dichloromethane. After dissolution of the prepolymer 5 mol % TBD (relative to lactide) was added. The solution was stirred for 5 min under nitrogen atmosphere, quenched with benzoic acid and precipitated in methanol.

PLLA_y-(PBiThx)₁₉-PLLA_y triblock copolymer: ¹H NMR (300.1 MHz, CDCl₃), δ (ppm): 5.2 (m, γ·2H, OCHCH₃), 4.69 (s, x·2H, OCHCH), 4.25 (s, x·4H, OCH₂CH₂), 1.76 (s, x·4H, OCH₂CH₂), 1.58 (d, γ·6H, OCHCH₃), 1.54 (s, x·6H, CH₃). ¹³C NMR (75.5 MHz, CDCl₃), δ (ppm): 169.5 (CO), 113.8, 77.0, 65.0, 26.2, 24.9.

7.2.3. Removal of isopropylidene groups of triblock copolyesters

General procedure of removal of isopropylidene groups of the acetal group was accomplished by treatment with trifluoroacetic acid (TFA). PLLA_y-(PBiThx)₁₉-PLLA_y block copolymer was stirred in aqueous TFA (4:1 v/v) for 30 min until complete solution. The mixture was poured into diethyl ether to precipitate the block copolymer containing free hydroxyl groups. The polymer was dried under vacuum and stored in a desiccator until needed.

PLLA_y-(PBThxOH)₁₉-PLLA_y block copolymer: ¹H NMR (300.1 MHz, TFA), δ (ppm): 5.32 (m, γ·2H, OCHCH₃), 4.91 (s, x·2H, COCHOH), 4.39 (s, x·4H, OCH₂CH₂), 1.86 (s, x·4H, OCH₂CH₂), 1.54 (s, 6H, CH₃) ¹³C NMR (75.5 MHz, CDCl₃/TFA), δ (ppm): 169.5 (CO), 113.8, 77.0, 65.0, 26.2, 24.9.

7.2.4. Hydrolytic degradation

Films for hydrolytic degradation and biodegradation studies were prepared with a thickness of 200 μm by casting from chloroform solution at a polymer concentration

of 100 g L^{-1} . The films were cut into 10 mm diameter, 20-30 mg weight disks and dried under vacuum to constant weight. For hydrolytic degradation, samples were immersed in vials containing 10 mL of either citric acid buffer (pH 2.0), sodium phosphate buffer (pH 7.4), and sodium carbonate buffer (pH 10) at $37 \text{ }^\circ\text{C}$ for 40 days. The disks were withdrawn from the incubation medium after scheduled periods of time, washed carefully with distilled water, dried to constant weight and analyzed by GPC chromatography and NMR spectroscopy. For the analysis of the products released to the incubation medium, samples were immersed in NMR tubes containing 1 mL of D_2O pH 2.0, pH 7.4 and pH 10 as well.

7.2.5. Nanoparticle formation

Nanoparticles of $\text{PLLA}_y\text{-(PBiThx)}_{19}\text{-PLLA}_y$ and $\text{PLLA}_y\text{-(PBThxOH)}_{19}\text{-PLLA}_y$ were prepared by the precipitation-dialysis method. 2 mg of the block copolyester were dissolved in 1 mL of DMSO and the same volume of water added to yield a translucent solution. This solution was dialyzed against distilled water for 72 h at room temperature using cellulose membrane tubes (2000 molecular weight cut-off) with frequent replacement of the external medium. The particles generated upon dialysis were subjected to SEM examination and light-scattering measurements.

7.2.6. Simulation studies

The morphological properties of the copolyesters containing protected and non-protected trearic units have been compared by molecular dynamics (MD) simulations. A cubic periodic box consisting on 64 polymer chains (with sequences $(\text{PLLA})_{17}\text{-(PBiThx)}_{17}\text{-(PLLA)}_{17}$ and $(\text{PLLA})_{17}\text{-(PBThxOH)}_{17}\text{-(PLLA)}_{17}$) has been simulated in the NPT ensemble at room temperature. Average box dimensions are 80 Å and 84 Å respectively.

The GAFF force field¹⁰ has been chosen to describe the potential energy. Atomic charge parameters have been obtained by fitting to the molecular electrostatic potential. The electrostatic potential have been computed at the B3LYP/6-31G* level for optimized geometries of the different repeat units. Ab initio calculations are done with Q-Chem.¹¹

The generation of starting structures for the MD has proceeded in the following way: random configurations have been generated with the packmol program,¹² taking

different polymer geometries obtained from a preliminar single-chain MD trajectory. The structure has been relaxed through an energy optimization and a NVT 1-ns MD at 300K. After that, the system has undergone a simulated annealing procedure, consisting on a progressive increase of the temperature up to 1000K during 1 ns in the NPT ensemble, followed with a 1000K NPT for 1 ns, and a slow cooling down NPT simulation to 300K for 10 ns. After this equilibration procedure, a production run of 5 ns in the NPT ensemble at 300K has been performed. All the MD simulations have been carried out with LAMMPS.¹³

7.3. Results and discussion

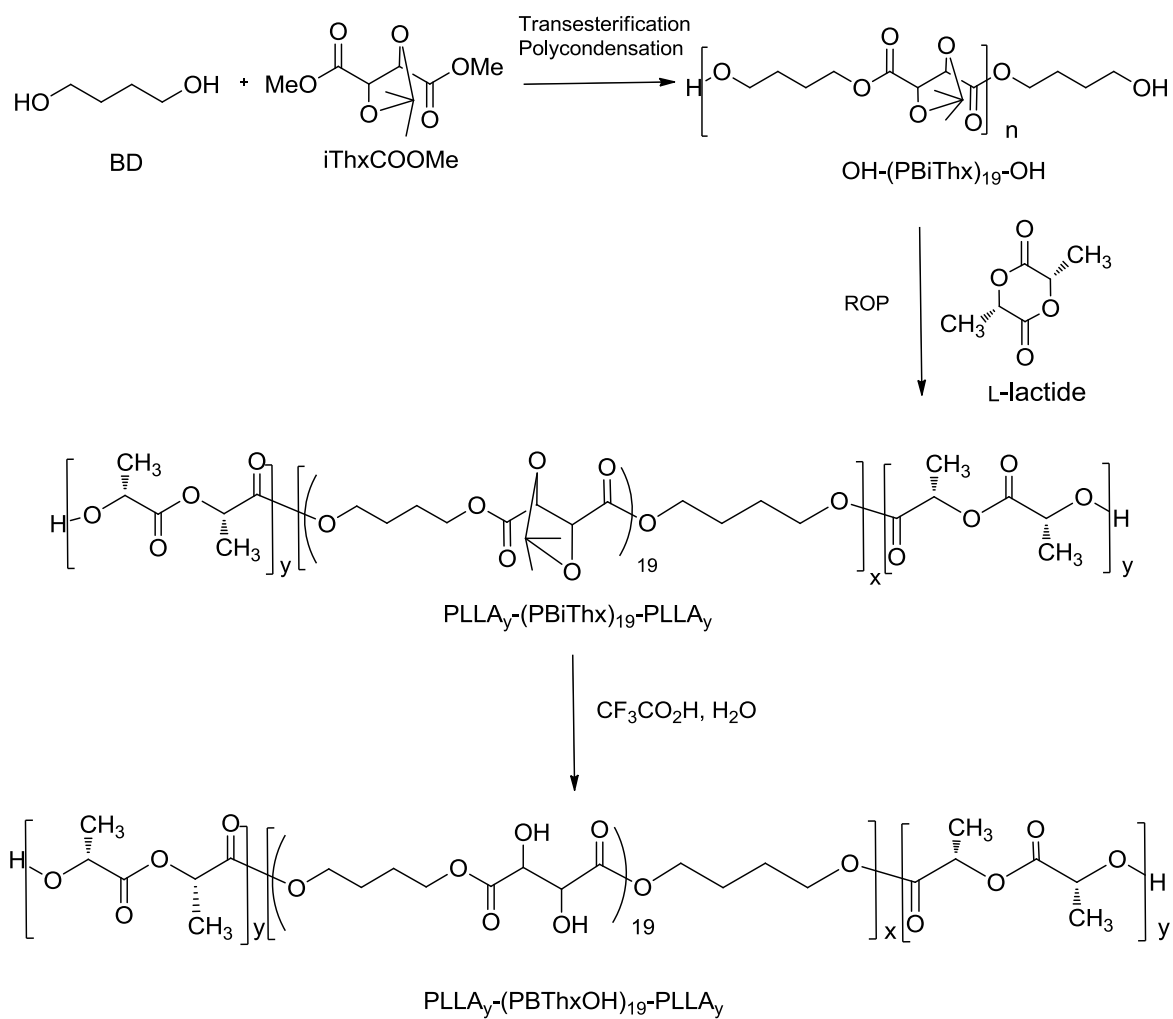
7.3.1. Synthesis and chemical structure

The synthetic route followed in this work to obtain the triblock copolyesters is depicted in Scheme 7.1. The OH-(PBiThx)₁₉-OH telechelic homopolyester was synthesized by a two-steps polymerization reaction in the melt from 1,4-butanediol and 2,3-di-O-methylene-L-tartrate using DBTO as catalyst. An excess of 30 mole-% of 1,4-butanediol was used in order to generate hydroxyl capped oligoesters containing around twenty repeating units. The first step was carried out at 100 °C under a nitrogen flow to sweep off the methanol generated by transesterification. The second step was carried out 110 °C under vacuum to remove the excess of BD and small amounts of remaining methanol. ¹H and ¹³C spectra of OH-(PBiThx)₁₉-OH homopolyester with indication of all signals assignments are provided in SI (Annex E). These spectra ascertained the chemical constitution expected for this telechelic homopolyester and a comparative quantification of the proton resonance signals arising from inner and ending threitylene units was used to estimate its number average polymerization degree which resulted to be 19.

Triblock copolyesters PLLA_y-(PBiThx)₁₉-PLLA_y were synthesized by ROP of L-lactide in the presence of OH-(PBiThx)₁₉-OH which operated as double macroinitiator. In order to prevent undesirable transesterifications leading to randomization, the reaction mixture was quenched with benzoic acid. The amounts of lactide and OH-(PBiThx)₁₉-OH made to react were accurately adjusted to target copolyesters with two selected y/x ratios, *i.e.* 4 and 6. Removal of isopropylidene groups of the acetal blocks was accomplished by treatment with aqueous trifluoroacetic acid for 5 min.

The chemical constitution and composition of the two triblock copolyesters synthesized in this work was definitely ascertained by NMR. The ^1H and ^{13}C NMR spectra of $\text{PLLA}_{38}\text{-(PBiThx)}_{19}\text{-PLLA}_{38}$ copolyester are depicted in Figure 7.1. for illustrating purposes, and those recorded for the another one is included in SI (Annex E). All signals could be straightforwardly assigned and no significant peaks revealing the presence of impurities were present in these spectra. Copolyester compositions were determined by integration of the proton signals arising from the respective block units. The obtained values were fairly close to those used in the respective feeds, which leads to conclude that L-lactide must have reacted almost completely by ROP. The characteristic peaks at 3.7 ppm corresponding to $-\text{CH}_2\text{OH}$ terminal groups disappeared as the conversion of $\text{OH-(PBiThx)}_{19}\text{-OH}$ increased, confirming the formation of ester functions (SI, Annex E).

Deprotected copolyesters were also characterized by NMR spectroscopy (Figure 7.2.). The composition of deprotected copolyesters were slightly rich in threarcic content, that could be explained by slight hydrolysis of PLLA blocks during deprotection treatment. GPC measurements showed that polyesters were obtained with M_w in the 4,000–7,000 g mol^{-1} range with dispersity indexes oscillating between 1.7 and 2.3. Composition and molecular weight data obtained for the telechelic homopolyester and the triblock copolyesters are collected in Table 7.1.



Scheme 7.1. Synthesis of OH-(PBiThx)₁₉-OH homopolyester, chain extension of main chain via ROP using L-lactide and deprotection of isopropylidene groups of PLLA_y-(PBiThx)₁₉-PLLA_y.

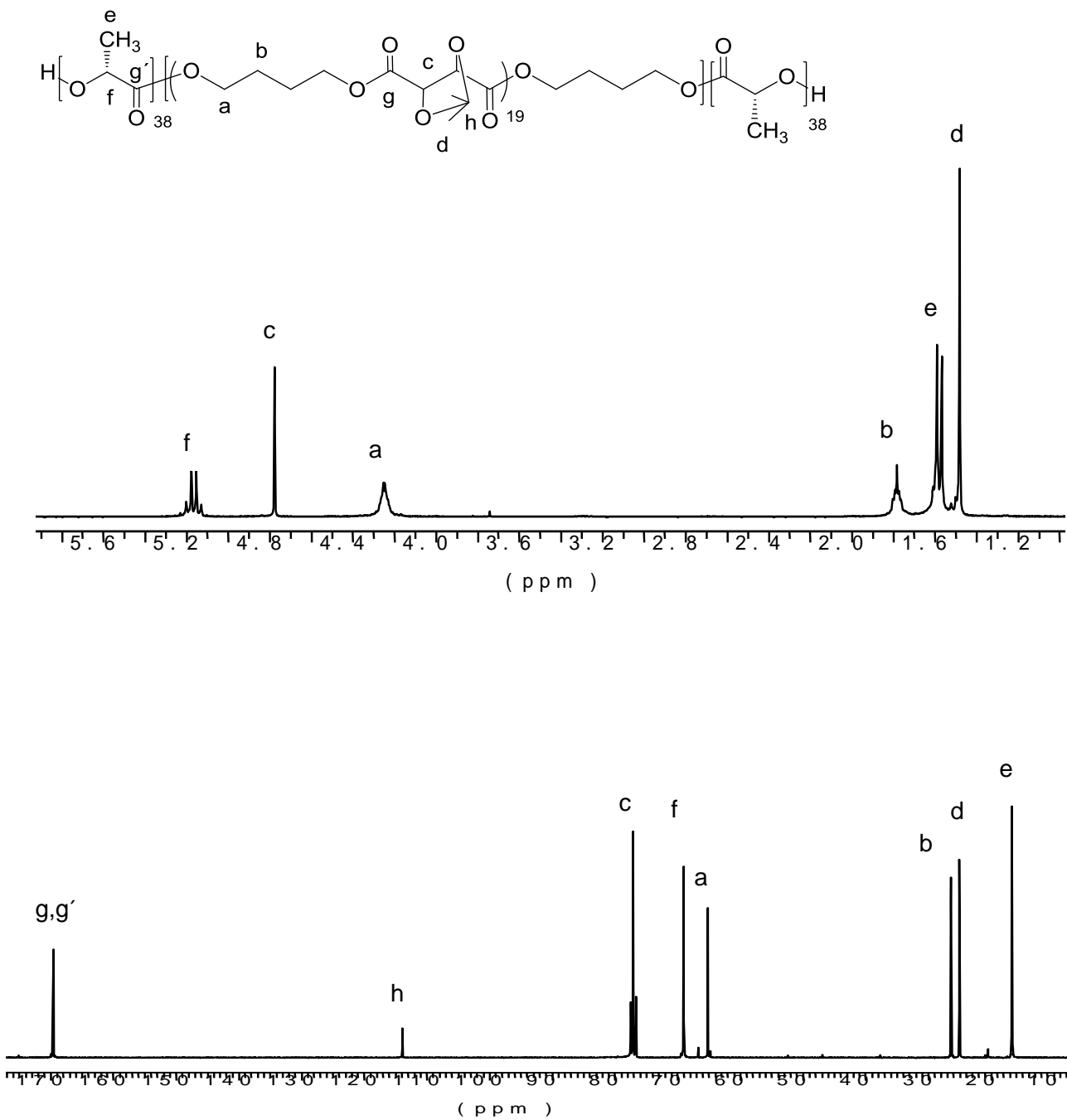


Figure 7.1. ¹H (up), ¹³C NMR spectra (bottom) of PLLA₃₈-(PBiThx)₁₉-PLLA₃₈ triblock copolymer.

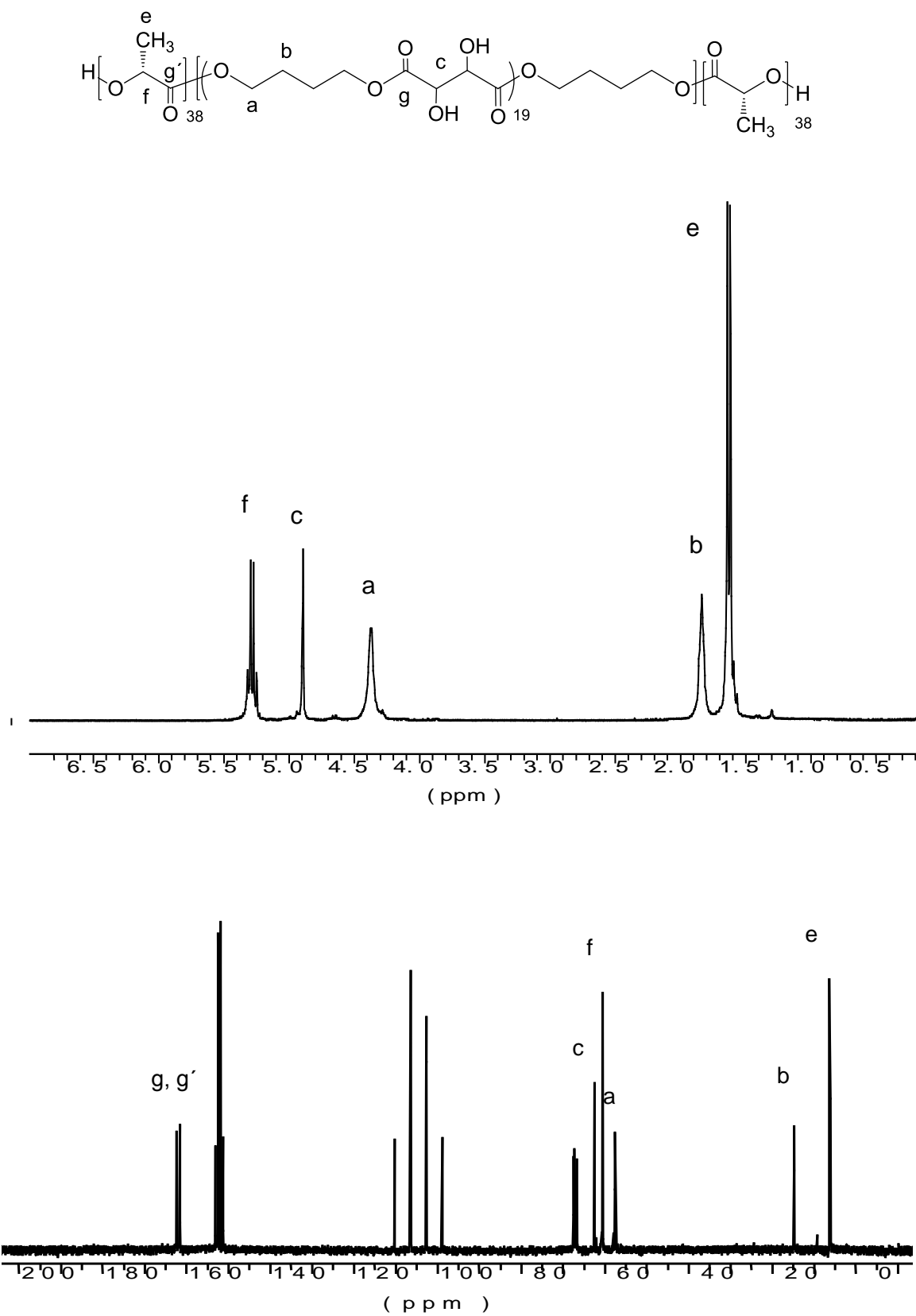


Figure 7.2. ¹H (up), ¹³C NMR spectra (bottom) of PLLA₃₈-PBThxOH₁₉-PLLA₃₈ triblock copolymer.

Table 7.1. Composition, molecular weights of telechelic homopolyesters and triblock copolyesters.

Polyester	Composition(mol/mol)		Molecular weights		
	Feed	Copolyester ^a	M_n^b	M_w^b (g·mol ⁻¹)	\mathcal{D}^b
OH-(PBiThx) ₁₉ -OH	100/0	100/0	3100	6600	2.1
PLLA ₃₈ -(PBiThx) ₁₉ -PLLA ₃₈	20.0/80.0	20.5/79.5	5300	12400	2.3
PLLA ₅₇ -(PBiThx) ₁₉ -PLLA ₅₇	14.3/85.7	15.4/84.6	7000	12400	1.8
PLLA ₃₈ -(PBThxOH) ₁₉ -PLLA ₃₈	20.0/80.0	21.4/78.6	4600	7800	1.7
PLLA ₅₇ -(PBThxOH) ₁₉ -PLLA ₅₇	14.3/85.7	17.5/82.5	6800	11800	1.7

^aMolar composition determined by integration of ¹H NMR spectra.

^bDetermined by GPC in HFIP against PMMA standards.

7.3.2. Thermal properties

The thermal behaviour of the telechelic homopolyester and the four triblock copolyesters has been comparatively studied by thermal gravimetric analysis (TGA) and differential scanning calorimetry (DSC). The main thermal parameters recorded from these assays are collected in Table 7.2.

The thermal stability was measured in the range of 30-600 °C range under a nitrogen flow, and the registered TGA traces are compared in Figure 7.3. As can be seen, the telechelic homopolyester starts to decompose approximately at 300 °C and displays a unique degradation step that proceeds at maximum rate at a temperature close to 350 °C. The triblock copolyesters started to decompose at rather lower temperatures due to lower stability of PLLA blocks. The protected copolyesters decompose through several degradation steps, while deprotected ones decompose in only one step. Main peaks corresponding to temperatures of maximum degradation rates were observed for the derivatives curves of the TGA traces in the ~ 300-360 °C range. In case of protected copolyesters, the weight loss taking place at the lower temperature step corresponds to the complete degradation of the PLLA blocks whereas that happening at higher temperature corresponds approximately to the decomposition of the (PBiThx)₁₉ block. Remaining weight after heating at 600 °C was maximum for the telechelic homopolyester (8%) whereas remaining weights for the triblock copolyesters oscillated within the 3-5% range. These TGA results lead to conclude that these compounds are rather heat resistant as to be comfortably handled by thermal processing.

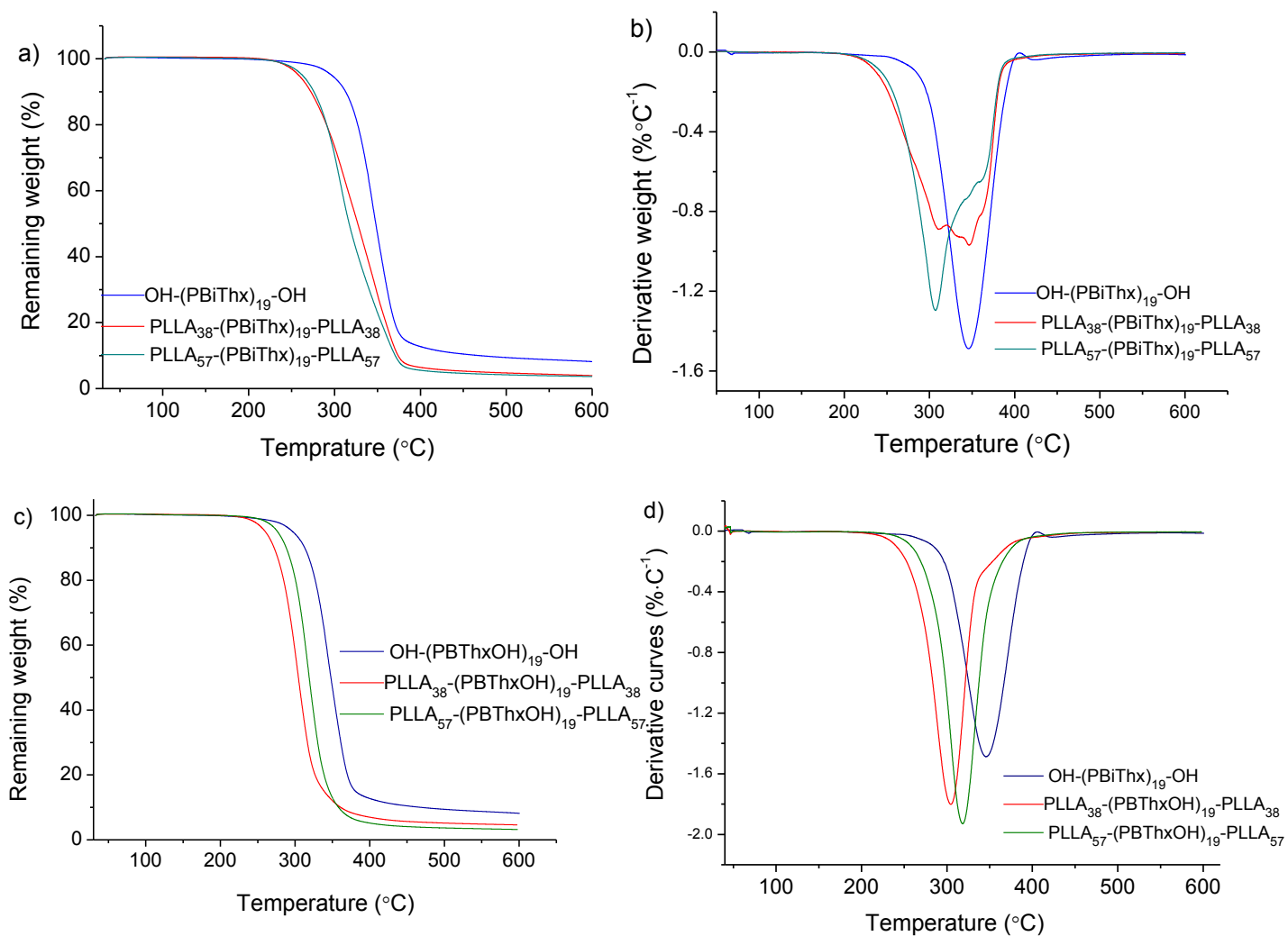


Figure 7.3. TGA traces of polyesters and its derivative curves.

Table 7.2. Thermal properties of telechelic homopolyester and triblock copolyesters.

Polyester	TGA ^a			DSC ^b								
				First heating			Cooling		Second heating			
	$^{\circ}T_d$ (°C)	$^{\max}T_d$ (°C)	RW(%)	T_g (°C)	T_m (°C)	ΔH_m (J·g ⁻¹)	T_c (°C)	ΔH_c (J·g ⁻¹)	T_c (°C)	ΔH_c (J·g ⁻¹)	T_m (°C)	ΔH_m (J·g ⁻¹)
OH-(PBiThx) ₁₉ -OH	297	346	8	-5	-	-	-	-	-	-	-	-
PLLA ₃₈ -(PBiThx) ₁₉ -PLLA ₃₈	258	310/347/359	4	24	137	24.6	-	-	100.6	-9.0	124/137	17.8
PLLA ₅₇ -(PBiThx) ₁₉ -PLLA ₅₇	263	307/344/359	4	30	154	36.7	80	16.0	-	-	153	25.7
PLLA ₃₈ -(PBThxOH) ₁₉ -PLLA ₃₈	260	304	5	35/48	146.9	39.7	-	-	107.5	-23.6	131/143	25.6
PLLA ₅₇ -(PBThxOH) ₁₉ -PLLA ₅₇	276	318	3	29/47	146.7	45.9	-	-	98.1	-26.3	145.1	37.1

^a Onset decomposition temperature corresponding to 5% of weight loss (T_d), temperature of maximum degradation rate ($^{\max}T_d$) and % of weight remaining after heating at 600 °C (RW).

^b Glass-transition temperature (T_g) taken as the inflection point of the heating DSC traces of melt-quenched samples recorded at 20 °C·min⁻¹. Melting temperatures (T_m) and melting enthalpy (ΔH_m) measured at heating/cooling rates of 10 °C·min⁻¹ of powdered samples coming directly from synthesis.

A DSC analysis of the OH-(PBiThx)₁₉-OH and triblock copolyesters was carried out in order to appraise their behavior regarding reversible thermal transitions. The DSC traces of telechelic homopolyester are shown in SI (Annex E) and the ones of triblock copolyesters are represented in Figure 7.4. The protected copolyesters were found to be semicrystalline and melted at 137 and 153 °C with respect to the fusion of PLLA blocks. As could be expected, the copolyester with longer PLLA blocks had higher T_m and ΔH_m as well. The deprotected copolyesters showed melting peaks at 147 °C with enhanced ΔH_m , corresponding to fusion of the (PBThxOH)₁₉ and PLLA block (Table 7.2).

The T_g of the polyesters were measured from the melt-quenched samples. The telechelic OH-(PBiThx)₁₉-OH homopolyester displayed a rather low T_g (-5 °C) as could be explained by the presense of isopropylidene groups in polymer chain. As it is known, the T_g of PLLA varies in the range of 50-80 °C depending on different parameters such as molecular weight and stereoisomeric content. The triblock copolyesters showed only one T_g at a value intermediate between those of OH-(PBiThx)₁₉-OH and PLLA, which increased with the LA/PBiThx ratio, that confirm the miscibility of the PBiThx and PLLA blocks. The deprotected copolyesters had two T_g , with the lower value corresponding to the transition of tartaric derived block and the higher temperature corresponding to PLLA block. The constitutional differences were evident in this case, as PLLA considered a hydrophobic polyester, while free hydroxyl groups give to the (PBThxOH) block a pronounced hydrophilic character.

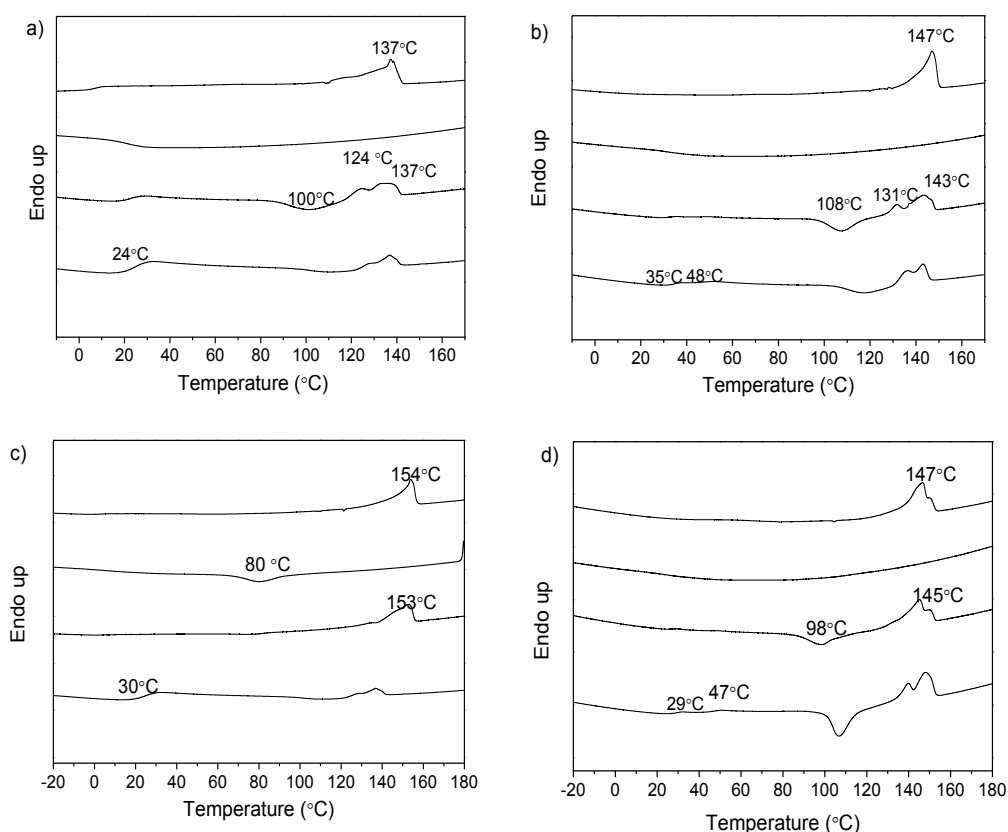


Figure 7.4. DSC traces of powdered samples of PLLA₃₈-(PBiThx)₁₉-PLLA₃₈ (a), PLLA₃₈-(PBThxOH)₁₉-PLLA₃₈ (b), PLLA₅₇-(PBiThx)₁₉-PLLA₅₇ (c), and PLLA₅₇-(PBThxOH)₁₉-PLLA₅₇ (d) copolyesters coming directly from synthesis: (1) heating at 10 °C·min⁻¹, (2) cooling at 10 °C·min⁻¹, (3) second heating at 10 °C·min⁻¹, (4) heating at 20 °C·min⁻¹ of a sample quenched from the melt.

7.3.3. Hydrolytic degradation

PLLA₃₈-(PBiThx)₁₉-PLLA₃₈ and PLLA₃₈-(PBThxOH)₁₉-PLLA₃₈ triblock copolyesters were incubated in citric acid buffer (pH 2.0), sodium phosphate buffer (pH 7.4) and sodium carbonate buffer (pH 10) at 37 °C for 40 days and degradation evolution was followed by monitoring the changes taking place in weight and M_w of the residue. According to what should be expected for aliphatic polyesters, a continuous decreasing in both sample weight and polymer M_w is observed for the two polyesters along incubation time with the noticeable remark that changes became more accentuated for hydrolytic degradation at pH 10 (Figure 7.5.). Firstly, at pH 2.0 the protected copolyester degraded at higher velocity than its deprotected analogue (SI, Annex E). After incubation its M_w reduced at 50%, while the deprotected one lost 35%. Under neutral conditions (pH 7.4) the degradation velocities of M_w of two copolyesters reached approximately the same values around 30%. At pH 10 hydrolytic degradation occurred faster than in other cases and led to almost totally destruction of incubated sample especially in case of deprotected copolyester.

To get insight into the hydrolytic degradation mechanism, the same polyesters were placed in NMR tubes at pH 10 aqueous buffer at 37 °C, and ¹H NMR spectra were recorded from the products released to the aqueous medium after incubation (Figure 7.6.). The spectrum contains signals corresponding to lactic, dilactic and tartatic acids, acetone and 1,4-butanediol. ¹H NMR of the PLLA₃₈-(PBThxOH)₁₉-PLLA₃₈ copolyester after incubation revealed that the content in PBiThx block of this sample had decreased about 10%, *i.e.* about one half of the PBiThx units were released upon degradation. This result is demonstrative that hydrolysis of triblock copolyesters mostly happens by breaking those ester groups in which the tartaric units are directly implied.

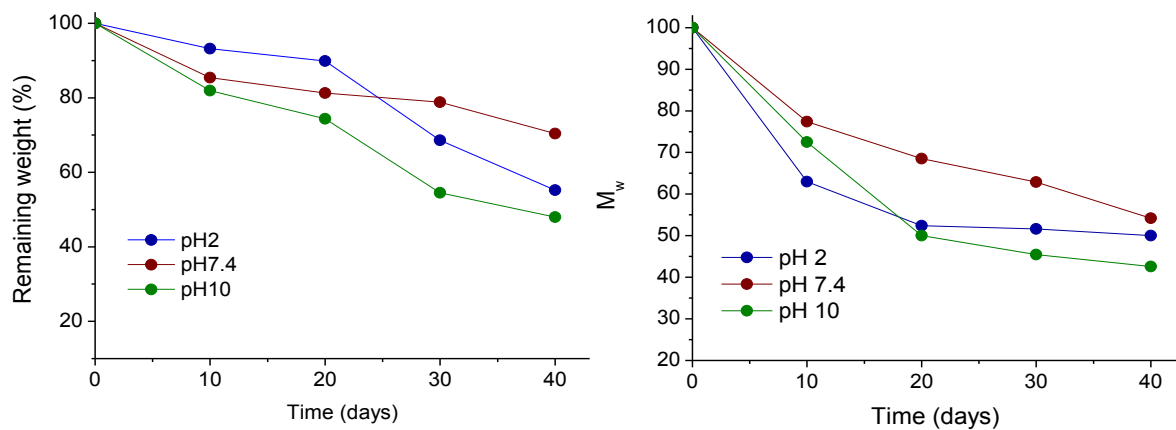


Figure 7.5. Remaining weight (a), molecular weight (b) of PLLA₃₈-(PBiThx)₁₉-PLLA₃₈ copolyester versus degradation time.

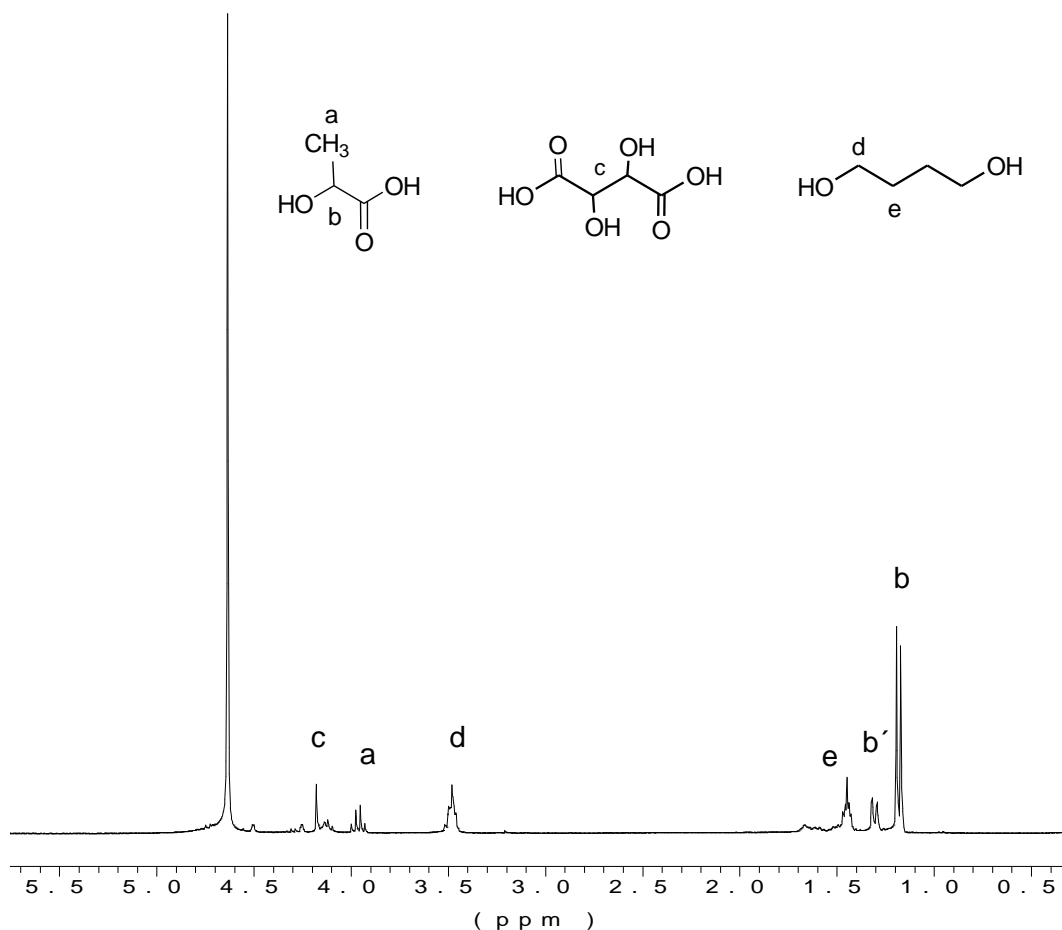


Figure 7.6. ¹H NMR spectrum in D₂O of the products released by PLLA₃₈-(PBThxOH)₁₉-PLLA₃₈ copolyester to the aqueous medium after incubation for 40 days at pH 10.

7.2.5. Nanoparticle formation

Nanotechnology has finally and firmly entered the realm of drug delivery. Performances of intelligent drug delivery systems are continuously improved with the purpose to maximize therapeutic activity and to minimize undesirable side-effects. Nanoparticles of $\text{PLLA}_{38}\text{-(PBiThx)}_{19}\text{-PLLA}_{38}$ and $\text{PLLA}_{38}\text{-(PBThxOH)}_{19}\text{-PLLA}_{38}$ were obtained by dialysis using DMSO, DMF and toluene as organic phase. The size distribution profiles of the nanoparticles obtained from the four copolyesters are compared in Figure 7.8. and the most characteristic parameters of them are collected in Table 7.3. As it is shown in Figure 7.7., well-shaped spherical particles with average diameters in the 190-440 nm range and satisfactory dispersities were obtained. Interestingly, that the size of nanoparticles formed by copolyesters with free hydroxyl groups were at two times larger than the size of nanoparticles formed by their protected analogues and it reduced as the length of the PLLA block increased.

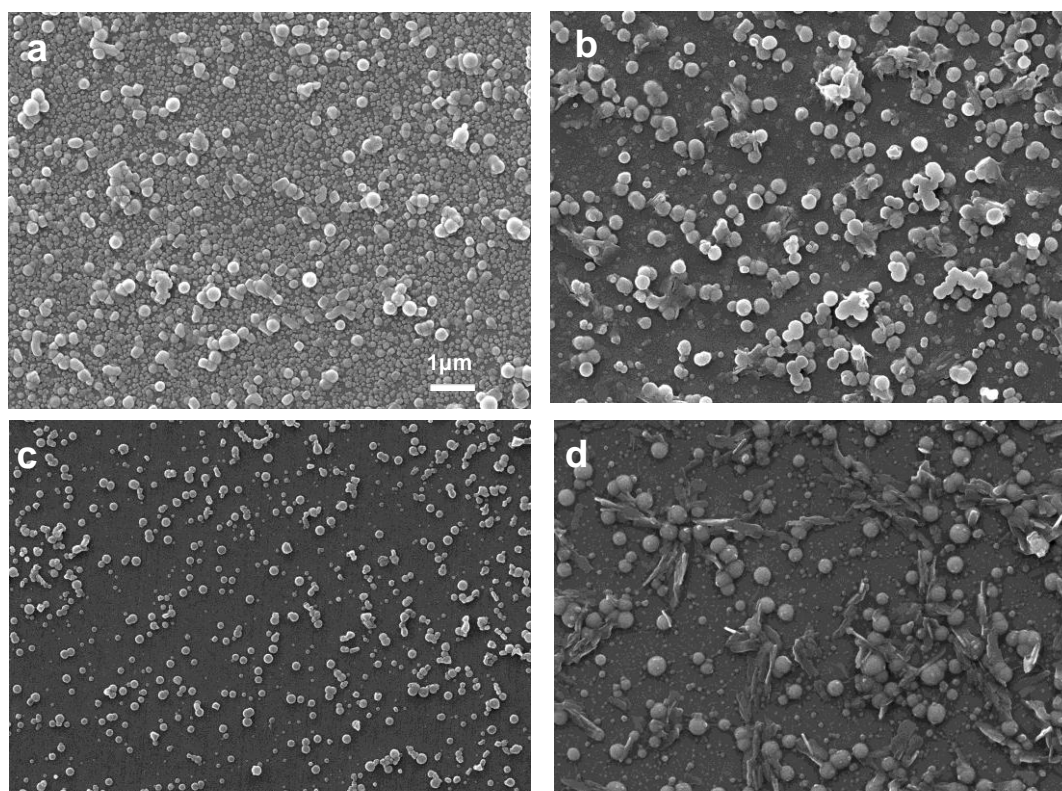
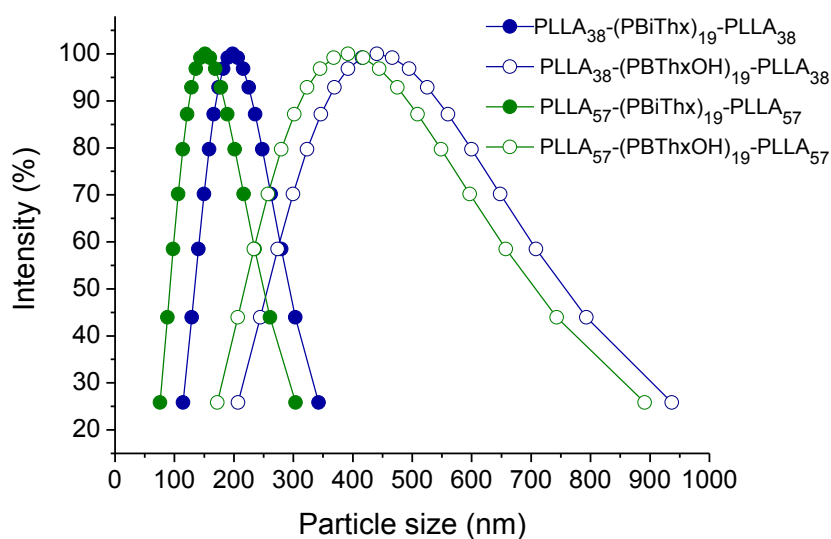


Figure 7.7. SEM images of nanoparticles made of $\text{PLLA}_{38}\text{-(PBiThx)}_{19}\text{-PLLA}_{38}$ (a), $\text{PLLA}_{38}\text{-(PBThxOH)}_{19}\text{-PLLA}_{38}$ (b), $\text{PLLA}_{57}\text{-(PBiThx)}_{19}\text{-PLLA}_{57}$ (c) and $\text{PLLA}_{57}\text{-(PBThxOH)}_{19}\text{-PLLA}_{57}$ (d) triblock copolyesters.

Table 7.3. Nanoparticle properties.

Triblock copolyester	Particle size (nm)	<i>D</i>	ζ -potential (mV)
PLLA ₃₈ -(PBiThx) ₁₉ -PLLA ₃₈	198	0.117	-23.0
PLLA ₃₈ -(PBThxOH) ₁₉ -PLLA ₃₈	440	0.234	-29.9
PLLA ₅₇ -(PBiThx) ₁₉ -PLLA ₅₇	151	0.196	-15.0
PLLA ₅₇ -(PBThxOH) ₁₉ -PLLA ₅₇	392	0.283	-18.0

**Figure 7.8.** Size distribution profiles of nanoparticles.

Zeta Potential is an important tool for understanding the state of the nanoparticle surface and predicting the long term stability of the nanoparticle. The Zeta-potential of the four triblock copolyesters was negative with values ranging between -23 and -18 mV. Such negative values are consistent with the presence of a high concentration of acetal groups or hydroxyl groups on the particle surface. Accordingly the structure of these nanoparticles can be interpreted as the (PBiThx)₁₉ and (PBThxOH)₁₉ segments are segregated to the outer part of the nanospheres whereas the PLLA blocks remain preferably located in the inner part.

The PLLA₃₈-(PBiThx)₁₉-PLLA₃₈ nanoparticles showed higher negative zeta potential value (~-23 mV), than the PLLA₅₇-(PBiThx)₁₉-PLLA₅₇ nanoparticles (~-15mV). The nanoparticles formed by copolyesters with deprotected hydroxyl groups distinguish in showing a slightly higher negative zeta potential value which is a favorable feature for

nanoparticle stability since aggregation will be hindered by electrostatic repulsion and avoid generation of aggregates.

7.2.6. Simulation studies

Figure 7.9. displays snapshots of the structure of the systems from the MD simulations. The difference between the different blocks becomes apparent in the resulting morphology, as lactic units (red) and butanediol-trearcic units (blue) appear to tend to aggregate in separate regions.

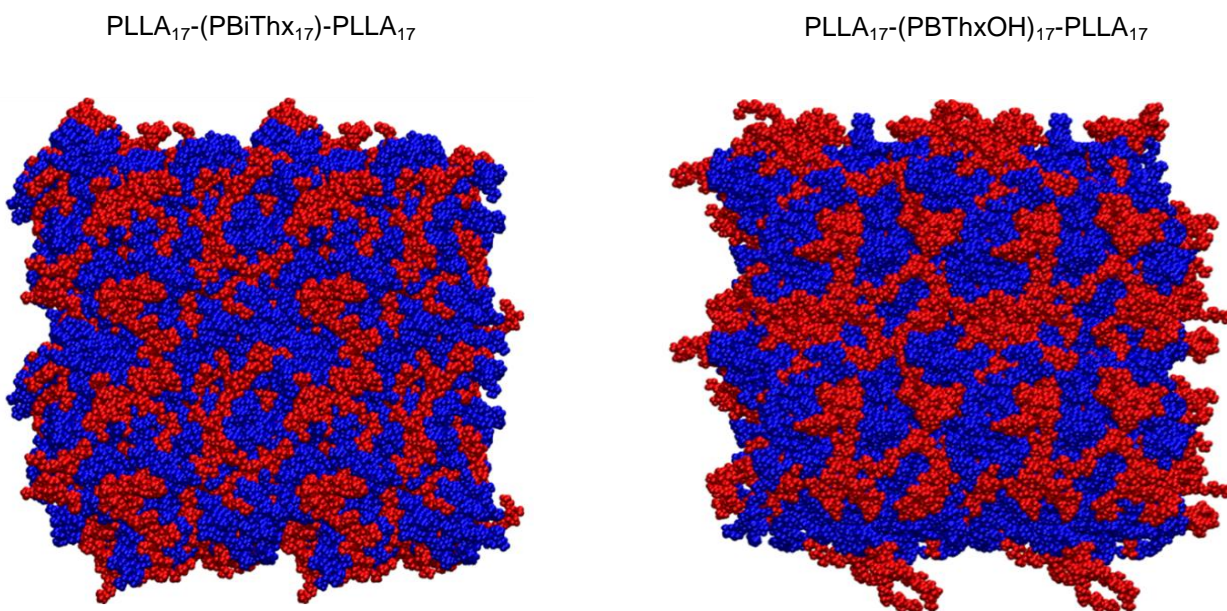


Figure 7.9. Snapshots of the molecular dynamics for the copolyesters with protected (left) and non-protected (right) trearcic units. Lactic acid blocks are depicted in red color, and butanediol-trearcic blocks in blue. Four periodic boxes are displayed.

The distribution of the different units can be described in terms of the radial distribution function. This function is defined as the population of pairs of molecules that are separated by a given distance; therefore, this function can provide information about the tendency of different units to come close or be separated.

Figure 7.10. displays a comparison of the radial distribution function between lactic units and butanediol-trearcic units for the two simulated systems. The profiles show that the proportion of pairs at short distances in the copolymer with non-protected trearcic units is significantly smaller than with protected units. This result confirms that the interaction

between lactic block and butanediol-treairic blocks is clearly lower in the non-protected copolyester.

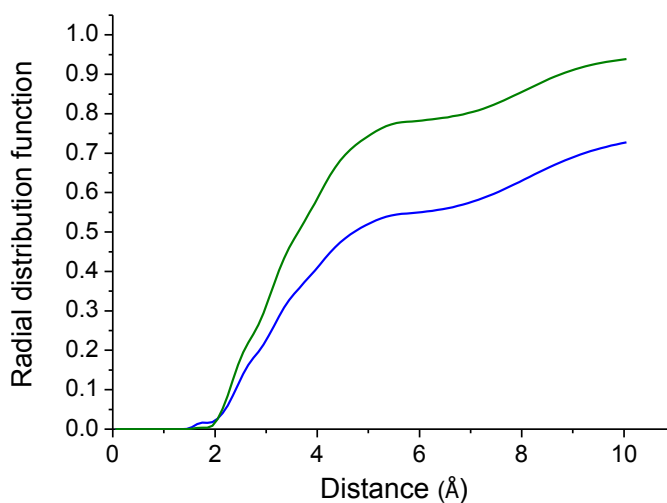


Figure 7.10. Radial distribution function between the lactate repeat units and the butanediol-treairic units for PLLA₁₇-(PBiThx)₁₇-PLLA₁₇ (green) and PLLA₁₇-(PBThxOH)₁₇-PLLA₁₇ (blue) copolyesters.

7.4. Conclusions

The triblock copolyesters PLLA_y-(PBiThx)₁₉-PLLA_y with two composition were successfully synthesized via ROP of L-lactide using as initiator a telechelic hydroxyl-capped homopolymer containing poly(butylene terephthalate) units. They were hydrolyzed leading to the copolyesters with free hydroxyl groups. They showed high thermal stability and were found to be semicrystalline. Protected copolyesters showed only one T_g intermediate between (PBiThx) and PLLA blocks, while deprotected ones demonstrated two characteristic T_g 's of each block. The copolyesters were able to form nanoparticles in nanoscale dimension suitable as hydrophobic drug carriers. They were easily hydrolysable especially under basic condition and has brought into evidence their potential application as drug delivery systems.

7.5. References

1. Bou, J. J.; Rodríguez-Galán, A.; Muñoz-Guerra, S. *Macromolecules* **1993**, *26*, 5664-5670.
2. Bou, J. J.; Iribarren, I.; Muñoz-Guerra, S. *Macromolecules* **1994**, *27*, 5263-5270.
3. Mathakiya, I. A.; Rakshit, A. K. *Int. J. Polym. Mater.* **2004**, *53*, 405-418.
4. Kimura, H.; Yoshinari, T.; Takeishi, M. *Polym. J.* **1999**, *31*, 388-392.
5. Villuendas, I.; Iribarren, J. I.; Muñoz-Guerra, S. *Macromolecules* **1999**, *32*, 8015-8023.
6. Alla, A.; Rodríguez-Galán, A.; Martínez de Ilarduya, A.; Muñoz-Guerra, S. *Polymer* **1997**, *38*, 4935-4944.
7. Acemoglu, M.; Bantle, S.; Mindt, T.; Nimmerfall, F. *Macromolecules* **1995**, *28*, 3030-3037.
8. Yokoe, M.; Aoi, K.; Okada, M. *J. Polym. Sci., Part A: Polym. Chem.* **2005**, *43*, 3909-3919.
9. Dhamaniya, S.; Jacob, J. *Polym. Bull.* **2012**, *68*, 1287-1304.
10. Wang, J., Wolf, R. M., Caldwell, J. W., Kollman, P. A.; Case, D. A. *J. Comput. Chem.* **2004**, *25*, 1157-1174.
11. Shao, Y. *et al. Mol. Phys.* **2015**, *113*, 184-215.
12. Martínez, L.; Andrade, R.; Birgin, E. G.; Martínez, J. M. *J. Comput. Chem.* **2009**, *30*, 2157-2164.
13. Plimpton, S. *J. Comp. Phys.* **1995**, *117*, 1-19.

Chapter 8

General conclusions

- Cyclic and bicyclic acetalized monomers derived from L-threose (Thx and iThx), D-glucose (Glux-diol) and D-mannose (Manx-diol), in addition to the bicyclic dianhydroglucitol known as isosorbide (Is), were successfully used as comonomers for copolyesters by both melt polycondensation and ROP in solution. Homopolyesters and a palette of random and block copolyesters could be synthesized under different reaction conditions.
- Organometallic DBTO was the catalyst used for melt polycondensation at high temperature leading to polyesters and random copolyesters with pretty high molecular weights. Organic TBD was the catalyst applied to assist ROP in solution at room temperature applied for building block copolyesters. It was observed along this thesis that poly(alkanoate)s synthesized from Is invariably showed lower molecular weight and needed longer reaction times than other cases, which is attributed to the relative lower reactivity of the secondary free hydroxyl functions present in this compound.
- It was concluded that the incorporation of sugar-derived units in the aliphatic polyesters did not produce significant alterations of their thermal stability. The decomposition temperature of copolyesters containing Thx units was found to be slightly lower than in homopolyesters whereas in copolyesters made from Glux-diol it remained practically unchanged for the whole range of compositions. The resistance to heat of all polyesters and copolyesters was high enough to allow their comfortable processing by conventional thermal methods.
- In general the statistical incorporation of sugar derived units in the aliphatic polyester entailed a noticeable decrease of both T_m and crystallinity. This depressing effect was weaker for the relatively smaller Thx units. Although the presence of Glux structure in copolyesters aliphatic appeared to be less influential than either Manx or Is for hindering crystallization, random copolyesters containing more than 30 mole-% of Glux units were definitely amorphous.
- The insertion of sugar-based acetalized units gave rise to an important increase of the T_g of all random copolyesters. This effect was much more pronounced when bicyclic sugar-based units were concerned, as it should be expected from their higher size and stiffness. The effect on T_g follows the order Glux>>Manx>Is>Thx in the three polyalkanoate series.

- The influence of copolymerization on the mechanical behavior was dependent on both the constitution and the content of the sugar-derived unit that was inserted. In general it can be stated that polyesters made from Glux-diol displayed much higher modulus and tensile strength than the other poly(alkanoate)s made from Thx, Manx-diol or Is, which in turn were much less extensible. Nevertheless, copolyesters with amounts of Glux units up to 30 mole-% showed a significant reduction in both Young modulus and tensile strength whereas the opposite effect was found for higher contents in such units.

- Degradation studies revealed that not only chemical degradation but also biodegradation of polyesters became enhanced by the insertion of either Thx or Glux units in the polyester chain. The hydrolytic degradation happened mostly by breaking the ester groups in which the sugar-based units were directly implied.

- Triblock copolyesters were synthesized by ROP of L-lactide initiated by diol macroinitiators made of poly(iThx or Glux succinate)s. Block copolyesters containing either Glux or iThx showed only one T_g whereas two T_g were displayed when the iThx units were desacetalized. Copolyesters containing Thx showed crystallinity that increased with desacetalization. All the triblock copolyesters were capable of self-assembling in nanoparticles with diameters in the 100-400 nm range. Molecular dynamics analysis supported the existence of a biphasic arrangement in these nanoparticles with hydrophilic units preferably located on the periphery. The copolyesters containing Thx units were readily hydrolysable under physiological conditions which brought into evidence their potential to be used as drug delivery systems.

Supplementary Information

Annex A. Modification of properties of poly(butylene succinate) by copolymerization with tartaric acid-based monomers

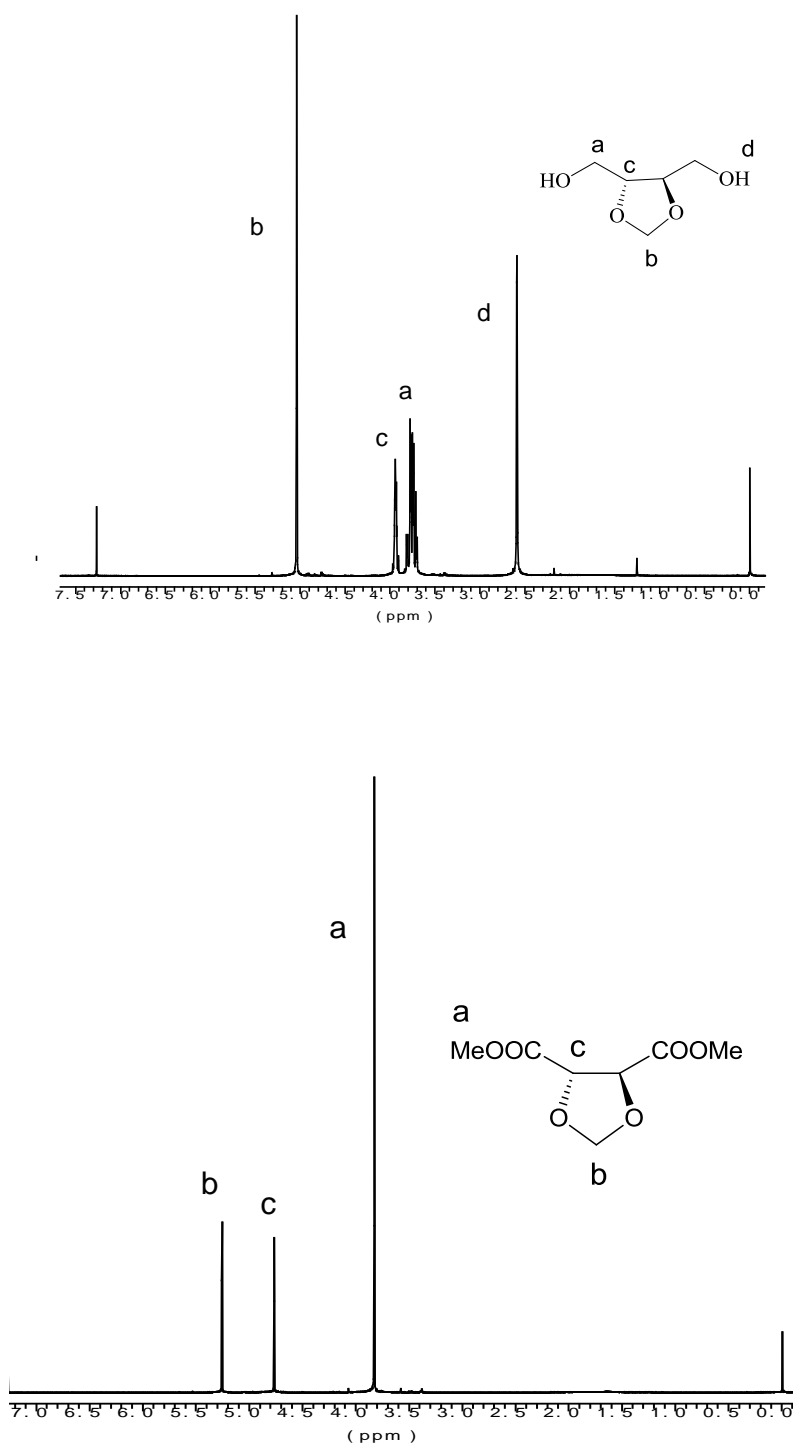


Fig.SI-A-1. ¹H NMR spectra of 2,3-di-O-methylene-L-threitol (up) and dimethyl 2,3-di-O-methylene-L-tartrate (bottom) with indication of peak assignments.

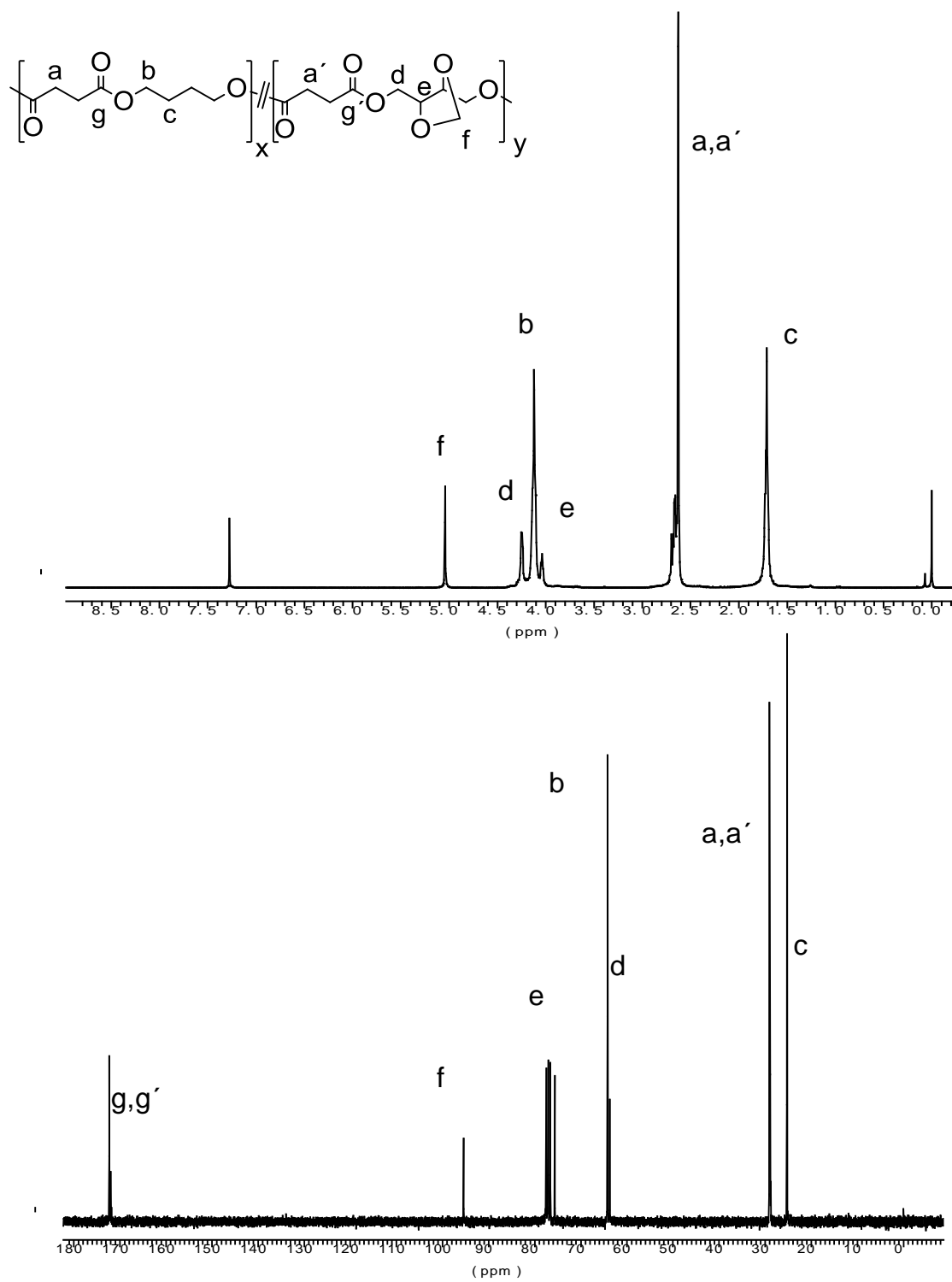


Fig.SI-A-2. ¹H- (top) and ¹³C- (bottom) NMR spectra of PB₈₀Thx₂₀S copolyesters.

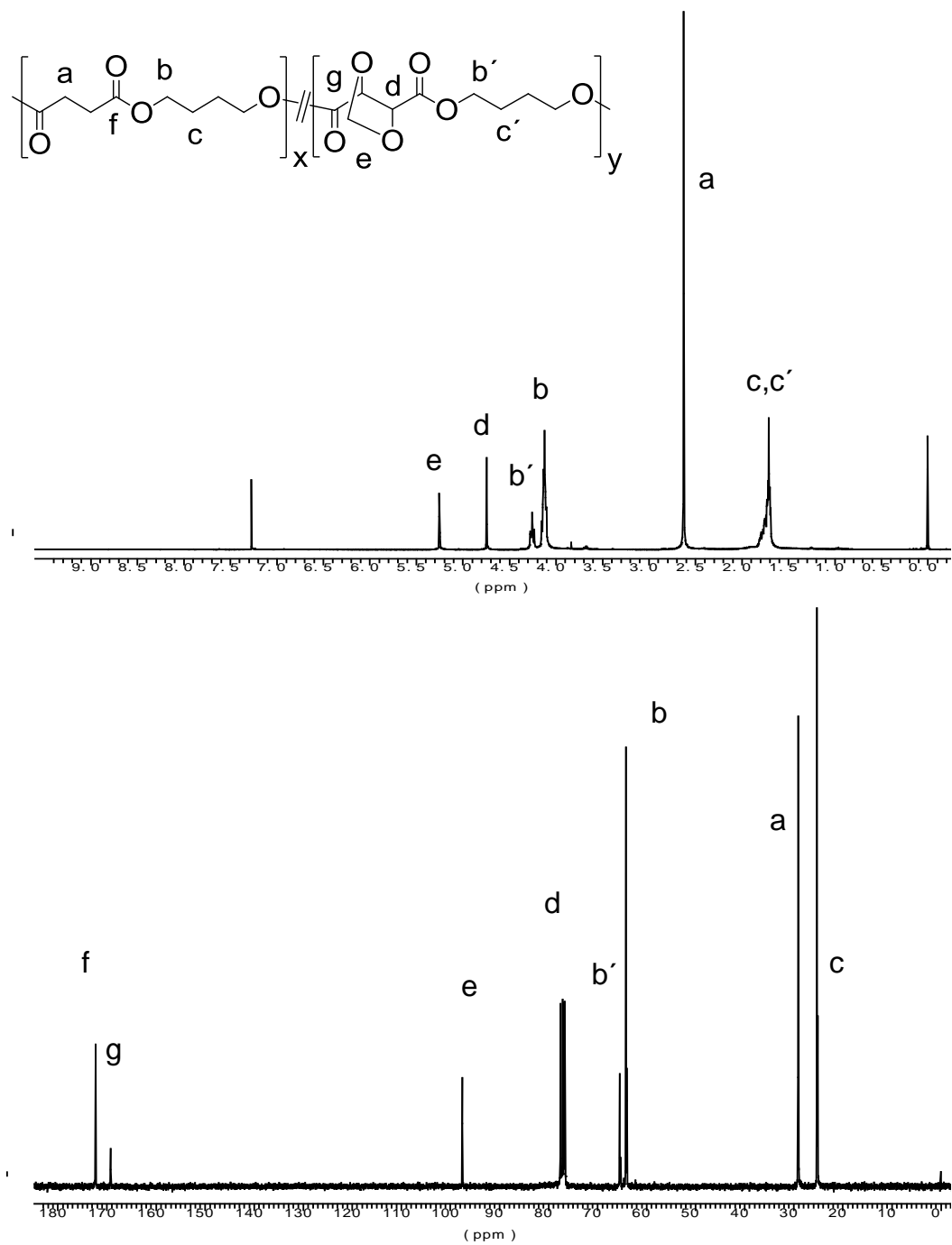


Fig. SI-A-3. ¹H- (top) and ¹³C- (bottom) NMR spectra of PBS₈₀Th₂₀ copolyesters.

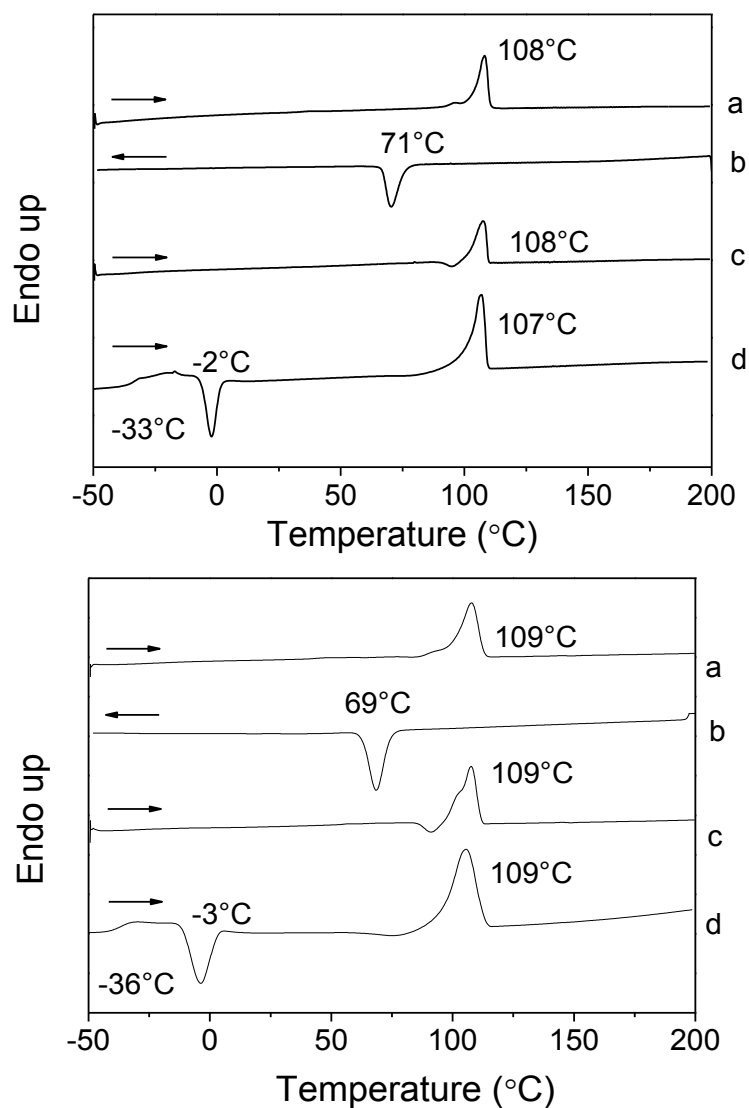


Fig. SI-A-4. DSC traces of PB₉₅Thx₅S (top) and PBS₉₅Thx₅ (bottom): (a) Heating at 10 °C·min⁻¹, (b) cooling at 10 °C·min⁻¹, (c) second heating at 10 °C·min⁻¹, (d) heating at 20 °C·min⁻¹ of a sample quenched from the melt.

Table SI-A-1. Powder X-ray diffraction data of PB_xTh_yS and PBS_xTh_y polyesters.

Polyester	<i>d</i> ^a (Å)									
PBS	6.5 w		4.5 m		4.0 m	3.9 s	3.4 w	3.0 w		2.6 w
PB ₈₀ Th ₂₀ S		5.4 w		4.5 m		3.9 s	3.4 w	3.1 w		2.6 w
PB ₆₀ Th ₄₀ S		5.4 w		4.5 m		4.0 m	3.4 w	3.1 w		2.6 w
PThxS										
PBS ₈₀ Th ₂₀	6.5 w	5.4 w		4.5 m		4.0 m	3.9 s	3.4 w	3.1 w	2.6 w
PBS ₆₀ Th ₄₀	6.5 w	5.4 w		4.5 m		3.9 m	3.4 w	3.1 w		2.6 w
PBS ₂₀ Th ₈₀	8.5 m	5.4 w	5.0 m		.4 m					2.7 w 2.5 w
PBThx	8.5 w	5.4 w	5.2 m	5.0 w	4.4 m	4.3 m	3.9 m			2.9 w 2.7 w 2.5 w

^a Bragg spacings measured in powder diffraction patterns after annealing. Intensities visually estimated as follows: m, medium strong; w, weak.

Crystallization kinetics

The Avrami equation (1) relates the fraction or amount of uncrystallized polymer that remains after time ($t-t_0$) during an isothermal processes to its growth rate parameter, k , and Avrami index, n .

$$X_c = 1 - \exp(-k(t-t_0)^n) \quad (1)$$

$$\log [-\ln(1-X_c)] = \log k + n \log(t-t_0) \quad (2)$$

The Avrami model is represented in logarithmic form (2), which allows to plot the following values $\log(t-t_0)$ vs $\log[-\ln(1-X_c)]$ and determine the parameters n and k , see Figure SI-3. Table SI-2 shows the values obtained from the Avrami fit.

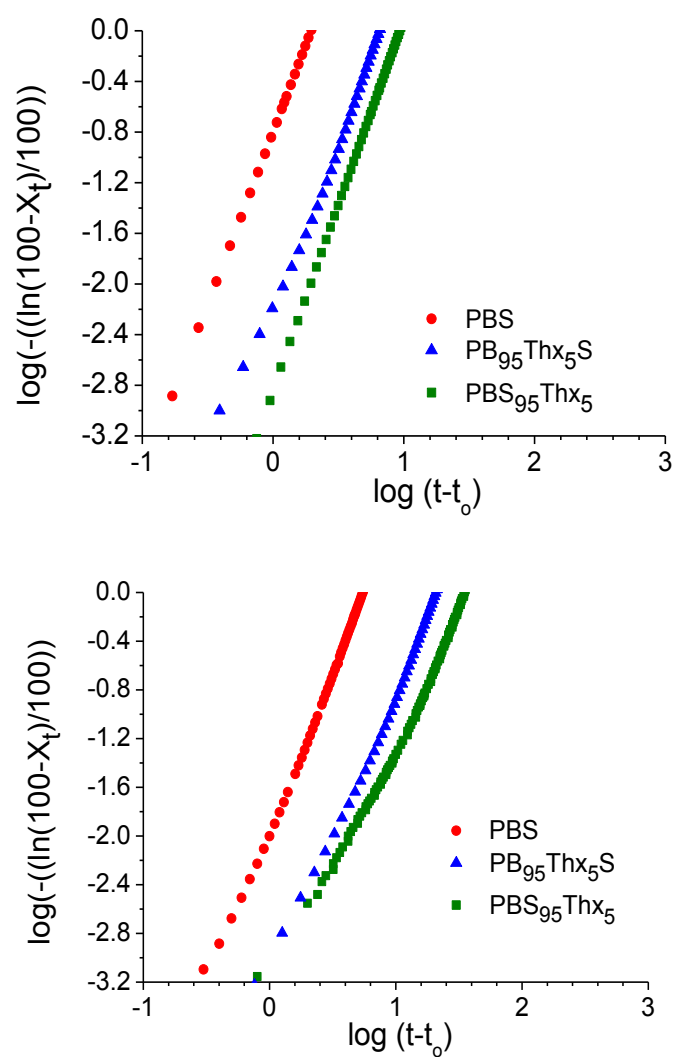


Fig. SI-A-5. Avrami plots of the Isothermal crystallization of polyesters at 85 °C (top) and 90 °C (bottom).

Table SI-A-2. Isothermal crystallization data of PBS, PB₉₅Thx₅S and PB₉₅Thx₅.

Polyester	T_c °C	t_0 min	$t_{1/2}$ min	n	$-\log k$	T_m^a °C
PBS	85	0.23	1.94	2.74	0.80	101/114
PBS	90	0.5	5.33	2.36	1.94	104/114
PB ₉₅ Thx ₅ S	85	0.41	6.16	2.20	2.11	100/108
PB ₉₅ Thx ₅ S	90	1.24	19.51	2.07	3.02	103/108
PBS ₉₅ Thx ₅	85	1.10	9.13	2.95	2.84	99/108
PBS ₉₅ Thx ₅	90	1.10	31.22	1.66	3.03	102/108

^aMultiple melting peak.

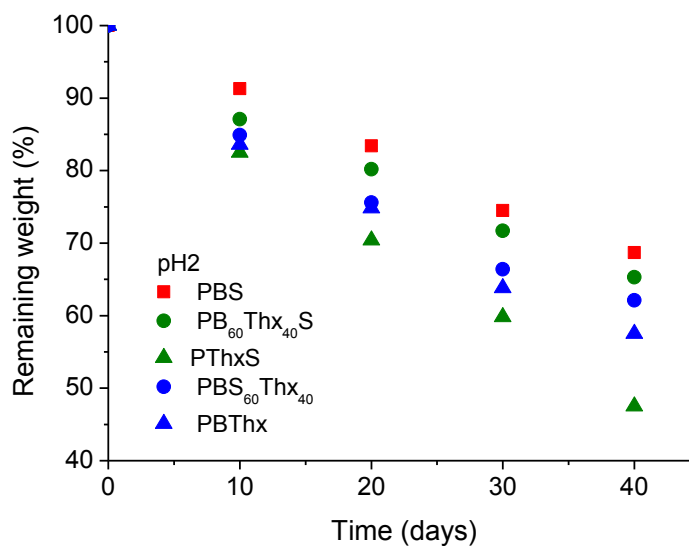


Fig. SI-A-6. Remaining weight of polyesters vs degradation time.

Annex B. Bio-based PBS copolyesters derived from a bicyclic D-glucitol

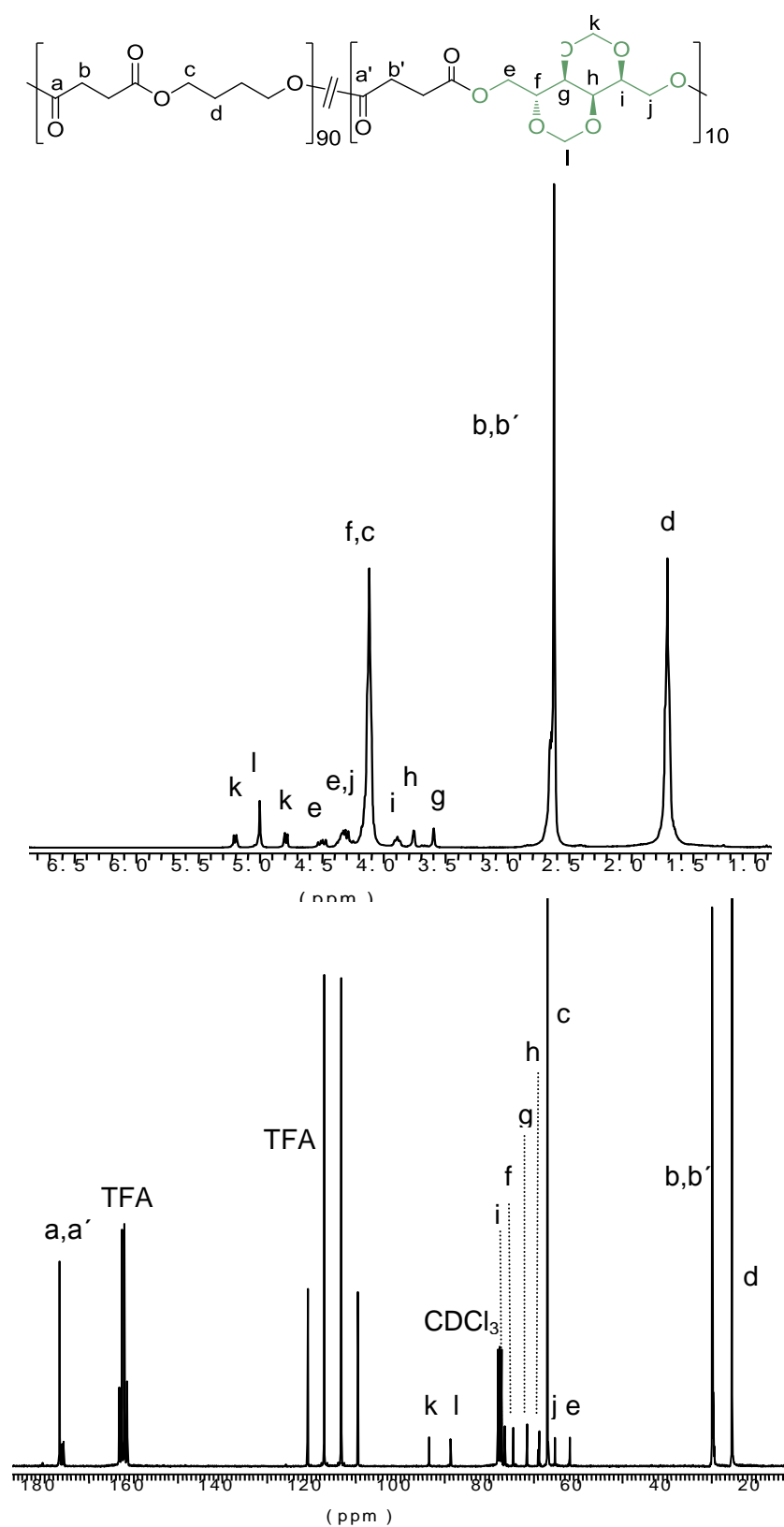


Fig. SI-B-1 ¹H NMR (top) and ¹³C (bottom) NMR spectra of PB₉₀Glux₁₀S copolyester with indication of peak assignments.

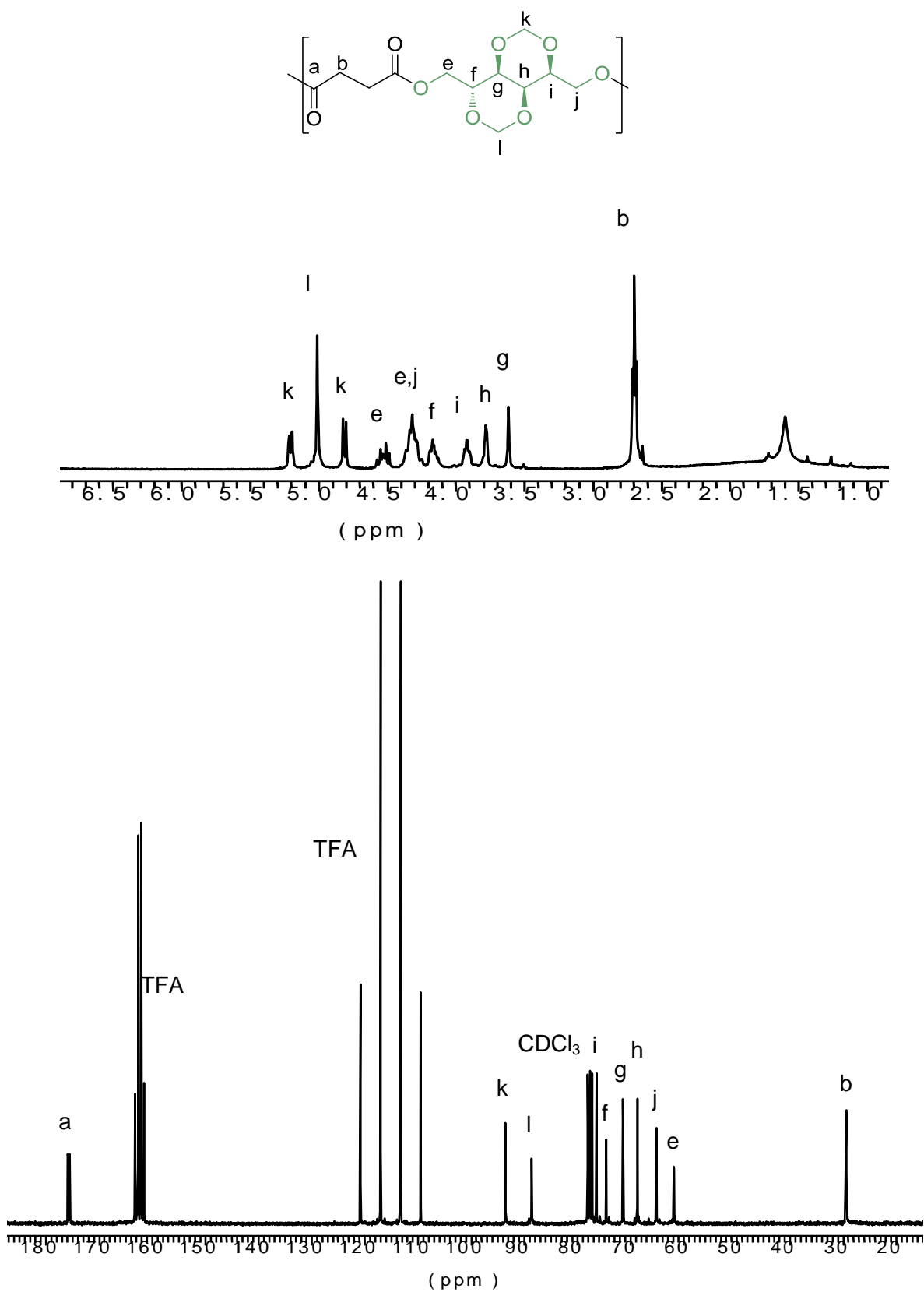


Fig. SI-B-2 ^1H NMR (top) and ^{13}C (bottom) NMR spectra of PGLuxS homopolyester with indication of peak assignments.

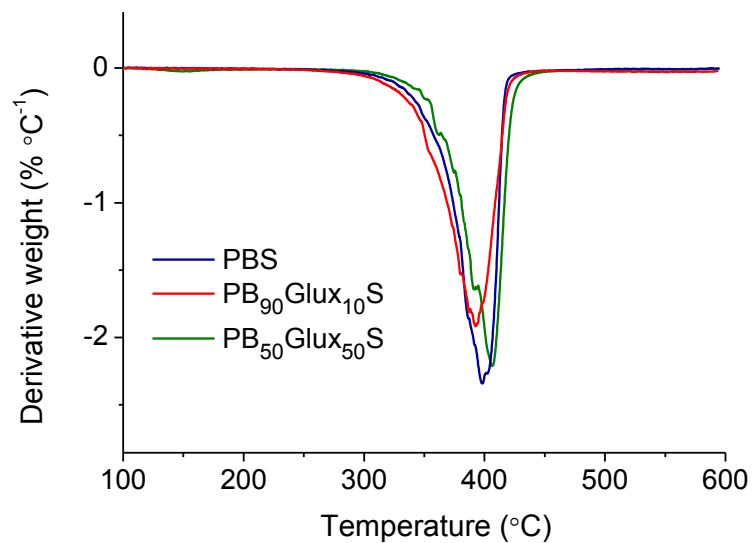


Fig. SI-B-3 Derivative curves of PBS, PB₉₀Glux₁₀S and PB₅₀Glux₅₀S.

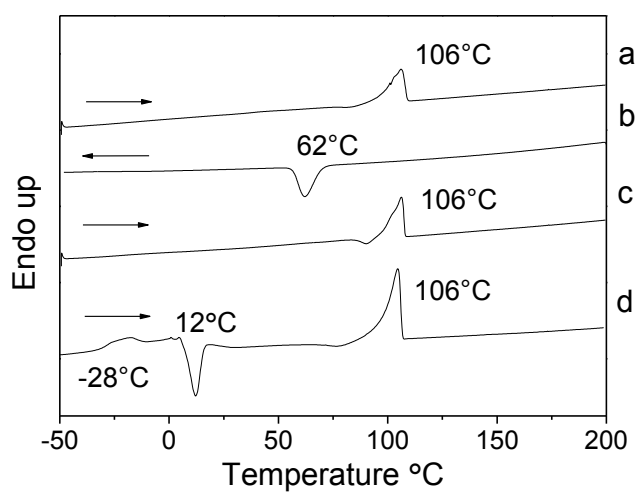


Fig. SI-B-4 DSC traces for PB₉₅Glux₅S: (a) Heating at 10 °C·min⁻¹, (b) Cooling at 10 °C·min⁻¹, (c) Second heating at 10 °C·min⁻¹, (d) Heating at 20 °C·min⁻¹ of a sample quenched from the melt.

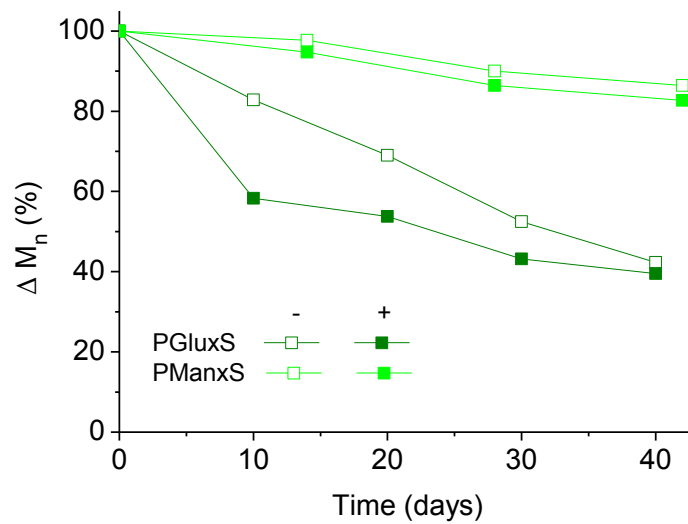


Fig. SI-B-5 Degradation curves representing the decay in molecular weight against incubation time for PGLuxS, PManxS at pH 7.4, (+) and (-) stand for presence of lipases.

Annex C. Sugar-based bicyclic monomers for aliphatic polyesters: a comparative appraisal of acetalized alditols and isosorbide

Signal assignments of the ^1H and ^{13}C NMR spectra recorded from polyesters

PGluxAdi: ^1H NMR (300.1 MHz, CDCl_3), δ (ppm): 5.2-4.8 (m, 4H, OCH_2O), 4.6-4.2 (m, 2H, OCH_2CH), 4.4-4.2 (m, 4H, OCH_2CH), 4.2 (m, 1H, OCH_2CHCH), 3.9 (m, 1H, OCH_2CHCH), 3.8 (m, 1H, OCH_2CHCH), 3.6 (m, 1H, $\text{OCH}_2\text{CHCHCHCH}$), 2.4 (m, 4H, COCH_2CH_2), 1.7 (m, 4H, COCH_2CH_2). ^{13}C NMR (75.5 MHz, CDCl_3), δ (ppm): 173.0-172.8 (CO), 92.9, 88.3, 75.5, 73.8, 70.9, 67.3, 63.2, 60.5, 33.6, 24.2.

PGluxSub: ^1H NMR (300.1 MHz, CDCl_3), δ (ppm): 5.2-4.8 (m, 4H, OCH_2O), 4.6-4.2 (m, 2H, OCH_2CH), 4.4-4.2 (m, 4H, OCH_2CH), 4.2 (m, 1H, OCH_2CHCH), 3.9 (m, 1H, OCH_2CHCH), 3.7 (m, 1H, OCH_2CHCH), 3.6 (m, 1H, $\text{OCH}_2\text{CHCHCHCH}$), 2.3 (t, 4H, COCH_2CH_2), 1.6 (m, 4H, COCH_2CH_2), 1.4 (m, 4H, $\text{COCH}_2\text{CH}_2\text{CH}_2$). ^{13}C NMR (75.5 MHz, CDCl_3), δ (ppm): 173.5-173.2 (CO), 92.9, 88.3, 75.6, 73.8, 70.9, 67.3, 63.2, 60.3, 33.9, 28.6, 24.6.

PGluxSeb: ^1H NMR (300.1 MHz, CDCl_3), δ (ppm): 5.2-4.8 (m, 4H, OCH_2O), 4.6-4.2 (m, 2H, OCH_2CH), 4.4-4.2 (m, 4H, OCH_2CH), 4.2 (m, 1H, OCH_2CHCH), 3.9 (m, 1H, OCH_2CHCH), 3.7 (m, 1H, OCH_2CHCH), 3.6 (m, 1H, $\text{OCH}_2\text{CHCHCHCH}$), 2.3 (m, 4H, COCH_2CH_2), 1.6 (m, 4H, COCH_2CH_2), 1.3 (m, 8H, $\text{COCH}_2\text{CH}_2\text{CH}_2\text{CH}_2$). ^{13}C NMR (75.5 MHz, CDCl_3), δ (ppm): 173.6-173.4 (CO), 92.9, 88.3, 75.6, 73.8, 71.0, 67.3, 63.4, 34.1, 29.1, 24.8.

PManxAdi: ^1H NMR (300.1 MHz, CDCl_3), δ (ppm): 4.9-4.8 (m, 4H, OCH_2O), 4.6-4.2 (m, 4H, OCH_2CH), 4.4 (m, 2H, OCH_2CH), 4.0 (m, 2H, OCH_2CHCH), 2.4 (m, 4H, COCH_2CH_2), 1.7 (m, 4H, COCH_2CH_2). ^{13}C NMR (75.5 MHz, CDCl_3), δ (ppm): 173.0 (CO), 88.3, 70.8, 66.3, 63.1, 33.6, 24.2.

PManxSub: ^1H NMR (300.1 MHz, CDCl_3), δ (ppm): 4.9-4.8 (m, 4H, OCH_2O), 4.5-4.2 (m, 4H, OCH_2CH), 4.4 (m, 2H, OCH_2CH), 4.1 (m, 2H, OCH_2CHCH), 2.4 (t, 4H, COCH_2CH_2), 1.8 (m, 4H, COCH_2CH_2), 1.3 (m, 4H, $\text{COCH}_2\text{CH}_2\text{CH}_2$). ^{13}C NMR (75.5 MHz, CDCl_3), δ (ppm): 173.4 (CO), 88.3, 70.9, 66.4, 63.0, 34.0, 29.0, 24.6.

PManxSeb: ^1H NMR (300.1 MHz, CDCl_3), δ (ppm): 4.9-4.8 (m, 4H, OCH_2O), 4.5-4.2 (m, 4H, OCH_2CH), 4.4 (m, 2H, OCH_2CH), 4.0 (m, 2H, OCH_2CHCH), 2.4-2.2 (t, 4H, COCH_2CH_2), 1.6 (m, 4H, COCH_2CH_2), 1.3 (m, 8H, $\text{COCH}_2\text{CH}_2\text{CH}_2\text{CH}_2$). ^{13}C NMR (75.5 MHz, CDCl_3), δ (ppm): 173.6 (CO), 88.3, 70.9, 66.4, 63.0, 34.0, 29.0, 24.8.

PIsAdi: ^1H NMR (300.1 MHz, CDCl_3), δ (ppm): 5.2 (m, 1H, CHO_{exo}), 5.1 (m, 1H, CHO_{endo}), 4.8 (m, 1H, $\text{CHCHO}_{\text{endo}}$), 4.6 (m, 1H, $\text{CHCHO}_{\text{exo}}$), 4.0-3.7 (m, 4H, $\text{CH}_2\text{CHO}_{\text{exo}}$ and $\text{CH}_2\text{CHO}_{\text{endo}}$), 2.4-2.2 (m, 4H, COCH_2CH_2), 1.7 (m, 4H, COCH_2CH_2). ^{13}C NMR (75.5 MHz, CDCl_3), δ (ppm): 172.6-172.2 (CO), 85.9, 80.7, 78.3, 73.9, 73.4, 70.4, 33.7-33.4, 24.2.

PIsSub: ^1H NMR (300.1 MHz, CDCl_3), δ (ppm): 5.2 (m, 1H, CHO_{exo}), 5.1 (m, 1H, CHO_{endo}), 4.8 (m, 1H, $\text{CHCHO}_{\text{endo}}$), 4.5 (m, 1H, $\text{CHCHO}_{\text{exo}}$), 4.0-3.7 (m, 4H, $\text{CH}_2\text{CHO}_{\text{exo}}$ and $\text{CH}_2\text{CHO}_{\text{endo}}$), 2.4-2.2 (m, 4H, COCH_2CH_2), 1.6 (m, 4H, COCH_2CH_2), 1.4 (m, 4H, $\text{COCH}_2\text{CH}_2\text{CH}_2$). ^{13}C NMR (75.5 MHz, CDCl_3), δ (ppm): 173.0-172.6 (CO), 86.0, 80.7, 77.9, 73.8, 73.5, 70.4, 34.0-33.8, 28.7, 24.6.

PIsSeb: ^1H NMR (300.1 MHz, CDCl_3), δ (ppm): 5.2 (m, 1H, CHO_{exo}), 5.1 (m, 1H, CHO_{endo}), 4.8 (m, 1H, $\text{CHCHO}_{\text{endo}}$), 4.5 (m, 1H, $\text{CHCHO}_{\text{exo}}$), 4.0-3.7 (m, 4H, $\text{CH}_2\text{CHO}_{\text{exo}}$ and $\text{CH}_2\text{CHO}_{\text{endo}}$), 2.4-2.2 (m, 4H, COCH_2CH_2), 1.6 (m, 4H, COCH_2CH_2), 1.3 (s, 8H, $\text{COCH}_2\text{CH}_2\text{CH}_2\text{CH}_2$). ^{13}C NMR (75.5 MHz, CDCl_3), δ (ppm): 173.1-172.8 (CO), 86.0, 80.7, 77.9, 73.7, 73.5, 70.4, 34.1-33.9, 29.0, 24.8.

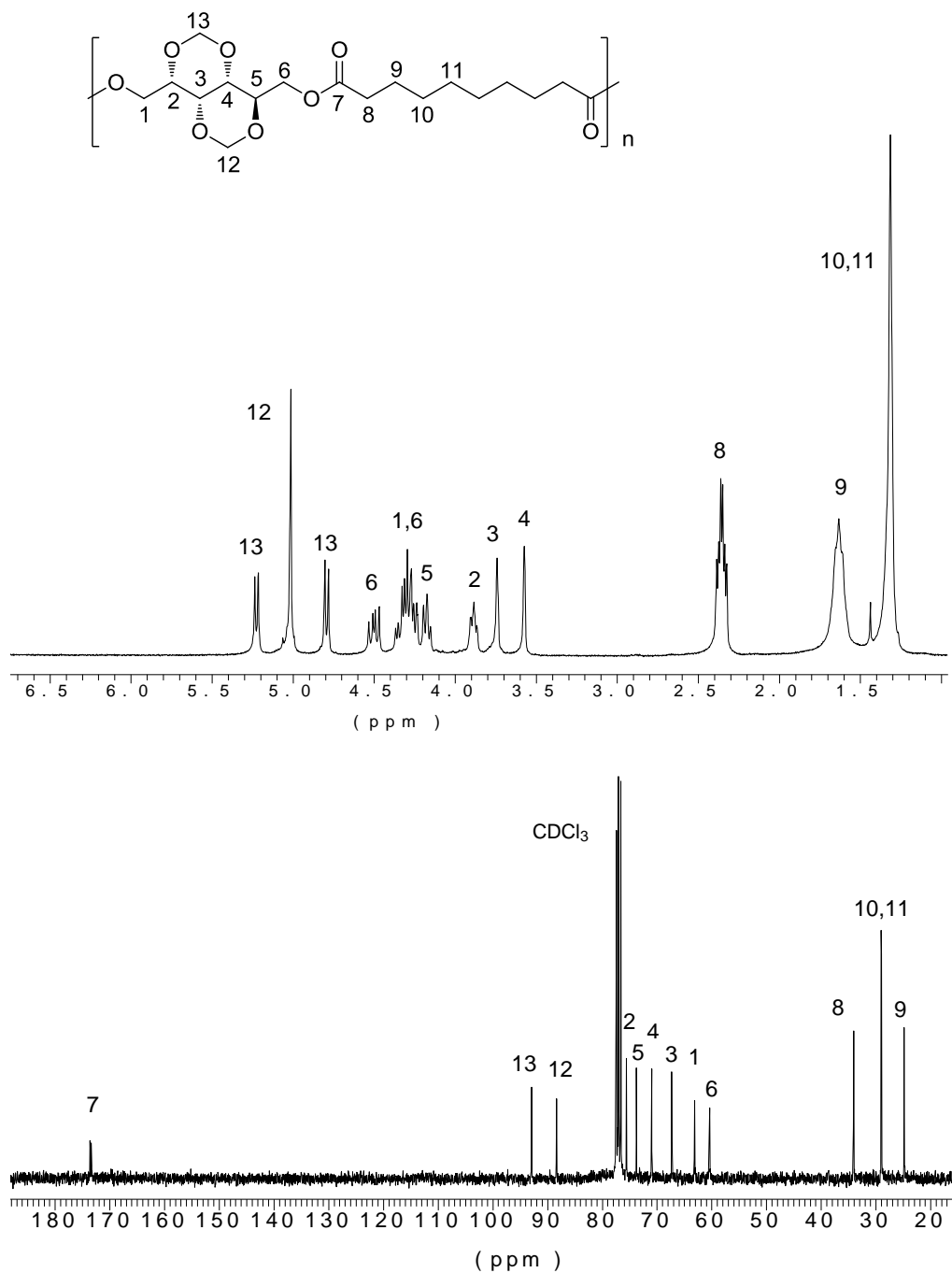


Fig.SI-C-1. ^1H NMR (top), ^{13}C (bottom) NMR spectra of PGluxSeb homopolyester.

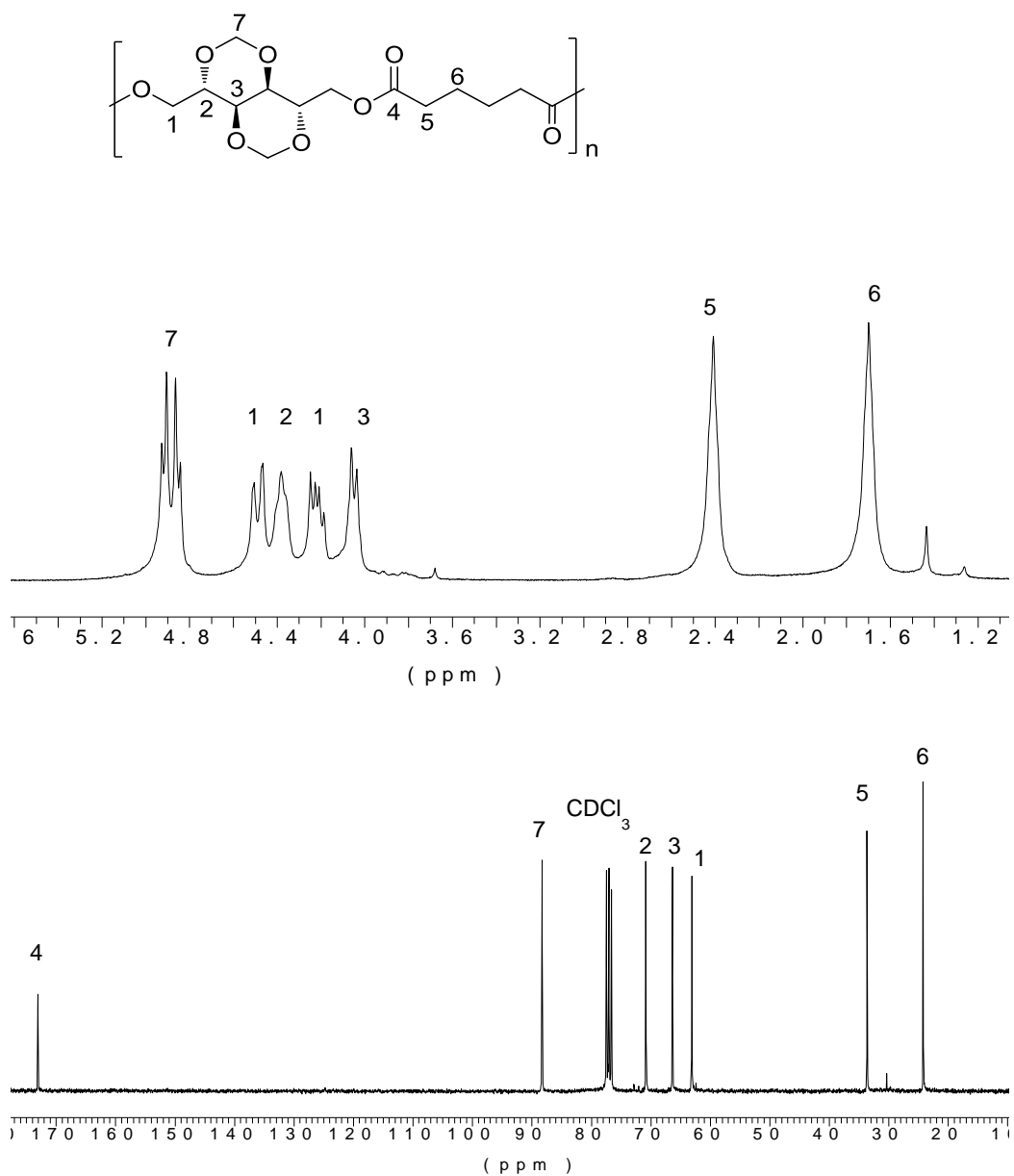


Fig. SI-C-2. ^1H NMR (top), ^{13}C (bottom) NMR spectra of PManxAdi homopolyester.

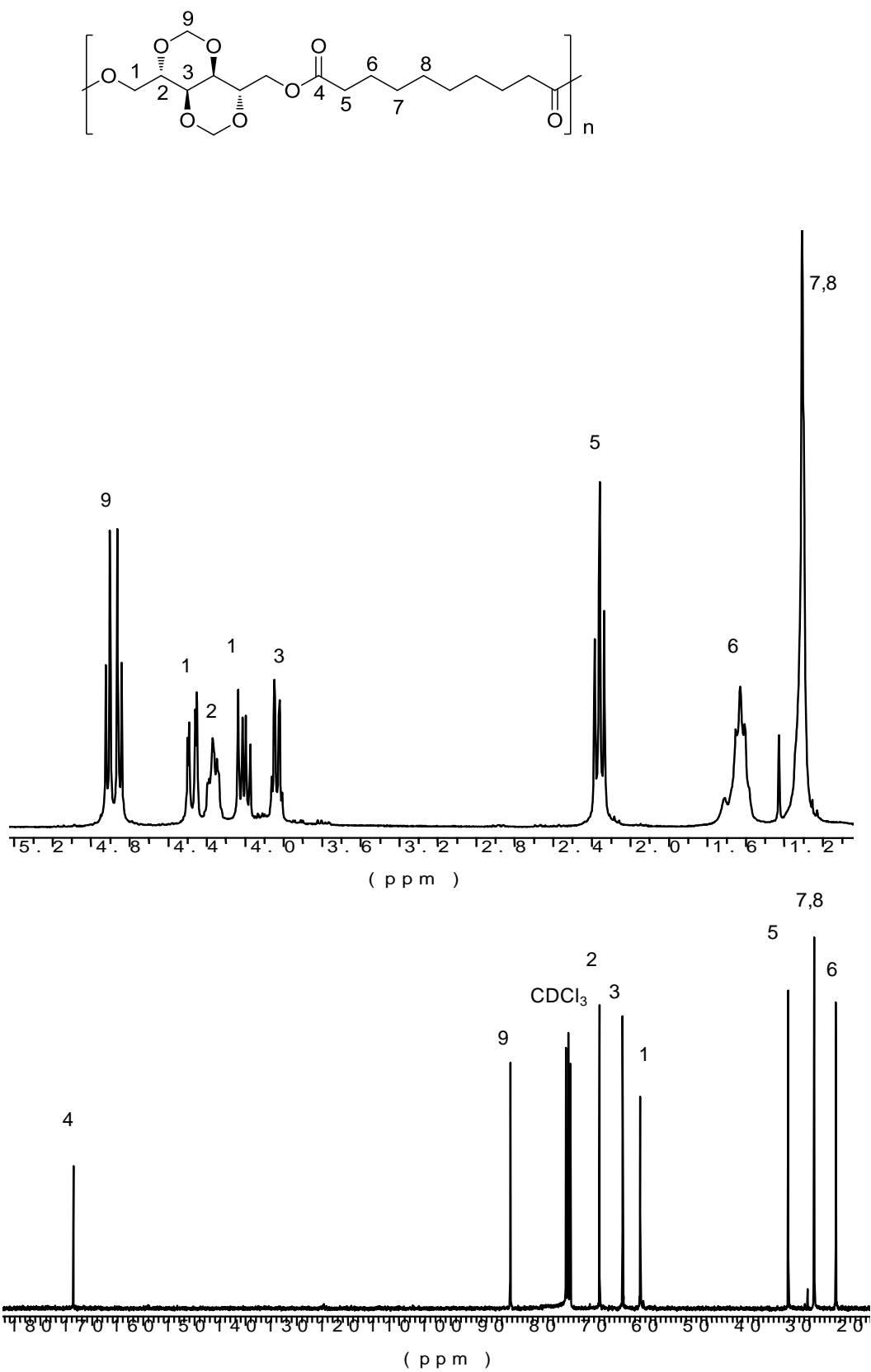


Fig. SI-C-3. ^1H NMR (top), ^{13}C (bottom) NMR spectra of PManxSeb homopolymer.

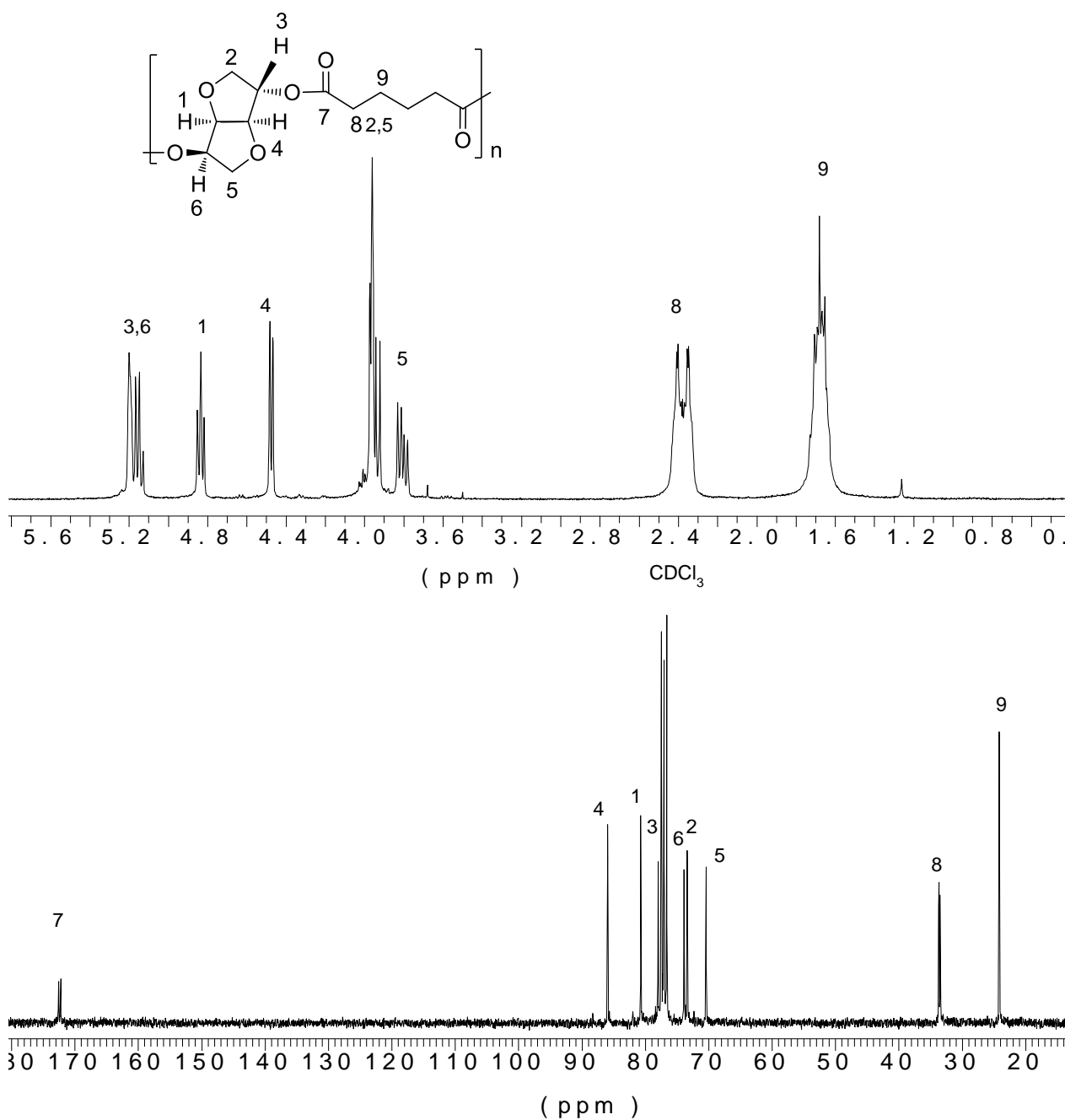


Fig. SI-C-4. ^1H NMR (top), ^{13}C (bottom) NMR spectra of PIsAdi homopolymer.

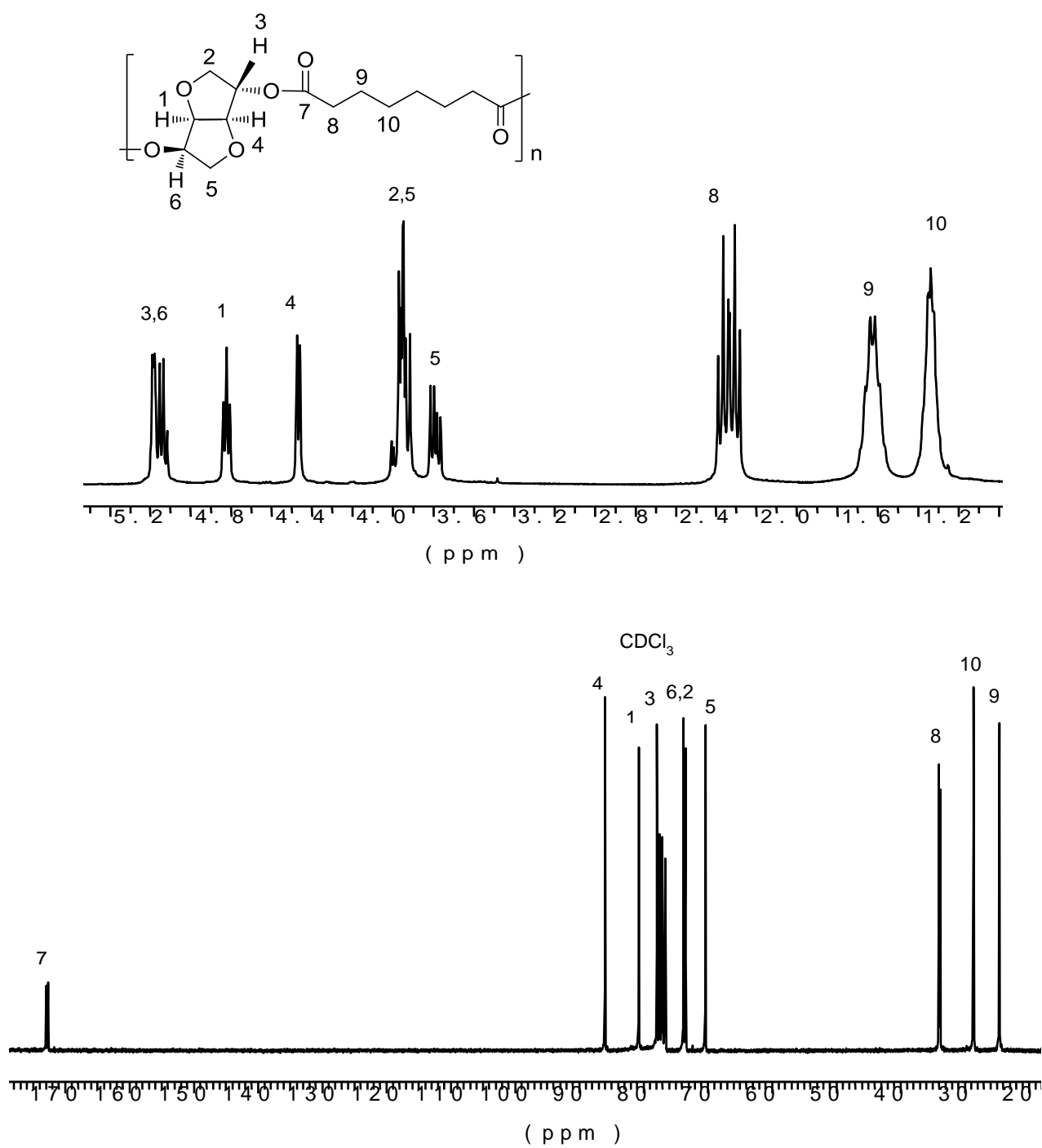


Fig.SI-C-5. ^1H NMR (top) and ^{13}C (bottom) NMR spectra of PlsSub homopolyester.

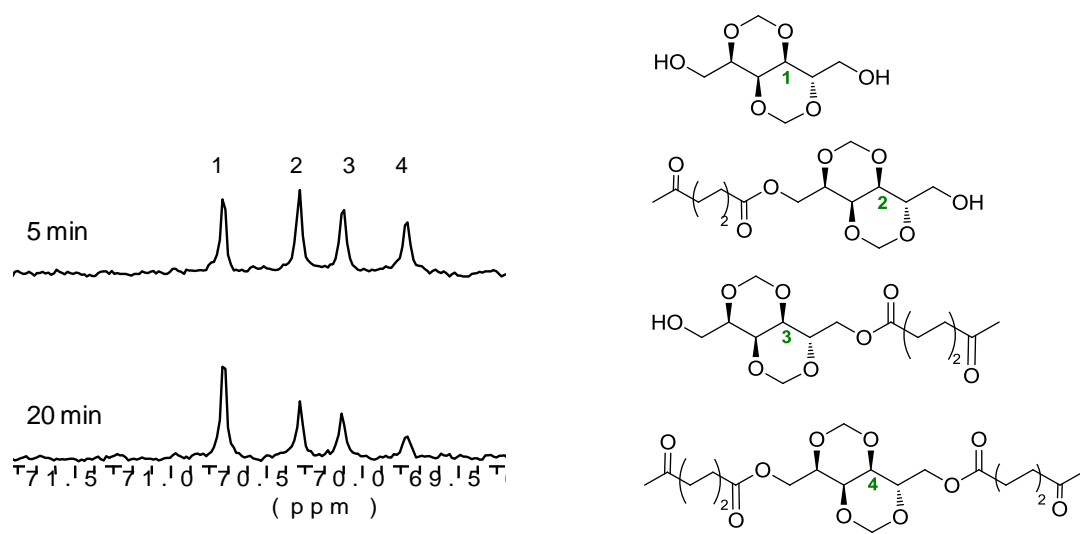


Fig. SI-C-6. ^{13}C -NMR spectra showing the different products generated by the transesterification of *exo* and *endo* groups of Glux-diol with dimethyl adipate.

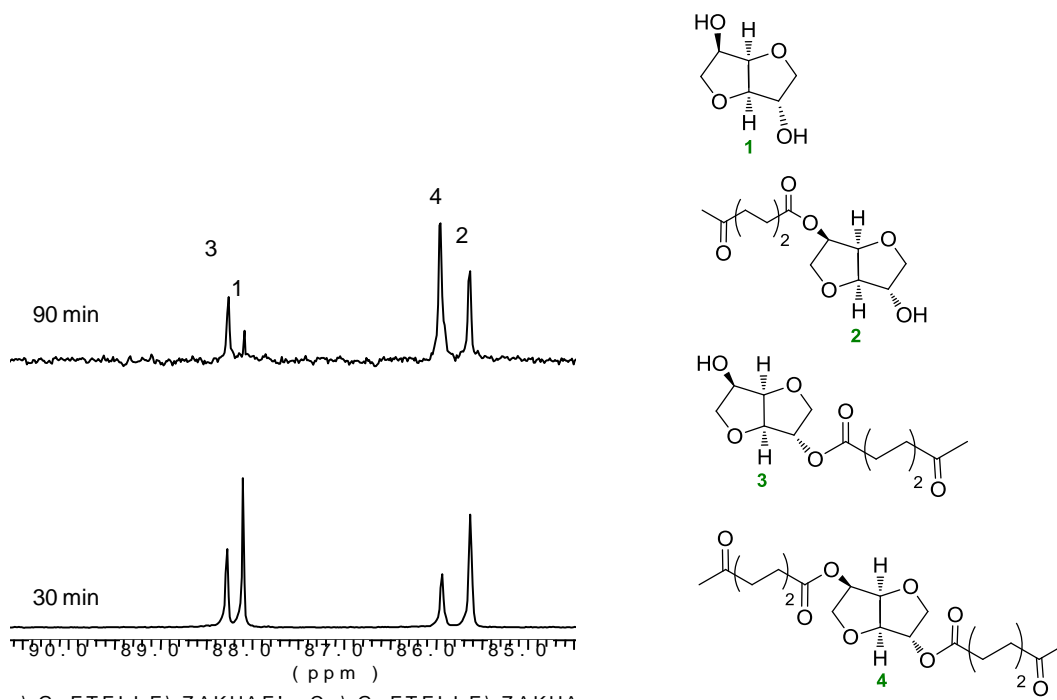


Fig. SI-C-7. ^{13}C -NMR spectra showing the different products generated by the transesterification of *exo* and *endo* groups of Is with dimethyl adipate.

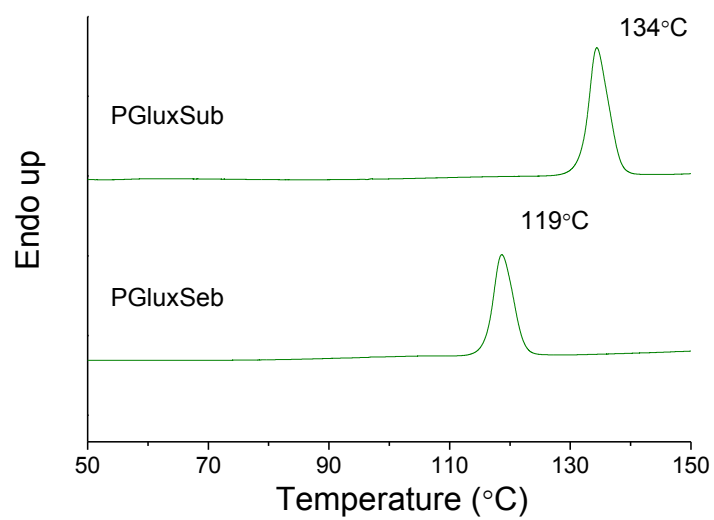


Fig. SI-C-8. First heating DSC traces of PGluxSeb annealed at 105 °C for 1 h, PGluxSub annealed at 120 °C for 1 h.

Annex D. Triblock copolyesters derived from lactic acid and glucose: Synthesis, nanoparticle formation and simulation

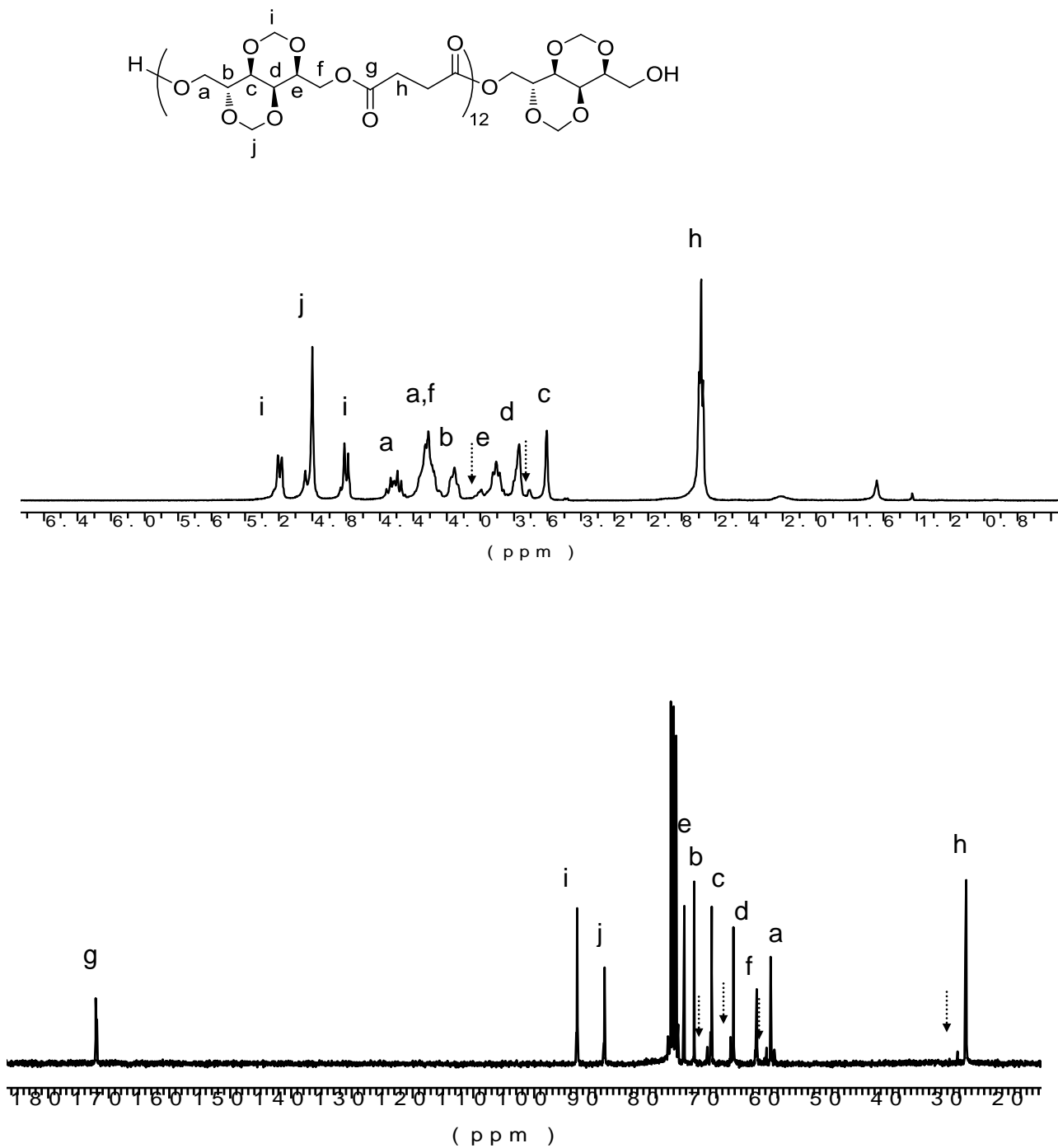


Fig. SI-D-1. ¹H (top), ¹³C (bottom) NMR spectra of telechelic OH-(PGLuxS)₁₂-OH homopolyester (the arrows show end groups).

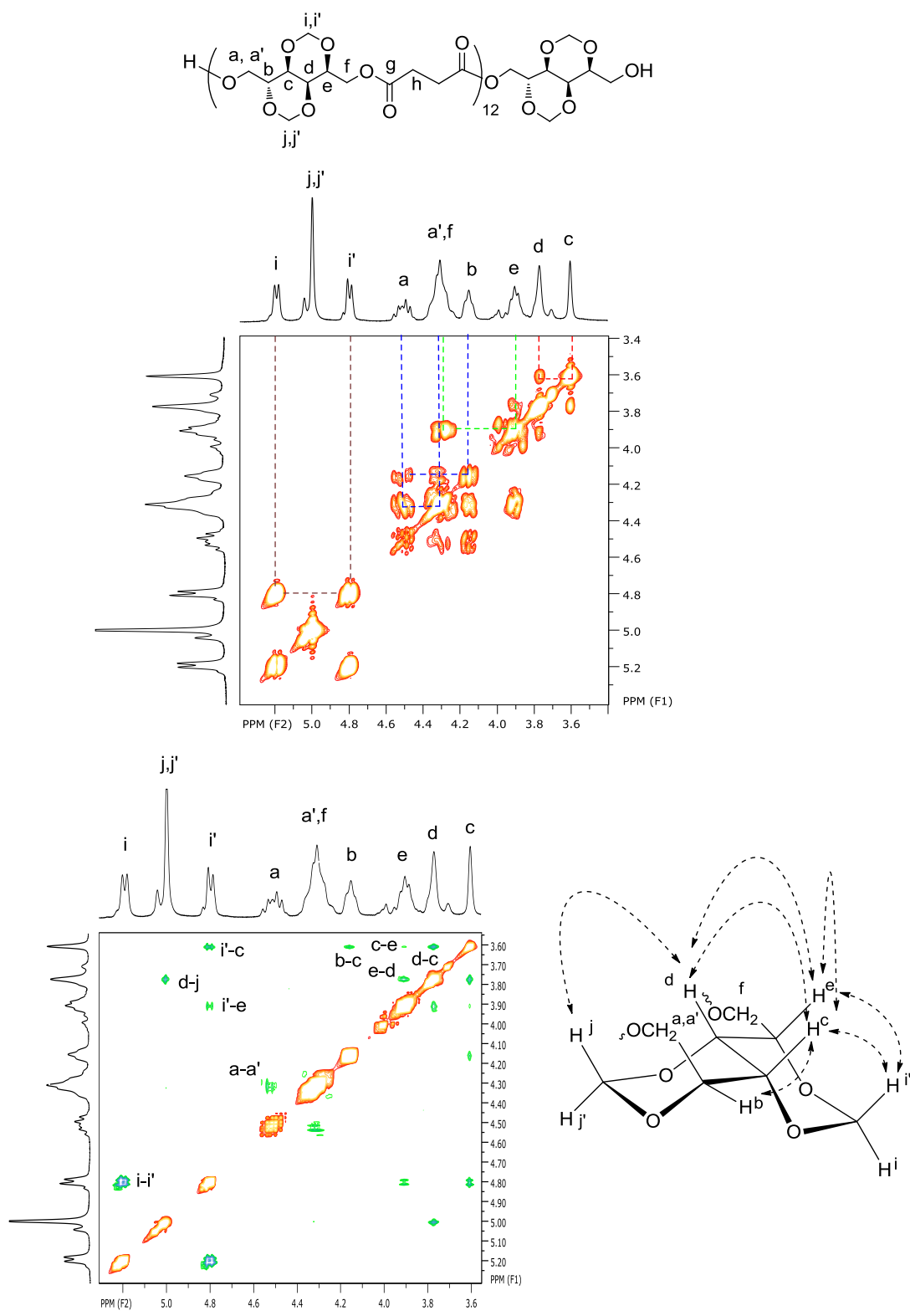


Fig. SI-D-2. ^1H - ^1H cosy (top) and noesy (bottom) NMR spectra of telechelic OH-(PGluxS)₁₂-OH homopolyester with peak assignments based on cross coupling signals and *nOe* interactions.

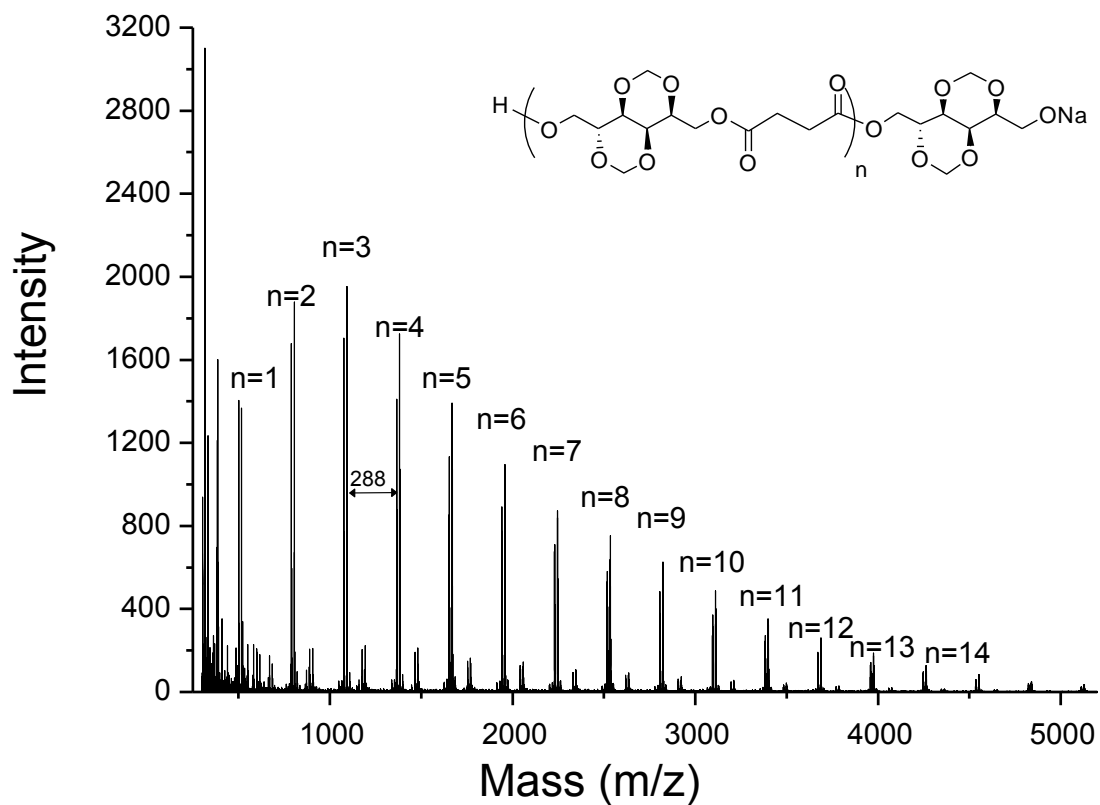


Fig. SI-D-3. MALDI-TOF mass spectra of telechelic OH-P(GluxS)₁₂-OH homopolyester. The two major peaks observed for every composition arise from quasimolecular ions (M+Na)⁺ and (M+Li)⁺, respectively.

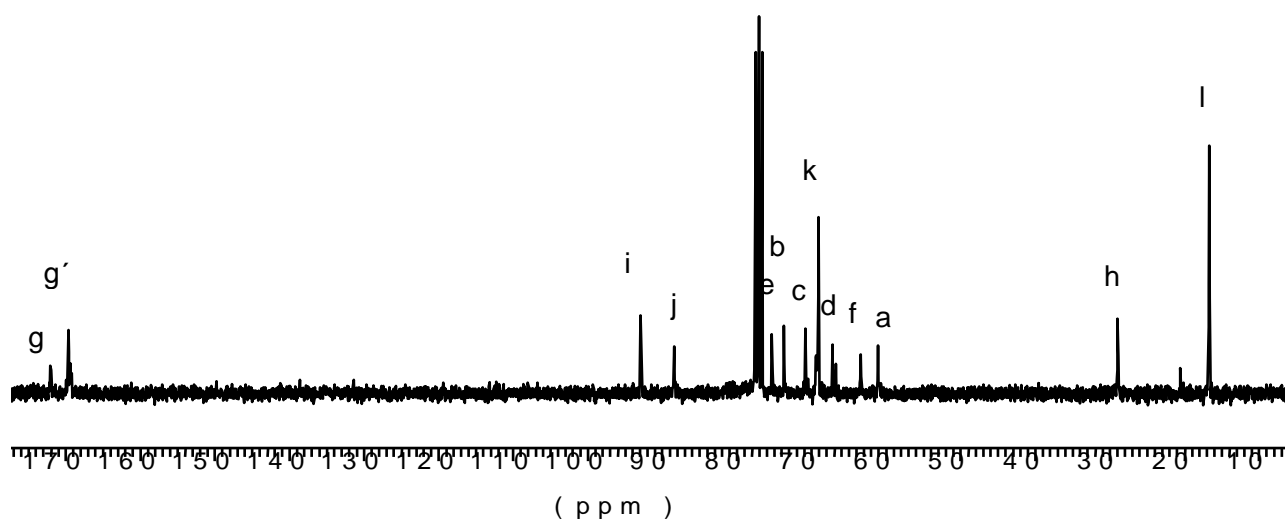
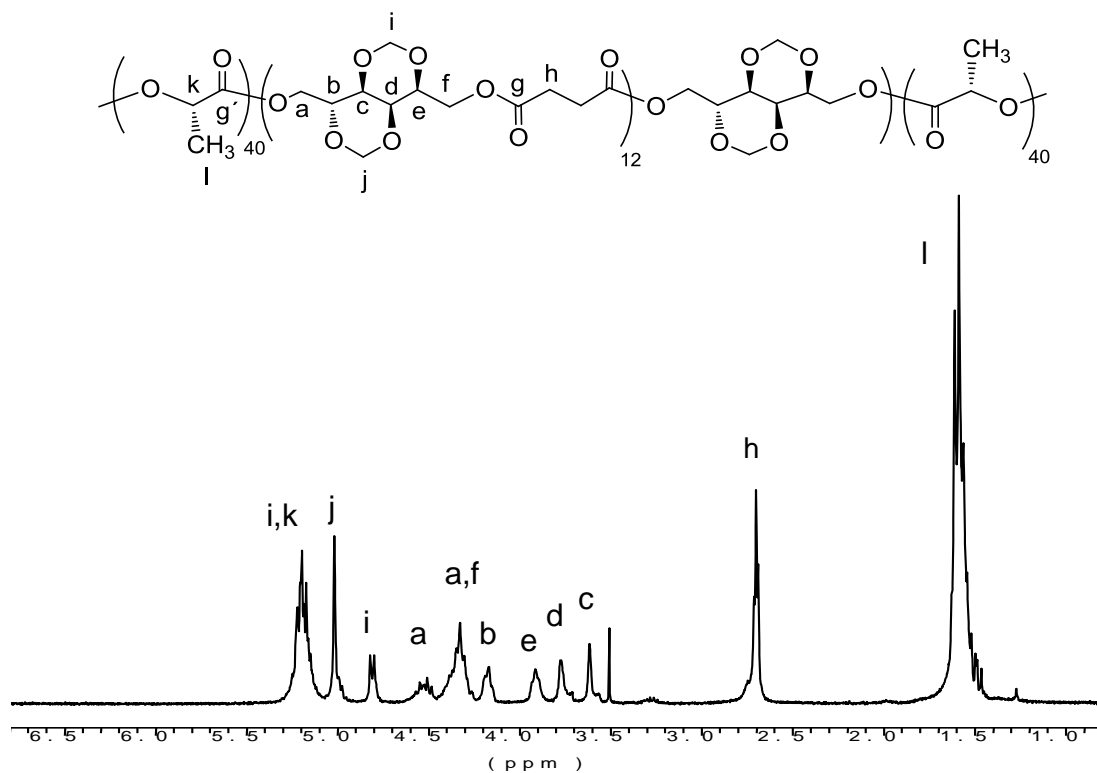


Fig. SI-C-4. ^1H (top) and ^{13}C (bottom) NMR spectra of $\text{PLA}_{40}\text{-(PGLuxS)}_{12}\text{-PLA}_{40}$ triblock copolyester.

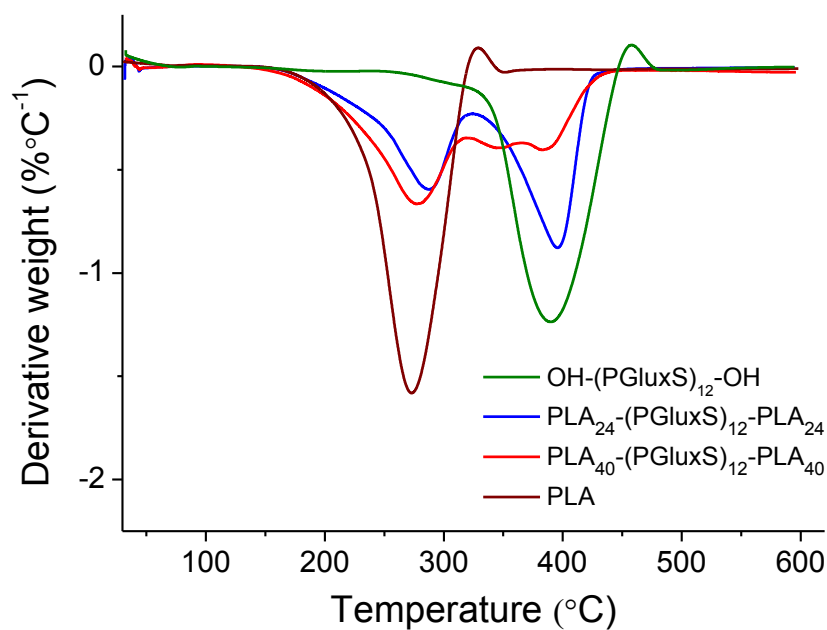


Fig. SI-D-5. Derivative curves of TGA traces of parent homopolyesters and triblock copolyesters.

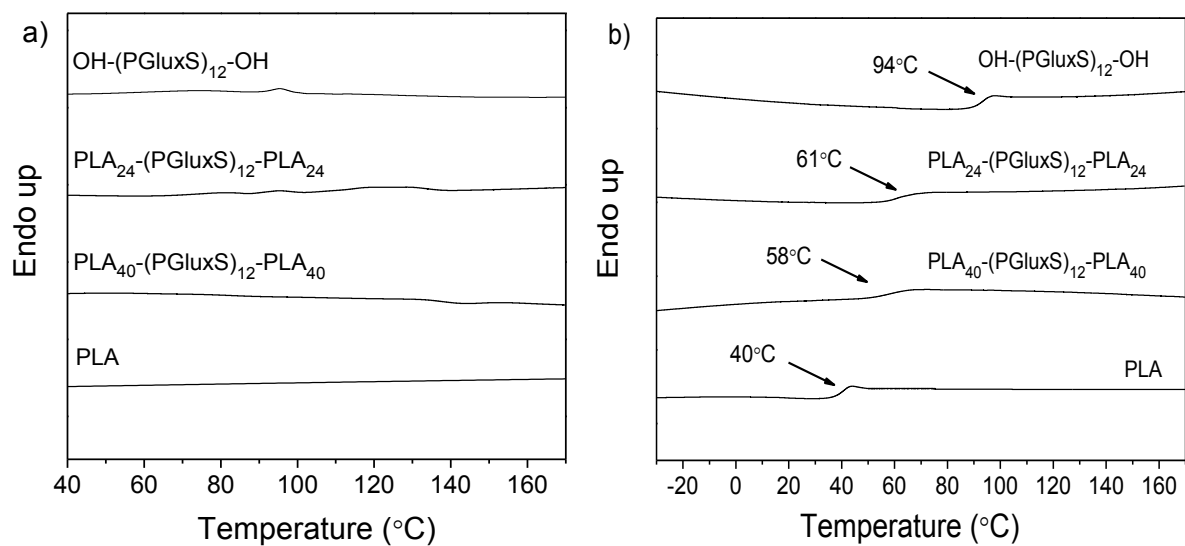


Fig. SI-D-6. a) First heating DSC traces of powdered samples coming directly from synthesis. b) DSC traces of melt-quenched samples for T_g observation.

Hydrolytic degradation and biodegradation

The hydrolytic degradation rate of PLA₂₄-(PGLuxS)₁₂-PLA₂₄ was evaluated by monitoring the changes taking place in molecular weight as a function of time in samples incubated in aqueous buffer pH 7.4 at 37 °C. The biodegradation of the same copolyester in the presence of pancreatic lipase was studied in parallel. For these studies, disks of a film of PLA₂₄-(PGLuxS)₁₂-PLA₂₄ were immersed in phosphate buffer and collected at scheduled times for GPC analysis. After incubation the triblock copolyester produced monomodal GPC chromatograms with peak values slightly decreasing with time. After three weeks of incubation, the copolyester had lost about 7-8% of the initial M_w (Fig. SI-7a), revealing a significant sensitivity to hydrolysis under neutral conditions. In the presence of lipase, degradation rate was slightly enhanced during the first weeks of incubation but final results were not very far from those achieved in the absence of enzymes. The ¹H NMR spectrum of the products released by the copolyester to the incubating medium is depicted in Fig. SI-D-7b. The spectrum contains signals corresponding to succinic, lactic acid and soluble oligomers.

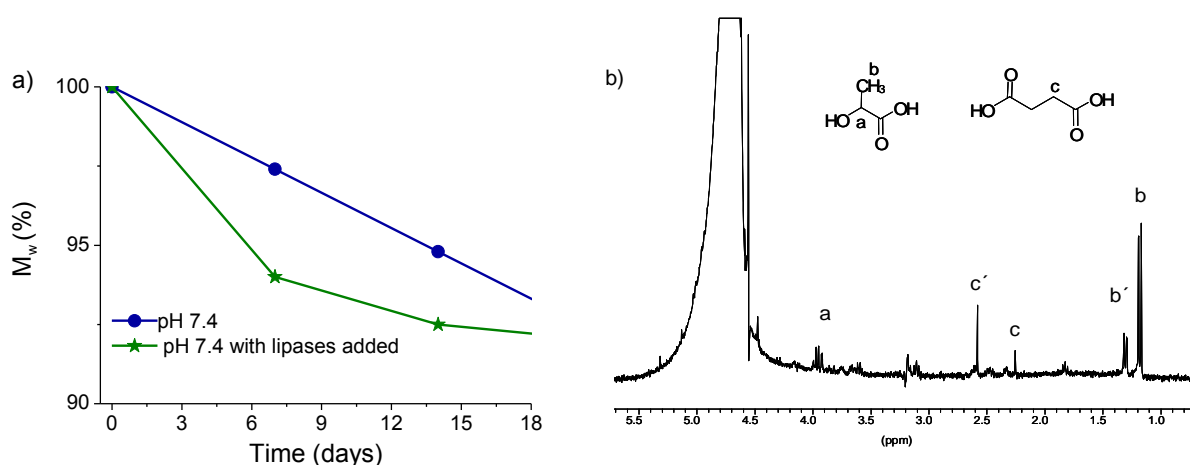


Fig. SI-D-7. a) Degradation plot of PLA₂₄-(PGLuxS)₁₂-PLA₂₄ copolyester at pH 7.4 with and without porcine pancreas enzyme added. b) ¹H NMR spectrum in D₂O of the products released to the aqueous medium after incubation for three weeks without porcine pancreas enzyme added.

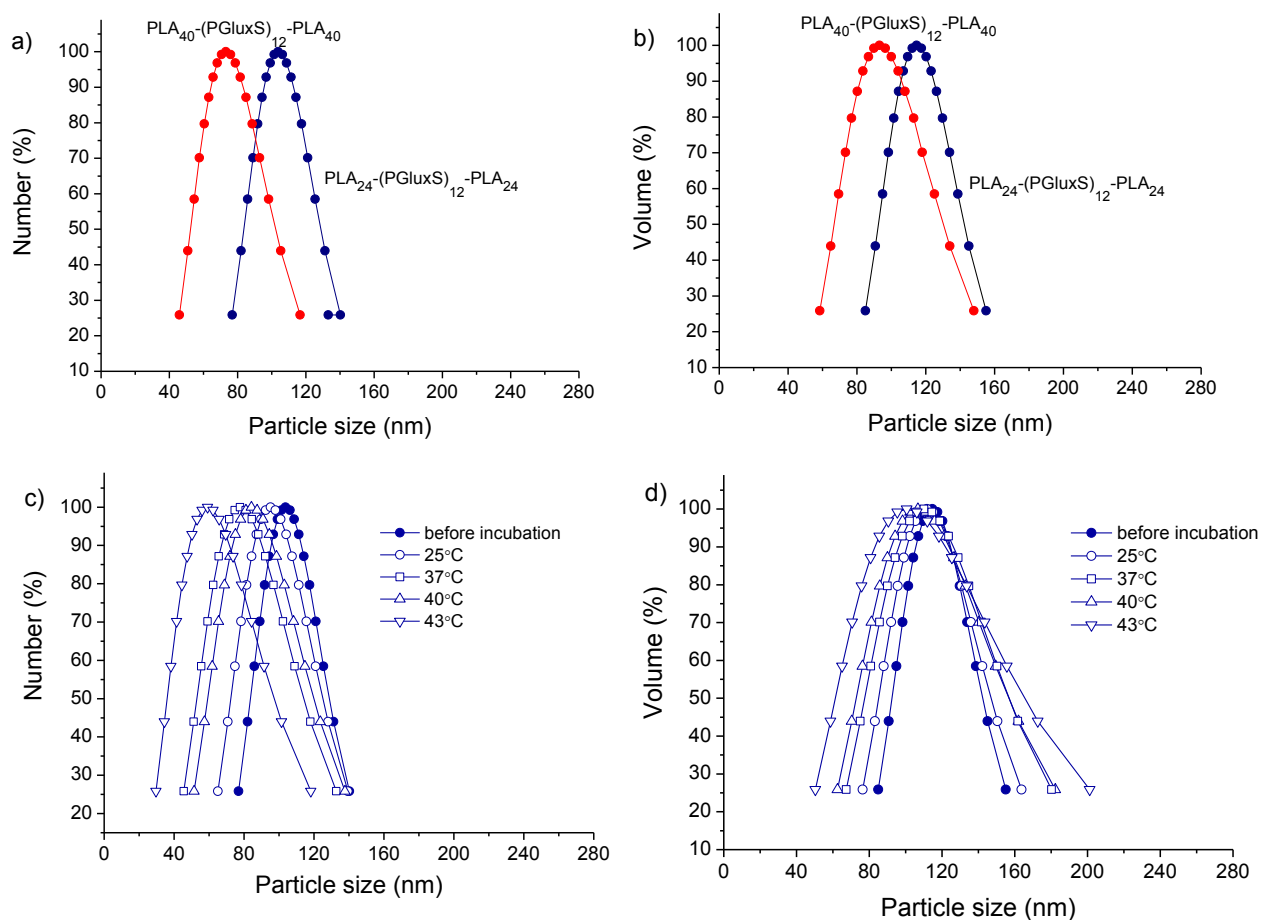


Fig. SI-D-8. Number (a) and volume size distribution plots (b) of $\text{PLA}_{24}\text{-(PGLuxS)}_{12}\text{-PLA}_{24}$ and $\text{PLA}_{40}\text{-(PGLuxS)}_{12}\text{-PLA}_{40}$ nanospheres. Number (c) and volume size distribution plots (d) of $\text{PLA}_{24}\text{-(PGLuxS)}_{12}\text{-PLA}_{24}$ nanospheres versus temperature after 5 days of incubation.

Table SI-D-1. Nanoparticle properties.

Triblock copolyester	Number particle size (nm)	Volume particle size (nm)
$\text{PLA}_{24}\text{-(PGLuxS)}_{12}\text{-PLA}_{24}$	104 ± 14.6	115.0 ± 7.0
$\text{PLA}_{40}\text{-(PGLuxS)}_{12}\text{-PLA}_{40}$	73.2 ± 13.0	94.2 ± 10.8

Atomistic simulations

Atomistic molecular dynamics simulations have been carried out to obtain the energy parameters within the MARTINI CG model on a system consisting on 4 $\text{PLA}_6\text{-(PGLuxS)}_{12}\text{-PLA}_6$ chains in aqueous solution. This simulation consisted on 2500 ps of production run, with a time step of 0.0005 ps, in the NVT ensemble at 300 K. The

GROMOS¹⁶ force-field has been used for these simulations, where the energy parameters for the three types of residue have been obtained through the ATB¹⁷⁻¹⁹ online tool.

Mapping scheme

Lactate, succinate and Glux units have been described by different types of coarse-grained beads within the framework of the MARTINI force-field in the paper. Each PLA repeat unit is represented by a single bead which corresponds to 5 heavy atoms (5:1 mapping scheme). The succinate monomer is represented by two spheres formed by 4 heavy atoms. The Glux unit is represented by 4 small beads corresponding to 3 heavy atoms: two terminal groups linked to the adjacent PLA or succinate units, and two central ones. The Glux groups directly bonded to PLA segments include an extra oxygen atom and thus have a larger size. Fig. SI-9 shows the bond connectivity between the beads in the CG model.

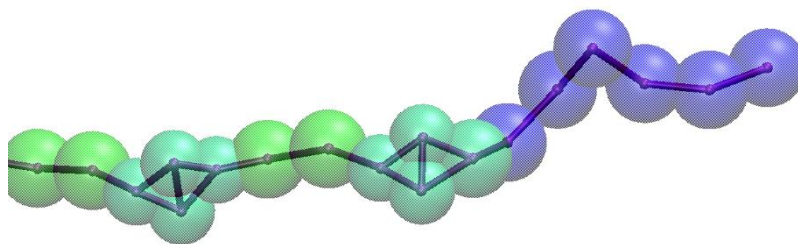


Fig. SI-D-9. Definition adopted for the CG particles used for the mesoscopic model of the PLA_y-(PGLuxS)_x-PLA_y copolymers, including the connectivity between the beads. Blue beads correspond to LA units, dark green to Glux, and light green to S.

The energy parameters are obtained by comparing the results obtained from the atomistic simulations with those from mesoscopic test simulations on the same system and under the same conditions (temperature, simulated time). Intramolecular energy parameters are chosen by fitting the bond length and angle distributions resulting from both methods.

Regarding intermolecular interactions, bead types have been assigned to produce a reasonable agreement between the pair-pair radial distribution functions obtained from the atomistic and CG simulations between the different groups and between the groups and the surrounding water molecules. According to that, the PLA units are assigned apolar character (type C1), the S beads are defined as polar (type P1), and the Glux spheres have hydrogen-bonded acceptor character (type SNa; type Na if linked to lactate groups). Within

the MARTINI framework, C1, P1 and Na particles have an effective interaction size $\sigma = 0.47$ nm, while SNa particles have a smaller effective size $\sigma = 0.43$ nm.

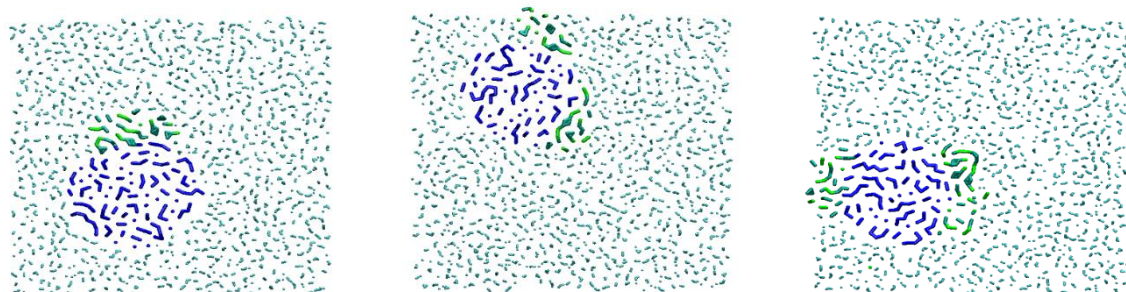


Fig. SI-D-10. Section of the $\text{PLA}_y\text{-(PGLuxS)}_{12}\text{-PLA}_y$ nanospheres. LA groups are depicted in blue color, Glux in dark green, Succ in light green, and water in cyan.

Annex E. Bio-based triblock copolyesters synthesized from tartaric acid derivative and poly(lactic acid), nanoparticle formation

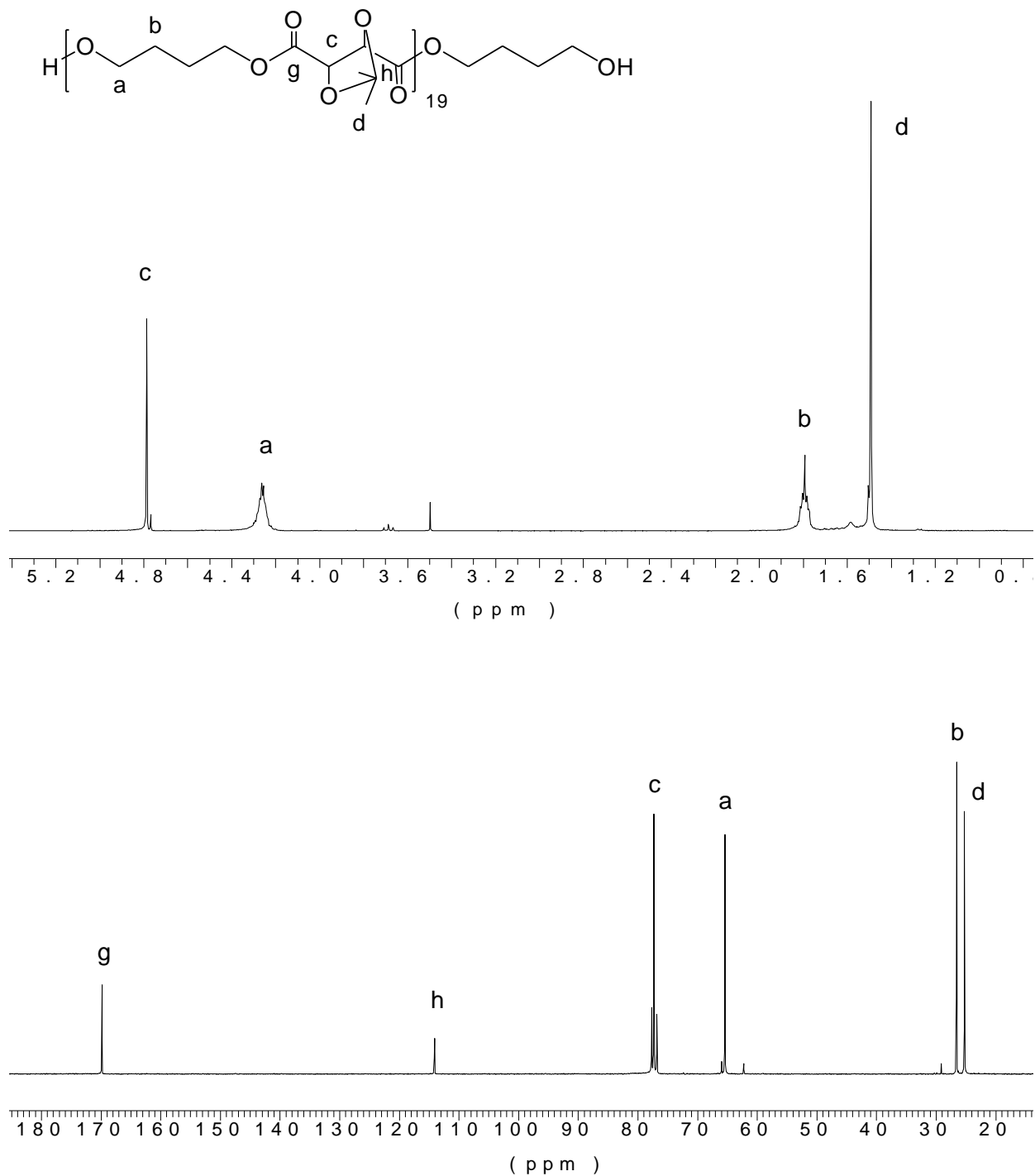


Fig. SI-E-1. ^1H (top), ^{13}C (bottom) NMR spectra of telechelic $\text{OH-(PBiThx)}_{19}\text{-OH}$ homopolyester (the arrows show end groups).

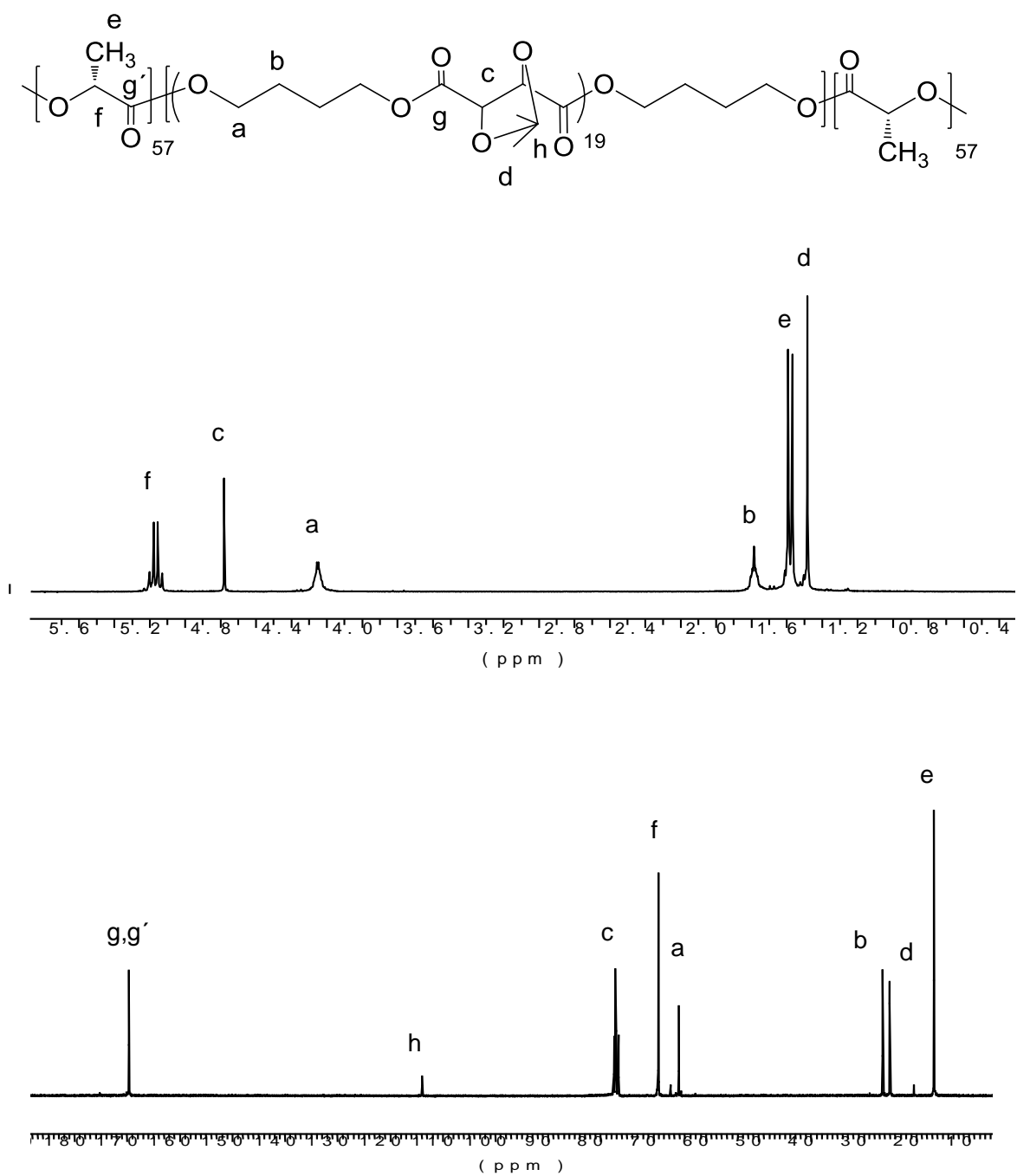


Fig. SI-E-2. ¹H (top) and ¹³C (bottom) NMR spectra of PLLA₅₇-(PBiThx)₁₉-PLLA₅₇ triblock copolyester.

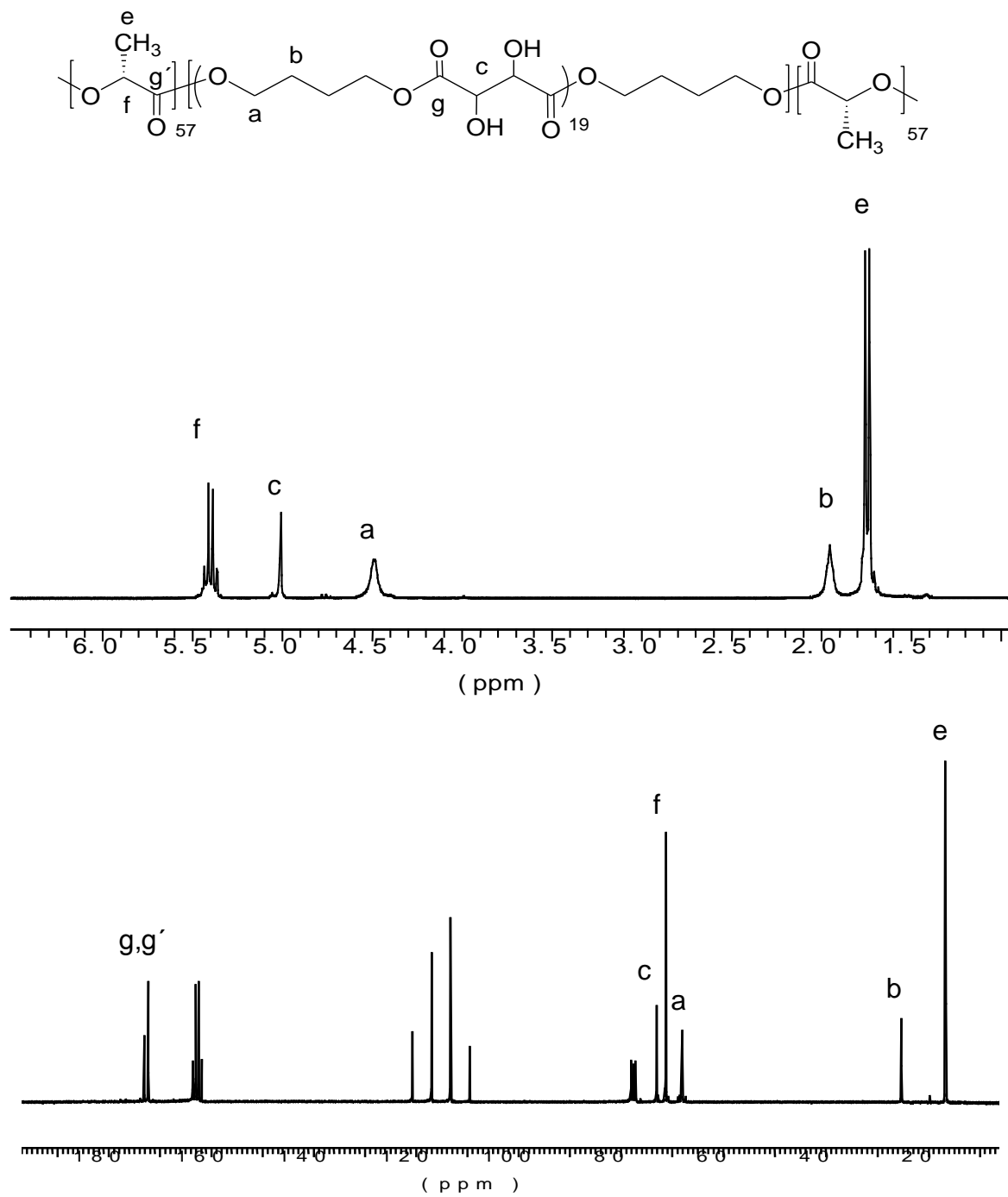


Fig. SI-E-3. ¹H (top) and ¹³C (bottom) NMR spectra of PLLA₅₇-(PBThxOH)₁₉-PLLA₅₇ triblock copolyesters.

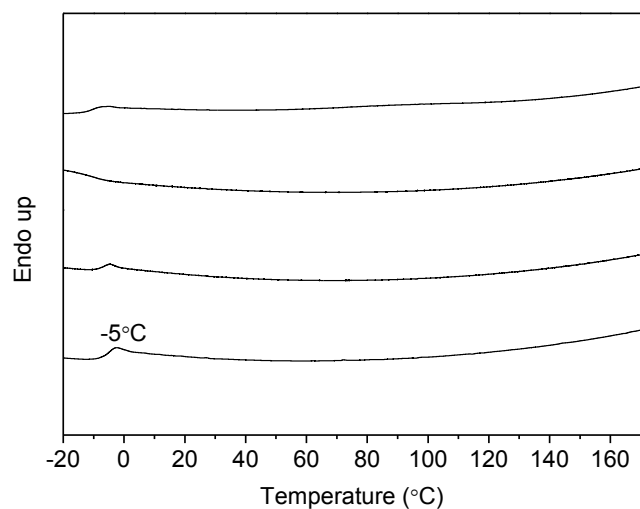


Fig. SI-E-4. DSC traces of powdered OH-(PBiThx)₁₉-OH telechelic homopolyester coming directly from synthesis: (1) heating at 10 °C·min⁻¹, (2) cooling at 10 °C·min⁻¹, (3) second heating at 10 °C·min⁻¹, (4) heating at 20 °C·min⁻¹ of a sample quenched from the melt.

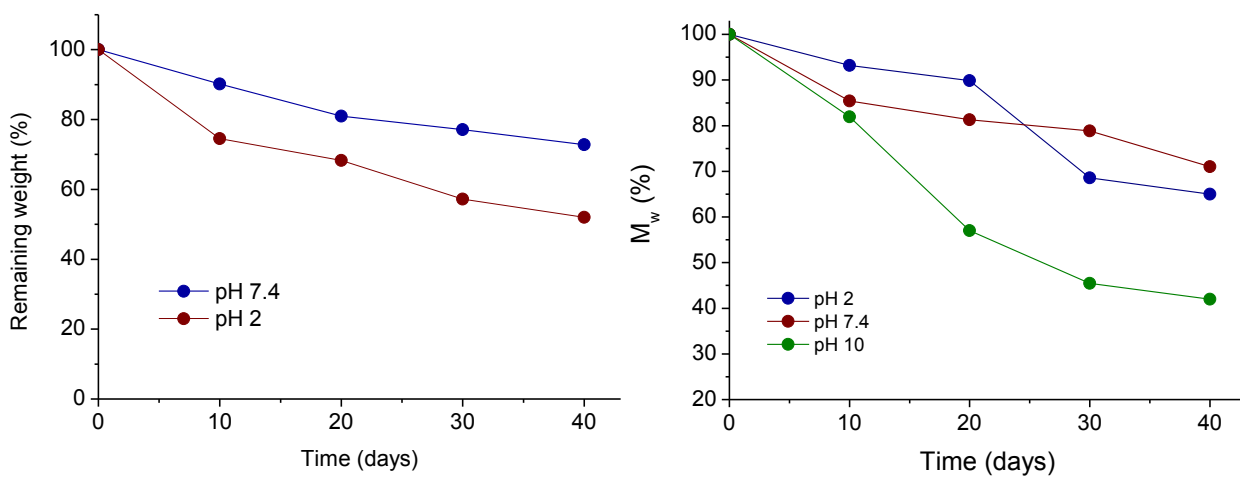


Fig. SI-E-5. Remaining weight (a), molecular weight (b) of PLLA₃₈-(PBThxOH)₁₉-PLLA₃₈ copolyester versus degradation time.

Acknowledgements

I would like to thank the whole research group of Polymers and Biopolymers in Polytechnical University of Catalonia.

Especially I am very grateful to Prof. Dr. Sebastián Muñoz-Guerra for giving me an opportunity to realize Ph.D thesis in his group, dedication for leading my project, interesting ideas and enthusiasm.

I would like to thank Dr. Antxon Martínez de Ilarduya for being codirector of my thesis, realizing brilliant NMR analyses and giving good advises.

I wish to thank Dr. Abdel Alla, for his cooperation in calorimetric and thermogravimetric experiments.

I am also grateful to all Ph.D. students Ana Gamarra, Juan Carlos Morales, Ernesto Tinajero, Cristina Lavilla, Cristina Japu, Alberto Lanz and Mayka Bautista. It was great sharing laboratory with you during these last four years.

A very special gratitude goes out to my parents Nadezda y Vladimir that gave me an opportunity to realize master studies in UPC. Thank you very much for your emotional support in the hardest moment of the Ph.D.

Thank you my grandfather Fedor Alekseevitch that you always was understanding with me, light memory to you.

I am grateful to Ulises for his eternal assistance and finding suitable words for overcoming numerous obstacles I have been facing through my research.

In addition I would like to express my gratitude to the Ministry of Education of Spain for the grant awarded to me for doing this research.

Thanks all for your encouragement!

Curriculum Vitae

Elena Zakharova was born on the 14th of August in Moscow, Russia. From 2005 to 2010 she studied Engineering of macromolecular compounds at the faculty of polymers in D.I. Mendeleev University of Chemical Technology (Moscow, Russia).

In 2012 she started master degree in Polymers and Biopolymers in Polytechnic University of Catalonia (Barcelona, Spain). In 2013 she presented her master dissertation entitled «Poly(butylene succinate) copolyesters containing cyclic acetalized tartrate units» under the supervision of Prof. Sebastián Muñoz-Guerra.

In 2013 she started her Ph.D. research entitled «Sustainable bioplastics derived from carbohydrates». During years of Ph.D. she gaved practical sessions in Organic Chemistry and Materials.

Publications

1. E. Zakharova, C. Lavilla, A. Alla, A. Martínez de Ilarduya, S. Muñoz-Guerra, Modification of properties of poly(butylene succinate) by copolymerization with tartaric acid-based monomers, *Eur. Polym. J.* 2014, 61, 263-273.
2. E. Zakharova, Alla, A. Martínez de Ilarduya, S. Muñoz-Guerra, Bio-based PBS copolyesters derived from a bicyclic D-glucitol, *RCS Adv.*, 2015, 46395-46404.
3. E. Zakharova, A. Martínez de Ilarduya, S. León, S. Muñoz-Guerra, Sugar-based bicyclic monomers for aliphatic polyesters: a comparative appraisal of acetalized alditols and isosorbide, *Des. Monomers Polym.* 2016, 20, 157-166.
4. E. Zakharova, S. Leon, A. Martínez de Ilarduya, S. Muñoz-Guerra, Triblock copolyesters derived from lactic acid and glucose: Synthesis, nanoparticle formation and simulation, *Eur. Polym. J.* 2017, 92, 1-12.
5. E. Zakharova, S. Leon, A. Martínez de Ilarduya, S. Muñoz-Guerra, Bio-based triblock copolyesters synthesized from tartaric acid derivative and poly(lactic acid), nanoparticle formation. *React. Funct. Polym.*, to be submitted.

Conference proceedings

1. E. Zakharova, C. Lavilla, A. Alla, A. Martínez de Ilarduya, S. Muñoz-Guerra, Modification of properties of poly(butylene succinate) by copolymerization with tartaric acid-based monomers. XIII Meeting of the specialized polymer group (RSEQ, RSEF), Girona, 7-10 September 2014, oral communication.
2. E. Zakharova, Alla, A. Martínez de Ilarduya, S. Muñoz-Guerra, Bio-based PBS copolyesters derived from a bicyclic D-glucitol. European polymer federation, Dresden, 21-26 June 2015, oral communication.
3. E. Zakharova, A. Martínez de Ilarduya, S. León, S. Muñoz-Guerra, Sugar-based bicyclic monomers for aliphatic polyesters: a comparative appraisal of acetalized alditols and isosorbide. XIV Meeting of the specialized polymer group (GEP), Burgos, 5-8 September 2016, poster.
4. E. Zakharova, S. Leon, A. Martínez de Ilarduya, S. Muñoz-Guerra, Triblock copolyesters derived from lactic acid and glucose: Synthesis, nanoparticle formation and simulation. IX congress of young researchers in polymers, (JIP), Tarragona, 5-9 June 2017, oral communication.